Time Delays in Control Systems

course notes

Leonid Mirkin
Faculty of Mechanical Engineering
Technion–IIT

draft, August 29, 2024

ii

Contents

Preface

T IME DELAYS are ubiquitous in control applications. They represent mass and heat transport phenomena, computation and communication time lags, many effects of unmodeled high-frequency dynamics, et cetera. Dynamics of continuous-time systems involving delays are intrinsically infinite dimensional, which complicates their analysis and associated control design methods. In many situations, delays have negative effects on the stability of control systems and impose severe limitations on their attainable performance. These factors suggest that understanding time-delay systems and corresponding control analysis and design methods is of vital importance.

These notes are intended to be an introduction to the realm of time-delay control systems. Their main emphasis is laid on the linear time-invariant (LTI) setting and input and / or output delays. The reason is twofold. First, this class, dubbed *dead-time systems*, is of great importance in applications, where a major harm is caused by loop delays. Second, these systems constitute the best understood class of time-delay systems, with plenty of rigorous, yet still transparent and intuitive, analysis and design methods available. Therefore, dead-time systems are a convenient class of time-delay systems, on which concepts can be explained without the need to dig into overly convoluted technicalities. Still, many ideas behind the studied systems are generic and extendable to more general settings.

Two aspects of the control of time-delay systems are highlighted throughout the text. The first one is prominence given to *dead-time compensation* (DTC) methods as *the* control architecture in the context of time-delay systems. I am convinced—and hope that the text conveys this opinion—that DTC is intrinsic to delayed dynamics and is a natural extension of classical concepts of state feedback and state observation. As such, quite a lot of space is devoted to motivating the DTC structure, its use in various control and estimation problems, as well as to related implementation issues. The second peculiarity is that the presentation is not dominated by stability analyses. Stability requirements comprise a compulsory part of requirements to control systems, of course. But the stabilization is hardly ever the ultimate goal of control design. Control is about imposing desired behaviors on controlled systems, reducing the sensitivity to disturbances on them, and so on. These aspects are extensively discussed in the notes.

This is an *engineering* text, so first and foremost it aims at developing an engineering insight into the impact of delays on control systems and at exploiting the structure of the delay element in various analysis and design situations. As a result—whether this is a welcome outcome or not depends on viewpoint—the notes are less concerned with such apparently fascinating issues as associated initial value problems, the smoothness of solutions, clustering closed-loop poles for systems with multiple incommensurate delays, and so on. Also, the math is not always self contained, some technical results are presented without proofs. Nonetheless, reasonable levels of rigorousness and self-containment are endeavored (although with only a partial success).

Haifa (32.7746,35.0230)   LEONID MIRKIN
October, 2019

Nomenclature

$\mathbb{N}$	set of positive integers (natural numbers)
$\mathbb{Z}$	set of integers
$\mathbb{Z}_+$	set of nonnegative integers
$\mathbb{Z}_-$	set of non-positive integers, $\mathbb{Z}_- = \mathbb{Z} \setminus \mathbb{N}$
$\mathbb{Z}_{i_1..i_2}$	integer interval from i_1 to and including i_2, i.e. $\mathbb{Z}_{i_1..i_2} := \{i \in \mathbb{Z} \mid i_1 \le i \le i_2\}$
$\mathbb{R}$	set of real numbers, $\mathbb{R} = (-\infty, \infty)$
$\mathbb{R}_+$	set of nonnegative real numbers, $\mathbb{R}_+ = [0, \infty)$
$\mathbb{R}_-$	set of non-positive real numbers, $\mathbb{R}_- = (\infty, 0]$
$j\mathbb{R}$	set of pure imaginary numbers
$\mathbb{C}$	set of complex numbers
$\operatorname{Re} z$	the real part of $z \in \mathbb{C}$
$\operatorname{Im} z$	the imaginary part of $z \in \mathbb{C}$
$\mathbb{C}_\alpha$	open right half-plain, to the right of $\alpha \in \mathbb{R}$, i.e. $\mathbb{C}_\alpha := \{z \in \mathbb{C} \mid \operatorname{Re} z > \alpha\}$
$\overline{\mathbb{C}}_\alpha$	closed right half-plain, to the right of $\alpha \in \mathbb{R}$, i.e. $\overline{\mathbb{C}}_\alpha := \{z \in \mathbb{C} \mid \operatorname{Re} z \ge \alpha\}$
$\mathbb{T}$	unit circle, $\mathbb{T} := \{z \in \mathbb{C} \mid |z| = 1\}$
$\mathbb{D}$	interior of $\mathbb{T}$ (open unit disk), $\mathbb{D} := \{z \in \mathbb{C} \mid |z| < 1\}$
$\overline{\mathbb{D}}$	closed unit disk, $\overline{\mathbb{D}} := \{z \in \mathbb{C} \mid |z| \le 1\} = \mathbb{D} \cup \mathbb{T}$
$\mathbb{F}$	generic field, frequently used as an alias of either $\mathbb{R}$ or $\mathbb{C}$
$C^{p \times m}(\mathbb{I})$	class of continuous functions $\mathbb{I} \to \mathbb{F}^{p \times m}$ for $\mathbb{I} \subset \mathbb{R}$ (it is denoted $C^p(\mathbb{I})$ if $m = 1$ and $C(\mathbb{I})$ if the dimensions are irrelevant or clear from the context)
$L_2^{p \times m}(\mathbb{I})$	Lebesgue space of square integrable functions $\mathbb{I} \to \mathbb{F}^{p \times m}$ (or $L_2(\mathbb{I})$)
$L_{2+}^{p \times m}(\mathbb{R})$	space of square integrable functions $\mathbb{R} \to \mathbb{F}^{p \times m}$ vanishing in $\mathbb{R} \setminus \mathbb{R}_+$ (or $L_{2+}(\mathbb{R})$)
$L_{2-}^{p \times m}(\mathbb{R})$	space of square integrable functions $\mathbb{R} \to \mathbb{F}^{p \times m}$ vanishing in $\mathbb{R} \setminus \mathbb{R}_-$ (or $L_{2-}(\mathbb{R})$)
$\ell_2^{p \times m}(\mathbb{I})$	space of square summable functions $\mathbb{I} \to \mathbb{F}^{p \times m}$ for $\mathbb{I} \subset \mathbb{Z}$ (or $\ell_2(\mathbb{I})$)
$\ell_{2+}^{p \times m}(\mathbb{Z})$	space of square summable functions $\mathbb{Z} \to \mathbb{F}^{p \times m}$ vanishing in $\mathbb{Z} \setminus \mathbb{Z}_+$ (or $\ell_{2+}(\mathbb{Z})$)
$\ell_{2-}^{p \times m}(\mathbb{Z})$	space of square summable functions $\mathbb{Z} \to \mathbb{F}^{p \times m}$ vanishing in $\mathbb{Z}_+$ (or $\ell_{2-}(\mathbb{Z})$)
$L_1^{p \times m}(\mathbb{I})$	space of absolute integrable functions $\mathbb{I} \to \mathbb{F}^{p \times m}$ (or $L_1(\mathbb{I})$)
$L_\infty^{p \times m}(\mathbb{I})$	space of essentially bounded functions $\mathbb{I} \to \mathbb{F}^{p \times m}$ (or $L_\infty(\mathbb{I})$)
$H_\infty^{p \times m}(\mathbb{A})$	Hardy space of holomorphic and bounded functions $\mathbb{A} \to \mathbb{F}^{p \times m}$ for some $\mathbb{A} \subset \mathbb{C}$ (or H_∞)
$\check{x}_t$	finite-window history of x at time t, $\check{x}_t(s) = x(t + s)$ for all $s \in [-\tau, 0]$ and some $\tau > 0$

$\mathbb{1}_{\mathbb{I}}$ indicator of either a set $\mathbb{I} \subset \mathbb{R}$, $\mathbb{1}_{\mathbb{I}}(t) = \begin{cases} 1 & \text{if } t \in \mathbb{I} \\ 0 & \text{otherwise} \end{cases}$, or $\mathbb{I} \subset \mathbb{Z}$, $\mathbb{1}_{\mathbb{I}}[t] = \begin{cases} 1 & \text{if } t \in \mathbb{I} \\ 0 & \text{otherwise} \end{cases}$

$\mathbb{1}$ unit step, either $\mathbb{1} := \mathbb{1}_{\mathbb{R}_+}$ or $\mathbb{1} := \mathbb{1}_{\mathbb{Z}_+}$

δ either Dirac (in the continuous time) or Kronecker (in the discrete time) delta

- -

e_i the ith standard basis in $\mathbb{F}^n$; $e_1 := \begin{bmatrix} 1 & 0 & 0 & \cdots & 0 \end{bmatrix}'$, $e_2 := \begin{bmatrix} 0 & 1 & 0 & \cdots & 0 \end{bmatrix}'$, et cetera

I_n $n \times n$ identity matrix (just I if the dimension is irrelevant)

M' transpose of a matrix $M \in \mathbb{R}^{n \times m}$ / complex-conjugate transpose of a matrix $M \in \mathbb{C}^{n \times m}$

$\lambda_i(M)$ ith eigenvalue of a matrix $M \in \mathbb{F}^{n \times n}$

$\text{spec}(M)$ spectrum of a matrix $M \in \mathbb{F}^{n \times n}$, i.e. the set of all its eigenvalues

$\rho(M)$ spectral radius of a matrix $M \in \mathbb{F}^{n \times n}$, $\rho(M) = \max\{|\lambda_1(M)|, \ldots, |\lambda_n(M)|\}$

$\lambda_{\min}(M)$ the minimum eigenvalue of a symmetric matrix $M = M' \in \mathbb{F}^{n \times n}$

$\lambda_{\max}(M)$ the maximum eigenvalue of a symmetric matrix $M = M' \in \mathbb{F}^{n \times n}$

$\bar{\sigma}(M)$ the maximum singular value of a matrix $M \in \mathbb{F}^{p \times m}$

$\underline{\sigma}(M)$ the minimum singular value of a matrix $M \in \mathbb{F}^{p \times m}$

$\text{tr}(M)$ trace of a matrix $M \in \mathbb{F}^{n \times n}$, $\text{tr}(M) = \sum_{i=1}^{n} m_{ii} = \sum_{i=1}^{n} \lambda_i(M)$

$\|M\|$ spectral norm of $M \in \mathbb{F}^{n \times m}$, $\|M\|^2 := \rho(M'M) = \rho(MM')$

$\|M\|_{\text{F}}$ Frobenius norm of $M \in \mathbb{F}^{n \times m}$, $\|M\|_{\text{F}}^2 := \text{tr}(M'M) = \text{tr}(MM') = \sum_{i=1}^{n} \sum_{j=1}^{m} |m_{ij}|^2$

$\text{diag}\{M_i\}$ block-diagonal matrix with M_i on its diagonal, i.e. $\text{diag}\{M_i\} := \begin{bmatrix} M_1 & & 0 \\ & \ddots & \\ 0 & & M_k \end{bmatrix}$

- -

$\text{sign}\, a$ sign of $a \in \mathbb{R}$, i.e. $\text{sign}\, a = 1$ if $a > 0$, $\text{sign}\, a = -1$ if $a < 0$, and $\text{sign}\, a = 0$ if $a = 0$

$\deg P(s)$ degree of a polynomial $P(s)$

lcf left coprime factorization over H_∞, like $G = \tilde{M}^{-1} \tilde{N}$

rcf right coprime factorization over H_∞, like $G = NM^{-1}$

$\mathcal{F}_\text{l}(G, R)$ lower linear fractional transformation, $\mathcal{F}_\text{l}(G, R) = G_{11} + G_{12} R (I - G_{22} R)^{-1} G_{21}$

$\mathcal{F}_\text{u}(G, R)$ upper linear fractional transformation, $\mathcal{F}_\text{u}(G, R) = G_{22} + G_{21} R (I - G_{11} R)^{-1} G_{12}$

$G \star \tilde{G}$ Redheffer star product, $G \star \tilde{G} = \begin{bmatrix} \mathcal{F}_\text{l}(G, \tilde{G}_{11}) & G_{12}(I - \tilde{G}_{11} G_{22})^{-1} \tilde{G}_{12} \\ \tilde{G}_{21}(I - G_{22} \tilde{G}_{11})^{-1} G_{21} & \mathcal{F}_\text{u}(\tilde{G}, G_{22}) \end{bmatrix}$

Chapter 1

Systems with Time Delays

$\mathbf{L}$ ATENCY is an intrinsic part of mass and information transfer. After all, no mass / information can travel faster than the speed of light. Information processing takes time as well. Hence, every control system should take potential latency into account. This chapter introduces the *delay element*, which is the basic module describing latency, and discusses its fundamental properties, in both continuous and discrete times, and effects on finite-dimensional dynamics.

1.1 Delay elements and their dynamics

1.1.1 Delay in discrete time

Although we are mostly concerned with continuous-time systems, throughout this text we occasionally use their discrete-time counterparts to gain insight into underlying ideas. This is because the dynamics of the delay element are more conventional in discrete time, which facilitates grasping ideas without the need to dig into advanced mathematical notions.

With this logic in mind, we start with defining the discrete-time delay element as a system $\bar{D}_\tau : u \mapsto y$, acting as

$$y[t] = u[t - \tau] \qquad \text{i.e.} \qquad \boxed{\bar{D}_\tau} \tag{1.1}$$

for some $\tau \in \mathbb{N}$, called the *delay*, and *all* $u : \mathbb{Z}_+ \to \mathbb{R}^m$. This is an ordinary linear shift-invariant (LSI) causal system, whose impulse response $d_\tau[t] = \delta[t - \tau]I_m$ and the (τm)-order transfer function, which is the z-transform of d_τ,

$$\bar{D}_\tau(z) = \frac{1}{z^\tau} I_m = \left[\begin{array}{cccc|c} 0 & I_m & \cdots & 0 & 0 \\ \vdots & \vdots & \ddots & \vdots & \vdots \\ 0 & 0 & \cdots & I_m & 0 \\ 0 & 0 & \cdots & 0 & I_m \\ \hline I_m & 0 & 0 & 0 & 0 \end{array} \right]. \tag{1.2}$$

The chosen state-space realization above is in the canonical companion form and is one of many possibilities, of course. Another route to end up with this realization is to construct the state vector of $\bar{D}_\tau$ first. This can be done via the interpretation of the state vector as a memory accumulator. It is readily seen that given an arbitrary time instance $t \geq 0$, the knowledge of $u[t + s]$ for all $s \in \mathbb{Z}_{-\tau..-1}$ is what we need to determine the present and future values of y given the inputs from t on. The (τm)-dimensional vector

$$x[t] := \begin{bmatrix} u[t - \tau] \\ \vdots \\ u[t - 1] \end{bmatrix} \tag{1.3}$$

1

is thus a logical candidate for the state vector of $\bar{D}_\tau$. Under this choice, the state propagation equation becomes

$$
\bar{D}_\tau : \begin{cases}
x[t+1] = \begin{bmatrix} 0 & I_m & \cdots & 0 \\ \vdots & \vdots & \ddots & \vdots \\ 0 & 0 & \cdots & I_m \\ 0 & 0 & \cdots & 0 \end{bmatrix} x[t] + \begin{bmatrix} 0 \\ \vdots \\ 0 \\ I_m \end{bmatrix} u[t] \\
y[t] = \begin{bmatrix} I_m & 0 & \cdots & 0 \end{bmatrix} x[t]
\end{cases}
\tag{1.4}
$$

and agrees with (1.2). As a matter of fact, the observability matrix of this realization equals $I_{\tau m}$ and its controllability matrix is the block-exchange matrix with m-dimensional blocks. Hence, realization (1.4) is minimal. If the delay element is not assumed to be in its zero equilibrium at $t = 0$, a nonzero initial condition $x[0]$, which is the history of its inputs in $\mathbb{Z}_{-\tau..-1}$, can be introduced.

The delay element $\bar{D}_\tau$ is $\ell_2(\mathbb{Z}_+)$-stable. This follows by the fact that all poles of its transfer function in (1.2) are at the origin, i.e. in the open unit disk $\mathbb{D}$. Another way to see that is via the readily verifiable relation $\|\bar{D}_\tau u\|_2 = \|u\|_2$, which holds for all $u \in \ell_2(\mathbb{Z}_+)$.

Remark 1.1 (varying delays). A natural generalization of $\bar{D}_\tau$ is the varying delay element $\bar{D}_{\tau[t]}$, which acts as $y[t] = u[t - \tau[t]]$ for a function $\tau[t] \geq 0$. This system is substantially knottier than the constant delay element, even its dimension varies from step to step. Another, somewhat surprising, fact is that $\bar{D}_{\tau[t]}$ might be $\ell_2(\mathbb{Z}_+)$-unstable for some $\tau[t]$. For example, if $\tau[t] = t$, then we have that $y[t] = u[0]$ for all $t \in \mathbb{Z}_+$. So the choice of $u[t] = \delta[t]$, which is an $\ell_2(\mathbb{Z}_+)$-signal, results in $y[t] = \mathbb{1}[t]$, which is not. Yet it can be shown that $\bar{D}_{\tau[t]}$ is $\ell_2(\mathbb{Z}_+)$-stable if $\tau[t]$ is uniformly bounded, say by $\bar{\tau} \in \mathbb{N}$, with its induced norm upperbounded by $\sqrt{1 + \bar{\tau}} > 1$ then. ∇

1.1.2   Delay in continuous time

The continuous-time delay element $\bar{D}_\tau : u \mapsto y$ is similar to its discrete-time counterpart from (1.1). It is defined as

$$
y(t) = u(t - \tau) \qquad \text{i.e.} \qquad \tag{1.5}
$$

for some constant delay $\tau > 0$ and all $u : \mathbb{R}_+ \to \mathbb{R}^m$. The similarity is not complete though. System (1.5) is more complex than that in (1.1), chiefly because the former is *infinite dimensional*.

Remember that the dimension of a dynamic system is the size of its minimal possible state vector, its smallest history accumulator. For the system in (1.5) the history, required to continue from a given time point $t_c \geq 0$, is clearly the whole trajectory of u in the time interval $[t_c - \tau, t_c]$. Indeed, this is exactly what we need to calculate $y(t)$ for $t \in [t_c, t_c + \tau]$. In other words, given an arbitrary time instance $t \geq 0$, we have to know the function $\breve{u}_t : [-\tau, 0] \to \mathbb{R}^m$ such that

$$
\breve{u}_t(s) = u(t + s), \quad \forall s \in [-\tau, 0],
\tag{1.6}
$$

to determine the present and future values of y given the inputs from t on. This is a perfect analogy with the discrete delay. Yet there is a qualitative difference between the discrete- and continuous-time cases. The set of all discrete m-dimensional functions over the finite interval $\mathbb{Z}_{-\tau..-1}$ is a finite-dimensional linear space, after all it is equivalent to the set of all τm-dimensional vectors, cf. (1.3). Unlike this, the set of all continuous-time functions over the finite interval $[-\tau, 0]$ is an infinite-dimensional linear space, because the number of linearly independent functions is unbounded there[1]. Hence, the continuous-time $\bar{D}_\tau$ in (1.5) is an infinite-dimensional system. Its state is $\breve{u}_t$ defined by (1.6). But writing down corresponding state equations would require advanced technical tools, which goes beyond the scope of these notes.

---

[1]For example, the functions $f_i(t) := e^{j2\pi i t / \tau}$ are linearly independent for all $i \in \mathbb{Z}_+$.

(a) Bode plot   (b) Nyquist plot   (c) Nichols chart
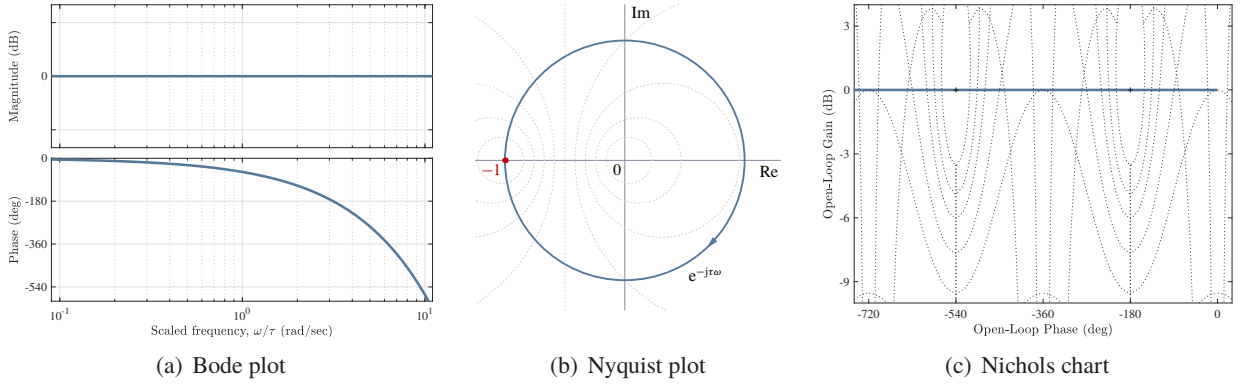
Fig. 1.1: Frequency response plots of the continuous-time delay element

If not stated otherwise, we assume that the initial conditions for (1.5) are zero, i.e. $\check{u}_0 = 0$. In this case $\bar{D}_\tau$ actually equals the shift operator S_τ defines by (B.2). The delay element is *LTI and stable*. Indeed,

$$[\bar{D}_\tau(\alpha u + \beta v)](t) = (\alpha u + \beta v)(t - \tau) = \alpha u(t - \tau) + \beta v(t - \tau) = \alpha(\bar{D}_\tau u)(t) + \beta(\bar{D}_\tau v)(t)$$

for all constants α and β and inputs u and v, which implies linearity. Because $\bar{D}_\tau S_\theta = S_{\tau+\theta} = S_\theta \bar{D}_\tau$, we have time invariance. And $L_2(\mathbb{R}_+)$-stability follows, similarly to the discrete-time case, from the fact that $\|\bar{D}_\tau u\|_2 = \|u\|_2$ for all $u \in L_2(\mathbb{R}_+)$. The delay element is obviously causal and its impulse response is

$$d_\tau(t) = \delta(t - \tau)I_m,$$

where m is the dimension of $u(t)$ and $y(t)$. Thus, $\bar{D}_\tau$ can be analyzed in transformed domains, like Fourier and Laplace.

The transfer function of $\bar{D}_\tau$ is

$$\bar{D}_\tau(s) := \mathcal{L}\{d_\tau\} = \mathrm{e}^{-\tau s} I_m. \tag{1.7}$$

It is a *non-rational* function of s, which is yet another indication that the continuous-time delay element is an infinite-dimensional system. The function $\mathrm{e}^{-\tau s}$ is an entire function of s (i.e. holomorphic in the whole $\mathbb{C}$). It is also bounded in every right-half plane $\mathbb{C}_\alpha := \{s \in \mathbb{C} \mid \mathrm{Re}\, s > \alpha\}$, as $|\mathrm{e}^{-\tau s}| < \mathrm{e}^{-\tau \alpha}$ for all $s \in \mathbb{C}_\alpha$ and $\tau > 0$. Hence, the transfer function $\bar{D}_\tau \in H_\infty$, which is the set of all holomorphic and bounded functions in $\mathbb{C}_0$. This is yet another proof that the continuous-time delay element is L_2-stable and causal.

The frequency response of the delay element is

$$\bar{D}_\tau(\mathrm{j}\omega) := \mathfrak{F}\{d_\tau\} = \mathrm{e}^{-\mathrm{j}\tau\omega} I_m. \tag{1.8}$$

In the scalar case, $m = 1$, its magnitude and phase are quite simple:

$$|\bar{D}_\tau(\mathrm{j}\omega)| = 1 \quad \text{and} \quad \arg \bar{D}_\tau(\mathrm{j}\omega) = -\tau\omega. \tag{1.9}$$

Thus, the frequency response magnitude of the delay element is unit for all frequencies and its phase is a linearly decreasing function of ω, i.e. the delay element adds a phase lag growing linearly with the frequency. The Bode, Nyquist, and Nichols plots of $\bar{D}_\tau$ are presented in Fig. 1.1. Expressions (1.9) facilitate the analysis of time-delay systems in the frequency domain, making it in some cases rather intuitive and substantially simpler than the analysis in the time domain.

Remark 1.2 (varying delays). Like in the discrete-time case, we can generalize $\bar{D}_\tau$ as the varying delay element $\bar{D}_{\tau(t)}$, which acts as $y(t) = u(t - \tau(t))$ for some function $\tau(t) \geq 0$. Curiously, this system might be $L_2(\mathbb{R}_+)$-unstable even if $|\tau(t)| \leq \bar{\tau}$ for all $t \in \mathbb{R}_+$ and an arbitrary upper bound $\bar{\tau} > 0$ (consider finding an example of such a delay function as a homework assignment). A yet more general situation is if the delay depends not only on time, but also on its input, so that $y(t) = u(t - \tau(t, u(t)))$. Such a delay element, $\bar{D}_{\tau(t),u}$, is nonlinear and its properties are yet more involved. ∇

(a) Sensing in rolling mill   (b) Actuating via conveyor belt
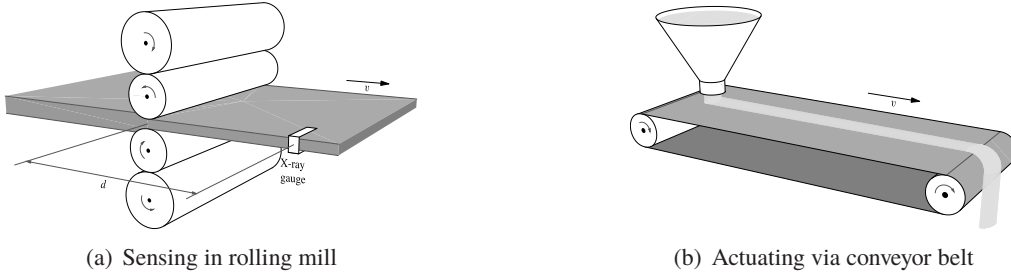
Fig. 1.2: Examples of systems with sensing and actuating delays

1.2 Interactions of delays with other dynamics

One seldom faces processes containing the delay element alone. In most situations delays interact with other dynamic processes. In this section some of such interactions are studied. For the sake of simplicity, we mostly consider systems with a single and constant delay, which simplifies their analysis. Remarks on multiple-delay systems and time-varying delays will be provided mostly to highlight potential differences.

1.2.1 Input and output delays

Arguably, the principal source of delays in feedback control applications are delays arising in the "control pass," i.e. in transferring information between the sensor and the actuator ends of the controller. These are

sensing delays, like that in measuring the thickness of a metal strip in rolling mills, see Fig. 1.2(a), where X-ray gauge measurements are on a distance, say d, from the roll gap and have access to measurements only $\tau = d/v$ time units after the rolls, where v is the velocity of the exist strip;

actuation delays, like that in the conveyor belt in Fig. 1.2(b), where a material through which some process is affected can reach the process only after $\tau = l/v$ time units after injecting into the system, where l is the length of the conveyor pass and v is its velocity;

communication delays, which are more and more common in light of the trend to distribute information acquisition and processing, with the use of communication networks to exchange local information between various components of control systems;

computational delays, which are inevitable if controllers are implemented on digital computers;

et cetera. From the plant modeling viewpoint, such delays can be viewed as input and / or output delays, that is delays connected in series with a controlled plant. A good collection of examples of systems with input / output delays arising in various, mostly process control, applications can be found in [53].

Let a plant P be LTI and input and output delays be uniform, say all input channels are delayed by the same $\tau_u \geq 0$ and all output channels are delayed the same by $\tau_y \geq 0$. This yields $\bar{D}_{\tau_y} P \bar{D}_{\tau_u}$ as the new plant. By the very time invariance, $\bar{D}_{\tau_y} P \bar{D}_{\tau_u} = P \bar{D}_{\tau_y + \tau_u}$, meaning that without loss of generality we may regard such systems as input delay systems $P\bar{D}_\tau$ with the transfer function

$$P_\tau(s) = P(s)\mathrm{e}^{-\tau s}, \tag{1.10}$$

where $\tau = \tau_y + \tau_u$. Systems of form (1.10) are known as *dead-time systems*.

Although P_τ is infinite dimensional, its properties are relatively intuitive. The impulse response of P_τ is $p_\tau(t) = p(t - \tau)$, by definition, with support in $[\tau, \infty)$. The addition of the delay element does not alter stability properties of the delay-free P. As $\mathrm{e}^{-\tau s}$ is an H_∞ function, it does not add any instability. In fact, it does not introduce additional poles, because it is entire. Moreover, $\mathrm{e}^{-\tau s} \neq 0$ for all $s \in \mathbb{C}$, so it cannot cancel poles of $P(s)$.

(a) Bode plot (b) Nyquist plot (c) Nichols chart
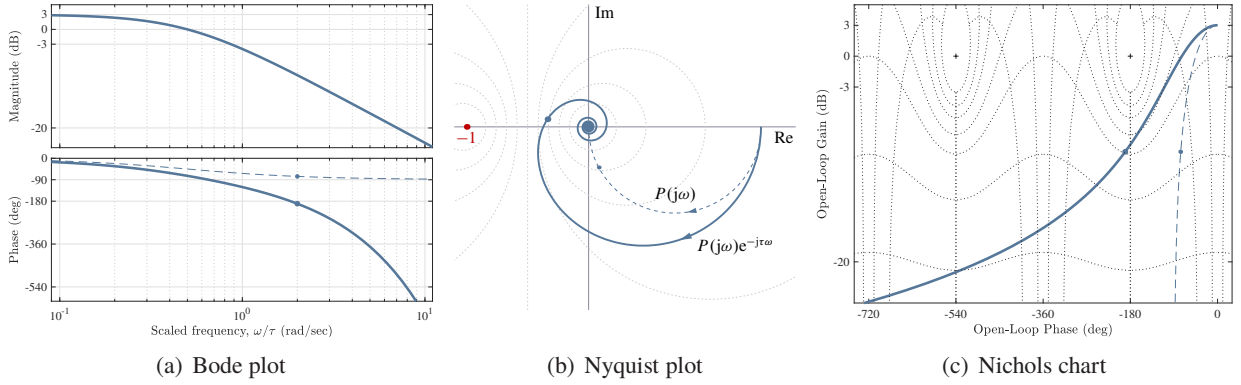
Fig. 1.3: Frequency response plots of $P(s) = \sqrt{2}/(2\tau s + 1)$ (dashed) and $P_\tau(s) = P(s)e^{-\tau s}$ (solid)

To gain insight into the state space structure of P_τ, consider its discrete-time counterpart, whose transfer function is $P_\tau(z) = P(z)z^{-\tau}$. This is a finite-dimensional system, provided of course P is finite dimensional itself, and its state-space realization can be derived from those of $P(z) = D + C(zI - A)^{-1}B$ and the discrete delay element in (1.2) using (B.25) on p. 169:

$$
P_\tau(z) = \left[\begin{array}{c|c} A & B \\ \hline C & D \end{array} \right]
\begin{bmatrix}
0 & I_m & \cdots & 0 & 0 \\
\vdots & \vdots & \ddots & \vdots & \vdots \\
0 & 0 & \cdots & I_m & 0 \\
0 & 0 & \cdots & 0 & I_m \\
\hline
I_m & 0 & 0 & 0 & 0
\end{bmatrix}
=
\left[\begin{array}{cc|ccc|c}
A & B & 0 & \cdots & 0 & 0 \\
\hdashline
0 & 0 & I_m & \cdots & 0 & 0 \\
\vdots & \vdots & \vdots & \ddots & \vdots & \vdots \\
0 & 0 & 0 & \cdots & I_m & 0 \\
0 & 0 & 0 & \cdots & 0 & I_m \\
\hline
C & D & 0 & 0 & 0 & 0
\end{array} \right].
\tag{1.11}
$$

The state vector of this system is the union of states of its components and includes thus both the state of P and the history of the input signal over the last τ steps, cf. (1.3). Following this logic, the state of the continuous-time input-delay system P_τ, with the transfer function as in (1.10), at a time instance t is $(x_P(t), \check{u}_t) \in \mathbb{R}^n \times \{[-\tau, 0] \to \mathbb{R}^m\}$, i.e. it comprises both the state x_P of the delay-free P and the history of the input signal over the time interval $[t - \tau, t]$. The space of all such states is infinite dimensional.

In the SISO case the frequency response of P_τ can be easily derived from that of P. It follows from (1.9) that

$$
|P_\tau(j\omega)| = |P(j\omega)| \quad \text{and} \quad \arg P_\tau(j\omega) = \arg P(j\omega) - \tau\omega.
\tag{1.12}
$$

In other words, the addition of the delay element does not alter the magnitude and adds extra phase lag, proportional to the frequency. These properties facilitate the construction of frequency-response plots of input-delay systems from those of their delay-free versions, see Fig. 1.3. Specifically, the Bode magnitude plot remains unchanged and its phase part shifts downward by $\tau\omega$ as shown in Fig. 1.3(a). Each point of the Nyquist plot of $P(j\omega)$ rotates clockwise, with the rotation angle increasing with the frequency. This normally results in spiral curves, like that in Fig. 1.3(b). Each point of the Nichols plot shifts leftward, see Fig. 1.3(c), by a distance increasing with the frequency.

Remark 1.3 (multiple delays). It may happen that different input and / or output channels of P have different delays. For example, if a thickness profile of the strip in the rolling mill system in Fig. 1.2(a) is controlled, then several points at different depths of the strip should be measured. Such sensors are normally located at different distances from the roll gap as well, causing different measurement delays. General multiple input and output delays can be described in the block-diagonal form $\mathrm{diag}\{\bar{D}_{\tau_{u,i}}\}$ and $\mathrm{diag}\{\bar{D}_{\tau_{y,i}}\}$, respectively, for some $\tau_{u,i} \geq 0$ and $\tau_{y,i} \geq 0$ and all relevant channel indices i. Such delay elements are still stable and do not alter stability properties and pole locations of the plant. At the same time, diagonal delays no

longer commute with the plant, unless the latter is block-diagonal itself. This non-trivially complicates the analysis of such systems.   ▽

Remark 1.4 (distributed delays). A yet more general description of the interconnection of delays and other dynamics is in the *distributed-delay*. An example of such a delay element is the system $u \mapsto y$ acting as

$$y(t) = \int_0^\tau \alpha(s)u(t-s)\,\mathrm{d}s = \int_{t-\tau}^t \alpha(t-s)u(s)\,\mathrm{d}s \tag{1.13}$$

for some (generalized) function $\alpha : [0, \tau] \to \mathbb{R}^{q \times m}$. This definition appears natural, as the integral can be seen as a weighted sum of delays in the range $[0, \tau]$ and standard lumped delays can be produced by Dirac delta components of α. However, this definition is also somewhat confusing. Indeed, by this logic any causal convolution as in (B.3) is a distributed-delay system. For example, think of the case where $\tau \to \infty$ and $\alpha(t) = \mathrm{e}^{-at}\mathbb{1}(t)$ for some $a > 0$. This yields ordinary first-order dynamics, whose treatment as a distributed-delay system would only complicate matters. Therefore, the term "distributed delay" is barely used throughout this text. When a system of form (1.13) with a finite τ arises, it is referred to as an FIR (finite impulse response) system. This is because (1.13) is a convolution representation of an LTI system, whose impulse response has support over a finite time interval $[0, \tau]$.   ▽

Remark 1.5 (varying delays). It may be safe to claim that constant lags are not widespread in applications. For example, if the strip velocity in the rolling mill system in Fig. 1.2(a) / the belt velocity in the conveyor actuator in Fig. 1.2(b) varies, then the corresponding measurement / actuation delay varies with time. In many cases such variations are small, so a constant-delay assumption is adequate. Still, there are applications, like networked control, where delay variations cannot be neglected. Properties of systems with time-varying delays might be less intuitive than those with constant delays. As an illustration, note that

$$\int_{\mathbb{R}_+} p(t-s)u(s-\tau(s))\,\mathrm{d}s \neq \int_{\mathbb{R}_+} p(t-\tau(t)-s)u(s)\,\mathrm{d}s$$

in general. Hence, the effect of an input delay $\tau(t)$ is not equivalent to that of the same output delay and vice versa. In fact, it might even happen that there is no equivalent output delay for a given non-constant input delay. Such issues render the analysis of systems with varying delays substantially more involved than that of systems with constant delays.   ▽

Delays as a compact modeling tool

In some situations input delays are used as a convenient modeling tool to represent high-order dynamics in a concise manner, with fewer parameters. Typical examples, omnipresent in process control, are first-order-plus-time-delay (FOPTD) and second-order-plus-time-delay (SOPTD) models, which comprise first- or second-order dynamics connected in series with a delay element. Such models are sufficiently rich to reflect complex dynamical phenomena with monotonic responses, while have only three or four parameters, viz. the static gain, time constant(s), and the delay, to identify.

To provide a flavor of this approach, consider a plant P_n with the transfer function of the form

$$P_n(s) = \frac{1}{(s+1)^n}$$

for a large enough $n \in \mathbb{N}$. This kind of model can describe n identical tanks, modeled as "flow $\mapsto$ level" systems, connected in series; a queue of n vehicles, modeled as integrators ("velocity $\mapsto$ position") and whose control signals are proportional to the position mismatch between the current and the next vehicle; et cetera. The frequency response of such a system has monotonically decreasing gain and phase, with a large phase lag at high frequencies. It can then be beneficial to approximate these dynamics by lower-order

(a) $n = 5$ (b) $n = 8$
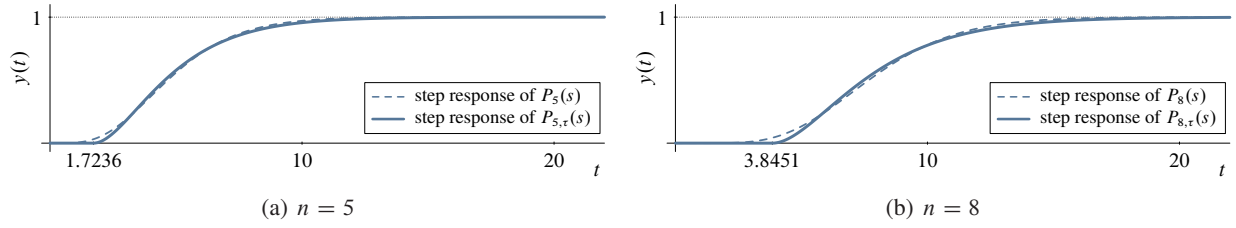
Fig. 1.4: Step response of P_n and its second-order-plus-time-delay (SOPTD) approximation $\tilde{P}_n$

ones connected in series with a delay element to account for the high-frequency phase lag. For example, for $n = 5$ and $n = 8$ the SOPTD approximations

$$P_{5,\tau}(s) = \frac{e^{-1.7236s}}{(1.6875s + 1)^2} \quad \text{and} \quad P_{8,\tau}(s) = \frac{e^{-3.8451s}}{(2.1626s + 1)^2}$$

fit the step responses of the plant reasonably well, see Fig. 1.4.

1.2.2   Internal delays

In some systems delays arise not as a result of control path latency, but rather in connection with internal interactions. To illustrate this phenomenon, consider a process described by the one-dimensional wave equation

$$\frac{\partial^2 w(x,t)}{\partial t^2} = c^2 \frac{\partial^2 w(x,t)}{\partial x^2} \quad \text{for } 0 < x < L \text{ and } t \geq 0, \tag{1.14}$$

where w is a physical variable of interest evolving both in time t and in space x, $c > 0$ is the speed of wave propagation in the medium, and $L > 0$ is the medium length. This kind of equations can describe a number of processes propagating in one-dimensional media, like acoustic waves in a duct, vibrations of a string, torsion of a rod, electrical transmission lines, et cetera. They vary in the nature of their excitation and interaction with the surrounding environment, which may be lumped (i.e. via boundary conditions) or distributed. Throughout this section we assume the former kind, which is simpler, of a type motivated by acoustic waves in a cylindrical duct, see [9] and the references therein for details. In this case $\partial w/\partial t$ and $-\rho_0 c^2 \partial w/\partial x$, where ρ_0 is the air density, are the velocity and pressure of the air in a duct.

Assume that the system is excited only at $x = 0$ via the boundary condition

$$\frac{\partial w(0,t)}{\partial t} = u(t) \tag{1.15}$$

for some exogenous signal u. Assume also that the other end, that at $x = L$, is passively connected to the environment and the interaction of waves in the medium with its surrounding at $x = L$ is characterized as

$$-cZ_m \frac{\partial w(x,t)}{\partial x}\bigg|_{x=L} = Z_L \frac{\partial w(L,t)}{\partial t} \tag{1.16}$$

for some end *impedance* operator Z_L, where $Z_m = \rho_0 c > 0$ is the impedance of the free propagation in the medium. The zero boundary impedance, $Z_L = 0$, corresponds to an open duct, for which the end pressure is zero. The infinite impedance $Z_L = \infty$ implies that the velocity at the end is zero, which may correspond to a sealed duct. The waves simply reflect in this case. If $Z_L = Z_m$, then we effectively have a semi-infinite duct, with waves totally transmitted. The end impedance need not be constant. In more realistic models Z_L is a dynamic system, frequently LTI, whose transfer function is positive real, i.e. such that $Z_L(s) \geq 0$ for all $s \in \bar{\mathbb{C}}_0$. It is not uncommon to have $Z_L(0) = 0$ and $Z_L(\infty) = Z_m$.

(a) $Z_L(s) = s/(s+1)$ and $R(s) = -1/(2s+1)$ (b) $Z_L(s) = 0$ and $R(s) = -1$
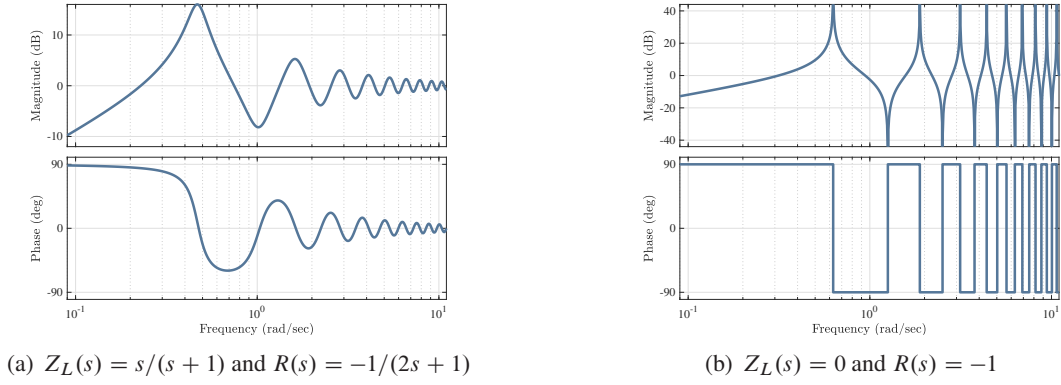
Fig. 1.5: Bode plots of $G_0(s)$ from (1.19) for $Z_m = 1$ and $\tau = 5$

The relation between u and w can be derived by taking the Laplace transform of (1.14) with respect to t, which results in the ordinary differential equation $c^2 \partial_x^2 W(x,s) = s^2 W(x,s)$ with the boundary conditions $sW(0,s) = U(s)$ and $sZ_L(s)W(L,s) + cZ_m\partial_x W(L,s) = 0$, where $\partial_x f := \partial f/\partial x$ and $\partial_x^2 f := \partial^2 f/\partial x^2$. The solution to this ODE is

$$\begin{bmatrix} W(x,s) \\ \partial_x W(x,s) \end{bmatrix} = \exp\left(\begin{bmatrix} 0 & 1 \\ s^2/c^2 & 0 \end{bmatrix} x\right) \begin{bmatrix} W(0,s) \\ \partial_x W(0,s) \end{bmatrix} = \begin{bmatrix} \cosh(sx/c)/s & c\sinh(sx/c)/s \\ \sinh(sx/c)/c & \cosh(sx/c) \end{bmatrix} \begin{bmatrix} U(s) \\ \partial_x W(0,s) \end{bmatrix},$$

where $\partial_x f(0,t)$ is meant for $\partial_x f(x,t)|_{x=0}$. The second boundary condition reads then

$$\begin{bmatrix} sZ_L(s) & cZ_m \end{bmatrix} \begin{bmatrix} \cosh(sL/c)/s & c\sinh(sL/c)/s \\ \sinh(sL/c)/c & \cosh(sL/c) \end{bmatrix} \begin{bmatrix} U(s) \\ \partial_x W(0,s) \end{bmatrix} = 0,$$

which is solved by $c\partial_x W(0,s) = V_0(s)U(s)$, where

$$V_0(s) := -\frac{1 + R(s)e^{-2(L/c)s}}{1 - R(s)e^{-2(L/c)s}} \quad \text{for } R(s) := \frac{Z_L(s) - Z_m}{Z_L(s) + Z_m}. \tag{1.17}$$

The parameter $R(s)$ is known the *reflectance* of the system at its end. If $Z_L(s)$ is positive real, then we have that $|R(s)| \le 1$ for all $s \in \bar{\mathbb{C}}_0$ and the equality holds iff $Z_L(s) = 0$ (think of it as Tustin's transform of $-Z_L/Z_m$). This is an important property of the considered system. Thus, we have that

$$\begin{bmatrix} sW(x,s) \\ c\partial_x W(x,s) \end{bmatrix} = \begin{bmatrix} \cosh(sx/c) & \sinh(sx/c) \\ \sinh(sx/c) & \cosh(sx/c) \end{bmatrix} \begin{bmatrix} 1 \\ V_0(s) \end{bmatrix} U(s). \tag{1.18}$$

If we are interested in the effect of u on the pressure $p_x = -cZ_m\partial_x w$ at the very point $x = 0$ of its application, then the transfer function of the system $G_0 : u \mapsto p_0$ is

$$G_0(s) = -V_0(s)Z_m = \frac{1 + R(s)e^{-\tau s}}{1 - R(s)e^{-\tau s}} Z_m, \tag{1.19}$$

where $\tau := 2L/c > 0$ is the time that takes a wave to travel to the end of the medium and back. This transfer function includes a delay element as its internal part, which renders $G_0(s)$ substantially more tangled than R. It might not be easy even to derive a closed-form impulse response of this system. This is possible in some special cases, for example for $R(s) = -1$ the impulse response is the impulse train $g_0(t) = \delta(t) - 2\delta(t - \tau) + 2\delta(t - 2\tau) - 2\delta(t - 3\tau) + \cdots$, cf. (B.4). Also, the Bode plots of the frequency-response $G_0(j\omega)$, shown in Fig. 1.5 for two different simple $R(s)$, exhibit a rich behavior, with numerous resonances, even though only a few parameters are required to model this system. Moreover, not for every
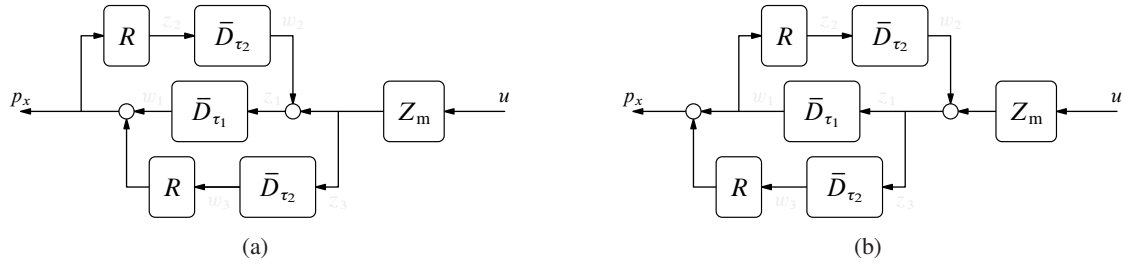
Fig. 1.6: Block-diagrams of G_x, whose transfer function is given by (1.21)

stable R this G_0 is stable. For example, the system with $R(s) = -1$, whose frequency response is depicted in Fig. 1.5(b), is unstable (stability issues in delay systems are discussed in Chapter 2).

Another complication is the location of poles of $G_0(s)$. They are among the roots of the function

$$\chi_\tau(s) = M_R(s) - N_R(s)\mathrm{e}^{-\tau s}, \tag{1.20}$$

where $N_R(s)$ and $M_R(s)$ the numerator and denominator polynomials of $R(s)$, assuming the latter is rational. This $\chi_\tau(s)$ is not a polynomial in s as it contains the transcendental term $\mathrm{e}^{-\tau s}$. Such functions are known as *quasi-polynomials*. In order to provide a flavor of difficulties associated with analyzing its roots, consider two simple cases with reflectances from Fig. 1.5. For $R(s) = -1$ we have $\chi_\tau(s) = 1 + \mathrm{e}^{-\tau s}$ and every $s_i = \mathrm{j}(2i + 1)\pi/\tau$, $i \in \mathbb{Z}$, as its root. In other words, this $\chi_\tau(s)$ has infinitely many roots. This is typical to quasi-polynomials. Not quite typical is the possibility to have these roots analytically. In fact, this possibility is essentially limited to the case when both $N_R(s)$ and $M_R(s)$ are constants. For example, if $R(s) = -1/(2s + 1)$, as in Fig. 1.5(a), then (1.20) reads $\chi_\tau(s) = 2s + 1 + \mathrm{e}^{-\tau s}$ and its roots cannot be expressed analytically. Nevertheless, some of its modal properties can be analyzed. For example, because the equality $|2s + 1| = |\mathrm{e}^{-\tau s}|$ must hold true at every root of this $\chi_\tau(s)$, we can conclude there are no roots in the closed right-half plane $\overline{\mathbb{C}}_0$. This is because $|2s + 1| > 1$ at all points there except the origin, whereas $|\mathrm{e}^{-\tau s}| \leq 1$ for $s \in \overline{\mathbb{C}}_0$. A simple check yields then that $\chi_\tau(0) = 2 \neq 0$ in this case. More details about properties of quasi-polynomials are presented in Section 2.1.

Yet more complex dynamics connect the exogenous input u with the pressure p_x at internal points $x \in (0, L)$. The transfer function of the system $G_x : u \mapsto p_x$, which is derived from (1.18), is

$$G_x(s) = \frac{\mathrm{e}^{-\tau_1 s} + R(s)\mathrm{e}^{-\tau_2 s}}{1 - R(s)\mathrm{e}^{-(\tau_1 + \tau_2)s}} Z_\mathrm{m}, \tag{1.21}$$

where $\tau_1 := x/c$ and $\tau_2 := (2L - x)/c$ are the times that take the original and reflected wave to reach the given x. Two alternative block-diagram representations of this system are presented in Fig. 1.6. Note that if the reflectance is zero, $R(s) = 0$, implying that the end impedance matches that of medium, then this system reduces to the scaled delay element $\bar{D}_{\tau_1} Z_\mathrm{m}$.

1.2.3 General interconnections

In light of the proliferation of interconnection configurations of the delay element(s) with finite-dimensional dynamics, it may be convenient to have a unified representation of systems involving delays. A possible choice for such a representation is presented in Fig. 1.7, where $\bar{D}_\tau$ is the $m_\tau \times m_\tau$ delay element and

$$G = \begin{bmatrix} G_{zw} & G_{zu} \\ G_{yw} & G_{yu} \end{bmatrix}$$
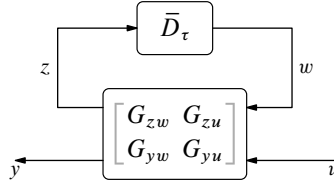
Fig. 1.7: General single-delay interconnection for $P_\tau : u \mapsto y$

is a finite-dimensional, i.e. delay-free, system. This is an upper linear-fractional transformation $\mathcal{F}_u(G, \bar{D}_\tau)$ of the type discussed in §A.3. It defines the system (plant)

$$P_\tau = \mathcal{F}_u(G, \bar{D}_\tau) = G_{yu} + G_{yw} \bar{D}_\tau (I - G_{zw} \bar{D}_\tau)^{-1} G_{zu}.$$

All single-delay systems studied so far can be viewed as particular cases of this setup for an appropriate choice of G. The dead-time system as in (1.10) corresponds to

$$G = G_{\text{inpd}} := \begin{bmatrix} 0 & I \\ P & 0 \end{bmatrix} \tag{1.22}$$

and the wave equation with the transfer function (1.19) corresponds to

$$G = G_{\text{wave},0} := \begin{bmatrix} R & Z_{\text{m}} \\ 2R & Z_{\text{m}} \end{bmatrix}. \tag{1.23}$$

Note that having a nilpotent "G_{zw}" part implies that the dependence of P_τ on the delay is affine (or linear, if $D_{yu} = 0$ as well). The choice of G producing a given P_τ is actually non-unique. Because $\bar{D}_\tau M = M \bar{D}_\tau$ for every time-invariant M, systems can be moved from the "z" to "w" channel without affecting the operator P_τ. In other words, if there is a multiplier M such that $G_{zw} = \tilde{G}_{zw} M$ and $G_{yw} = \tilde{G}_{yw} M$, then

$$G = \begin{bmatrix} \tilde{G}_{zw} & G_{zu} \\ \tilde{G}_{yw} & G_{yu} \end{bmatrix} \begin{bmatrix} M & 0 \\ 0 & I \end{bmatrix} \quad \leftrightarrow \quad \begin{bmatrix} M & 0 \\ 0 & I \end{bmatrix} \begin{bmatrix} \tilde{G}_{zw} & G_{zu} \\ \tilde{G}_{yw} & G_{yu} \end{bmatrix} =: \tilde{G}$$

and thus

$$\begin{aligned} \mathcal{F}_u(G, \bar{D}_\tau) &= \mathcal{F}_u\left(\begin{bmatrix} \tilde{G}_{zw} & G_{zu} \\ \tilde{G}_{yw} & G_{yu} \end{bmatrix} \begin{bmatrix} M & 0 \\ 0 & I \end{bmatrix}, \bar{D}_\tau \right) = \mathcal{F}_u\left(\begin{bmatrix} \tilde{G}_{zw} & G_{zu} \\ \tilde{G}_{yw} & G_{yu} \end{bmatrix}, M \bar{D}_\tau \right) \\ &= \mathcal{F}_u\left(\begin{bmatrix} \tilde{G}_{zw} & G_{zu} \\ \tilde{G}_{yw} & G_{yu} \end{bmatrix}, \bar{D}_\tau M \right) = \mathcal{F}_u\left(\begin{bmatrix} M & 0 \\ 0 & I \end{bmatrix} \begin{bmatrix} \tilde{G}_{zw} & G_{zu} \\ \tilde{G}_{yw} & G_{yu} \end{bmatrix}, \bar{D}_\tau \right) \\ &= \mathcal{F}_u(\tilde{G}, \bar{D}_\tau) \end{aligned}$$

regardless of M. This transformation can always be carried out for a square and nonsingular M. In some situations it is also possible to use non-invertible and even non-square multiplies, which might help in reducing problem dimensions as is seen in the example below.

Example 1.1. Let
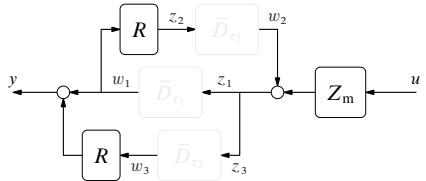
$$G(s) = \left[\begin{array}{cc|cc|c} 0 & 1 & 1 & 1 & 0 \\ 0 & 0 & 1 & 1 & 1 \\ \hline 1 & 0 & 0 & 0 & 0 \\ 0 & 1 & 0 & 0 & 0 \\ \hline 1 & 0 & 0 & 0 & 0 \end{array} \right] = \left[\begin{array}{cc|c|c} 0 & 1 & 1 & 0 \\ 0 & 0 & 1 & 1 \\ \hline 1 & 0 & 0 & 0 \\ 0 & 1 & 0 & 0 \\ \hline 1 & 0 & 0 & 0 \end{array} \right] \left[\begin{array}{cc|c} 1 & 1 & 0 \\ 0 & 0 & 1 \end{array} \right],$$

which interacts with a 2×2 delay element $\bar{D}_\tau$. Taking $M = \begin{bmatrix} 1 & 1 \end{bmatrix}$, the system can be equivalently generated by

$$\tilde{G}(s) = \left[\begin{array}{cc:c} 1 & 1 & 0 \\ \hdashline 0 & 0 & 1 \end{array}\right] \left[\begin{array}{cc:cc} 0 & 1 & 1 & 0 \\ 0 & 0 & 1 & 1 \\ \hline 1 & 0 & 0 & 0 \\ 0 & 1 & 0 & 0 \\ \hline 1 & 0 & 0 & 0 \end{array}\right] = \left[\begin{array}{cc:cc} 0 & 1 & 1 & 0 \\ 0 & 0 & 1 & 1 \\ \hdashline 1 & 1 & 0 & 0 \\ \hline 1 & 0 & 0 & 0 \end{array}\right]$$

interacting with a *scalar* delay, which is a more economical description. $\qquad \nabla$

Remark 1.6 (multiple delays). Systems with multiple delays can also be presented in the form of Fig. 1.7. It is only required to replace the single-delay operator $\bar{D}_\tau$ with its block-diagonal counterpart $\mathrm{diag}\{\bar{D}_{\tau_i}\}$. For instance, the wave equation with the transfer function (1.21) can be expressed in this form by removing all three delay blocks at the block-diagram in Fig. 1.6(b) and connecting the inputs (w_1, w_2, w_3, u) with the outputs (z_1, z_2, z_3, y) for $y = p_x$,

$$\Longrightarrow \qquad G = G_{\mathrm{wave},x} := \left[\begin{array}{ccc:c} 0 & 1 & 0 & Z_\mathrm{m} \\ R & 0 & 0 & 0 \\ 0 & 1 & 0 & Z_\mathrm{m} \\ \hdashline 1 & 0 & R & 0 \end{array}\right] \qquad (1.24)$$

and taking $\mathrm{diag}\{\bar{D}_{\tau_1}, \bar{D}_{\tau_2}\}$ as its delay element, where $\bar{D}_{\tau_1}$ is scalar and $\bar{D}_{\tau_2}$ is 2×2. $\qquad \nabla$

The separation of delay-free and delayed parts is conceptually appealing. It facilitates manipulating time-delay systems. For example, closing a feedback loop between y and u of the form

$$u = R(y + v)$$

for some delay-free "controller" R and a "reference signal" v results in the the same configuration, just now with a different, yet still delay-free, "G" part and v instead of u. For example, for a dead-time system with G as in (1.22) we end up with

$$G = G_{PR} := \begin{bmatrix} RP & R \\ P & 0 \end{bmatrix}, \qquad (1.25)$$

which can be verified by simple signal tracing ($z = R(y + v) = RPw + Rv$). This G_{PR} has a nonzero "G_{zw}" part, meaning that it is no longer a system with input delay. The separation in Fig. 1.7 is also convenient in numerical simulations (this is how delay systems are implemented in MATLAB, as a matter of fact), since standard tools can be used for the finite-dimensional part and all infinite-dimensionality is concentrated in the relatively simple pure delay element. For example, simulating $\mathcal{F}_\mathrm{u}(G_{\mathrm{wave},0}, \bar{D}_\tau)$ may be easier than that of the corresponding wave PDE.

The separation of the delay element from the delay-free dynamics also facilitates the use of convenient state-space machinery in analyzing time-delay systems. Bring in a *minimal* state-space realization of the transfer function

$$G(s) = \begin{bmatrix} G_{zw}(s) & G_{zu}(s) \\ G_{yw}(s) & G_{yu}(s) \end{bmatrix} = \left[\begin{array}{c:cc} A & B_w & B_u \\ \hline C_z & D_{zw} & D_{zu} \\ C_y & D_{yw} & D_{yu} \end{array}\right]. \qquad (1.26)$$

This transfer function defines the following time-domain relation:

$$G : \begin{cases} \dot{x}(t) = Ax(t) + B_w w(t) + B_u u(t) \\ z(t) = C_z x(t) + D_{zw} w(t) + D_{zu} u(t) \\ y(t) = C_y x(t) + D_{yw} w(t) + D_{yu} u(t) \end{cases}$$

These equations should be complemented by the delayed relation $w(t) = z(t - \tau)$, resulting in

$$P_\tau : \begin{cases} \begin{bmatrix} \dot{x}(t) \\ z(t) \end{bmatrix} = \begin{bmatrix} A & B_w \\ C_z & D_{zw} \end{bmatrix} \begin{bmatrix} x(t) \\ z(t - \tau) \end{bmatrix} + \begin{bmatrix} B_u \\ D_{zu} \end{bmatrix} u(t) \\ \\ y(t) = \begin{bmatrix} C_y & D_{yw} \end{bmatrix} \begin{bmatrix} x(t) \\ z(t - \tau) \end{bmatrix} + D_{yu} u(t) \end{cases} \tag{1.27}$$

describing the mapping $P_\tau : u \mapsto y$. Equations of this kind are known as *delay-differential equations* (DDEs), aka *differential-difference equation*, which are a subclass of *functional-differential equations*. The "x" part of its propagation is governed by a differential equation and the "z" part is governed by a delay (difference) equation. Equation (1.27) is a general single-delay DDE. Its state at every time instance $t \geq 0$ comprises the state $x(t)$ of G and the whole time history of z over the interval $[t - \tau, t]$ (c.f. the discussion in §1.1.2), i.e. it is $(x(t), \breve{z}_t) \in \mathbb{R}^n \times \{[-\tau, 0] \to \mathbb{R}^{m_\tau}\}$. The transfer function of P_τ is readily derived using standard properties of the Laplace transform and assuming zero history in $t \leq 0$:

$$P_\tau(s) = D_{yu} + \begin{bmatrix} C_y & D_{yw} e^{-\tau s} \end{bmatrix} \begin{bmatrix} sI - A & -B_w e^{-\tau s} \\ -C_z & I - D_{zw} e^{-\tau s} \end{bmatrix}^{-1} \begin{bmatrix} B_u \\ D_{zu} \end{bmatrix}. \tag{1.28}$$

Because $e^{-\tau s}$ vanishes as $\operatorname{Re} s \to \infty$, the matrix that is inverted in (1.28) has full normal rank and thus the inversion is well defined. The function $P_\tau(s)$ above is normally a non-rational function of s. Namely, each its element is a *quotient of quasi-polynomials* of a more general form than (1.20) (see §2.1.1 for details).

Remark 1.7. The transfer function (1.28) can be equivalently presented as

$$P_\tau(s) = D_{yu} + \begin{bmatrix} C_y & D_{yw} \end{bmatrix} \begin{bmatrix} sI - A & -B_w \\ -C_z & e^{\tau s} I - D_{zw} \end{bmatrix}^{-1} \begin{bmatrix} B_u \\ D_{zu} \end{bmatrix}, \tag{1.28$'$}$$

which is a more symmetric form of $P_\tau(s)$. However, it is conventional to use $e^{-\tau s}$ in transfer functions with delay elements and quasi-polynomials, so we proceed with (1.28). $\triangledown$

Form (1.27) of delay-differential equations in is not quite orthodox. Two its special cases frequently studied in the literature are presented below.

1. If $D_{zw} = 0$, then the second row of (1.27) reads $z(t) = C_z x(t) + D_{zu} u(t)$. Substituting this expression to the first row, we end up with the following dynamics:

$$\dot{x}(t) = Ax(t) + A_\tau x(t - \tau) + B_u u(t) + B_\tau u(t - \tau) \tag{1.29}$$

   for $A_\tau := B_w C_z$ and $B_\tau := B_w D_{zu}$. This is a conventional form of so-called (single-delay) *retarded* DDEs, in which the derivative term does not include delays. Note that its state at a time instance t is still $(x(t), \breve{z}_t) \in \mathbb{R}^n \times \{[-\tau, 0] \to \mathbb{R}^{m_\tau}\}$, rather than $(\breve{x}_t, \breve{u}_t) \in \{[-\tau, 0] \to \mathbb{R}^n\} \times \{[-\tau, 0] \to \mathbb{R}^m\}$.

2. If $D_{zw} \neq 0$, but there exists a square matrix E_τ such that $B_w D_{zw} = -E_\tau B_w$ (take the lowest rank E_τ satisfying it), then pre-multiplying the second row of (1.27) by B_w and using the first row we have:

$$\begin{aligned} B_w z(t) &= B_w C_z x(t) - E_\tau B_w z(t - \tau) + B_w D_{zu} u(t) \\ &= B_w C_z x(t) - E_\tau (\dot{x}(t) - Ax(t) - B_u u(t)) + B_w D_{zu} u(t). \end{aligned}$$

   Hence, we end up with the dynamical equation

$$\dot{x}(t) + E_\tau \dot{x}(t - \tau) = Ax(t) + A_\tau x(t - \tau) + B_u u(t) + B_\tau u(t - \tau) \tag{1.30}$$

   for $A_\tau := B_w C_z + E_\tau A$ and $B_\tau := B_w D_{zu} + E_\tau B_u$. This is a conventional form of so-called *neutral* DDEs (single-delay, again), in which the derivative term is delayed as well.

Throughout this text the general DDE (1.27) corresponding to the setup in Fig. 1.7 is preferred, partially by pure aesthetic considerations.

1.3 Finite-dimensional approximations of the delay element

The continuous-time delay element (1.5) is infinite dimensional and so are its interconnections. To avoid associated complications, one may consider to approximate the delay element by a finite-dimensional system, so that standard methods can be used. Such approximations are addressed in this section.

Remark 1.8 (to approximate, or not to approximate). Before discussing approximations techniques, a brief disclaimer is in order. One of the central themes of these notes is the exploitation of the structure of the delay element, especially in various control design problems. Approximating delays by finite-dimensional systems might damage this structure, rendering the problem in hand less transparent. Approximations are thus suggested to be used as merely a convenience, e.g. a tool for performing quick initial screening or simulations. As such, their simplicity and transparency are preferable to accuracy to some extent.   ▽

First, consider perspectives of approximating the pure delay element $\bar{D}_\tau$ by a *stable* finite-dimensional LTI system, say R_τ. We say that R_τ approximates $\bar{D}_\tau$ if the *approximation error* $\epsilon_R := \|\bar{D}_\tau - R_\tau\|$ is "small," where $\|\cdot\|$ stands for a system norm of choice. If the H_∞ norm is chosen as the measure to the approximation accuracy, then

$$\epsilon_R = \|\bar{D}_\tau - R_\tau\|_\infty = \sup_{\omega \in \mathbb{R}} |\bar{D}_\tau(j\omega) - R_\tau(j\omega)| = \sup_{\omega \in \mathbb{R}} |e^{-j\tau\omega} - R_\tau(j\omega)|.$$

Because $R_\tau(s)$ is rational, the argument of its frequency response is bounded and approaches some finite value as ω grows. At the same time, it follows from (1.9) that the phase lag of $\bar{D}_\tau(j\omega)$ is unbounded. Hence, there is an infinite increasing sequence of frequencies, say $\{\omega_i\}_{i\in\mathbb{N}}$, such that

$$\arg R_\tau(j\omega_i) - \arg \bar{D}_\tau(j\omega_i) = \pi + 2\pi k_i \iff e^{j(\arg R_\tau(j\omega_i) - \arg \bar{D}_\tau(j\omega_i))} = -1$$

for some $k_i \in \mathbb{Z}$. At those frequencies we have that

$$|\bar{D}_\tau(j\omega_i) - R_\tau(j\omega_i)| = |\bar{D}_\tau(j\omega_i)| + |R_\tau(j\omega_i)| = 1 + |R_\tau(j\omega_i)|.$$

Therefore,

$$\epsilon_R \geq 1 + \sup_{i\in\mathbb{N}} |R_\tau(j\omega_i)| \geq 1 = \|\bar{D}_\tau - 0\|_\infty.$$

The lower bound $\epsilon_R = 1$ above is attained only if $|R_\tau(j\omega_i)| = 0$ for all $i \in \mathbb{N}$. Because $R_\tau(s)$ is rational, the only possible choice here is $R_\tau = 0$. In other words, the best finite-dimensional approximation of $\bar{D}_\tau$ is the zero system. This *optimal* approximation is useless and effectively implies that any attempt to approximate the pure delay element in the H_∞ metric[2] is futile.

However, we might never *need* to approximate the delay element over the whole frequency range. In most engineeringly-motivated control problems only a finite frequency band is of interest, just because realistic processes have finite bandwidths. As the phase lag of $\bar{D}_\tau$ over any finite frequency range is finite, the approximation problem in this setting does make sense. A possible approach to that end is to approximate $F\bar{D}_\tau$ for a stable low-pass filter F, whose bandwidth defines the frequency range of interest.

There are various approaches to approximate $F\bar{D}_\tau$ by finite-dimensional systems, see [58, Sec. 6.3] and the references therein for an overview. Similarly to model order reduction methods for finite-dimensional systems, delay approximation methods can be roughly divided into those oriented on singular value decompositions and those based on power series expansions of the delay element in the Laplace domain. The first group has normally built-in stability and performance guarantees and are thus more accurate. An example is the balanced truncation procedure, popular for finite-dimensional systems and based on calculating Hankel singular values of the original system and corresponding Schmidt pairs (singular vectors). This approach does extend to systems of the form $F\bar{D}_\tau$, with calculable Hankel singular values and

---

[2]The same conclusion is immediate for approximating $\bar{D}_\tau$ in the $\mathcal{A}$-norm, which is the $L_\infty(\mathbb{R}_+)$-induced system norm.

Schmidt pairs. Yet involved calculations entail transcendental equations and are not quite easy to use, even in the simplest case of a first-order $F(s)$. For that reason, results based on singular value are far less popular than those based on power series expansions. The idea there is to truncate a power expansion of $e^{-\tau s}$, or a function involving it, up to some term and under certain additional (interpolation) constraints. Such methods are frequently rather easy to implement. On the downside, accuracy and even stability are often not their natural by-products. For instance, it might appear natural to approximate the transfer function of $\bar{D}_\tau$ via the relation

$$e^{-\tau s} = \frac{e^{-\tau s/2}}{e^{\tau s/2}} \approx \frac{Q_n(-\tau s/2)}{Q_n(\tau s/2)},$$

where the polynomial $Q_n(s) := 1 + s + s^2/2! + \cdots + s^n/n!$ is the nth order partial sum of the Maclaurin series of e^s. However, this $Q_n(s)$ is Hurwitz only for $n \leq 4$, which renders this approach quite limited.

1.3.1 Padé approximant of $e^{-\tau s}$

Perhaps the best known truncation-based approach is to approximate the delay element by its Padé approximant of a given degree. Consider first the general logic of this approach. Let $\phi(s)$ be a complex function, analytic in some neighborhood of the origin. A rational function

$$R_{m,n}(s) = \frac{P_m(s)}{Q_n(s)} = \frac{p_m s^m + \cdots + p_1 s + p_0}{q_n s^n + \cdots + q_1 s + 1},$$

is said to be the $[m, n]$-Padé approximant of $\phi(s)$ if the first $n + m + 1$ terms of the Maclaurin series of $\phi(s)$ and $R_{m,n}(s)$ coincide. In other words, the $[m, n]$-Padé approximant matches $\phi(s)$ and its $n + m$ derivatives at $s = 0$, i.e. $\phi^{(i)}(0) = R^{(i)}(0)$ for all $i \in \mathbb{Z}_{0..n+m}$. An alternative condition for the Padé approximant, which is useful for computing the required coefficients q_i and p_i, is that $\phi(s) - R_{m,n}(s) = O(s^{m+n+1})$ or, equivalently,

$$\phi(s)Q_n(s) - P_m(s) = O(s^{m+n+1}) \quad \text{as } s \to 0. \tag{1.31}$$

This Bézout-like identity is solvable iff $\phi(s)$ and -1 are coprime, i.e. have no common roots, which is obviously always true. Hence, the sought polynomials always exist and are unique. The $m + n + 1$ free coefficients of $P_m(s)$ and $Q_n(s)$ can be selected from (1.31) by the use of the Maclaurin series expansion of $\phi(s)$ and zeroing the coefficients of all powers of s from 0 to $m + n$. The latter procedure can, in turn, be expressed as the following set of $n + m + 1$ linear equations (here we assume that $n \geq m$, i.e. that $R_{m,n}(s)$ is proper):

$$\underbrace{\begin{bmatrix} \phi_0 & 0 & \cdots & 0 & 0 & \cdots & 0 & -1 & 0 & \cdots & 0 \\ \phi_1 & \phi_0 & \cdots & 0 & 0 & \cdots & 0 & 0 & -1 & \cdots & 0 \\ \vdots & \vdots & \ddots & \vdots & \vdots & & \vdots & \vdots & \vdots & \ddots & \vdots \\ \phi_m & \phi_{m-1} & \cdots & \phi_0 & 0 & \cdots & 0 & 0 & 0 & \cdots & -1 \\ \phi_{m+1} & \phi_m & \cdots & \phi_1 & \phi_0 & \cdots & 0 & 0 & 0 & \cdots & 0 \\ \vdots & \vdots & & \vdots & \vdots & \ddots & \vdots & \vdots & \vdots & & \vdots \\ \phi_n & \phi_{n-1} & \cdots & \phi_{n-m} & \phi_{n-m-1} & \cdots & \phi_0 & 0 & 0 & \cdots & 0 \\ \vdots & \vdots & & \vdots & \vdots & & \vdots & \vdots & \vdots & & \vdots \\ \phi_{n+m} & \phi_{n+m-1} & \cdots & \phi_n & \phi_{n-1} & \cdots & \phi_m & 0 & 0 & \cdots & 0 \end{bmatrix}}_{\text{permutated Sylvester matrix}} \begin{bmatrix} 1 \\ q_1 \\ \vdots \\ q_m \\ q_{m+1} \\ \vdots \\ q_n \\ p_0 \\ p_1 \\ \vdots \\ p_m \end{bmatrix} = 0, \tag{1.32}$$

where $\phi_i = \phi^{(i)}(0)/i!$ for all $i \in \mathbb{Z}_+$ are the coefficients of the Maclaurin expansion of $\phi(s)$. Thus, all we need is to solve n linear equations (the last n rows above) in q_i and then calculate the coefficients of $P_m(s)$

from the first $m + 1$ rows of (1.32). As a matter of fact, those n equations for the coefficients of $Q_n(s)$ are of the form $Mq = b$ for an $n \times n$ Toeplitz matrix M. This structure can be exploited to solve the equation more efficiently.

Our interest is the $[n, n]$-Padé approximant of $e^{-\tau s}$. So consider first

$$\phi(s) = e^s = \sum_{i=0}^{\infty} \frac{1}{i!} s^i =: \sum_{i=0}^{\infty} \phi_i \, s^i.$$

The $[n, n]$-Padé approximant of the transfer function $e^{-\tau s}$ of the delay element $\bar{D}_\tau$ is then obtained by the substitution $s \to -\tau s$. Also, although any $m \le n$ can be considered, the choice $m = n$ appears natural and is by far the most common one. Still, arguments below extend to $m < n$ seamlessly. For $m = n$ equality (1.32) reads

$$\begin{bmatrix} \phi_0 & 0 & \cdots & 0 & -1 & 0 & \cdots & 0 \\ \phi_1 & \phi_0 & \cdots & 0 & 0 & -1 & \cdots & 0 \\ \vdots & \vdots & \ddots & \vdots & \vdots & \vdots & \ddots & \vdots \\ \phi_n & \phi_{n-1} & \cdots & \phi_0 & 0 & 0 & \cdots & -1 \\ \hline \phi_{n+1} & \phi_n & \cdots & \phi_1 & 0 & 0 & \cdots & 0 \\ \vdots & \vdots & \ddots & \vdots & \vdots & \vdots & & \vdots \\ \phi_{2n} & \phi_{2n-1} & \cdots & \phi_n & 0 & 0 & \cdots & 0 \end{bmatrix} \begin{bmatrix} 1 \\ q_1 \\ \vdots \\ q_n \\ \hline p_0 \\ p_1 \\ \vdots \\ p_n \end{bmatrix} = 0. \tag{1.33}$$

Define

$$\xi(t) = \begin{bmatrix} \xi_1(t) \\ \vdots \\ \xi_n(t) \end{bmatrix} := \begin{bmatrix} \psi_{n+1}(t) & \psi_n(t) & \cdots & \psi_1(t) \\ \vdots & \vdots & \ddots & \vdots \\ \psi_{2n}(t) & \psi_{2n-1}(t) & \cdots & \psi_n(t) \end{bmatrix} \begin{bmatrix} 1 \\ q_1 \\ \vdots \\ q_n \end{bmatrix}, \quad \text{where } \psi_i(t) := \frac{t^i}{i!}$$

(so that $\phi_i = \psi_i(1)$). Clearly, the last n rows in the left-hand side of (1.33) are exactly $\xi(1)$. Hence, the choice of $Q_n(s)$ in the $[n, n]$-Padé approximant of e^s is equivalent to the choice of n scalars q_i such that $\xi(1) = 0$. Two more facts, which follow directly from the definition of $\psi_i(t)$, are important. First, $\xi(0) = 0$ for all q_i. Second, $\psi_i(t) = \dot{\psi}_{i+1}(t)$ for all $i \in \mathbb{N}$, so that $\xi_i(t) = \xi_n^{(n-i)}(t)$. Thus, we look for a

- polynomial function $\xi_n(t)$ of order $2n$ such that $\xi_n^{(i)}(t) = 0$ at $t = 0$ and $t = 1$ for all $i \in \mathbb{Z}_{0..n-1}$.

All such polynomials can be described as $\alpha t^n (t-1)^n$ for some constant α. Hence, we have the equality

$$\xi_n(t) = \frac{t^{2n}}{(2n)!} + \sum_{i=1}^{n} \frac{t^{2n-i}}{(2n-i)!} q_i = \alpha t^n (t-1)^n, \quad \forall t \in [0, 1]. \tag{1.34}$$

It follows then by the binomial theorem that $\alpha = 1/(2n)!$ and

$$q_i = (-1)^i \binom{n}{i} \frac{(2n-i)!}{(2n)!} = (-1)^i \frac{(2n-i)! \, n!}{(2n)! \, (n-i)! \, i!}$$

for all $i \in \mathbb{Z}_{1..n}$. Note that an alternative expression for q_i can be obtained by differentiating (1.34) $2n - i$ times at $t = 0$, to have

$$q_i = \xi_n^{(2n-i)}(0)$$

It is only left to obtain the coefficients p_i from the first $n+1$ rows of (1.33). The first row yields $p_0 = 1$. By repeating the arguments about the last n rows and taking into account that $\xi_n^{(i)}(1) = (-1)^i \xi_n^{(i)}(0)$, we have that

$$p_i = \xi_n^{(2n-i)}(1) = (-1)^{2n-i} \xi_n^{(2n-i)}(0) = (-1)^i q_i, \quad \forall i \in \mathbb{Z}_{1..n}.$$

This implies that $P_n(s) = Q_n(-s)$ and the resulting $R_{n,n}(s)$ is all-pass, in the sense that $|R_{n,n}(j\omega)| = 1$ for all $\omega \in \mathbb{R}$.

Summarizing, the $[n, n]$-Padé approximant of the delay element $\bar{D}_\tau$ has the transfer function

$$e^{-\tau s} \approx R_{n,n}(\tau s) = \frac{Q_n(-\tau s)}{Q_n(\tau s)}, \quad \text{where } Q_n(s) = \sum_{i=0}^{n} \binom{n}{i} \frac{(2n-i)!}{(2n)!} s^i \tag{1.35}$$

(mind substituting $s \rightarrow -\tau s$ to derive the approximant of $e^{-\tau s}$ from that of e^s). The five lowest-order polynomials $Q_n(s)$ are

$$Q_1(s) = 1 + \frac{1}{2} s,$$

$$Q_2(s) = 1 + \frac{1}{2} s + \frac{1}{12} s^2,$$

$$Q_3(s) = 1 + \frac{1}{2} s + \frac{1}{10} s^2 + \frac{1}{120} s^3,$$

$$Q_4(s) = 1 + \frac{1}{2} s + \frac{3}{28} s^2 + \frac{1}{84} s^3 + \frac{1}{1680} s^4,$$

$$Q_5(s) = 1 + \frac{1}{2} s + \frac{1}{9} s^2 + \frac{1}{72} s^3 + \frac{1}{1008} s^4 + \frac{1}{30240} s^5.$$

Two properties of the Padé approximation method are given below without proofs. The first one is about the stability of $R_{n,n}$, which should be an essential property of any approximation of $\bar{D}_\tau$:

Proposition 1.1. *The polynomials $Q_n(s)$ defined in (1.35) are Hurwitz for all $n \in \mathbb{N}$.*

The second result provides a simple, yet tight at very low frequencies, upper bound on the approximation error in the frequency domain. To formulate it, we need the normalized Butterworth polynomials, which are k-order Hurwitz polynomials $B_k(s)$ satisfying $|B_k(j\omega)|^2 = 1 + \omega^{2k}$. For $k = 2n + 1$

$$B_{2n+1}(s) = (s + 1) \prod_{i=1}^{n} \left(s^2 + 2\cos\left(\frac{n + 1 - i}{2n + 1} \pi\right) s + 1 \right)$$

and its roots are equidistant on the left unit semi-circle.

Proposition 1.2. *The Padé approximant (1.35) satisfies $|e^{-j\omega} - R_{n,n}(j\omega)| \leq 2.02|H_{2n+1}(j\omega)|$ for all $\omega \in \mathbb{R}$, where*

$$H_{2n+1}(s) = \frac{(s/\omega_n)^{2n+1}}{B_{2n+1}(s/\omega_n)}$$

is the high-pass Butterworth filter, whose cutoff frequency

$$\omega_n := \left(2 \frac{(2n)!(2n + 1)!}{(n!)^2} \right)^{1/(2n+1)}$$

is such that $\{\omega_n\} = \{2.8845, 4.2823, 5.7251, 7.1814, 8.6435, \ldots\}$ and $\lim_{n\to\infty} \omega_n/n = 4/e \approx 1.4715$.

Although the bound of Proposition 1.2 is conservative, it does show that the Padé approximant is accurate at low frequencies and the approximations accuracy increases with n. These conclusions are intuitive. Indeed, the equality $e^{-s} - R_{n,n}(s) = O(s^{2n+1})$, which defines the method, effectively says that $R_{n,n}(s)$ interpolates e^{-s} and its $2n$ derivatives at the origin, i.e. at $\omega = 0$. An immediate consequence of the result of Proposition 1.2 is that $\|(\bar{D}_1 - R_{n,n})F\|_\infty \leq 2.02\|H_{2n+1}F\|_\infty$ for all $F \in H_\infty$. If F is a low-pass filter, then the lower its bandwidth is, the smaller is $\|H_{2n+1}F\|_\infty$. This is also intuitive.

(a) $R(s) = -1/(2s + 1)$ (b) $R(s) = -1$
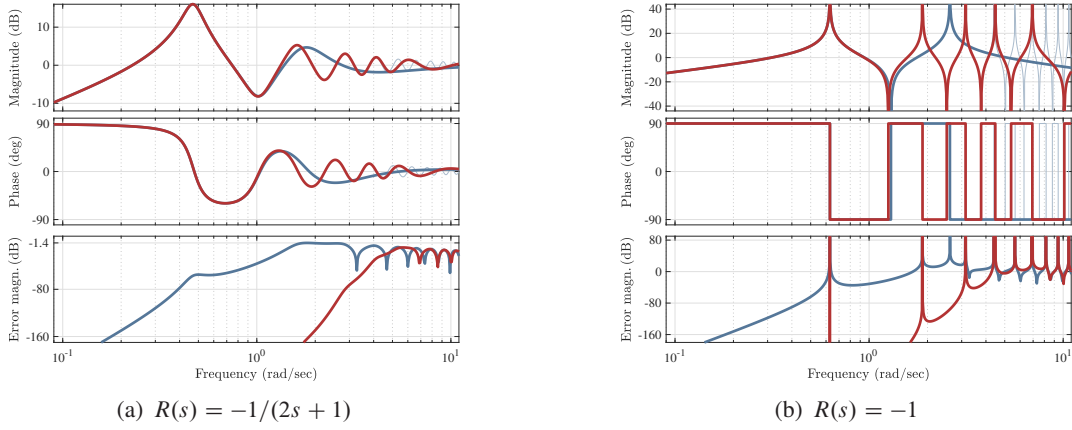
Fig. 1.8: $G_0(s)$ from (1.19) for $Z_m = 1$ and $\tau = 5$ with [4, 4]- and [12, 12]-Padé approximants of the delay

To illustrate traits of Padé approximants, consider the system G_0 driven by the wave equation (1.14), whose transfer function is given by (1.19) on p. 8 and the frequency responses are presented in Fig. 1.5. If the reflectance R has a finite bandwidth, i.e. if its transfer function $R(s)$ is strictly proper, then the delay has a limited effect on the high-frequency dynamics of G_0. We can then expect that the use of a Padé approximant of a sufficiently high degree will result in a good approximation of G_0. This is indeed the case, as can be seen from the plots in Fig. 1.8(a) for the strictly proper $R(s) = -1/(2s + 1)$, representing the original system (thin pale line) and its [4, 4]- and [12, 12]-Padé approximants (thick lines). It is also clear that the higher-order Padé results in a higher approximation accuracy. The situation is different if the bandwidth of $R(s)$ is infinite. As no finite-dimensional approximation of the delay element succeeds over all frequencies, the high-frequency dynamics of G_0 can no longer be captured by its approximation. This is seen from the plots in Fig. 1.8(b), where the approximation error for the bi-proper $R(s) = -1$ is unbounded, no matter what degree of the Padé approximant is chosen.

Remark 1.9. The approximation of the delay element in $G_0(s) = Z_m(1 + R(s)e^{-\tau s})/(1 - R(s)e^{-\tau s})$ might not be the best way to approximate this function. A more accurate approximation could be obtained via deriving a Padé approximant of $\phi(s) = G_0(s)$ directly. But this would require to develop new formulae and software, rather than to use widely available ones for $\phi(s) = e^{-\tau s}$.   ▽

Chapter 2

Stability Analysis

S TABILITY IS A VITAL PROPERTY of every control system. So the first analytic chapter of these notes addresses the stability analysis of the single-delay system $P_\tau : u \mapsto y$ in Fig. 2.1 for a finite-dimensional G, given in terms of its state-space realization (1.26), and an $m_\tau \times m_\tau$ delay element $\bar{D}_\tau$ of the form defined by (1.5). Both i/o stability (in the L_2 sense) and Lyapunov stability are studied below. In both these cases the analysis reduces to that of autonomous versions of the system, much in parallel to what happens in the finite-dimensional case. Details are more delicate and involved though.

2.1 I/O stability and modals

We start with analysing the i/o stability. We say that a linear system $G : u \mapsto y$ is L_2-stable (or simply stable) if $y \in L_2(\mathbb{R})$ for all $u \in L_2(\mathbb{R})$ and $\|y\|_2$ is bounded for all u such that $\|u\|_2 = 1$. If G is LTI, then it is stable iff its transfer function $G(s)$ belongs to H_∞, which is the space of holomorphic and bounded functions in $\mathbb{C}_0$, see (B.17). If G is finite-dimensional, then $G(s)$ is rational and $G \in H_\infty$ iff $G(s)$ is proper and its poles are in the open left-half plane $\mathbb{C} \setminus \bar{\mathbb{C}}_0$. An appropriately defined properness is also required in delay systems and it always holds for the system in Fig. 2.1 with a proper $G(s)$. In this section we thus concentrate on "poles" of $P_\tau(s)$ or, more accurately, on its characteristic function.

2.1.1 Characteristic function of delay-differential equations

A direct verification of whether a transfer function like

$$P_\tau(s) = D_{yu} + \begin{bmatrix} C_y & D_{yw}\mathrm{e}^{-\tau s} \end{bmatrix} \begin{bmatrix} sI - A & -B_w\mathrm{e}^{-\tau s} \\ -C_z & I - D_{zw}\mathrm{e}^{-\tau s} \end{bmatrix}^{-1} \begin{bmatrix} B_u \\ D_{zu} \end{bmatrix} \tag{2.1}$$

belongs to H_∞ might not be an easy task in general. In the rational case, corresponding to $m_\tau = 0$ and having $P_\tau(s) = D_{yu} + C_y(sI - A)^{-1}B_u$, there is a simple alternative. It is based on the observation that $P_\tau \in H_\infty$ whenever so does $(sI - A)^{-1}$, which represents the autonomous state dynamics $\dot{x}(t) = Ax(t)$.
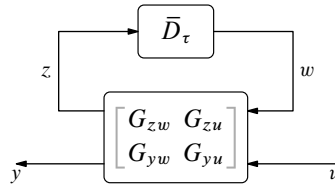
Fig. 2.1: General single-delay interconnection

19

The function $(sI - A)^{-1}$ is not holomorphic only at the eigenvalues of A and is bounded (actually, vanishes) as $|s| \to \infty$. Thus, if all roots of the *characteristic function* (polynomial) $\det(sI - A)$ are in the open left-half plane $\mathbb{C} \setminus \bar{\mathbb{C}}_0$, then $P_\tau \in H_\infty$. Moreover, this condition becomes necessary if (A, B_u) is stabilizable and (C_y, A) is detectable.

The counterpart of the characteristic function for a general P_τ in (2.1) is naturally

$$\chi_\tau(s) := \det \begin{bmatrix} sI - A & -B_w \mathrm{e}^{-\tau s} \\ -C_z & I - D_{zw}\mathrm{e}^{-\tau s} \end{bmatrix}, \tag{2.2}$$

which also represents the free motion of the state of the system in Fig. 2.1, that is

$$\begin{bmatrix} \dot{x}(t) \\ z(t) \end{bmatrix} = \begin{bmatrix} A & B_w \\ C_z & D_{zw} \end{bmatrix} \begin{bmatrix} x(t) \\ z(t - \tau) \end{bmatrix}.$$

The roots of $\chi_\tau(s)$, dubbed the *modes* of P_τ, represent then nontrivial solutions of the free motion dynamics. Modes are the poles of $\Phi_\tau^{-1}(s)$, where

$$\Phi_\tau(s) := \begin{bmatrix} sI - A & -B_w \mathrm{e}^{-\tau s} \\ -C_z & I - D_{zw}\mathrm{e}^{-\tau s} \end{bmatrix}, \tag{2.3}$$

which is the only factor in (2.1) that might not be in H_∞. We may thus anticipate that the absence of modes of P_τ in $\bar{\mathbb{C}}_0$ is indicative of the stability of P_τ. This may indeed be the case, although not always, with the analysis complications caused by potentially intricate properties of $\Phi_\tau(s)$ at $|s| \to \infty$. On top of this, finding roots of $\chi_\tau(s)$ for a nonzero τ might be a hard task in itself. Still, stability analysis via the characteristic function is frequently a practical approach. All this will be discussed in the remaining subsections of Section 2.1. But before that, some terminology is introduced.

It can be shown that the characteristic function (2.2) is of the form

$$\chi_\tau(s) = \sum_{i=0}^{k} Q_i(s)\mathrm{e}^{-i\tau s} \tag{2.4}$$

for some $k \in \mathbb{Z}_+$ and finite polynomials $Q_i(s)$ such that $\deg Q_0(s) \geq \deg Q_i(s)$ for all $i \in \mathbb{Z}_{1..k}$. As we already know from the discussion on p. 9, this kind of functions is known as *quasi-polynomials*. Because $Q_0(s) = \det(sI - A)$, its roots are the eigenvalues of A. If the condition $\deg Q_0(s) > \deg Q_i(s)$ holds for all $i \in \mathbb{Z}_{1..k}$, then the quasi-polynomial (2.4) is termed *retarded*. Otherwise, i.e. if there is at least one $j \in \mathbb{Z}_{1..k}$ such that $\deg Q_0(s) = \deg Q_j(s)$, it is called *neutral*. The same terminology is used with respect to DDE (1.27) itself. There are classes of delay systems, whose characteristic quasi-polynomials have $\deg Q_0(s) < \deg Q_j(s)$ for at least one j. They are known as *advanced* and not studied in this text. They cannot result from the system in Fig. 2.1 with a proper $G(s)$ and should not be expected in realistic situations. If $k = 1$, then $\chi_\tau(s)$ in (2.4) is said to be a quasi-polynomial with a *single delay*, like that in (1.20). If $k > 1$, then (2.4) is a quasi-polynomial with multiple *commensurate delays*, as all its delays are integer multiples of one $\tau > 0$. It should be emphasized that a single-delay system, like that in Fig. 2.1, can potentially have a multiple-delay characteristic function, see Example 2.3 below. Yet such a function is always of the commensurate type. In multiple-delay systems, like that in Remark 1.6, characteristic quasi-polynomials can be of the form $Q_0(s) + \sum_i Q_i(s)\mathrm{e}^{-\tau_i s}$ with at least one irrational τ_{i_1}/τ_{i_2}. Such multiple-delay quasi-polynomials are said to have *incommensurate* delays and their properties are normally way messier than those of their commensurate counterparts.

Example 2.1. Consider an input-delay system as in (1.10) for the plant $P(s) = D + C(sI - A)^{-1}B$. From (1.22), the state-space realization

$$G_{\mathrm{inpd}}(s) = \left[\begin{array}{c|cc} A & B & 0 \\ \hline 0 & 0 & I \\ C & D & 0 \end{array} \right] \quad \implies \quad \chi_\tau(s) = \det \begin{bmatrix} sI - A & -B\mathrm{e}^{-\tau s} \\ 0 & I \end{bmatrix} = \det(sI - A).$$

This $\chi_\tau(s)$ is a standard polynomial, agreeing with the discussion in §1.2.1. $\triangledown$

Example 2.2. If the reflectance R in (1.19) has $R(s) = D + C(sI - A)^{-1}B$, then

$$
G_{\text{wave},0}(s) = \left[\begin{array}{c|cc} A & B & 0 \\ \hline C & D & Z_m \\ 2C & 2D & Z_m \end{array}\right] \implies \chi_\tau(s) = \det\left[\begin{array}{cc} sI - A & -Be^{-\tau s} \\ -C & 1 - De^{-\tau s} \end{array}\right]
$$

The static $R(s) = -1$ as in Fig. 1.5(b) results in the already familiar, from a discussion on p. 9, $\chi_\tau(s) = 1 + e^{-\tau s}$, which is a single-delay neutral quasi-polynomial. If $R(s) = -1/(2s + 1)$, as in Fig. 1.5(a), then

$$
\chi_\tau(s) = \det\left[\begin{array}{cc} s + 1/2 & -e^{-\tau s} \\ 1/2 & 1 \end{array}\right] = \left(s + \frac{1}{2}\right) + \frac{1}{2}e^{-\tau s},
$$

which is a single-delay retarded quasi-polynomial. $\triangledown$

Example 2.3. Let

$$
G(s) = \left[\begin{array}{cc|cc:c} 0 & 1 & 0 & 1 & 0 \\ -q_{00} & -q_{01} & -q_{10} & 1 & 1 \\ \hline 1 & 0 & 0 & 0 & 0 \\ 0 & \alpha & 0 & 0 & 0 \\ \hdashline 1 & 0 & 0 & 0 & 0 \end{array}\right]
$$

for some $\alpha \in \mathbb{R}$. The corresponding characteristic function is

$$
\chi_\tau(s) = s^2 + q_{01}s + q_{00} + (-\alpha s + q_{10} + \alpha q_{00})e^{-\tau s} + \alpha q_{10}e^{-2\tau s}.
$$

If $\alpha \neq 0$, this is a *multiple-delay* commensurate quasi-polynomial. If $\alpha = 0$, $\chi_\tau(s)$ has only one delay. In fact, in the latter case

$$
G(s) = \left[\begin{array}{c:c} 1 & 0 \\ 0 & 0 \\ \hdashline 0 & 1 \end{array}\right]\left[\begin{array}{cc|cc:c} 0 & 1 & 0 & 1 & 0 \\ -q_{00} & -q_{01} & -q_{10} & 1 & 1 \\ \hline 1 & 0 & 0 & 0 & 0 \\ \hdashline 1 & 0 & 0 & 0 & 0 \end{array}\right]
$$

and $M = \left[\begin{smallmatrix} 1 \\ 0 \end{smallmatrix}\right]$ can be moved through the 2×2 delay element and then $\mathcal{F}_u(G, \bar{D}_\tau) = \mathcal{F}_u(\tilde{G}, \bar{D}_\tau)$ for

$$
\tilde{G}(s) = \left[\begin{array}{cc|cc:c} 0 & 1 & 0 & 1 & 0 \\ -q_{00} & -q_{01} & -q_{10} & 1 & 1 \\ \hline 1 & 0 & 0 & 0 & 0 \\ \hdashline 1 & 0 & 0 & 0 & 0 \end{array}\right]\left[\begin{array}{c:c} 1 & 0 \\ 0 & 0 \\ \hdashline 0 & 1 \end{array}\right] = \left[\begin{array}{cc|c:c} 0 & 1 & 0 & 0 \\ -q_{00} & -q_{01} & -q_{10} & 1 \\ \hline 1 & 0 & 0 & 0 \\ \hdashline 1 & 0 & 0 & 0 \end{array}\right]
$$

and the 1×1 delay element $\bar{D}_\tau$, which is a simpler setup (cf. Example 1.1). $\triangledown$

Example 2.4. If $D_{zw} = 0$, then the corresponding characteristic function is always retarded, cf. (1.29). Yet $D_{zw} \neq 0$ does not necessarily lead to a neutral $\chi_\tau(s)$. To see this, consider

$$
G(s) = \left[\begin{array}{c|cc:c} 0 & -1 & 1 & 1 \\ \hline 1 & 0 & 1 & 0 \\ 1 & 0 & 0 & 0 \\ \hdashline 1 & 0 & 0 & 0 \end{array}\right],
$$

whose $D_{zw} = \left[\begin{smallmatrix} 0 & 1 \\ 0 & 0 \end{smallmatrix}\right] \neq 0$ (although it is nilpotent), but the characteristic function $\chi_\tau(s) = s + e^{-2\tau s}$ is still retarded. $\triangledown$

(a) Neutral chains, $\alpha_i \in \{1/4, 1, 2\}$ (b) Asymptotic retarded chain, $\alpha_1 = 13$
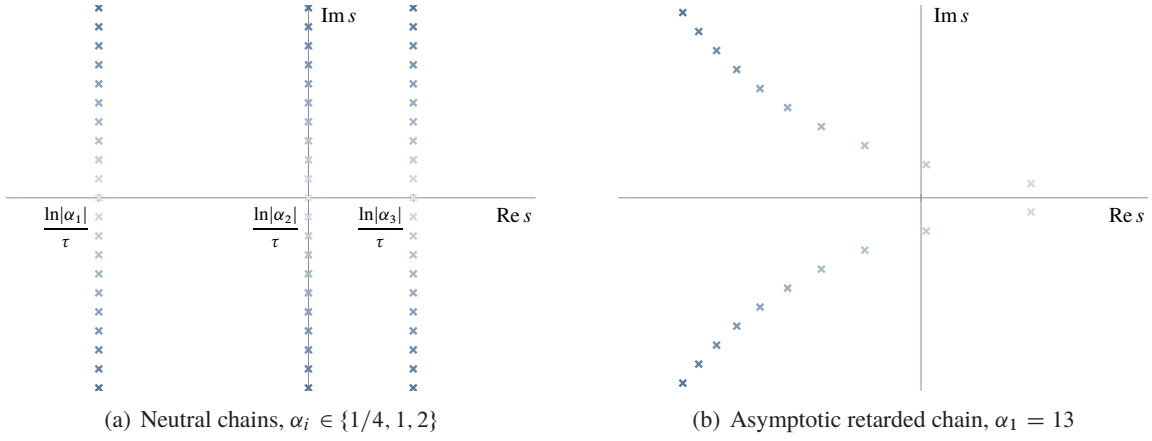
Fig. 2.2: Asymptotic chains of roots of $\chi_\tau(s)$

2.1.2 Asymptotic root properties

The quasi-polynomial $\chi_\tau(s)$ in (2.4) is an entire function of s, i.e. it is holomorphic in the whole $\mathbb{C}$. Hence, the set of roots of $\chi_\tau(s)$ is countable and there are no accumulation points [65, Thm. 10.18]. This, in turn, implies that the number of roots of (2.4) in every bounded region of $\mathbb{C}$ if finite.

Because quasi-polynomials have an infinite number of roots, there must be root sequences with unbounded magnitudes. Although calculating those sequences exactly is seldom possible, their asymptotic behavior is understood rather well. For commensurate quasi-polynomials of the form (2.4), which are either neutral or retarded, roots for large $|s|$ are always organized in a finite number of chains of two possible kinds (follows by Rouché's arguments).

1. *Neutral chains* are asymptotic, under sufficiently large $|s|$, to the solutions of the equations $e^{\tau s} = \alpha_i$ for some $\alpha_i \in \mathbb{C} \setminus \{0\}$. Those solutions are at the sequence $\{s_{ik}\}_{k \in \mathbb{Z}}$ with

$$s_{ik} = \frac{\ln|\alpha_i|}{\tau} + j\frac{2\pi k + \arg \alpha_i}{\tau}.$$

   All these s_{ik} are on a vertical line, either in the left-half plane (if $|\alpha_i| < 1$), or in the right-half plane (if $|\alpha_i| > 1$), or on the imaginary axis (if $|\alpha_i| = 1$), see Fig. 2.2(a).

2. *Retarded chains* are asymptotic, under sufficiently large $|s|$, to the solutions of the equations $se^{\tau s} = \alpha_i$ for some $\alpha_i \in \mathbb{C} \setminus \{0\}$. Those solutions *asymptotically* approach [58, Lem. 6.1.2] the sequence $\{s_{ik}\}_{k \in \mathbb{N}}$ with

$$s_{ik} = -\frac{\ln(2\pi k) - \ln|\tau \alpha_i|}{\tau} + j\frac{2\pi k + \arg \alpha_i - \pi/2}{\tau}$$

   for sufficiently large k, as well as their complex conjugates. The real parts of these s_{ik} approach $-\infty$ irrespective of α_i, although slower than their imaginary parts approach $\pm\infty$, see Fig. 2.2(b).

If (2.4) is retarded, i.e. if $\deg Q_0(s) > \deg Q_i(s)$ for all $i \in \mathbb{Z}_{1..k}$, there are only retarded chain(s). Otherwise, there is at least one neutral chain and, possibly, also retarder chain(s). More details can be found in [6, Ch. 12] or [58, Sec. 6.1], but digging into this issue is beyond the scope of these notes.

Remark 2.1 (incommensurate delays). The asymptotic roots behavior for quasi-polynomials with incommensurate delays, i.e. of the form $P(s) + \sum_i Q_i(s)e^{-\tau_i s}$ with at least one irrational ratio τ_{i_1}/τ_{i_2}, is slightly different. While retarded chains, if exist, are the same as in the commensurate case, neutral modes do not approach infinity in a regular way. Nonetheless, they are asymptotically confined to the vertical strip $|\operatorname{Re} s| \leq \beta$ for some finite $\beta > 0$. $\triangledown$

Neutral chains can be quantified in terms of the matrix $D_{zw} \in \mathbb{R}^{m_\tau \times m_\tau}$. To this end, note that $sI - A$ is nonsingular whenever $|s|$ is large enough (whenever $|s| > \rho(A)$, to be precise). By (A.5a),

$$\chi_\tau(s) = \det(sI - A)\det(I - D_{zw}\mathrm{e}^{-\tau s} - C_z(sI - A)^{-1}B_w\mathrm{e}^{-\tau s})$$

and only roots of the second factor are of interest. At every neutral chain we have that $|s| \to \infty$, whereas $|\mathrm{e}^{-\tau s}|$ remains bounded. Hence, the term $C_z(sI - A)^{-1}B_w\mathrm{e}^{-\tau s}$ vanishes and we end up with

$$\det(I - D_{zw}\mathrm{e}^{-\tau s}) = 0 \quad \Longleftrightarrow \quad \det(\mathrm{e}^{\tau s}I - D_{zw}) = 0.$$

Thus, all neutral chains are along the vertical lines $\mathrm{Re}\, s = \ln|\lambda_i|/\tau$ for distinct nonzero eigenvalues λ_i of D_{zw}. There are no neutral chains iff D_{zw} is nilpotent, which agrees with Example 2.4.

2.1.3 Stability and roots of characteristic function

Our next step is to connect the modes of P_τ, which are the roots of the characteristic function (2.2), with its stability. It should be clear that if $\chi_\tau(s)$ has a root in $\overline{\mathbb{C}}_0$, then $P_\tau \notin H_\infty$, unless this root is a hidden modes, canceled by other factors of $P_\tau(s)$. Yet would the absence of RHP modes be sufficient to guarantee stability? Unlike the finite-dimensional case, answering this question for time-delay systems might not be trivial. The main delicacy lies in the behavior of $\Phi_\tau(s)$ defined by (2.3) at $|s| \to \infty$. What helps to sort that out in most cases is the understanding of asymptotic properties of roots of $\chi_\tau(s)$. Depending on the spectral radius of the matrix D_{zw}, three situations may be considered separately.

The case $\rho(D_{zw}) > 1$ is fairly straightforward and technically simple. Namely, there is clearly an infinite number of roots of $\chi_\tau(s)$ in $\overline{\mathbb{C}}_0$ and thus an infinite number of unstable poles of $\Phi_\tau^{-1}(s)$. Unless all of them are canceled by other terms in (2.1), which is possible only if the setup in Fig. 2.1 is redundant, we may conclude that $P_\tau \notin H_\infty$, which is quite in line with the finite-dimensional intuition.

The case $\rho(D_{zw}) < 1$ is also uncomplicated. Indeed, by (A.2a) we have that

$$\Phi_\tau^{-1}(s) = \begin{bmatrix} I & (sI - A)^{-1}B_w\mathrm{e}^{-\tau s} \\ 0 & I \end{bmatrix}$$
$$\times \begin{bmatrix} (sI - A)^{-1} & 0 \\ 0 & (I - D_{zw}\mathrm{e}^{-\tau s} - C_z(sI - A)^{-1}B_w\mathrm{e}^{-\tau s})^{-1} \end{bmatrix} \begin{bmatrix} I & 0 \\ C_z(sI - A)^{-1} & I \end{bmatrix}.$$

Because $(sI - A)^{-1}$ vanishes as $|s| \to \infty$ and $|\mathrm{e}^{-\tau s}| < 1$ in $s \in \mathbb{C}_0$, we have that

$$\limsup_{s \in \mathbb{C}_0, |s| \to \infty} \|\Phi_\tau^{-1}(s)\| = \limsup_{s \in \mathbb{C}_0, |s| \to \infty} \|(I - D_{zw}\mathrm{e}^{-\tau s})^{-1}\|$$

$$\leq \sup_{s \in \mathbb{C}_0} \|(I - D_{zw}\mathrm{e}^{-\tau s})^{-1}\| = \max_{\zeta \in \mathbb{D}} \|(I - D_{zw}\zeta)^{-1}\| < \infty$$

because D_{zw} is a Schur stable matrix (the "max" term is the H_∞ norm of a discrete system with the proper transfer function $z(zI - D_{zw})^{-1} = I + (zI - D_{zw})^{-1}D_{zw}$). Thus, $\Phi_\tau^{-1}(s)$ might become unbounded only at its poles and the following result can be formulated.

Proposition 2.1. *If $\rho(D_{zw}) < 1$, then $P_\tau(s)$ given by (1.28) belongs to H_∞ whenever the characteristic function (2.2) has no roots in $\overline{\mathbb{C}}_0$.*

The condition of Proposition 2.1 is only sufficient. Similarly to the finite-dimensional case, it might be that $P_\tau \in H_\infty$ even if χ_τ has RHP roots. This happens if all unstable roots of χ_τ are hidden modes of P_τ, i.e. if

$$\mathrm{rank} \begin{bmatrix} A - sI_n & B_w & B_u \\ C_z & D_{zw} - \mathrm{e}^{\tau s}I_{m_\tau} & D_{zu} \end{bmatrix} < n + m_\tau \quad \text{or} \quad \mathrm{rank} \begin{bmatrix} A - sI_n & B_w \\ C_z & D_{zw} - \mathrm{e}^{\tau s}I_{m_\tau} \\ C_y & D_{yw} \end{bmatrix} < n + m_\tau$$

at all roots s of $\chi_\tau(s)$ in $\overline{\mathbb{C}}_0$.

Example 2.5. Consider the system in Fig. 2.1 with $\tau = 1$ and

$$G(s) = \frac{1}{s}\begin{bmatrix} \alpha e^\alpha & s-\alpha \\ \alpha e^\alpha & -\alpha \end{bmatrix} = \left[\begin{array}{c|cc} 0 & \alpha e^\alpha & -\alpha \\ \hline 1 & 0 & 1 \\ 1 & 0 & 0 \end{array}\right] \implies P_\tau(s) = \frac{\alpha(e^{\alpha-s}-1)}{s-\alpha e^{\alpha-s}}$$

for $\alpha > 0$. Its

$$\chi_\tau(s) = \det\begin{bmatrix} s & -\alpha e^{\alpha-s} \\ -1 & 1 \end{bmatrix} = s - \alpha e^{\alpha-s}$$

is a single-delay retarded quasi-polynomial. Because $\chi_\tau(\alpha) = 0$, this characteristic function has at least one root in $\overline{\mathbb{C}}_0$, at $s = \alpha$. However, the singularity of $P_\tau(s)$ at $s = \alpha$ is removable, because $\lim_{s\to\alpha} P_\tau(s) = -\alpha/(1+\alpha)$, which follows by applying L'Hôpital's rule. This could have been expected, because

$$\begin{bmatrix} A-sI & B_w & B_u \\ C_z & D_{zw}-e^{\tau s}I & D_{zw} \end{bmatrix}\bigg|_{s=\alpha} = \begin{bmatrix} -s & \alpha e^\alpha & -\alpha \\ 1 & -e^s & 1 \end{bmatrix}\bigg|_{s=\alpha} = \begin{bmatrix} -\alpha & \alpha e^\alpha & -\alpha \\ 1 & -e^\alpha & 1 \end{bmatrix}$$

has reduced rank for every α. In fact, $P_\tau \in H_\infty$ if α is sufficiently small. To see that, rewrite

$$P_\tau(s) = -\frac{\phi(s)}{1+\phi(s)}, \quad \text{where } \phi(s) := \alpha\frac{1-e^{\alpha-s}}{s-\alpha} = \int_0^1 \alpha e^{(\alpha-s)t}\,dt.$$

The function $\phi(s)$ is a finite integral of an entire function, $\alpha e^{(\alpha-s)t}$, and is therefore entire itself. Moreover,

$$\sup_{\text{Re }s>0}|\phi(s)| \le \sup_{\text{Re }s>0}\int_0^1 |\alpha e^{(\alpha-s)t}|\,dt = \sup_{\text{Re }s>0}\int_0^1 \alpha e^{\alpha t}e^{-\text{Re }s\,t}\,dt = \int_0^1 \alpha e^{\alpha t}\,dt = e^\alpha - 1 = \phi(0) < \infty,$$

so that $\phi \in H_\infty$ and $\|\phi\|_\infty = e^\alpha - 1$. If $\alpha < \ln 2 \approx 0.693$, then $\|\phi\|_\infty < 1$ and we have that $P_\tau \in H_\infty$ by the Small Gain Theorem. Actually, this bound on α is conservative and $P_\tau \in H_\infty$ for all $\alpha < \alpha_*$, where $\alpha_* \approx 1.293$ is the real solution to $\alpha_* e^{\alpha_*} = 1.5\pi$ (see Example 2.9 on p. 32 for explanations). $\triangledown$

The case $\rho(D_{zw}) = 1$ is the most delicate one. On the one hand, we can no longer bound $\|\Phi_\tau^{-1}(s)\|$ in $\{s \in \overline{\mathbb{C}}_0 \mid |s| \to \infty\}$ as was done under $\rho(D_{zw}) < 1$. On the other hand, we may have no poles in the RHP, even if as they asymptotically approach the imaginary axis. This is where our finite-dimensional insight might betray us, as demonstrated by the example below.

Example 2.6. Consider the system in Fig. 2.1 for $\tau = 1$ and

$$G(s) = \begin{bmatrix} -s/(s+1) & -s/(s+1) \\ 1/(s+1) & 1/(s+1) \end{bmatrix} = \left[\begin{array}{c|cc} -1 & 1 & 1 \\ \hline 1 & -1 & -1 \\ 1 & 0 & 0 \end{array}\right] \implies P_\tau(s) = \frac{1}{s+1+se^{-s}}.$$

Hence,

$$\chi_\tau(s) = \det\begin{bmatrix} s+1 & -e^{-s} \\ -1 & 1+e^{-s} \end{bmatrix} = s+1+se^{-s},$$

which is a single-delay neutral quasi-polynomial. Now, $\chi_\tau(s) = 0$ iff s satisfies $-e^{-s} = 1+1/s$. Assuming that $s = \sigma + j\omega$ is a root of this $\chi_\tau(s)$, the magnitude equality $|e^{-s}| = |1+1/s|$ can be expressed as

$$e^{-\sigma} = \left|1+\frac{1}{\sigma+j\omega}\right| = \left|\left(1+\frac{\sigma}{\sigma^2+\omega^2}\right) - j\frac{\omega}{\sigma^2+\omega^2}\right| \ge \left|1+\frac{\sigma}{\sigma^2+\omega^2}\right|.$$

First, let $\sigma = 0$. The first equality above reads then $1 = 1+1/|\omega|$, which holds for none $\omega \in \mathbb{R}$. Now, let $\sigma > 0$. In this case the inequality above leads to $e^{-\sigma} > 1$, which is again impossible. Thus, $P_\tau(s)$ has no

poles in the closed RHP. Nevertheless, this $P_\tau \notin H_\infty$. To see this, let $\{s_i\} \in \mathbb{C} \setminus \overline{\mathbb{C}}_0$ be a sequence of roots of $\chi_\tau(s)$ such that

$$s_i + 1 + s_i e^{-s_i} = 0, \quad \text{with } \lim_{i \to \infty} |s_i| = \infty,$$

which always exists as we already know. Define then another sequence, $\{\tilde{s}_i\} \in \mathbb{C}_0$ with $\tilde{s}_i = -s_i$, such that $\lim_{i \to \infty} |\tilde{s}_i| = \infty$ as well. The values of $P_\tau(s)$ at each $\tilde{s}_i$ are

$$P_\tau(\tilde{s}_i) = \frac{1}{1 - s_i - s_i e^{s_i}} = \frac{1}{1 - s_i + s_i^2/(1 + s_i)} = 1 + s_i.$$

So we have a sequence in $\mathbb{C}_0$ at which $\lim_{i \to \infty} |P_\tau(\tilde{s}_i)| = \infty$. Thus, $P_\tau(s)$ is not bounded in $\mathbb{C}_0$. $\triangledown$

Thus, if $\rho(D_{zw}) = 1$, it might happen that a system having no poles in $\overline{\mathbb{C}}_0$ is nevertheless unstable, which has no counterparts for finite-dimensional systems. To muddle even more, the transfer function

$$\frac{1}{(s + 1)(s + 1 + se^{-s})},$$

which has the same poles as the transfer function in Example 2.6, plus an additional pole at $s = -1$, does belong to H_∞, see [59], and is thus stable. Moreover, there are systems with $\rho(D_{zw}) = 1$ that have infinitely many roots in $\mathbb{C}_0$.

It is possible to characterize all these situations, which is intricate and might not be quite important from the engineering point of view. This is because of an observation that even if a system with $\rho(D_{zw}) = 1$ is stable, this property is extremely fragile and thus impractical. Indeed, a very small perturbation to D_{zw} can render $\rho(D_{zw}) > 1$ and the system unstable, with an infinite number of poles in $\mathbb{C}_0$. For that reason, we regard delay systems with $\rho(D_{zw}) = 1$ as *practically unstable*, which simplifies the analysis and does not entail any loss of engineering generality.

Remark 2.2 (regaining the link). The discussion above effectively says that the connection between stability and roots of the characteristic function is conventional for the class of systems of interest, those with $\rho(D_{zw}) < 1$. Still, we do not have this connection for a general D_{zw} anymore. But it can be regained with a slight modification of the stability area in the complex plane. Namely, the system is stable whenever there is $\epsilon > 0$ such that all roots of $\chi_\tau(s)$ lie in $\mathbb{C} \setminus \mathbb{C}_{-\epsilon}$. The price to pay for this modification is the loss of a clear intuition for transfer functions along this new stability boundary, $-\epsilon + j\mathbb{R}$. Because the problematic case of $\rho(D_{zw}) = 1$ is ruled out anyway, we proceed with the standard definition. $\triangledown$

2.1.4 Nyquist stability criterion

The Nyquist criterion is an elegant way to count the number of unstable closed-loop poles using the knowledge of the number of unstable open-loop poles and the behavior of the polar plot of the loop frequency response. Mathematically, the criterion is an application of Cauchy's argument principle to the open-loop transfer function with respect to the Nyquist contour. The latter comprises a semicircular arc connecting $+jr$ and $-jr$ in the clockwise direction, i.e. $r \cos \theta + jr \sin \theta$ for $\theta \in [-\pi, \pi]$, for $r \to \infty$, which is closed along the imaginary axis (encircling pure imaginary poles of the loop transfer function from the right, if present). A key factor enabling stability analysis with this approach is that all unstable poles of both open- and closed-loop systems lie inside the Nyquist contour. The criterion also complements well the loop shaping design method, because the loop transfer function on the Nyquist contour is merely its frequency response, with values at the semicircular arc collapsing to a point in the finite-dimensional case.

Projecting these ideas to the system in Fig. 2.1 in the case when G_{zw} is SISO, we may consider analyzing its unstable poles on the basis of the polar plot of the "loop gain"

$$L_\tau(s) := G_{zw}(s)e^{-\tau s}. \tag{2.5}$$

A clear advantage here is that G_{zw} is finite dimensional, i.e. standard, and effects of the delay on the frequency response of L_τ are simple and intuitive, as discussed in §1.2.1 on p. 5. Certain care should be taken to analyze poles of $P_\tau(s)$ properly. This is because the Nyquist analysis of L_τ is only concerned with the poles of $(I - L_\tau)^{-1} = (I - G_{zw}\bar{D}_\tau)^{-1}$, whereas $P_\tau = G_{yu} + G_{yw}\bar{D}_\tau(I - G_{zw}\bar{D}_\tau)^{-1}G_{zu}$ might contain additional modes, those of G_{yu}, G_{yw}, and G_{zu}, or might have some modes canceled. Still, accounting for those potential additions / cancellations is not a challenge because G is finite dimensional. A simplest way to do that is to use a potentially nonminimal form of $G_{zw}(s)$, with all poles of $G(s)$ included into it. In fact, if such canceled poles are unstable, the system is unstable for all τ. If these poles are stable, they have no effect on the stability of P_τ.

So, let G_{zw} be SISO and assume that $|G_{zw}(\infty)| < 1$ (otherwise the system is unstable anyway). With the assumption above, we know that there may be only a finite number of "closed-loop" poles in $\bar{\mathbb{C}}_0$. Hence, the Nyquist contour still encircles all possible unstable poles and can be used as is. The only subtle point here is the values of $G_{zw}(s)$ at the semicircular arc of the contour, whose radius approaches infinity. If $G_{zw}(s)$ is strictly proper, then $G_{zw}(s)$ is zero at all its parts, exactly as in the finite-dimensional case. But if $G_{zw}(\infty) = \gamma \neq 0$ for some $|\gamma| < 1$, then

$$L_\tau(r\cos\theta + jr\sin\theta) \xrightarrow{r\to\infty} \gamma e^{-\tau r\cos\theta} e^{-j\tau r\sin\theta}$$

is no longer a point. Rather, it is a curve connecting γe^{jr} and γe^{-jr} through the origin and remaining within the closed disk $|\gamma|\bar{\mathbb{D}} \subset \mathbb{D}$. Although this behavior deviates from that in the finite-dimensional case, it does not affect the stability analysis, as the connecting curve remains within the open unit disk $\mathbb{D}$. Thus, the Nyquist stability criterion extends to delay systems in Fig. 2.1 with $|G_{zw}(\infty)| < 1$ *verbatim*.

Example 2.7. To illustrate the use of the Nyquist criterion in the context of the stability analysis of the delay system in Fig. 2.1 and insights one can gain from it, consider the system with

$$G(s) = \left[\begin{array}{cc|c:c} 0 & 1 & 0 & 0 \\ -q_{00} & -q_{01} & -q_{10} & 1 \\ \hline 1 & 0 & 0 & 0 \\ \hdashline 1 & 0 & 0 & 0 \end{array}\right] = \frac{1}{s^2 + q_{01}s + q_{00}}\begin{bmatrix} -q_{10} & 1 \\ -q_{10} & 1 \end{bmatrix}, \tag{2.6}$$

which is the system studied in Example 2.3 on p. 21 (under $\alpha = 0$). It is readily seen that poles of $P_\tau(s)$ coincide with those of $1/(1 - L_\tau)$ in this case. Let $q_{00} = 1$, $q_{01} = 0.1$, and $q_{10} = 0.4$. For this choice of the parameters the system G_{zw} is itself stable, so the system is stable iff the Nyquist plot of L_τ does not encircle the critical point. It might be easier to analyze the behavior of $L_\tau(j\omega)$ on the Nichols chart, because it is cleaner than the Nyquist plot for systems with large phase lags and several crossover frequencies. The Nichols plots of the studied system for several values of τ are presented in Fig. 2.3. We can readily conclude
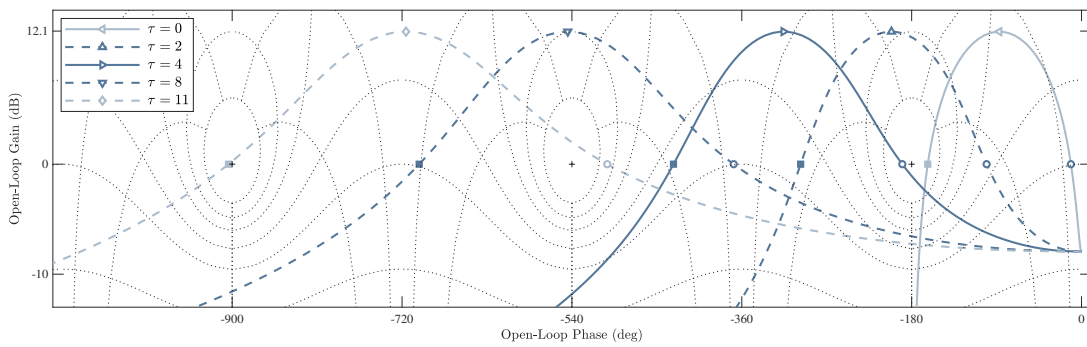

Fig. 2.3: Nichols plots of the loop frequency response of (2.6)

that P_τ is stable for $\tau = 0$ and $\tau = 4$ (solid lines) and unstable for $\tau = 2$, $\tau = 8$, and $\tau = 11$ (dashed lines). As a matter of fact, if $\tau = 2$ or $\tau = 8$, there are 2 unstable poles of $P_\tau(s)$, while if $\tau = 11$, there are 4 of them.

Because the impact of τ on $L_\tau(j\omega)$ is uncomplicated—only the phase is affected by τ, linearly—Nyquist arguments offer a valuable insight into the effect of $\bar{D}_\tau$ on the stability of the system. Indeed, with G from (2.6), $L_\tau(j\omega)$ has two crossover frequencies, i.e. the frequencies at which $|L_\tau(j\omega)| = |G_{zw}(j\omega)| = 0$ [dB]. They are $\omega_{c,1} \approx 0.7795$ and $\omega_{c,2} \approx 1.1757$ (rad/s), denoted by round and square markers, respectively, on Fig. 2.3. Poles of $P_\tau(s)$ cross the imaginary axis when the Nichols plot of $L_\tau(s)$ crosses any of the critical points $(-180 - 360k, 0)$, $k \in \mathbb{Z}$. Because the delay does not affect the magnitude of $L_\tau(j\omega)$, a critical point can only be crossed at either of the crossover frequencies. Being stable at $\tau = 0$, the system clearly remains stable for sufficiently small $\tau > 0$. But as τ becomes sufficiently large, the plot crosses the critical point $(-180, 0)$ at $\omega = \omega_{c,2}$ and the system loses stability, see the dashed line for $\tau = 2$ in Fig. 2.3. Then, as τ grows further, the second point crosses that critical point, this time at $\omega = \omega_{c,1}$. It happens that at this very τ the point $L_\tau(j\omega_{c,2})$ is still to the right of the next critical point, $(-540, 0)$. Hence, as soon as $L_\tau(j\omega_{c,1})$ passes $(-180, 0)$, the system becomes stable again, cf. the solid line for $\tau = 4$. As τ keeps growing, $L_\tau(j\omega_{c,2})$ eventually crosses $(-540, 0)$ at which point stability is lost again, see the dashed line for $\tau = 8$. And the system never becomes stable again after that. To understand the reason, note that the angular distance between $L_\tau(j\omega_{c,1})$ and $L_\tau(j\omega_{c,2})$ grows with τ, just because the phase lag due to the delay element is proportional to the frequency and $\omega_{c,2} > \omega_{c,1}$. Hence, there is a delay $\tau = \tau_\star$ such that

$$\arg L_{\tau_\star}(j\omega_{c,2}) = \arg L_{\tau_\star}(j\omega_{c,1}) - 2\pi \quad \Longleftrightarrow \quad \tau_\star = \frac{2\pi + \arg G_{zw}(j\omega_{c,2}) - \arg G_{zw}(j\omega_{c,1})}{\omega_{c,2} - \omega_{c,1}}$$

(in our case $\tau_\star \approx 9.1775$) and the angular distance between $L_\tau(j\omega_{c,1})$ and $L_\tau(j\omega_{c,2})$ exceeds $360°$ for all $\tau > \tau_\star$. Thus, there is at least one critical point (and for larger delays even more, like for the pale dashed curve in Fig. 2.3 corresponding to $\tau = 11$) between them for all such delays. $\triangledown$

The arguments above apply to a general situation. Although details might be knotty and stability conditions are not readily formulated for every possible frequency-response curve, some qualitative conclusions can be drawn. In particular, it is not hard to convince oneself that the following properties hold:

- if there are no nonzero crossover frequencies, then stability / instability property of the zero-delay system holds for all $\tau > 0$ (delay-independent condition);

- stability / instability of the zero-delay system is preserved for "sufficiently small" $\tau > 0$;

- unless there are no nonzero crossover frequencies, there is a finite $\tau_\star$ such that the system is unstable for all $\tau > \tau_\star$.

This said, the Nyquist criterion might still not the the most convenient tool for computing intervals of τ for which the system is stable. Direct analyses of characteristic quasi-polynomials studied in the next two subsections, might be advantageous in this respect.

2.1.5 Delay sweeping (direct method of Walton–Marshall)

A fundamental property of quasi-polynomials $\chi_\tau(s)$ as in (2.2) under $\rho(D_{zw}) < 1$ is that the rightmost frontier of their roots, i.e. $\sup_{\chi_\tau(s)=0} \text{Re } s$, is a continuous function of τ for all $\tau \geq 0$, see [11, Thms. 2.2 and 2.3]. Consequently, as τ changes in $\mathbb{R}_+$, the roots might migrate from the left-half plane $\mathbb{C} \setminus \bar{\mathbb{C}}_0$ to the right-half plane $\mathbb{C}_0$ or vice versa through the imaginary axis only. Thus, we can start with counting unstable roots of the zero-delay version of it, $\chi_0(s)$, which is a standard polynomial analysis problem, and then count crossings the imaginary axis by the roots of $\chi_\tau(s)$ as τ sweeps the whole positive semi-axis. Each time roots cross from left to right, which is referred to as a *switch*, we add to the count of unstable

poles. If roots cross from right to left, a *reversal*, we subtract that count. John E. Walton and Keith Marshall in [78] showed that this count can be carried out efficiently, using only finite polynomial analysis and most of its steps depend only on properties of $Q_i(s)$ and are independent of τ.

Single-delay quasi-polynomials

Let us start with the single-delay version of (2.4), which is the quasi-polynomial

$$\chi_\tau(s) = Q_0(s) + Q_1(s)e^{-\tau s}, \tag{2.7}$$

where the real polynomials $Q_0(s)$ and $Q_1(s)$ satisfy the following assumptions:

$\mathcal{A}_1$: $\deg Q_0(s) \geq \deg Q_1(s)$,

$\mathcal{A}_2$: $|\lim_{s \to \infty} Q_1(s)/Q_0(s)| < 1$,

$\mathcal{A}_3$: $Q_0(s)$ and $Q_1(s)$ have no common roots in $\overline{\mathbb{C}}_0$,

$\mathcal{A}_4$: $Q_0(0) + Q_1(0) \neq 0$.

Assumption $\mathcal{A}_1$ just says that $\chi_\tau(s)$ is either neutral or retarded. $\mathcal{A}_2$ guarantees that there are no neutral root chains in $\overline{\mathbb{C}}_0$. Indeed, roots of (2.7) satisfy the relation $e^{\tau \operatorname{Re} s} = |Q_1(s)/Q_0(s)|$, meaning that as $s \to \infty$ they are all in the open left-half plane. In other words, $\mathcal{A}_2$ is equivalent to $\rho(D_{zw}) < 1$ for the system in Fig. 2.1. Common unstable roots of $Q_0(s)$ and $Q_1(s)$ are roots of $\chi_\tau(s)$ regardless of τ, which justifies $\mathcal{A}_3$. If $\mathcal{A}_4$ does not hold, then $\chi_\tau(s)$ has an (unstable) root at the origin for all τ. Thus, $\mathcal{A}_{1\text{-}4}$ do not impose any loss of generality, if they do not hold, then the stability analysis is futile.

By the logic of the method, we now analyze pure imaginary roots of $\chi_\tau(s)$ for $\tau > 0$. In other words, we seek for $\omega \in \mathbb{R}$ that solve

$$Q_0(j\omega) + Q_1(j\omega)e^{-j\tau\omega} = 0 \quad \Longleftrightarrow \quad e^{j\tau\omega} = -\frac{Q_1(j\omega)}{Q_0(j\omega)}.$$

The latter equation, in turn, is equivalent to the following two equalities:

$$|Q_0(j\omega)| = |Q_1(j\omega)| \tag{2.8a}$$

($Q_0(j\omega)$ and $Q_1(j\omega)$ cannot vanish simultaneously by $\mathcal{A}_3$), known as the *magnitude relation*, and

$$\tau\omega = \arg Q_1(j\omega) - \arg Q_0(j\omega) + (2k - 1)\pi \quad \text{for some } k \in \mathbb{Z}, \tag{2.8b}$$

dubbed the *phase relation*. Three observations on potential solutions of (2.8) in ω and τ are in order. First, if $\omega = 0$ solves the gain relation (2.8a), then the phase relation (2.8b) is not valid because of $\mathcal{A}_4$. This agrees with the intuition that roots cannot cross the imaginary axis at the origin, τ has no effect on $\chi_\tau(s)$ there. Second, if $\omega = \omega_i \neq 0$ solves (2.8a), then so does $\omega = -\omega_i$ and every τ solving (2.8b) for ω_i does that for $-\omega_i$ too. Therefore, roots always migrate in pairs. Third, if $\omega = \omega_i > 0$ solves (2.8a), then (2.8b) is solved by all positive

$$\tau_{ik} = \tau_{i0} + \frac{2\pi}{\omega_i}k, \quad k \in \mathbb{Z}_+, \tag{2.9}$$

where τ_{i0} is the smallest nonnegative solution of the phase relation for ω_i. Thus, to find pure imaginary roots of $\chi_\tau(we)$ s only need to find all positive solutions of the magnitude relation (2.8a), which are known as *crossing frequencies*. It is readily seen that these frequencies are the positive roots of

$$\phi(\omega) = Q_0(j\omega)Q_0(-j\omega) - Q_1(j\omega)Q_1(-j\omega), \tag{2.10}$$

which is an even polynomial whose leading coefficient is positive, by $\mathcal{A}_{1,2}$, and whose effective degree, i.e. the degree with respect to ω^2, equals that of $Q_0(s)$. If $\phi(\omega)$ has no positive real roots, no imaginary

axis crossings can take place and stability properties are delay independent. If (2.10) is solvable, then there are an infinite number of crossings as τ increases. But if roots of (2.7) do cross $j\mathbb{R}$ as τ grows, it happens only at a *finite number of points, independent of τ*. This is an important property, which facilitates the characterization of stability regions in terms of τ.

Having found crossing frequencies, the next step is to understand directions of those crossings. The following result clarifies this issue:

Lemma 2.2. *Let $\omega_i > 0$ be a solution of $\phi(\omega_i) = 0$. Each pure imaginary point $j\omega_i$ is*

1. *a switch iff $\phi(\omega)$ changes its sign from minus to plus at $\omega = \omega_i$ as ω increases,*
2. *a reversal iff $\phi(\omega)$ changes its sign from plus to minus at $\omega = \omega_i$ as ω increases,*
3. *a tangential point, at which no roots of $\chi_\tau(s)$ cross the imaginary axis, otherwise.*

In particular, the point is a switch (reversal) if $\mathrm{d}\phi(\omega)/\mathrm{d}\omega|_{\omega=\omega_i} > 0$ ($\mathrm{d}\phi(\omega)/\mathrm{d}\omega|_{\omega=\omega_i} < 0$).

Proof. Crossing directions are determined by the function

$$\sigma(\omega) = \operatorname{sign} \operatorname{Re} \left. \frac{\mathrm{d}s}{\mathrm{d}\tau} \right|_{s=j\omega}.$$

Namely, we have a switch at ω_i if $\sigma(\omega_i) > 0$, a reversal if $\sigma(\omega_i) < 0$, and an uncertain situation if $\sigma(\omega_i) = 0$, where higher derivatives are required. Thus, our first goal is to calculate $\sigma(\omega)$ at the imaginary roots of $\chi_\tau(s)$. To this end, differentiate the characteristic function by τ along any of its roots:

$$0 = \frac{\mathrm{d}\chi_\tau(s)}{\mathrm{d}\tau} = \frac{\mathrm{d}Q_0(s)}{\mathrm{d}s}\frac{\mathrm{d}s}{\mathrm{d}\tau} + \frac{\mathrm{d}Q_1(s)}{\mathrm{d}s}\frac{\mathrm{d}s}{\mathrm{d}\tau}e^{-\tau s} - Q_1(s)e^{-\tau s}\left(\tau\frac{\mathrm{d}s}{\mathrm{d}\tau} + s\right).$$

Hence,

$$\frac{\mathrm{d}s}{\mathrm{d}\tau} = \frac{sQ_1(s)e^{-\tau s}}{Q_0'(s) + Q_1'(s)e^{-\tau s} - \tau Q_1(s)e^{-\tau s}} = -s\left(\frac{Q_0'(s)}{Q_0(s)} - \frac{Q_1'(s)}{Q_1(s)} + \tau\right)^{-1},$$

where equality $Q_1(s)e^{-\tau s} = -Q_0(s)$ was used and $(\cdot)'$ stands for the differentiation with respect to s. Because $\operatorname{sign} \operatorname{Re} z^{-1} = \operatorname{sign} \operatorname{Re} z$,

$$\sigma(\omega) = \operatorname{sign} \operatorname{Re}\left[-\frac{1}{j\omega}\left(\frac{Q_0'(j\omega)}{Q_0(j\omega)} - \frac{Q_1'(j\omega)}{Q_1(j\omega)} + \tau\right)\right]$$

$$= \operatorname{sign} \operatorname{Re}\left[\frac{j}{\omega}\left(\frac{Q_0'(j\omega)}{Q_0(j\omega)} - \frac{Q_1'(j\omega)}{Q_1(j\omega)}\right)\right] \qquad \left(\text{because } \operatorname{Re}\frac{\tau}{j\omega} = 0\right)$$

$$= \operatorname{sign} \operatorname{Re}\left[j\left(\frac{Q_0'(j\omega)}{Q_0(j\omega)} - \frac{Q_1'(j\omega)}{Q_1(j\omega)}\right)\right] \qquad (\text{because } \omega > 0)$$

Multiplying expression under "sign" by $Q_0(j\omega)Q_0(-j\omega) = Q_1(j\omega)Q_1(-j\omega) > 0$ we get:

$$\sigma(\omega) = \operatorname{sign} \operatorname{Re}\left[j\left(\frac{\mathrm{d}Q_0(j\omega)}{\mathrm{d}(j\omega)}Q_0(-j\omega) - \frac{\mathrm{d}Q_1(j\omega)}{\mathrm{d}(j\omega)}Q_1(-j\omega)\right)\right]$$

$$= \operatorname{sign} \operatorname{Re}\left[\frac{\mathrm{d}Q_0(j\omega)}{\mathrm{d}\omega}Q_0(-j\omega) - \frac{\mathrm{d}Q_1(j\omega)}{\mathrm{d}\omega}Q_1(-j\omega)\right].$$

Because $\operatorname{sign} \operatorname{Re} z = \operatorname{sign}(z + \bar{z})$,

$$\sigma(\omega) = \operatorname{sign}\left(\frac{\mathrm{d}Q_0(j\omega)}{\mathrm{d}\omega}Q_0(-j\omega) - \frac{\mathrm{d}Q_1(j\omega)}{\mathrm{d}\omega}Q_1(-j\omega) + \frac{\mathrm{d}Q_0(-j\omega)}{\mathrm{d}\omega}Q_0(j\omega) - \frac{\mathrm{d}Q_1(-j\omega)}{\mathrm{d}\omega}Q_1(j\omega)\right)$$

$$= \operatorname{sign}\frac{\mathrm{d}\phi(\omega)}{\mathrm{d}\omega}.$$
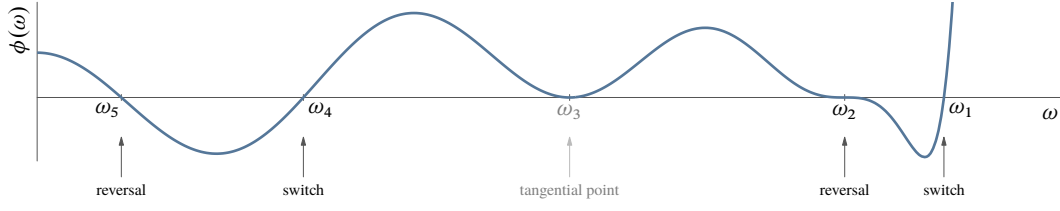
Fig. 2.4: Qualitative sketch of $\phi(\omega)$

This proves the last statement.

To complete the proof we need to address the singular case of $\sigma(\omega_i) = 0$. Its handling is quite technical and can be found in [78, §6.2]. $\qquad\qquad\qquad\qquad\qquad\qquad\qquad\qquad\qquad\qquad\qquad\qquad\qquad$ $\square$

Remarkably, not only crossing frequencies, but also crossing directions are independent of τ. Moreover, because $\phi(\omega)$ is even and its leading coefficient is positive (by $\mathcal{A}_2$), $\lim_{\omega\to\infty}\phi(\omega) = +\infty$. This means that the last, at the highest ω, cross of the zero level by it is always a point where the sign changes from minus to plus. Hence, the highest non-tangential crossing frequency is always a switch. Also, switch and reversal frequencies always alternate, see Fig. 2.4 for a qualitative picture.

Having understood crossing directions at each crossing frequency, it is time to return to the delay chains in (2.9), which solve the phase relation (2.8b). Each crossing frequency determines such a chain and each chain is stuck with the same crossing direction. All we need now is to order all crossing delays as an ascendant sequence $\{\tau_j\}_{j\in\mathbb{Z}_+}$ with $\tau_0 = 0$, still marked by their crossing direction, and start counting the number of $\mathbb{C}_0$ roots of $\chi_\tau(s)$, say $\nu\in\mathbb{Z}_+$, as τ grows from $\tau = 0$ up. At each τ_j the counter ν changes, so we end up with a sequence $\{\nu_j\}_{j\in\mathbb{Z}_+}$. Its starting point is the zero-delay ν_0 and ν_j at each $j \in \mathbb{N}$ are updated as

$$\nu_j = \begin{cases} \nu_{j-1} + 2 & \text{if } \tau_j \text{ corresponds to a switch} \\ \nu_{j-1} - 2 & \text{if } \tau_j \text{ corresponds to a reversal} \\ \nu_{j-1} & \text{if } \tau_j \text{ corresponds to a tangential point} \end{cases} \qquad (2.11)$$

(the counter changes by 2 as roots migrate at both $j\omega_j$ and $-j\omega_j$). The system is then stable in each interval $\tau \in (\tau_j, \tau_{j+1})$ with $\nu_j = 0$. There number of such intervals might be arbitrary and the first stable interval is not necessarily $[0, \tau_1)$, meaning that the delay might have a stabilizing effect. Anyhow, unless all crossing frequencies are tangential points, there is always a finite $j_\star \in \mathbb{Z}_+$ such that $\nu_j > 0$ for all $j \geq j_\star$, i.e. the counting may stop at a finite j. This is because the highest non-tangential crossing frequency ω_l is always a switch, so the distance between two successive switch delays in that chain, $\tau_{l,k+1} - \tau_{lk} = 2\pi/\omega_l$, is always smaller than that between any possible reversal delays. Hence, switches accumulate faster and the sequence $\{\nu_j\}$ is unbounded.

Example 2.8. Now, consider again the system from (2.6) for $q_{00} = 1$, $q_{01} = 0.1$, and some $q_{10} > 0$. The zero-delay characteristic polynomial is $\chi_0(s) = s^2 + 0.1s + 1 + q_{10}$ in this case and it is Hurwitz, i.e. $\nu_0 = 0$. The polynomial

$$\phi(\omega) = (-\omega^2 + j0.1\omega + 1)(-\omega^2 - j0.1\omega + 1) - q_{10}^2 = \omega^4 - 2\cdot 0.995\,\omega^2 + 1 - q_{10}^2$$

and $\dot\phi(\omega) = 4\omega(\omega^2 - 0.995)$ is zero only if $\omega^2 = 0.995$. Four scenarios are possible, depending on q_{10}.

1. If $0 < q_{10} < \sqrt{1 - 0.995^2} \approx 0.0999$, there are no real roots of $\phi(\omega)$. Hence, taking into account that $\nu_0 = 0$, the system is stable for all $\tau \geq 0$, i.e. it is *delay-independent stable*.

2. If $q_{10} = \sqrt{1 - 0.995^2}$, there is a double positive real roots of $\phi(\omega)$,

$$\omega_{1,2}^2 = 0.995.$$

Because $\phi(\omega) = (\omega^2 - 0.995)^2 \geq 0$ for this q_{10}, $\phi(\omega)$ does not change its sign at crossing frequencies and we have a tangential point. The delays at which the roots of $\chi_\tau(s)$ are on the imaginary axis can be determined from the phase relation (2.8b). To this end, note that

$$\arg Q_1(j\omega) - \arg Q_0(j\omega) = \arg q_{10} - \arg(1 - \omega^2 + j0.1\omega) = \begin{cases} \arctan \frac{0.1\omega}{\omega^2 - 1} & \text{if } 0 \leq \omega \leq 1 \\ \arctan \frac{0.1\omega}{\omega^2 - 1} - \pi & \text{if } \omega \geq 1 \end{cases}$$

Because $\omega_{1,2} < 1$, (2.8b) reads

$$\tau\omega_{1,2} = \arctan \frac{0.1\omega_{1,2}}{\omega_{1,2}^2 - 1} + (2k - 1)\pi \approx -1.5207 + (2k - 1)\pi$$

and crossing delays are positive iff $k \in \mathbb{N}$. Thus, the system is stable iff

$$\tau \neq 1.62495 + 6.31476k, \quad k \in \mathbb{Z}_+.$$

3. If $\sqrt{1 - 0.995^2} < q_{10} < 1$, there are two positive real roots of $\phi(\omega)$,

$$\omega_1^2 = 0.995 + \sqrt{0.995^2 - 1 + q_{10}^2} \quad \text{and} \quad \omega_2^2 = 0.995 - \sqrt{0.995^2 - 1 + q_{10}^2},$$

the first of which is a switch and the second is a reversal. To illustrate properties of the system, select $q_{10} = 0.4$, like in the Nyquist analysis of Example 2.7. With this choice $\omega_1 \approx 1.1757$ and $\omega_2 \approx 0.7795$ and the phase relations read

$$\tau_{1k} \approx 0.2537 + 5.3441k = \{0.2537, 5.5978, 10.9419, 16.286, 21.6301, 26.9742, \ldots\}$$

for switches and

$$\tau_{2k} \approx 3.7785 + 8.0602k = \{3.7785, 11.8387, 19.8989, 27.9591, 36.0193, \ldots\}$$

for reversals. The sequence of all crossing delays is then (gray elements mark reversals)

$$\{\tau_j\} = \{0, 0.2537, 3.7785, 5.5978, 10.9419, 11.8387, 16.286, 19.8989, 21.6301, 26.9742, 27.9591, \ldots\}.$$

Hence, the counter of unstable poles reads $\{\nu_j\} = \{0, 2, 0, 2, 4, 2, 4, 2, 4, 6, 4, \ldots\}$ in this case. At $j = 3$ and $j = 4$ we have two successive switches (and, expectably, never two successive reversals). Thus, we may stop counting after $j = 4$ and conclude the system is stable iff

$$\tau \in [0, 0.2537) \cup (3.7785, 5.5978),$$

which agrees with what we have via the Nichols chart in Fig. 2.3.

4. If $q_{10} \geq 1$, there is one positive real root of $\phi(\omega)$,

$$\omega_1^2 = 0.995 + \sqrt{0.995^2 - 1 + q_{10}^2} \geq 1.99$$

and it is a switch, of course. This implies that the system is stable only until the first crossing delay, τ_{10}. The phase relation (2.8b) reads now (mind that $\omega_1 > 1$)

$$\tau\omega_1 = \arctan \frac{0.1\omega_1}{\omega_1^2 - 1} - \pi + (2k - 1)\pi = \arctan \frac{0.1\omega_1}{\omega_1^2 - 1} + 2(k - 1)\pi,$$

so its minimum positive solution corresponds to $k = 1$. Hence, the system is stable iff

$$0 \leq \tau < \frac{1}{\omega_1} \arctan \frac{0.1\omega_1}{\omega_1^2 - 1}, \quad \text{where } \omega_1^2 = 0.995 + \sqrt{q_{10}^2 - 0.009975}$$

which is a decreasing function of $q_{10} \geq 1$, as a matter of fact.

Ugh, that was long, but nevertheless quite straightforward ...   ▽

Example 2.9. Let us return to the system studied in Example 2.5, whose transfer function

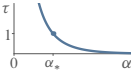$$P_\tau(s) = \frac{\alpha(e^{\alpha-s} - 1)}{s - \alpha e^{\alpha-s}}.$$

We already saw that the root of its characteristic function at $s = \alpha$ is a removable singularity of $P_\tau(s)$. Moreover, it is readily seen that no other root of the denominator may be canceled by a root of the numerator (any zero must satisfy $e^{\alpha-s} = 1$, at which points the roots of the denominator satisfy $s = \alpha$). Therefore, $P_\tau \in H_\infty$ iff the denominator has no other roots in $\bar{\mathbb{C}}_0$. To apply the delay sweeping analysis to this task, we need to consider a general delay τ, so the characteristic function of interest

$$\chi_\tau(s) = s - \alpha e^\alpha e^{-\tau s}.$$

It clearly satisfies $\mathcal{A}_{1\text{-}4}$. The zero-delay version of it, $\chi_0(s) = s - \alpha e^\alpha$, has its only root at $s = \alpha e^\alpha$, in $\mathbb{C}_0$, so it is not Hurwitz. Moreover, the polynomial $\phi(\omega) = \omega^2 - \alpha^2 e^{2\alpha}$ has only one positive real root, at $\omega_1 = \alpha e^\alpha$, which must be a switch. Hence, P_τ with $\tau = 1$ is stable iff the first crossing delay $\tau < 1$. By (2.8b), the crossing delays satisfy, for $k \in \mathbb{Z}$,

$$\tau \omega_1 = \arg j\omega_1 - \arg \alpha e^\alpha + (2k-1)\pi = \frac{\pi}{2} - 0 + (2k-1)\pi \implies \tau = \frac{(4k-1)\pi}{2\alpha e^\alpha}.$$

The smallest positive solution

$$\tau = \frac{3\pi}{2\alpha e^\alpha} = \quad \text{}$$

then. This crossing delay is a strictly decreasing function of α ranging the whole $\mathbb{R}_+$. Hence, there is a unique α_* satisfying $\alpha_* e^{\alpha_*} = 1.5\pi$ at which $\tau = 1$ (in fact, $\alpha_* \approx 1.29313$) and P_τ is stable iff $\alpha < \alpha_*$. This explains how the upper bound on α was obtained in Example 2.5.   ▽

Remark 2.3 (necessary condition). An interesting, and sometimes useful, observation from the developments above is that roots can cross the imaginary axis only in pairs. Therefore, if $\chi_0(s)$ has an odd number of unstable poles, the system is delay-independent unstable. Using Vieta's formulae, this observation leads to a simple necessary condition for the existence of τ for which all roots of $\chi_\tau(s)$ are in $\mathbb{C} \setminus \bar{\mathbb{C}}_0$. Namely, if $\chi_0(s) = s^n + \chi_{0,n-1}s^{n-1} + \cdots + \chi_{01}s + \chi_{00}$, then there is no $\tau \geq 0$ for which all roots of $\chi_\tau(s)$ are stable whenever $\chi_{00} \leq 0$. The case of $\chi_{00} < 0$ is exactly the condition for $\chi_0(s)$ to have an odd number of unstable roots. The case of $\chi_{00} = 0$ corresponds to the situation when $\chi_\tau(0) = 0$ for all τ.   ▽

Remark 2.4 (Nyquist connections). Comparing the results of the third scenario of Example 2.8 with those in §2.1.4, we can see that crossing frequencies of the former match the crossover frequencies of the latter. This is not a coincidence and is a general property, just because $Q_1(s)/Q_0(s)$ is exactly the "open-loop" transfer function $G_{zw}(s)$. In the same vein, the quantities τ_{i0} in (2.9) can be interpreted as delay margins of the loop L_τ from (2.5). Still, there are qualitative differences. For instance, while the Nyquist arguments are based on the number of unstable roots of $Q_0(s)$, the delay sweeping method uses unstable roots of $Q_0(s) + Q_1(s)$ as its starting point. It might be that this very difference renders the direct method easier to "algoritmize" than the Nyquist criterion. At the same time, the Nyquist criterion arguably offers more insight into properties of the system and is more visual.   ▽

Multiple-delay quasi-polynomials

Arguments above extend to general commensurate quasi-polynomials of form (2.4), although technicalities become rather cumbersome. To provide a flavor of the approach and associate complications, consider the two-delay version of the problem for

$$\chi_\tau(s) = Q_0(s) + Q_1(s)e^{-\tau s} + Q_2(s)e^{-2\tau s},$$

such that counterparts of $\mathcal{A}_{1\text{-}4}$ hold (i.e. no neutral chains in $\overline{\mathbb{C}}_0$, no common unstable roots of all $Q_i(s)$, and $\sum_i Q_i(0) \neq 0$). The underlying idea is still to count imaginary crossings of roots of this $\chi_\tau(s)$ as τ increases from $\tau = 0$. Because $\chi_\tau(s)$ is real, its pure imaginary roots coincide with those of

$$e^{-2\tau s}\chi_\tau(-s) = Q_2(-s) + Q_1(-s)e^{-\tau s} + Q_0(-s)e^{-2\tau s}.$$

But then, every imaginary root of $\chi_\tau(s)$ is also a root of yet another quasi-polynomial

$$\begin{aligned}
\tilde{\chi}_\tau(s) &:= Q_0(-s)\chi_\tau(s) - Q_2(s)e^{-2\tau s}\chi_\tau(-s) \\
&= Q_0(-s)Q_0(s) - Q_2(-s)Q_2(s) + \big(Q_0(-s)Q_1(s) - Q_1(-s)Q_2(s)\big)e^{-\tau s},
\end{aligned}$$

which is a single-delay quasi-polynomial of the form (2.7) and whose imaginary roots we can analyze. The catch is that $\tilde{\chi}_\tau(s)$ might have additional imaginary roots, which are an artifact of the procedure. To understand these additional roots, consider the magnitude equality part of the equation $\tilde{\chi}_\tau(j\omega) = 0$, which is

$$(|Q_0(j\omega)| - |Q_2(j\omega)|)|\chi_\tau(j\omega)| = 0.$$

This equality holds if either $|\chi_\tau(j\omega)| = 0$, which is what we are interested in, or $|Q_0(j\omega)| = |Q_2(j\omega)|$, which is an artifact in potentia (it might not be, there is also a phase relation to satisfy). Thus, all positive frequencies at which the magnitudes of Q_0 and Q_2 coincide should be checked separately. There might be only a finite number of such frequencies (otherwise, we necessarily have $Q_0(s) = Q_2(s)$ and a neutral chain on the imaginary axis, which contradicts our assumptions). Assuming that $|Q_0(j\omega_i)| \neq |Q_2(j\omega_i)|$ at all imaginary roots $j\omega_i$ of $\chi_\tau(s)$, it can be shown [78, Sec. 6.3] that the crossing directions of $\tilde{\chi}_\tau(s)$ and $\chi_\tau(s)$ coincide iff $|Q_0(j\omega_i)| > |Q_2(j\omega_i)|$ and are opposite iff $|Q_0(j\omega_i)| < |Q_2(j\omega_i)|$ at each crossing frequency ω_i.

Example 2.10. Let

$$\chi_\tau(s) = s + e^{-\tau s} + e^{-2\tau s},$$

for which $\chi_0(s) = s + 2$ is Hurwitz. The only positive frequency at which $|Q_0(j\omega)| = |Q_2(j\omega)|$ is $\omega = 1$ then. Now,

$$\tilde{\chi}_\tau(s) = -s^2 - 1 - (s+1)e^{-\tau s}$$

and the corresponding $\tilde{\phi}(\omega) = (1 - \omega^2)^2 - (1 + \omega^2) = \omega^2(\omega^2 - 3)$ has one admissible solution, $\omega_1 = \sqrt{3}$. As this $\omega_1 \neq 1$, there are no artifact crossing frequencies. All crossings of $\tilde{\chi}_\tau(s)$ at this frequency are switches and, because $|Q_0(j\omega_1)| = \sqrt{3} > 1 = |Q_2(j\omega_1)|$, so are the crossings of $\chi_\tau(s)$. To find the smallest positive τ at which this switch takes place, consider the phase relation for $\tilde{\chi}_\tau(s)$, which is

$$\tau\omega_1 = \arg(-1 - j\omega_1) - \arg(\omega_1^2 - 1) + (2k - 1)\pi = \arctan\omega_1 + 2\pi k = \frac{\pi}{3} + 2\pi k.$$

Its smallest positive solution is $\tau = \pi/(3\sqrt{3}) \approx 0.6046$. Hence,

$$0 \leq \tau < \frac{\pi}{3\sqrt{3}}$$

is the range of delays for which this $\chi_\tau(s)$ has no unstable roots. $\qquad\triangledown$

The procedure outlined above applies to general quasi-polynomials of the form (2.2) recursively, each step reducing one delay. It should be clear that even in a general commensurate case crossing frequencies and root directions are independent of the delay, which is a useful insight. Computational details are rather dull though. Also, dimensions of involved polynomials grow rapidly in those iterations, so the approach might not be quite practical for quasi-polynomials of the form (2.4) with a large k.

Remark 2.5 (incommensurate delays). The situation is way more complicated for quasi-polynomials with incommensurate delays. Roots crossings there no longer happen at a finite number of frequencies, so the analysis is a nightmare even for quasi-polynomials with 2 delays and constant $Q_1(s)$ and $Q_2(s)$. $\qquad\triangledown$
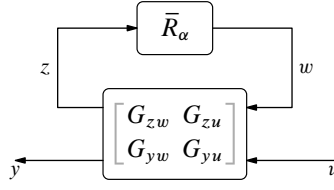
Fig. 2.5: General interconnection with Rekašius substitution

2.1.6   Bilinear (Rekašius) transformation

An alternative take on the idea of checking crossings of the imaginary axis by roots of $\chi_\tau(s)$ as τ sweeps the whole positive semi-axis was proposed by Zenonas V. Rekašius in [63]. A key observation is that at each frequency $\omega \in \mathbb{R}$, the locus of $\mathrm{e}^{-\mathrm{j}\tau\omega}$ in the complex plane as τ sweeps $\mathbb{R}_+$ (which is the unit circle $\mathbb{T}$, as a matter of fact) coincides with that of $\bar{R}_\alpha(\mathrm{j}\omega)$, where

$$\bar{R}_\alpha(s) := \frac{-s + \alpha}{s + \alpha}, \tag{2.12}$$

as α sweeps the whole real axis $\mathbb{R}$. Moreover, for every $\omega_i \in \mathbb{R} \setminus \{0\}$ and $\tau_i \in \mathbb{R}_+$ there is $\alpha_i \in \mathbb{R}$, viz.

$$\alpha_i = \omega_i \cot \frac{\tau_i \omega_i}{2}, \tag{2.13}$$

such that the equality $\mathrm{e}^{-\mathrm{j}\tau_i\omega_i} = \bar{R}_{\alpha_i}(\mathrm{j}\omega_i)$ holds.

These observations suggest that frequency-response properties of the delay systems in Fig. 2.1 can be studied in terms of those of the finite-dimensional system in Fig. 2.5, which is obtained by the substitution $\bar{D}_\tau \to \bar{R}_\alpha$. A state-space realization of this finite-dimensional system can be derived similarly to that of the delay system (1.27). The only difference is the replacement of the relation $w(t) = z(t - \tau)$ with

$$\begin{cases} \dot{x}_{\mathrm{R}}(t) = -\alpha x_{\mathrm{R}}(t) + z(t) \\ w(t) = 2\alpha x_{\mathrm{R}}(t) - z(t) \end{cases}$$

which represents the Laplace-domain relation $W(s) = (-s + \alpha)/(s + \alpha)Z(s)$. Eliminating z and w from the model we then end up with the transfer function of $P_\tau : u \mapsto y$ in terms of its state-space realization

$$P_\tau(s) = \left[\begin{array}{cc|c} A - B_w R_{zw} C_z & 2\alpha B_w R_{zw} & B_u - B_w R_{zw} D_{zu} \\ R_{zw} C_z & \alpha(D_{zw} - I) R_{zw} & R_{zw} D_{zu} \\ \hline C_y - D_{yw} R_{zw} C_z & 2\alpha D_{yw} R_{zw} & D_{yu} - D_{yw} R_{zw} D_{zu} \end{array} \right], \tag{2.14}$$

where $R_{zw} := (I + D_{zw})^{-1}$ is well defined if we assume that $\rho(D_{zw}) < 1$. The corresponding characteristic function is

$$\chi_\alpha(s) := \det \left[\begin{array}{cc} sI - A + B_w R_{zw} C_z & 2\alpha B_w R_{zw} \\ R_{zw} C_z & sI + \alpha(I - D_{zw}) R_{zw} \end{array} \right] = \bar{\chi} \sum_{i=0}^{k} (s + \alpha)^{k-i} (\alpha - s)^i Q_i(s), \tag{2.15}$$

where the last expression follows from (2.4) for $\bar{\chi} \neq 0$ such that $\chi_\alpha(s)$ is monic. Nonzero pure imaginary roots of $\chi_\tau(s)$ in (2.4) coincide then with those of $\chi_\alpha(s)$ in (2.13). Moreover, crossing directions of such roots of $\chi_\alpha(s)$ are closely related to those of $\chi_\tau(s)$, as established by the result below.

Lemma 2.3. *Let s_τ and s_α be roots of $\chi_\tau(s)$ and $\chi_\alpha(s)$, respectively. If $\mathrm{j}\omega_i \neq 0$ is a root of both these functions, then*

$$\mathrm{sign} \, \mathrm{Re} \left. \frac{\mathrm{d}s_\tau}{\mathrm{d}\tau} \right|_{s=\mathrm{j}\omega_i} = -\mathrm{sign} \, \mathrm{Re} \left. \frac{\mathrm{d}s_\alpha}{\mathrm{d}\alpha} \right|_{s=\mathrm{j}\omega_i}.$$

Proof. Consider the equation

$$\det \begin{bmatrix} sI - A & -B_w \zeta \\ -C_z & I - D_{zw}\zeta \end{bmatrix} = 0$$

and let $\zeta(s)$ denote its solution. Clearly,

$$e^{-\tau s_\tau} = \zeta(s_\tau) \quad \text{and} \quad \frac{-s_\alpha + \alpha}{s_\alpha + \alpha} = \zeta(s_\alpha).$$

Thus,

$$\frac{d}{d\tau} e^{-\tau s_\tau} = -e^{-\tau s_\tau} \left(s_\tau + \tau \frac{ds_\tau}{d\tau} \right) = \zeta'(s_\tau) \frac{ds_\tau}{d\tau}$$

and

$$\frac{d}{d\alpha} \frac{-s_\alpha + \alpha}{s_\alpha + \alpha} = \frac{2}{(s_\alpha + \alpha)^2} \left(s_\alpha - \alpha \frac{ds_\alpha}{d\alpha} \right) = \zeta'(s_\alpha) \frac{ds_\alpha}{d\alpha},$$

where $\zeta'(s) := d\zeta(s)/ds$. Hence,

$$-e^{-\tau s_\tau} \left(s_\tau \left(\frac{ds_\tau}{d\tau} \right)^{-1} + \tau \right) = \frac{2}{(s_\alpha + \alpha)^2} \left(s_\alpha \left(\frac{ds_\alpha}{d\alpha} \right)^{-1} - \alpha \right)$$

whenever $s_\tau = s_\alpha$. In particular, at $s_\tau = s_\alpha = j\omega_i \neq 0$ we have that $e^{-j\tau\omega_i} = (-j\omega_i + \alpha)/(j\omega_i + \alpha)$ and

$$\tau + j\omega_i \left(\frac{ds_\tau}{d\tau} \right)^{-1} = \frac{2}{\omega_i^2 + \alpha^2} \left(\alpha - j\omega_i \left(\frac{ds_\alpha}{d\alpha} \right)^{-1} \right)$$

or, equivalently,

$$\left(\frac{ds_\tau}{d\tau} \right)^{-1} = -\frac{2}{\omega_i^2 + \alpha^2} \left(\frac{ds_\alpha}{d\alpha} \right)^{-1} + j\frac{1}{\omega_i} \left(\tau - \frac{2\alpha}{\omega_i^2 + \alpha^2} \right).$$

The result then follows by the fact that $\text{sign Re } z = \text{sign Re } z^{-1}$. $\qquad\blacksquare$

Thus, we can analyze imaginary crossings of $\chi_\tau(s)$ via those of $\chi_\alpha(s)$. A good news is that this $\chi_\alpha(s)$ is a standard polynomial, rather than a quasi-polynomial from (2.4). A bad news is that the parameters of $\chi_\alpha(s)$ are functions of α, so the analysis has to be carried out in parametric form. This can be done via the Routh–Hurwitz stability criterion, although handling singular cases there might be a mess. Arguably, the delay sweeping method is more streamlined and easier to use, especially in the analysis of various low-order applications, see Section 3.1. Still, the bilinear transformation may also be helpful in analyzing properties of delay systems, examples can be found in §4.1.1.

Example 2.11. Return to the system with G as in (2.6). Assume that $q_{00} = 1$, $q_{01} = 0.1$, and $q_{10} = 0.4$, like in the third item of Example 2.8. The counterpart of $\chi_\tau(s) = s^2 + 0.1s + 1 + 0.4e^{-\tau s}$ in this case is

$$\chi_\alpha(s) = s^3 + (\alpha + 0.1)s^2 + 0.1(\alpha + 6)s + 1.4\alpha.$$

We can construct its Routh array, of course, but for third-order polynomials the condition of having a pair of nonzero pure imaginary roots is

$$1.4\alpha = 0.1(\alpha + 6)(\alpha + 0.1) \quad \Longrightarrow \quad \alpha_{1,2} = \frac{7.9 \pm \sqrt{60.01}}{2}.$$

The corresponding imaginary roots (with positive frequencies) are then

$$s_{1,2} = j\sqrt{0.1(\alpha + 6)}|_{\alpha = \alpha_{1,2}},$$
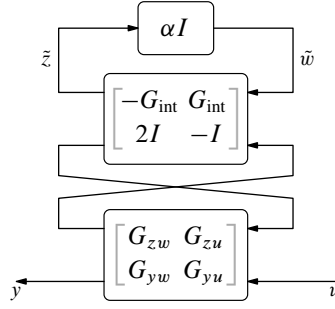
Fig. 2.6: Equivalent form of the system in Fig. 2.5 with isolated α, here $G_{\text{int}}(s) = 1/s \cdot I$

which yields crossing frequencies $\omega_1 \approx 1.1757$ and $\omega_2 \approx 0.7795$, exactly as in Example 2.8. Crossing directions can be found by constructing the corresponding root locus plot. But we already know, from the analysis in §2.1.5, that the highest crossing frequency is a switch and the next one is a reversal. Inverting (2.13), we then get

$$\tau_{ik} = \frac{2}{\omega_i}\left(\arctan\frac{\omega_i}{\alpha_i} + \pi k\right), \quad \forall k \in \mathbb{Z}$$

from which the results derived in Example 2.8 are recovered.   ▽

Remark 2.6 (pulling α out). It is readily seen that $\bar{R}_\alpha(s) = \mathcal{F}_u(\left[\begin{smallmatrix} -1/s & 1/s \\ 2 & -1 \end{smallmatrix}\right], \alpha)$. This form facilitates extracting α from the LFT in Fig. 2.5 in the equivalent form presented in Fig. 2.6. The latter system, in turn, is equivalent to $\mathcal{F}_u(\tilde{G}, \alpha I)$, where

$$\tilde{G}(s) = \left[\begin{array}{cc|cc} 0 & (I + D_{zw})^{-1}C_z & (D_{zw} - I)(I + D_{zw})^{-1} & (I + D_{zw})^{-1} \\ 0 & A - B_w(I + D_{zw})^{-1}C_z & 2B_w(I + D_{zw})^{-1} & B_u - B_w(I + D_{zw})^{-1}D_{zu} \\ \hline I & 0 & 0 & 0 \\ 0 & C_y - D_{yw}(I + D_{zw})^{-1}C_z & 2D_{yw}(I + D_{zw})^{-1} & D_{yu} - D_{yw}(I + D_{zw})^{-1}D_{zu} \end{array}\right]$$

is the Redheffer start product $\tilde{G} = \left[\begin{smallmatrix} -G_{\text{int}} & G_{\text{int}} \\ 2I & -I \end{smallmatrix}\right] \star G$, where G_{int} is the integrator with the transfer function $G_{\text{int}}(s) = 1/s \cdot I$.   ▽

2.2 Lyapunov stability and Lyapunov's direct method

Another way to address the stability of dynamic systems is to analyze the Lyapunov stability of unforced motion via Lyapunov functions. These methods are not in the center of these notes, mainly because of personal preferences (Lyapunov methods do not appear to be well suited to analyze meaningful control performance and to design dynamic controllers). So such methods are only outlined below. There is hefty literature on this subject, which can be consulted for more details and (sometimes) insight, see e.g. [22, 28] and the references therein.

2.2.1 Ordinary differential equations

We start with a brief overview of the Lyapunov stability and Lyapunov's direct (aka second) method for finite-dimensional systems described by equations of the form

$$\dot{x}(t) = f(x(t)), \tag{2.16}$$

where $x : \mathbb{R}_+ \to \mathbb{R}^n$ is a state and $f : \mathbb{R}^n \to \mathbb{R}^n$ is a locally Lipschitz continuous function. Assume that $x_{\text{eq}} \in \mathbb{R}$ is its equilibrium, i.e. $f(x_{\text{eq}}) = 0$. We say that this equilibrium is *stable* if for every $\epsilon > 0$ there

is $\delta = \delta(\epsilon) > 0$ such that $\|x(0) - x_{eq}\| < \delta \implies \|x(t) - x_{eq}\| < \epsilon$ for all $t \in \mathbb{R}_+$. *Asymptotic stability* requires, in addition, that there is $\delta > 0$ such that $\|x(0) - x_{eq}\| < \delta \implies \lim_{t\to\infty} \|x(t) - x_{eq}\| = 0$. The set of initial conditions that generate converging states is known as the region of attraction of an asymptotically stable equilibrium. If the region of attraction is the whole $\mathbb{R}^n$, then the equilibrium is said to be *globally asymptotically stable*.

A key idea of Lyapunov's direct method is that the stability of (2.16) can be analyzed without the need to solve it explicitly. Rather, stability can be concluded from properties of the derivative of certain function $V : \mathbb{R}^n \to \mathbb{R}$, known as a *Lyapunov function*, along trajectories of (2.16). Without loss of generality we assume hereafter that $x_{eq} = 0$, in which case $f(0) = 0$ (otherwise, shifting $x \to x - x_{eq}$ does the trick). In this case a legitimate Lyapunov function shall be continuously differentiable and satisfy $V(x) > 0$ for all $x \neq 0$ and $V(0) = 0$. The derivative of V along trajectories of (2.16) is defined as

$$\dot{V}(x) := \frac{dV(x)}{dt} = \frac{\partial V(x)}{\partial x} \frac{dx}{dt} = \frac{\partial V(x)}{\partial x} f(x).$$

The following results hold true:

1. if $\dot{V}(x) \leq 0$ for all x, then (2.16) is Lyapunov stable;

2. if $\dot{V}(x) < 0$ for all $x \neq 0$, then (2.16) is stable asymptotically;

3. if $\dot{V}(x) \leq 0$ for all x and $\dot{V}(x) \equiv 0$ implies $x \equiv 0$, then (2.16) is also stable asymptotically

(the last condition follows by LaSalle's invariance principle, which says that if $\dot{V} \leq 0$, then all trajectories accumulate in the set $\{x \mid \dot{V}(x) = 0\}$). If the statements "for all x" above are understood as "for all x in some neighborhood of the origin," then properties are local. For global stability the statements above should be valid for all $x \in \mathbb{R}^n$ and the condition $\lim_{\|x\|\to\infty} V(x) = \infty$ hold.

A catch in the use of this method is to find a Lyapunov function, which might be a highly nontrivial task in its own. Still, in some situations such functions can be constructed. This is the case when a Lyapunov function can be interpreted as an energy function of the system, for instance. The problem is perhaps best understood for linear systems, where $f(x) = Ax$ for certain $A \in \mathbb{R}^{n \times n}$. A handy choice here is the *quadratic Lyapunov function*

$$V(x) = x'Px, \quad P = P' > 0. \tag{2.17}$$

With this choice $\dot{V}(x) = 2x'PAx = x'(PA + A'P)x$ and the system is stable if there is $P > 0$ such that $PA + A'P \leq 0$. This requirement can be formulated as the existence of $P > 0$ satisfying the Lyapunov equation $PA + A'P + C'C = 0$ for some C. In this case $\dot{V} = -\|Cx\|^2 \leq 0$. If C has full row rank, then $\|Cx\| > 0$ for all $x \neq 0$ and we have asymptotic stability. In fact, it is sufficient to have (C, A) observable, because in that case $Cx \equiv 0$ iff $x \equiv 0$ and we can apply LaSalle's invariance principle to conclude about asymptotic stability. Note that asymptotic stability does not imply that $\|x(t)\|$ is a monotonically decreasing function of t. Yet the existence of a quadratic Lyapunov function implies that in some coordinate bases, namely $P^{1/2}x$, the state of an asymptotically stable system does decay monotonically. This property is useful in analyzing various classes of switched systems.

2.2.2 Delay-differential equations

Now consider the delay system in Fig. 2.1. Because the purpose of this section is to provide mainly a flavor of the approach, in the analysis of its Lyapunov stability we consider only the particular case of retarded DDEs, for $D_{zw} = 0$, and concentrate on systems described by

$$\dot{x}(t) = Ax(t) + A_\tau x(t - \tau), \tag{2.18}$$

where $A_\tau := B_w C_z$. This is the autonomous version of (1.29) and we may consider $\check{x}_t \in C^n([-\tau, 0])$ as its state at a time instance t. If rank $A_\tau < n$, this is not a minimal state, cf. a comment after (1.29). Still,

this choice is sufficient for our purposes. If we assume that the initial condition $\check{x}_0 \in C^n([-\tau, 0])$, i.e. is continuous, then the solution of (2.18) exists on all $\mathbb{R}_+$ and is continuous as well, i.e. $\check{x}_t \in C^n(\mathbb{R})$ for all t.

Once the definition of state is clear, the extension of the notion of Lyapunov stability and of Lyapunov's direct method to (2.18) is conceptually straightforward. All we need is to replace the vector $x(t)$ with the function $\check{x}_t$. As such, the stability of (2.18) is defined as the existence of $\delta = \delta(\epsilon)$ such that (mind that the equilibrium is taken zero) $\|\check{x}_t\| < \epsilon$ for all t whenever $\|\check{x}_0\| < \delta$, where $\|\cdot\|$ is a norm on $C^n([-\tau, 0])$. The Lyapunov function is also supposed to be of the form $V(\check{x})$, possessing infinite-dimensional counterparts of properties stated in §2.2.1. The analogy would be even more evident if DDE (2.18) was cast as an operator differential equation in terms of $\check{x}_t$, see [10, Sec. 2.4]. However, dealing with such functions might be quite cumbersome. This motivated other approaches, developed via attempts to extend Lyapunov's method for DDEs like (2.18) while keeping conditions expressed in terms of $x(t)$ whenever possible. Two best known of them, outlined below, were put forward by Boris Razumikhin [62] and Nikolay Krasovskii [31].

Lyapunov–Razumikhin approach

The idea here is to still use a Lyapunov function based only on the vector $x(t)$, yet then replace the condition on its derivative with a weaker requirement. The result, which is an LTI version of [22, Thm. 5.4.2], is as follows.

Theorem 2.4 (Razumikhin). *If there is a continuous $V : \mathbb{R}^n \to \mathbb{R}$ such that $V(0) = 0$,*

$$\alpha(\|x\|) \le V(x) \le \beta(\|x\|), \tag{2.19a}$$

and

$$\dot{V}(x(t)) \le -\gamma(\|x(t)\|) \quad \text{whenever } V(x(t+\theta)) \le \rho(V(x(t))) \text{ for all } \theta \in [-\tau, 0] \tag{2.19b}$$

for continuous non-decreasing functions $\alpha, \beta, \gamma, \rho : \mathbb{R}_+ \to \mathbb{R}_+$ such that $\lim_{\|x\| \to \infty} \alpha(\|x\|) = \infty$ and $\rho(V) \ge V$, then (2.18) is Lyapunov stable. If in addition $\rho(V) > V$ for all $V > 0$, then (2.18) is stable asymptotically.

Loosely speaking, the Razumikhin approach does not require to keep the derivative of V negative all the time. Rather, it has to be enforced only when the current value of the Lyapunov function exceeds all those over the past history of the length τ. The example below illustrates the use of this approach. Although its procedure is not the state of the art, it does help to gain some insight into the method.

Example 2.12. Consider DDE (2.18) and select the quadratic Lyapunov function (2.17) for it. Condition (2.19a) holds then for $\alpha(\|x\|) = \lambda_{\min}(P)\|x\|^2$ and $\beta(\|x\|) = \lambda_{\max}(P)\|x\|^2$. Now,

$$\dot{V}(x(t)) = 2x'(t)P(Ax(t) + A_\tau x(t-\tau)) = \begin{bmatrix} x'(t) & x'(t-\tau) \end{bmatrix} \begin{bmatrix} A'P + PA & PA_\tau \\ A_\tau'P & 0 \end{bmatrix} \begin{bmatrix} x(t) \\ x(t-\tau) \end{bmatrix}.$$

This derivative cannot be negative for all t if we allow arbitrary $x(t)$ and $x(t-\tau)$, for the matrix in that quadratic form is not negative definite (its $(2,2)$ entry is zero). Yet we need its negativity only at time instanced when the second condition of (2.19b) holds. To exploit this fact, select $\rho(V) = \eta V$ for some $\eta > 1$, which is perhaps just an expedient choice. Condition (2.19b) is ensured then by the existence of $\zeta > 0$ such that

$$\dot{V}(x(t)) \le -\zeta x'(t)Px(t) \quad \text{whenever } x'(t+\theta)Px(t+\theta) \le \eta x'(t)Px(t) \text{ for all } \theta \in [-\tau, 0], \tag{2.20}$$

which corresponds to $\gamma(\|x\|) = \zeta \lambda_{\min}(P)\|x\|^2$. Checking (2.20) precisely, only at time instances when its second inequality holds, would not be easy. The trick is to relax it. Namely, consider the function

$$W(t) := \dot{V}(x(t)) + a(\eta x'(t)Px(t) - x'(t-\tau)Px(t-\tau)), \quad a > 0.$$

Clearly, $\eta x'(t) P x(t) \geq x'(t-\tau) P x(t-\tau)$ whenever $\eta x'(t) P x(t) \geq x'(t+\theta) P x(t+\theta)$ for all $\theta \in [-\tau, 0]$. Therefore, if $W(t) \leq -\zeta x'(t) P x(t)$, then (2.20) holds and we may endeavor to guarantee that

$$W(t) + \zeta x'(t) P x(t) = \begin{bmatrix} x'(t) & x'(t-\tau) \end{bmatrix} \begin{bmatrix} A'P + PA + (a\eta + \zeta)P & PA_\tau \\ A_\tau'P & -aP \end{bmatrix} \begin{bmatrix} x(t) \\ x(t-\tau) \end{bmatrix} \leq 0.$$

The latter is ensured if

$$\begin{bmatrix} A'P + PA + (a\eta + \zeta)P & PA_\tau \\ A_\tau'P & -aP \end{bmatrix} \leq 0 \iff \begin{bmatrix} A'P + PA + aP & PA_\tau \\ A_\tau'P & -aP \end{bmatrix} \leq -\begin{bmatrix} \epsilon P & 0 \\ 0 & 0 \end{bmatrix},$$

where $\epsilon := a(\eta - 1) + \zeta > 0$ may be arbitrarily small, as $\eta > 1$ and $\zeta > 0$ may be chosen freely. Thus, we end up with the inequality

$$\begin{bmatrix} A'P + PA + aP & PA_\tau \\ A_\tau'P & -aP \end{bmatrix} < 0. \tag{2.21}$$

If $P = P' > 0$ and $a > 0$ guaranteeing it exist, then system (2.18) is asymptotically stable. If a is fixed, then (2.21) is linear in its remaining free parameter P. Such inequalities are known as *linear matrix inequalities* (LMIs) and can be solved efficiently, see [66]. In fact, (2.21) is equivalent to a simpler LMI, $QA' + AQ + aQ - a^{-1}A_\tau Q A_\tau' < 0$ under $Q = P^{-1} > 0$. The scalar a may then be sought out by whatever ad hoc parametric search. On the downside, the condition derived here is normally conservative, i.e. the failure to solve (2.21) does not necessarily implies that the system is unstable for some τ. $\qquad \triangledown$

Lyapunov–Krasovskii approach

The idea here is to use a function of the whole state $\check{x}_t$, $V : C^n([-\tau, 0]) \to \mathbb{R}$, as a Lyapunov candidate. A simplification is that conditions on its positively and the negativity of its derivative can still be formulated in terms of $x(t)$, not the whole $\check{x}_t$. The following result is a linear version of [22, Cor. 5.3.1].

Theorem 2.5 (Krasovskii). *If there is a continuous $V(\check{x}) : C^n([-\tau, 0]) \to \mathbb{R}$ such that $V(0) = 0$,*

$$V(\check{x}) \geq \alpha(\|x\|), \quad and \quad \dot{V}(\check{x}) \leq -\beta(\|x\|) \tag{2.22}$$

for functions $\alpha, \beta : \mathbb{R}_+ \to \mathbb{R}_+$ such that $\lim_{\|x\| \to \infty} \alpha(\|x\|) = \infty$, then (2.18) is Lyapunov stable. If in addition $\beta(\|x\|) > 0$ for all $\|x\| > 0$, then (2.18) is stable asymptotically.

The dependencies of functions α and β only on $\|x(t)\|$ is a relaxation of expected conditions in terms of a norm of $\check{x}_t$ (although the bound on the derivative can be interpreted in terms of LaSalle's invariance principle, because $x \equiv 0$ obviously implies $\check{x} \equiv 0$). These conditions imply that, in principle, the choice of the Lyapunov function like in (2.17) is still legitimate, which is not quite obvious. However, such a choice would be futile in most situations, because it is not sufficiently rich for dynamics like (2.18). Hence, finding conditions on P guaranteeing stability is not normally possible for it, see the discussion in Example 2.12. This is why more elaborate functions are considered.

A natural general counterpart of the quadratic Lyapunov function (2.17) for DDE (2.18) would be

$$V(\check{x}_t) = x'(t) P_0 x(t) + 2x'(t) \int_{-\tau}^0 P_{0\tau}(s) x(t+s) \mathrm{d}s + \int_{-\tau}^0 \int_{-\tau}^0 x'(t+r) P_{\tau\tau}(r, s) x(t+s) \mathrm{d}s \, \mathrm{d}r \tag{2.23}$$

for some matrix $P_0 = P_0'$ and functions $P_{0\tau} : [-\tau, 0] \to \mathbb{R}^{n \times n}$ and $P_{\tau\tau} : [-\tau, 0] \times [-\tau, 0] \to \mathbb{R}^{n \times n}$ such that $P_{\tau\tau}(r, s) = P_{\tau\tau}'(s, r)$. Moreover, these function have to guarantee that $V(\check{x}_t) \geq \alpha \|x(t)\|^2$ for some $\alpha > 0$ to satisfy the condition of Theorem 2.5. Such functions are conventionally dubbed *Lyapunov–Krasovskii functionals*. However, the form above might be "too rich." Finding matrix functions for (2.23) might be a hard problem to handle. For this reason, simpler particular cases of the quadratic function (2.23) are typically sought. The example below illustrates the idea (other uses are discussed in Section 4.3).

Example 2.13. Consider DDE (2.18) and now select

$$V(\check{x}_t) = x'(t) P_0 x(t) + \int_{-\tau}^{0} x'(t+s) P_\tau x(t+s)\,\mathrm{d}s = x'(t) P_0 x(t) + \int_{t-\tau}^{t} x'(s) P_\tau x(s)\,\mathrm{d}s$$

for matrices $P_0 = P_0' > 0$ and $P_\tau = P_\tau' > 0$, which corresponds to $P_{0\tau}(s) = 0$ and $P_{\tau\tau}(r,s) = \delta(r-s) P_\tau$ in (2.23). This choice satisfies the first inequality in (2.22) for $\alpha(\|x\|) = \lambda_{\min}(P_0)\|x\|^2$, so it is a legitimate candidate. To take the derivative of this function along trajectories of (2.18), remember the Leibniz integral rule,

$$\frac{\mathrm{d}}{\mathrm{d}t} \int_{a(t)}^{b(t)} f(s,t)\,\mathrm{d}s = \int_{a(t)}^{b(t)} \frac{\partial}{\partial t} f(s,t)\,\mathrm{d}s + \frac{\mathrm{d}b(t)}{\mathrm{d}t} f(b(t),t) - \frac{\mathrm{d}a(t)}{\mathrm{d}t} f(a(t),t). \tag{2.24}$$

It is then readily seen that

$$\begin{aligned}
\dot{V}(\check{x}_t) &= 2x'(t) P_0 \dot{x}(t) + x'(t) P_\tau x(t) - x'(t-\tau) P_\tau x(t-\tau) \\
&= 2x'(t) P_0 A x(t) + 2x'(t) P_0 A_\tau x(t-\tau) + x'(t) P_\tau x(t) - x'(t-\tau) P_\tau x(t-\tau) \\
&= \begin{bmatrix} x'(t) & x'(t-\tau) \end{bmatrix} \begin{bmatrix} A' P_0 + P_0 A + P_\tau & P_0 A_\tau \\ A_\tau' P_0 & -P_\tau \end{bmatrix} \begin{bmatrix} x(t) \\ x(t-\tau) \end{bmatrix}.
\end{aligned}$$

Thus, if we can find P_0 and P_τ such that

$$\begin{bmatrix} A' P_0 + P_0 A + P_\tau & P_0 A_\tau \\ A_\tau' P_0 & -P_\tau \end{bmatrix} < 0, \tag{2.25}$$

then $M_0 := -A' P_0 - P_0 A - P_\tau - P_0 A_\tau P_\tau^{-1} A_\tau' P_0 > 0$ and the condition of Theorem 2.5 holds for $\beta(\|x\|) = \lambda_{\min}(M_0)\|x\|^2$, so that the system is asymptotically stable (in fact, for every delay τ, so we end up with delay-independent stability). The condition above is again an LMI in its two free parameters, P_0 and P_τ. Condition (2.25) is also conservative, i.e. the failure to solve the LMI above does not necessarily implies that the system is unstable for some τ. Still, it is less conservative than the Razumikhin condition (2.21). Indeed, the latter is a special case of (2.25) for $P_0 = P$ and $P_\tau = aP$, constraining P_τ if $n > 1$. $\triangledown$

Remark 2.7 (conservatism). Stability results derived via Lyapunov's method tend to be quite conservative. There are several sources of that. It might be that the chosen Lyapunov function is not the "best" one, which is especially common in the Lyapunov–Krasovskii approach. Showing that the derivative is negative normally involves bounding cross-terms and strengthening condition (2.19b) or (2.22), like was done in Examples 2.12 and 2.13 with including terms depending on $x(t-\tau)$, which also induces conservatism. Moreover, conservatism sources are often non-transparent, resulting in many seemingly different, but actually equivalent results, see [83, §3.3].

Nevertheless, sometimes Lyapunov-based may be non-conservative. For example, consider the conditions in Example 2.13 in the scalar case with $A = -1$ and $A_\tau = a_\tau$. The LMI (2.25) reads then

$$\begin{bmatrix} P_\tau - 2P_0 & P_0 a_\tau \\ a_\tau P_0 & -P_\tau \end{bmatrix} < 0 \iff P_\tau > 0 \wedge P_\tau - 2P_0 + \frac{a_\tau^2 P_0^2}{P_\tau} < 0 \iff (P_\tau - P_0)^2 < (1 - a_\tau^2) P_0^2,$$

where the first equivalence relation follows by (A.6). The last inequality is solvable in $P_0 > 0$ and $P_\tau > 0$ iff $|a_\tau| < 1$, as in that case an appropriate P_τ can be found for every given P_0. At the same time, the use of any of the methods discussed in Section 2.1 yields that the system is delay-independent stable iff $a_\tau \in (-1, 1]$. This implies that the Lyapunov–Krasovskii (and Lyapunov–Razumikhin, which is equivalent if $n = 1$) method misses only stability under $a_\tau = 1$, i.e. it is practically non-conservative in this case. $\triangledown$

Remark 2.8 (neutral DDEs). In the neutral delay case, like in (1.30), the Lyapunov analysis is quite similar. An important fact is that, much like the i/o stability case, the system is Lyapunov unstable whenever $\rho(E_\tau) > 1$ and might be either stable or unstable if $\rho(E_\tau) = 1$, see [61] for more details. If $\rho(E_\tau) < 1$, then essentially the only alteration to the conditions of Theorem 2.5 is the replacement of $\alpha(\|x(t)\|)$ with $\alpha(\|x(t) - E_\tau x(t-\tau)\|)$. $\triangledown$

Chapter 3

Stabilization of Time-Delay Systems

H AVING GRASPED BASIC IDEAS about the stability analysis of time-delay systems, we turn to stabilization problems in this chapter. We shall be mostly concerned with dead-time systems, i.e. systems comprising a finite-dimensional system connected in series with a delay element, like (1.10) on p. 4. The morale of this chapter is that a right choice of the controller architecture can substantially simplify the solution, rendering it essentially finite dimensional.

3.1 Stabilization of FOPTD systems by fixed-structure controllers

We start with a brief flirt with stabilization ideas for fixed-structure (finite-dimensional fixed-structure, to be precise) controllers. To simplify the exposition, we consider only unstable FOPTD (first-order-plus-time-delay) plants of the form

$$P_\tau(s) = \frac{e^{-\tau s}}{s - 1} \tag{3.1}$$

As discussed in §1.2.1, such models are important in applications, like process control. Moreover, in some situations this model represents dynamics, left after other parts, stable and stably invertible, are canceled by the controller. The choice of the plant pole at $s = 1$ does not inflict any loss of generality. If $P(s) = a/(s - a)$ for some $a > 0$, the pole can always be normalized by the substitution $s \to as$ and scaling $\tau \to a\tau$. In other words, the delay τ in (3.1) should always be though of as the ratio between the loop delay and the time constant $1/a$ of the finite-dimensional part of the plant dynamics.

The stabilization setup for this system is the standard unity-feedback architecture shown in Fig. 3.1. As only the stability of this system is analyzed, the exogenous signals are not relevant. The characteristic function of the closed-loop system in this case is

$$\chi_\tau(s) = (s - 1)M_R(s) + N_R(s)e^{-\tau s}, \tag{3.2}$$
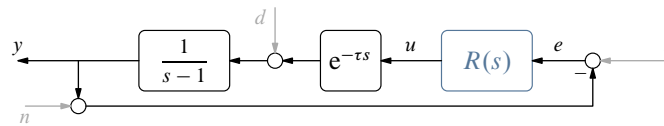
Fig. 3.1: Unity-feedback control setup for a FOPTD plant

where $N_R(s)$ and $M_R(s)$ are the numerator and denominator of the controller, $R(s) = N_R(s)/M_R(s)$, cf. (1.25). This is a single-delay quasi-polynomial of the form (2.4), which can be analyzed by the delay sweeping method of §2.1.5 for a given $R(s)$. In this section we consider a more challenging problem of analyzing $\chi_\tau(s)$ as functions of controller parameters.

3.1.1   Stabilizing PI controllers

Assume that the class of controllers to be analyzed is of the form

$$R(s) = R_{\text{PI}}(s) := k_p\left(1 + \frac{1}{T_i s}\right) \tag{3.3}$$

for some nonzero real k_p (known as the proportional gain) and T_i (integral time or reset time). In this case $N_R(s) = k_p(T_i s + 1)$ and $M_R(s) = T_i s$ and the characteristic function (3.2) reads

$$\chi_\tau(s) = T_i s(s-1) + k_p(T_i s + 1)e^{-\tau s}.$$

Form

$$\phi(\omega) = T_i^2 \omega^2(\omega^2 + 1) - k_p^2(T_i^2 \omega^2 + 1) = T_i^2 \omega^4 - T_i^2(k_p^2 - 1)\omega^2 - k_p^2.$$

according to (2.10). The only positive-real solution of this equation, the crossing frequency, satisfies

$$\omega_c^2 = \frac{1}{2}\left(k_p^2 - 1 + \sqrt{(k_p^2 - 1)^2 + 4\frac{k_p^2}{T_i^2}}\right), \tag{3.4}$$

which is a switch because $d\phi(\omega)/d\omega = 2T_i^2 \omega(1 - k_p^2 + 2\omega^2) = 0$ only at $\omega = 0$ and $\omega^2 = (k_p^2 - 1)/2$, both smaller than ω_c^2. Hence, the closed-loop system can be stable for some delays only if it is stable for $\tau = 0$. The zero-delay characteristic polynomial,

$$\chi_0(s) = T_i s^2 + T_i(k_p - 1)s + k_p,$$

is Hurwitz iff all its coefficients are nonzero and have the same sign. If $k_p < 0$, then we must have $T_i < 0$ and $T_i(k_p - 1) < 0$, which is a contradiction. Hence, all coefficients must be positive, which is the case iff

$$k_p > 1 \quad \text{and} \quad T_i > 0. \tag{3.5}$$

As a matter of fact, this implies that $T_i \omega_c^2 > k_p > 1$. The phase relation (2.8b) for this $\chi_\tau(s)$ reads

$$\tau\omega_c = \arg(jT_i\omega_c + 1) - \arg(j\omega_c - 1) - \frac{\pi}{2} + (2k-1)\pi = \arg\frac{jT_i\omega_c + 1}{j\omega_c - 1} + \left(2k - \frac{3}{2}\right)\pi$$

$$= \arg\frac{(jT_i\omega_c + 1)(j\omega_c + 1)}{\omega_c^2 + 1} + \left(2k - \frac{1}{2}\right)\pi = \arg(1 - T_i\omega_c^2 + j(T_i + 1)\omega_c) + \left(2k - \frac{1}{2}\right)\pi.$$

Because $T_i\omega_c^2 > 1$, we have that $\arg(1 - T_i\omega_c^2 + j(T_i + 1)\omega_c) \in (\pi/2, \pi)$ and the smallest crossing delay corresponds to $k = 1$. Therefore, the closed-loop system is stable iff (3.5) holds and

$$0 \le \tau < \frac{1}{\omega_c}\arctan\frac{T_i\omega_c^2 - 1}{(T_i + 1)\omega_c} < 1 \tag{3.6}$$

for ω_c given by (3.4). This is a simple condition on τ for given k_p and T_i, but is far from being simple in terms of controller parameters. Even in the P controller case, which corresponds to $T_i = \infty$, the condition

$$0 \le \tau < \frac{\arctan\sqrt{k_p^2 - 1}}{\sqrt{k_p^2 - 1}} \tag{3.6'}$$

(a) in the $(k_\mathrm{p}, 1/T_\mathrm{i})$-plane

(b) in the $(\omega_\mathrm{c}, 1/T_\mathrm{i})$-plane
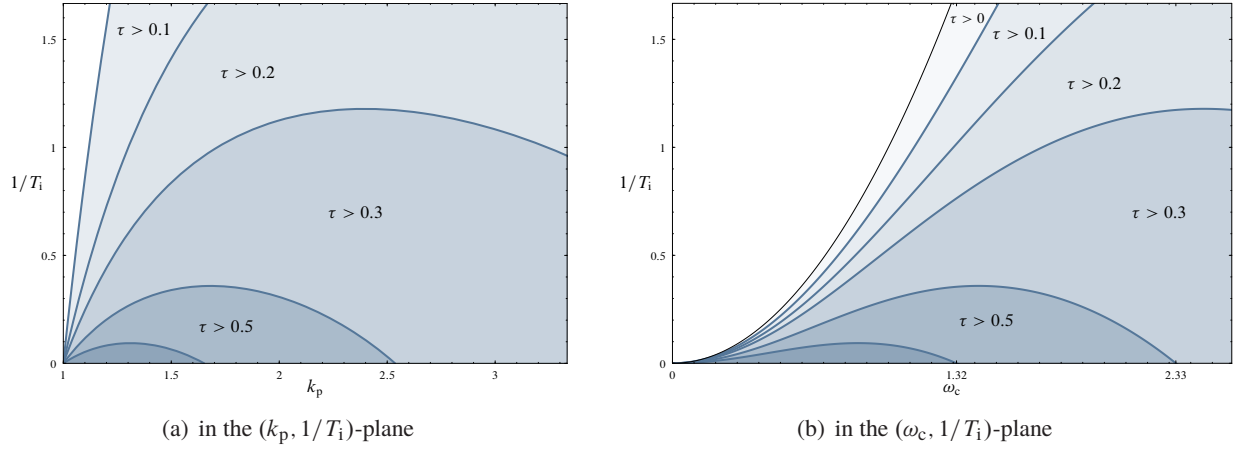
Fig. 3.2: Maximum stabilizing delay contours for the PI controller (3.3)

is not solvable in k_p analytically. As such, controller parameters may be chosen graphically, from the plot of stability contours of the delay in the $(k_\mathrm{p}, 1/T_\mathrm{i})$-plane, shown in Fig. 3.2(a). A suitable, viz. stabilizing in this case, PI controller (3.3) may be then selected for each given delay τ.

The crossing frequency ω_c in (3.4) is the crossover frequency of the loop $P_\tau R$. This is an important characteristic of the control system in Fig. 3.1, it roughly indicates the frequency range in which feedback is useful and the closed-loop bandwidth. It follows from (3.4) that any given crossover frequency can be attained by the choice

$$k_\mathrm{p} = T_\mathrm{i}\omega_\mathrm{c}\sqrt{\frac{1+\omega_\mathrm{c}^2}{1+T_\mathrm{i}^2\omega_\mathrm{c}^2}},$$

which is admissible, i.e. results in $k_\mathrm{p} > 1$, iff $\omega_\mathrm{c} > 1/\sqrt{T_\mathrm{i}}$. In other words, there is a one-to-one correspondence between $\omega_\mathrm{c} > 1/\sqrt{T_\mathrm{i}}$ and $k_\mathrm{p} > 1$, so we can analyze the stability of the system in terms of its crossover frequency instead of the proportional gain. This analysis may actually be more informative and it facilitates deriving the analytic bound on the integral time under a given delay $\tau > 0$,

$$\frac{1}{T_\mathrm{i}} < \frac{\omega_\mathrm{c}(\omega_\mathrm{c} - \tan(\tau\omega_\mathrm{c}))}{1 + \omega_\mathrm{c}\tan(\tau\omega_\mathrm{c})}. \tag{3.7}$$

Because $\tau \in [0, 1)$, the numerator in the right-hand side above is positive iff $\omega_\mathrm{c} \in (0, \omega_\tau)$, where ω_τ is the smallest positive solution to $\omega_\tau = \tan(\tau\omega_\tau)$. Such ω_τ always exists and satisfies $\tau\omega_\tau \in [0, \pi/2)$. At the same time, the denominator in the right-hand side of (3.7) is positive for all $\tau\omega_\mathrm{c} \in [0, \pi/2)$. Therefore, there exist $T_\mathrm{i} > 0$ satisfying (3.7) iff ω_c is strictly smaller than ω_τ, which is a strictly monotonically increasing function of τ. The corresponding level curves of the upper bounds on $1/T_\mathrm{i}$ as functions of ω_c for several values of τ are presented in Fig. 3.2(b).

3.1.2 Stabilizing PD controllers

Now consider the class of PD controllers of the form

$$R(s) = R_\mathrm{PD}(s) := k_\mathrm{p}(1 + T_\mathrm{d}s) \tag{3.8}$$

for some nonzero proportional gain k_p and real T_d (derivative time). The characteristic function (3.2) for this choice is

$$\chi_\tau(s) = s - 1 + k_\mathrm{p}(1 + T_\mathrm{d}s)\mathrm{e}^{-\tau s}.$$

(a) in the (k_p, T_d)-plane

(b) in the (ω_c, T_d)-plane
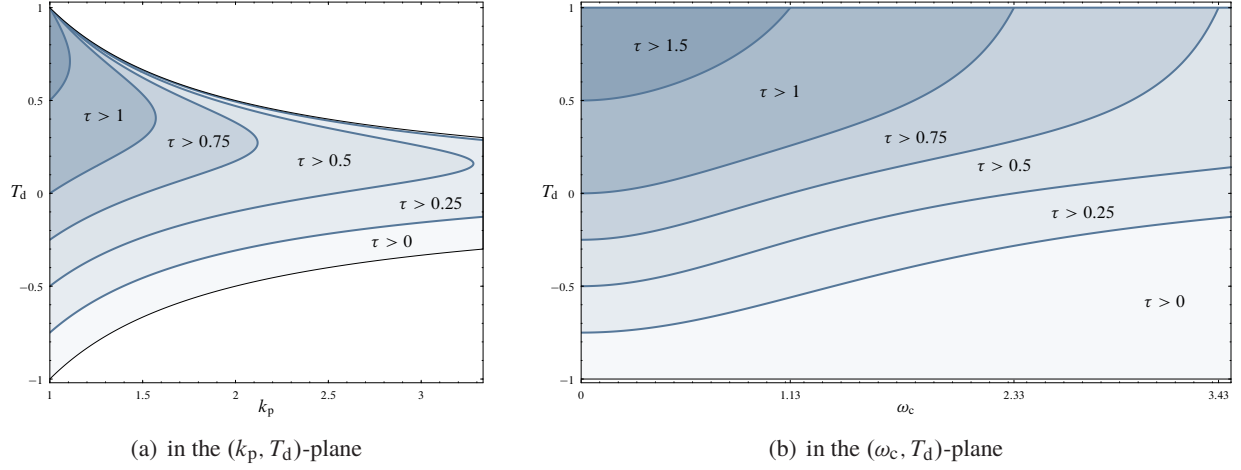
Fig. 3.3: Maximum stabilizing delay contours for the PD controller (3.8)

This is a neutral quasi-polynomial, so we first have to guarantee $\mathcal{A}_2$ on p. 28. This requires $|k_p T_d| < 1$, which is assumed hereafter. The corresponding $\phi(\omega)$ is then

$$\phi(\omega) = (1 - k_p^2 T_d^2)\omega^2 - (k_p^2 - 1).$$

Clearly, its solution must satisfy

$$\omega_c^2 = \frac{k_p^2 - 1}{1 - k_p^2 T_d^2}. \tag{3.9}$$

Taking into account that $|k_p T_d| < 1$, this $\phi(\omega)$ has positive roots iff $|k_p| > 1$. If this is the case, then the crossing frequency is is a switch, because $\mathrm{d}\phi(\omega)/\mathrm{d}\omega = 2(1 - k_p^2 T_d^2)\omega$ is positive there. Consider now properties of the zero-delay version of the characteristic equation,

$$\chi_0(s) = (1 + k_p T_d)s + k_p - 1.$$

Because $|k_p T_d| < 1$, its leading coefficient is positive, so this polynomial is Hurwitz iff $k_p > 1$. Thus, the system is delay-independent unstable whenever $k_p \leq 1$ and is stable for all delays below the first crossing delay if $k_p > 1$. This crossing delay can be found from the phase relation (under $k_p > 0$)

$$\tau\omega_c = \arg(1 + \mathrm{j}T_d\omega_c) - \arg(-1 - \mathrm{j}\omega_c) + (2k - 1)\pi = \arctan(T_d\omega_c) + \arctan\omega_c + 2k\pi.$$

Because each one of the two first terms above is a function in $(0, \pi/2)$, the minimum positive solution of this equation corresponds to $k = 0$. Hence, the system is stable iff

$$k_p > 1, \quad |T_d| < \frac{1}{k_p} < 1, \quad \text{and} \quad 0 \leq \tau < \frac{1}{\omega_c}\big(\arctan(T_d\omega_c) + \arctan\omega_c\big) \leq 2 \tag{3.10}$$

for ω_c given by (3.9). The last relation is again not quite transparent in terms of the controller parameters for a fixed τ. The level curves in the (k_p, T_d)-plane presented in Fig. 3.3(a) can be used to choose k_p and T_d.

Like in the PI case, the analysis is simplified if we consider the crossover frequency ω_c as the parameter of choice instead of k_p. This is always possible, owing to the relation

$$k_p = \sqrt{\frac{1 + \omega_c^2}{1 + T_d^2\omega_c^2}},$$
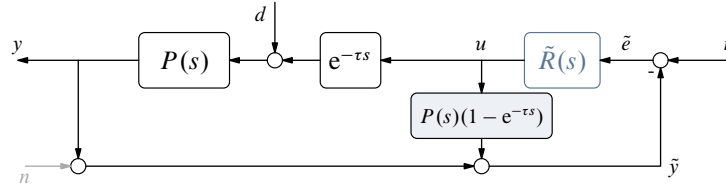
Fig. 3.4: Unity-feedback system with Smith controller

which defines a one-to-one correspondence between $\omega_c > 0$ and $k_p > 1$ provided $|T_d| < 1$. The bound on τ in (3.10) translated then to the following bound on the derivative time as a function of τ and ω_c:

$$-1 < \frac{\tan(\tau\omega_c - \arctan\omega_c)}{\omega_c} < T_d < 1, \tag{3.11}$$

which is nonempty iff $0 < \tau\omega_c < \arctan\omega_c + \pi/2 < \pi$. These bounds are presented in Fig. 3.3(b) and may be useful to see limitations, imposed by the loop delay, on the attainable crossover frequency.

Although the examples above discuss simple controllers for a simple time-delay system, they can be used to appreciate problems arising in more general situations. Namely, it is not hard to extrapolate that finding precise stabilizability conditions might be tremendously challenging and even if such conditions can be found, they are seldom transparent and it might not be trivial to find a meaningful re-parametrization, for which the result is intuitive. For these reasons, the design of fixed-structure finite-dimensional stabilizing controllers is normally addressed via conservative methods, based on various kinds of approximations and the use of robustness techniques (some of the are studied in Chapter 4).

3.2 Problem-oriented controller architectures: historical developments

The design of (low-order) fixed-structure controllers is a challenge even for finite-dimensional plants with high-order dynamics. Conventional wisdom has it then that the complexity of the controller should be comparable to that of the controlled process. In particular, there are systematic and intuitive methods to design at least $(n - p)$-dimensional stabilizing controllers for n-dimensional LTI plants with p measured non-redundant outputs, whereas no such methods exist for lower-order controllers in general.

The observation above suggests that the stabilization of (infinite-dimensional) time-delay systems may require the use of infinite-dimensional controllers. This section aims at presenting developments in the control literature since the late '50s on methods to design infinite-dimensional controllers for time-delay, mainly dead-time, systems, which exploit the structure of the delay element. These developments bore several fruitful concepts, resulting in intuitive design procedures and implementable controller architectures. The presentation below is technical, its main goal is to present a historical overview. The underlying insights and somewhat more streamlined derivations of these approaches are then revealed in the next section.

3.2.1 Dead-time compensation: Smith predictor and its modifications

The first problem-oriented controller architecture for dead-time systems was proposed by Otto J. M. Smith back in 1957 [70]. The controller, presented in Fig. 3.4, comprises two parts, a *primary controller* $\tilde{R}$ and a *Smith predictor* $P(1 - \bar{D}_\tau)$ in the internal feedback path of the controller. The overall controller $R : y \mapsto u$ in this case has the transfer function

$$R(s) = \frac{\tilde{R}(s)}{1 + \tilde{R}(s)P(s)(1 - e^{-\tau s})}. \tag{3.12}$$
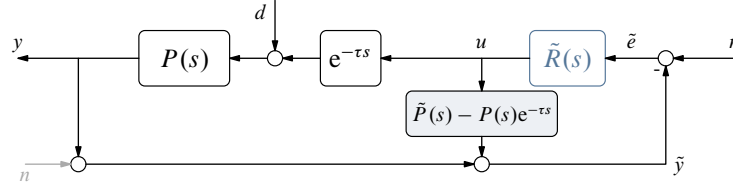
Fig. 3.5: Unity-feedback system with modified Smith predictor

Although the controller is quite complex, the setup makes closed-loop properties more transparent. The underlying logic of this architecture can be seen from the behavior of the signal

$$\tilde{y} = y + P(1 - \bar{D}_\tau)u = P(\bar{D}_\tau u + d) + P(1 - \bar{D}_\tau)u = P(u + d),$$

which can thus be seen as a *predicted* version of y. The use of the predicted output in lieu of y leads to simpler closed-loop dynamics, as can be seen from the resulting control sensitivity,

$$T_c(s) = \frac{R(s)e^{-\tau s}}{1 + P(s)R(s)e^{-\tau s}} = \frac{\tilde{R}(s)e^{-\tau s}}{1 + \tilde{R}(s)P(s)(1 - e^{-\tau s}) + P(s)\tilde{R}(s)e^{-\tau s}} = \frac{\tilde{R}(s)}{1 + P(s)\tilde{R}(s)} =: \tilde{T}_c(s),$$

and complementary sensitivity,

$$T(s) = P(s)e^{-\tau s}T_c(s) = \frac{P(s)\tilde{R}(s)}{1 + P(s)\tilde{R}(s)}e^{-\tau s} =: \tilde{T}(s)e^{-\tau s},$$

transfer functions. Thus, the control sensitivity function turns completely delay free and the complementary sensitivity function is left with only an input delay. From the stabilization point of view, a key fact is that the delay is not present in the denominators of both these closed-loop transfer functions. As a result, if the primary controller $\tilde{R}$ stabilizes the delay-free systems $\tilde{T}$ and $\tilde{T}_c$, then R defined by (3.12) renders the actual T and T_c stable as well. This remarkable property facilitates the design of the primary controller for the delay-free version of the plant, P, and then implementing it in the Smith form of Fig. 3.4. Also note that although the overall controller in (3.12) is infinite dimensional, it is readily implementable. All we need is to realize a delay line and a finite-dimensional plant model in the internal feedback of the controller.

The situation is not that simple though. Consider the disturbance sensitivity transfer function

$$T_d(s) = P(s)(1 - T(s)) = P(s)\left(1 - \frac{P(s)\tilde{R}(s)}{1 + P(s)\tilde{R}(s)}e^{-\tau s}\right) = \frac{P(s)}{1 + P(s)\tilde{R}(s)} + \frac{[P(s)]^2\tilde{R}(s)(1 - e^{-\tau s})}{1 + P(s)\tilde{R}(s)}$$

$$=: \tilde{T}_d(s) + \tilde{T}(s)P(s)(1 - e^{-\tau s}).$$

Unless plant poles are canceled in the predictor $P(s)(1 - e^{-\tau s})$, they are the poles of the disturbance sensitivity $T_d(s)$ as well. Hence, if $P(s)$ has unstable poles other than single poles at $j2k\pi/\tau$ for $k \in \mathbb{Z}$, the closed-loop system is internally unstable as well, no matter what primary controller is chosen. This implies that the Smith controller is not applicable to unstable plants in most cases.

However, instability under unstable plants is not an intrinsic property of predictor-based schemes. A possible fix was proposed by Keiji Watanabe and Masami Itō in [80]. The idea is paraphrased in Fig. 3.5, where the prediction element $\tilde{P} - P\bar{D}_\tau$ is based on a finite-dimensional system $\tilde{P}$, which is not necessarily the same as the plant P. With this choice, the signal $\tilde{y} = \tilde{P}u + Pd$ is no longer a prediction of the zero-delay output. Still, this is a delay-free response, so that the architecture presented in Fig. 3.5 is dubbed the *dead-time compensator*. The four closed-loop transfer functions of interest are then

$$\begin{bmatrix} S(s) & T_d(s) \\ T_c(s) & T(s) \end{bmatrix} = \begin{bmatrix} 1 & \tilde{P}(s) - P(s)e^{-\tau s} \\ 0 & 1 \end{bmatrix} \begin{bmatrix} \tilde{S}(s) & \tilde{T}_d(s) \\ \tilde{T}_c(s) & \tilde{T}(s) \end{bmatrix} \begin{bmatrix} 1 & -\tilde{P}(s) + P(s)e^{-\tau s} \\ 0 & 1 \end{bmatrix}, \tag{3.13}$$

where

$$
\begin{bmatrix} \tilde{S}(s) & \tilde{T}_{\mathrm{d}}(s) \\ \tilde{T}_{\mathrm{c}}(s) & \tilde{T}(s) \end{bmatrix} := \frac{1}{1 + \tilde{P}(s)\tilde{R}(s)} \begin{bmatrix} 1 \\ \tilde{R}(s) \end{bmatrix} \begin{bmatrix} 1 & \tilde{P}(s) \end{bmatrix}
$$

are the closed-loop transfer functions associated with the unity-feedback interconnection of delay-free $\tilde{P}$ and $\tilde{R}$. If the finite-dimensional system $\tilde{P}$ is such that the prediction block $\tilde{P} - P\bar{D}_\tau$ is itself stable, then

$$
\begin{bmatrix} 1 & 0 \\ \tilde{P}(s) - P(s)\mathrm{e}^{-\tau s} & 1 \end{bmatrix} \quad \text{and} \quad \begin{bmatrix} 1 & 0 \\ -\tilde{P}(s) + P(s)\mathrm{e}^{-\tau s} & 1 \end{bmatrix} = \begin{bmatrix} 1 & 0 \\ \tilde{P}(s) - P(s)\mathrm{e}^{-\tau s} & 1 \end{bmatrix}^{-1}
$$

are bi-stable and

$$
\begin{bmatrix} S & T_{\mathrm{c}} \\ T_{\mathrm{d}} & T \end{bmatrix} \in H_\infty \iff \begin{bmatrix} \tilde{S} & \tilde{T}_{\mathrm{c}} \\ \tilde{T}_{\mathrm{d}} & \tilde{T} \end{bmatrix} \in H_\infty.
$$

This, in turn, implies that the stabilization problem for the input-delay plant $P\bar{D}_\tau$ reduces to that for the delay-free $\tilde{P}$.

Thus, the stabilization problem boils down to finding a finite-dimensional $\tilde{P}$ for which $\tilde{P} - P\bar{D}_\tau$ is stable. This turns out to be always possible. The choice proposed in [80], based on the state-space realization of $P(s) = C(sI - A)^{-1}B$, is

$$
\tilde{P}(s) = C\mathrm{e}^{-A\tau}(sI - A)^{-1}B \tag{3.14}
$$

and has the same order and the same poles as $P(s)$. In this case the transfer function of the predictor, known as the *modified Smith predictor* (MSP), is

$$
\tilde{P}(s) - P(s)\mathrm{e}^{-\tau s} = C(\mathrm{e}^{-A\tau} - \mathrm{e}^{-\tau s}I)(sI - A)^{-1}B = C\mathrm{e}^{-A\tau}\int_0^\tau \mathrm{e}^{-(sI-A)t}\,\mathrm{d}t\,B. \tag{3.15}
$$

This is an entire function bounded in $\mathbb{C}_0$, cf. a discussion in Example 2.5 on p. 24. Hence, it belongs to H_∞ and the MSP is stable. There are other choices, some of which are proposed in [80], all of them are based on canceling unstable poles of $P(s)$ in the predictor $\tilde{P}(s) - P(s)\mathrm{e}^{-\tau s}$. Because of those cancellations, certain care should be taken in implementing such predictors, this issue is discussed in Chapter 7. But, in any case, the use of the dead-time compensation (DTC) architecture renders the stabilization problem essentially finite dimensional, which is a clear advantage in comparison with the methods discussed in Section 3.1.

3.2.2 Finite spectrum assignment

Consider now the system

$$
\dot{x}(t) = Ax(t) + Bu(t - \tau), \tag{3.16}
$$

which is a dead-time system with the whole state of its delay-free part measurable. We assume that (A, B) is stabilizable. Conceptually, the stabilization problem for it would be simple if we measured the future vector $x(t + \tau)$ at each t. The control law $u(t) = Kx(t + \tau) + K_v v(t)$, where v is an exogenous signal and K_v is some gain, is obviously stabilizing if $A + BK$ is Hurwitz. Finding an appropriate K is a standard step of designing a state feedback controller for the zero-delay version of (3.16). Of course, the control law above, based on $x(t + \tau)$, is not implementable. But we may try to imitate it by replacing $x(t + \tau)$ with its *prediction*. This logic is reminiscent of that of observer-based feedback, where unmeasurable state is replaced with its estimate.

A prediction of x can be obtained by solving (3.16),

$$
x(t + \tau) = \mathrm{e}^{A\tau}x(t) + \int_t^{t+\tau} \mathrm{e}^{A(t+\tau-r)}Bu(r - \tau)\,\mathrm{d}r = \mathrm{e}^{A\tau}x(t) + \int_{t-\tau}^t \mathrm{e}^{A(t-r)}Bu(r)\,\mathrm{d}r.
$$

This is a linear function of the state of (3.16), which is $(x(t), \breve{u}_t)$ as discussed in §1.2.1, and is causally implementable. Thus, a candidate for the predictor-based feedback is

$$u(t) = K\left(e^{A\tau} x(t) + \int_{t-\tau}^{t} e^{A(t-r)} B u(r) \, dr\right) + K_v v(t), \tag{3.17}$$

where K is such that $A + BK$ is Hurwitz.

To analyze the stability of the closed-loop system with the control law (3.17), rewrite it in the Laplace domain. To this end, note that the last term in it is the convolution of $u(t)$ and $e^{At} B \mathbb{1}_{[0,\tau]}(t)$, where $\mathbb{1}_{[0,\tau]}(t)$ is the indicator function of the interval $[0, \tau]$. As such, the Laplace transform of it is the product of the Laplace transforms of each one of these functions, i.e.

$$\mathcal{L}\left\{\int_{t-\tau}^{t} e^{A(t-r)} B u(r) \, dr\right\} = \int_{0}^{\infty} e^{At} B \mathbb{1}_{[0,\tau]}(t) e^{-st} \, dt \, U(s) = \int_{0}^{\tau} e^{-(sI-A)t} \, dt \, B U(s). \tag{3.18}$$

Thus, (3.17) can be written as

$$\left(I - K \int_{0}^{\tau} e^{-(sI-A)t} \, dt \, B\right) U(s) = K e^{A\tau} X(s) + K_v V(s).$$

Combining this relation with the Laplace-domain version of (3.16), we end up with the closed-loop equations

$$\begin{bmatrix} sI - A & -B e^{-\tau s} \\ -K e^{A\tau} & I - K \int_{0}^{\tau} e^{-(sI-A)t} \, dt \, B \end{bmatrix} \begin{bmatrix} X(s) \\ U(s) \end{bmatrix} = \begin{bmatrix} 0 \\ K_v \end{bmatrix} V(s).$$

The stability of these dynamics can be analyzed via its characteristic function, which determines the existence of a nontrivial free motion under $v = 0$. By the logic of §2.1.1, this function is

$$\chi_{\tau,\mathrm{cl}}(s) = \det \begin{bmatrix} sI - A & -B e^{-\tau s} \\ -K e^{A\tau} & I - K \int_{0}^{\tau} e^{-(sI-A)t} \, dt \, B \end{bmatrix}. \tag{3.19}$$

Although the task of finding its roots appears complicated, it is actually not. Just note that

$$e^{-A\tau}(sI - A) \int_{0}^{\tau} e^{-(sI-A)t} \, dt \, B = e^{-A\tau} B - B e^{-\tau s},$$

cf. the second equality of (3.15). Therefore,

$$\begin{bmatrix} sI - A & -B e^{-\tau s} \\ -K e^{A\tau} & I - K \int_{0}^{\tau} e^{-(sI-A)t} \, dt \, B \end{bmatrix} = \begin{bmatrix} sI - A & e^{-A\tau}(sI - A) \int_{0}^{\tau} e^{-(sI-A)t} \, dt \, B - e^{-A\tau} B \\ -K e^{A\tau} & I - K \int_{0}^{\tau} e^{-(sI-A)t} \, dt \, B \end{bmatrix}$$

$$= \begin{bmatrix} sI - A & -e^{-A\tau} B \\ -K e^{A\tau} & I \end{bmatrix} \begin{bmatrix} I & e^{-A\tau} \int_{0}^{\tau} e^{-(sI-A)t} \, dt \, B \\ 0 & I \end{bmatrix}$$

and

$$\chi_{\tau,\mathrm{cl}}(s) = \det \begin{bmatrix} sI - A & -e^{-A\tau} B \\ -K e^{A\tau} & I \end{bmatrix} = \det(sI - A - e^{-A\tau} BK e^{A\tau}) = \det(e^{-A\tau}(sI - A - BK)e^{A\tau})$$

$$= \det(sI - A - BK),$$

where the second equality follows by (A.5b). In other words, $\chi_{\tau,\mathrm{cl}}(s)$ in (3.19) is actually a plain polynomial of degree n, whose roots are the eigenvalues of $A + BK$, exactly as in the delay-free case. For this reason, the strategy behind control law (3.17) is called the *finite spectrum assignment* (FSA). The term was coined by Andrzej Manitius and Andrzej W. Olbrot in their 1979 paper [34], where the stabilization problem in a slightly different, albeit essentially equivalent, form was studied. The ideas behind controller (3.17) can be traced back to the late '60s, see [17, 36, 30], where similar configurations were discussed in various contexts.

Remark 3.1 (multiple delays). Remarkably, the FSA approach extends to a rather general class of multiple input delay systems. Although such kinds of extensions are not as intuitive as the predictor-based approach described above, they can be deduced from the analysis above and still produce finite closed-loop spectra. For example, consider a plant described by the equation $\dot{x}(t) = Ax(t) + \sum_i B_i u(t - \tau_i)$ for delays $\tau_i \geq 0$. The control law

$$u(t) = K\left(x(t) + \sum_i \int_{t-\tau_i}^t e^{A(t-\tau_i-r)} Bu(r)\,dr \right) + K_v v(t)$$

assigns the spectrum of the closed-loop system to the roots of $\det(sI - A - \sum_i e^{-A\tau_i} B_i K)$, which is a polynomial of degree n, and the stabilization is possible iff $(A, \sum_i e^{-A\tau_i} B_i)$ is stabilizable. $\qquad\triangledown$

If only a part of the vector x is measured, say if (3.16) is complemented by the measurement equation $y(t) = Cx(t)$, then (3.17) should be complemented by an observer of x, resulting in the control law

$$\dot{\hat{x}}(t) = A\hat{x}(t) + Bu(t - \tau) - L(y(t) - C\hat{x}(t)) \tag{3.20a}$$

$$u(t) = K\left(e^{A\tau}\hat{x}(t) + \int_{t-\tau}^t e^{A(t-r)} Bu(r)\,dr \right) + K_v v(t), \tag{3.20b}$$

for some L such that $A + LC$ is Hurwitz, which exists iff (C, A) is detectable. With the standard trick of replacing $\hat{x}(t)$ with the observer error $e(t) := x(t) - \hat{x}(t)$ by a similarity transformation, the closed-loop system reads in the Laplace domain as

$$\begin{bmatrix} sI - A - LC & 0 & 0 \\ 0 & sI - A & -Be^{-\tau s} \\ Ke^{A\tau} & -Ke^{A\tau} & I - K\int_0^\tau e^{-(sI-A)t}\,dt\,B \end{bmatrix} \begin{bmatrix} E(s) \\ X(s) \\ U(s) \end{bmatrix} = \begin{bmatrix} 0 \\ 0 \\ K_v \end{bmatrix} V(s).$$

Its characteristic function

$$\chi_{\tau,\text{cl}}(s) = \det \begin{bmatrix} sI - A - LC & 0 & 0 \\ 0 & sI - A & -Be^{-\tau s} \\ Ke^{A\tau} & -Ke^{A\tau} & I - K\int_0^\tau e^{-(sI-A)t}\,dt\,B \end{bmatrix} = \det(sI - A - LC)\det(sI - A - BK)$$

is again a polynomial, now having the degree $2n$, coinciding with that in the delay-free observer-based feedback. Controller (3.20), dubbed *observer-predictor*, was analyzed by Toshio Furukawa and Etsujiro Shimemura in [18], although perhaps appeared for the first time in Davis Q. Mayne's paper [36] of 1968 and also as a part of the LQG optimal control law in David L. Kleinman's paper [30] of 1969.

3.2.3 Kwon–Pearson–Artstein reduction

A related, albeit a bit more general, approach was proposed by Wook Hyun Kwon and Allan E. Pearson in [32] and then extended by Zvi Artstein in [3]. Consider again (3.16) and introduce the variable

$$\tilde{x}(t) := x(t) + \int_{t-\tau}^t e^{A(t-\tau-r)} Bu(s)\,dr,$$

which is effectively a prediction of $e^{-A\tau} x(t + \tau)$. Differentiating this variable results in the relation

$$\dot{\tilde{x}}(t) = \dot{x}(t) + A\int_{t-\tau}^t e^{A(t-\tau-r)} Bu(r)\,dr + e^{-A\tau} Bu(t) - Bu(t - \tau)$$

$$= Ax(t) + A\int_{t-\tau}^t e^{A(t-\tau-r)} Bu(r)\,dr + e^{-A\tau} Bu(t),$$

where the first equality is obtained via the Leibniz integral rule (2.24) on p. 40 and the second equality follows by (3.16). Thus, the variable $\tilde{x}$ satisfies the ODE

$$\dot{\tilde{x}}(t) = A\tilde{x}(t) + e^{-A\tau}Bu(t). \tag{3.21}$$

Note that controllability-related characteristics of $(A, e^{-A\tau}B)$ are equivalent to those of (A, B). System (3.21) is called the *reduced system* and it can be stabilized by standard methods. For example, if the state-feedback $u(t) = \tilde{K}\tilde{x}(t) + K_v v(t)$ is used for it, then the reduced system is stable iff $A + e^{-A\tau}B\tilde{K}$ is Hurwitz. But then

$$x(t) = \tilde{x}(t) - \int_{t-\tau}^{t} e^{A(t-\tau-r)}B\tilde{K}\tilde{x}(r)\,\mathrm{d}r$$

is bounded whenever so is $\tilde{x}$, merely by the triangle inequality and the boundedness of $\|e^{-As}B\tilde{K}\|$ for $s \in [0, \tau]$. Thus, the stabilization problem for (3.16) is yet again reduced to the stabilization of a delay-free system, this time (3.21). The stabilizing controller in terms of the original vector x is given by

$$u(t) = \tilde{K}\left(x(t) + \int_{t-\tau}^{t} e^{A(t-\tau-r)}Bu(r)\,\mathrm{d}r\right) + K_v v(t), \tag{3.22}$$

which actually equals the FSA control law (3.17) under $\tilde{K} = Ke^{A\tau}$.

Remark 3.2 (time-varying delays). The main difference of the reduction approach from the FSA is in their analyses of the closed-loop stability. While the FSA does that via the characteristic function, the reduction approach uses time-domain arguments. As such, they can be applied to time-varying delays as well. As an example, consider the system $\dot{x}(t) = Ax(t) + Bu(\theta(t))$ for some absolutely continuous function $\theta(t) \leq t$ such that $\dot{\theta}(t) > 0$, which is a special case of the system analyzed in [3, Ex. 5.6]. This is an input-delay system with the time-varying delay $\tau(t) = t - \theta(t) \geq 0$. Denote by $\theta^{-1}(t)$ the inverse of $\theta(t)$, i.e. the value of r for which $\theta(r) = t$. It is unique whenever $\dot{\theta}(t) > 0$ and satisfies $\theta^{-1}(t) \geq t$. The function

$$\tilde{x}(t) = x(t) + \int_{\theta(t)}^{t} e^{A(t-\theta^{-1}(r))}B\dot{\theta}^{-1}(r)u(r)\,\mathrm{d}r$$

satisfies then the reduced equation

$$\dot{\tilde{x}}(t) = A\tilde{x}(t) + e^{-A(\theta^{-1}(t)-t)}B\dot{\theta}^{-1}(t)\,u(t),$$

which is free of delays. Actually, the variable $\bar{x}(t) := e^{A(\theta^{-1}(t)-t)}\tilde{x}(t)$ is the prediction of $x(\theta^{-1}(t))$, so the variable $\theta^{-1}(t) - t \geq 0$ can be thought of as the prediction horizon required for the delay $t - \theta(t)$. Moreover, it can be shown that $\dot{\bar{x}}(t) = A\bar{x}(t) + Bu(t)$, so its dynamics are time invariant. Yet, similarly to the discussion in Remark 3.1, the prediction interpretation is not evident in extending the approach to multiple-delay systems of the form $\dot{x}(t) = Ax(t) + \sum_i B_i u(\theta_i(t))$, in which case reduced dynamics are intrinsically time varying. ∇

3.2.4 Connections

Remarkably, all three approaches studied in Section 3.2 share essentially the same structure of their controllers. Namely, they all result in controllers having internal feedback of the form presented in Fig. 3.6, where the "primary controller" $\tilde{R}$ is designed for a delay-free system and the "dead-time compensation" block Π is determined by the plant (exogenous signals are taken zero for brevity). Indeed, the Smith controller in Fig. 3.4 corresponds to this form under $\Pi(s) = P(s)(1 - e^{-\tau s})$ and the primary controller $\tilde{R}$
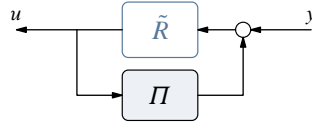
Fig. 3.6: Common controller structure (DTC, FSA, reduction)

designed for P. The MSP in Fig. 3.5 chooses $\Pi(s)$ in form (3.15). The FSA controller (3.17) can be cast in the form presented in Fig. 3.6 under $y = x$, the static $\tilde{R}(s) = Ke^{A\tau}$, and

$$\Pi(s) = \mathcal{L}\{e^{A(t-\tau)}B\mathbb{1}_{[0,\tau]}\} = e^{-A\tau}\int_0^\tau e^{-(sI-A)t}\,dt\,B,$$

cf. (3.18). Likewise, the controller of (3.22) is the same modulo the choice of $\tilde{R}(s) = \tilde{K}$. In fact, the multiple-delay extension discussed in Remark 3.1 can also be cast in the form presented in Fig. 3.6 with a static $\tilde{R}$ and a more elaborate Π.

Moreover, the observer-predictor in (3.20) is also of the same form. This is not obvious, but can be proved. To this end, introduce the variable

$$\bar{x}(t) := e^{A\tau}\hat{x}(t) + \int_{t-\tau}^t e^{A(t-r)}Bu(r)\,dr,$$

with which (3.20b) reads $u(t) = K\bar{x}(t)$ (remember, we assume here that $v = 0$). Using again the Leibniz integral rule (2.24), we have:

$$\dot{\bar{x}}(t) = e^{A\tau}\big(A\hat{x}(t) + Bu(t-\tau) - L(y(t) - C\hat{x}(t))\big) + A\int_{t-\tau}^t e^{A(t-r)}Bu(r)\,dr + Bu(t) - e^{A\tau}Bu(t-\tau)$$

$$= A\bar{x}(t) + Bu(t) - e^{A\tau}L(y(t) - C\hat{x}(t)).$$

Substituting $\hat{x}(t) = e^{-A\tau}\bar{x}(t) - e^{-A\tau}\int_{t-\tau}^t e^{A(t-r)}Bu(r)\,dr$ to this expression, we end up with the following equivalent form of (3.20):

$$\dot{\bar{x}}(t) = (A + e^{A\tau}LCe^{-A\tau})\bar{x}(t) + Bu(t) - e^{A\tau}L\left(y(t) + Ce^{-A\tau}\int_{t-\tau}^t e^{A(t-r)}Bu(r)\,dr\right) \qquad (3.20a')$$

$$u(t) = K\bar{x}(t). \qquad (3.20b')$$

But this control law is exactly in the form presented in Fig. 3.6, with

$$\tilde{R}(s) = \left[\begin{array}{c|c} A + BK + e^{A\tau}LCe^{-A\tau} & -e^{A\tau}L \\ \hline K & 0 \end{array}\right],$$

which is the observer-based controller for $\tilde{P}$ given by (3.14), and $\Pi(s)$ in form (3.15). In other words, the MSP of Watanabe–Ito with the observer-based primary controller is identical to the observer-predictor controller of Furukawa–Shimemura. These two controllers were regarded different for some time, until their equivalence was shown in [47].

3.3 Problem-oriented controller architectures: control-theoretic insight

The fact that independently developed control methods produce the same controller architecture is intriguing. A somewhat superficial explanation of that might be given via recalling that these methods have prediction ideas in their origin. However, prediction is not a part of the classical control-theoretic toolkit

and is often viewed as an incautious business, especially from the robustness point of view. On top of this, neither the MSP nor multiple-delay extensions of the FSA / reduction approaches is readily interpretable as a predictor-based controller. Moreover, however natural and clever the guesses discussed in this section might be, there is no indication whether they are really justified. We thus shall look for more solid control-theoretic explanations, for which we yet again turn to the discrete-time version of the problem.

3.3.1 Gaining insight via discrete-time systems: state feedback

Consider the input-delay system

$$x[t + 1] = Ax[t] + Bu[t - \tau], \tag{3.23}$$

where $x[t] \in \mathbb{R}^n$, $u[t] \in \mathbb{R}^m$, $\tau \in \mathbb{N}$, and the whole x is measurable. To simplify the exposition, assume that (A, B) is reachable. We already know, cf. (1.11) on p. 5, that the state equation of this system is

$$\underbrace{\begin{bmatrix} x[t+1] \\ \hline u[t-\tau+1] \\ \vdots \\ u[t-1] \\ u[t] \end{bmatrix}}_{x_\tau[t+1]} = \underbrace{\begin{bmatrix} A & B & 0 & \cdots & 0 \\ \hline 0 & 0 & I & \cdots & 0 \\ \vdots & \vdots & \vdots & \ddots & \vdots \\ 0 & 0 & 0 & \cdots & I \\ 0 & 0 & 0 & \cdots & 0 \end{bmatrix}}_{A_\tau} \underbrace{\begin{bmatrix} x[t] \\ \hline u[t-\tau] \\ \vdots \\ u[t-2] \\ u[t-1] \end{bmatrix}}_{x_\tau[t]} + \underbrace{\begin{bmatrix} 0 \\ \hline 0 \\ \vdots \\ 0 \\ I \end{bmatrix}}_{B_\tau} u[t]. \tag{3.24}$$

The first important observation regarding the model above is that if x is assumed to be measurable, then so should be the whole state x_τ of (3.24). Indeed, the other components of x_τ are the history of the input signal u, which is generated by us and thus should be available in virtually every reasonable scenario. Consequently, we can implement the standard state-feedback law for (3.24) and it is of the form

$$u[t] = \begin{bmatrix} K_x & K_\tau & \cdots & K_2 & K_1 \end{bmatrix} x_\tau[t] = K_x x[t] + \sum_{i=1}^{\tau} K_i u[t - i]. \tag{3.25}$$

This is a dynamic control law if considered as a mapping $x \mapsto u$ and its structure is reminiscent of that in Fig. 3.6, under $y = K_x x$, $\tilde{R} = I$, and $\Pi(z) = \sum_i K_i z^{-i}$. This suggests that the internal feedback in Fig. 3.6 with an FIR Π, whose impulse response has support in $[0, \tau]$, is merely a *static state feedback* acting on the component $\check{u}_i$ of the state of input-delay systems. This is a well-justified choice from the control-theoretic perspective.

The second important observation about model (3.24) is that not all modes of A_τ would make sense to move by feedback. To see this, note that

$$\text{rank} \begin{bmatrix} A_\tau - \lambda I & B_\tau \end{bmatrix} = \text{rank} \begin{bmatrix} A - \lambda I & B & 0 & 0 & \cdots & 0 & 0 \\ \hline 0 & -\lambda I & I & 0 & \cdots & 0 & 0 \\ 0 & 0 & -\lambda I & I & \cdots & 0 & 0 \\ \vdots & \vdots & \vdots & \vdots & \ddots & \vdots & \vdots \\ 0 & 0 & 0 & 0 & \cdots & I & 0 \\ 0 & 0 & 0 & 0 & \cdots & -\lambda I & I \end{bmatrix} = \text{rank} \begin{bmatrix} A - \lambda I & B \end{bmatrix} + \tau m,$$

so the only possibly reachable modes of the realization in (3.24) are those of (A, B). As the latter pair is assumed to be reachable, so is (A_τ, B_τ) and all $n + m\tau$ modes of (3.24) can be freely assigned by static state feedback of the form (3.25). But $m\tau$ eigenvalues of A_τ are already in a perfect location, at the origin. Such kind of eigenvalues, known as *deadbeat*, are obviously stable and are normally considered welcome, albeit expensive to attain. Yet now we have deadbeat modes for free, so it would make perfect sense to keep them untouched, which would also keep the control energy low. With this logic in mind, the choice of the feedback gain in (3.25) should aim only at assigning a subset of the modes of A_τ, those of A. To understand this kind of pole assignment problem, some preliminary results are required.

Preliminary: partial pole placement by state feedback

Consider the state-feedback problem for the n-order delay-free system

$$x[t + 1] = Ax[t] + Bu[t]$$

and suppose that only $\tilde{n} < n$ eigenvalues of A should be moved by feedback, while the other $n - \tilde{n}$ are to remain untouched. Perhaps the easiest way to visualize this process, while avoiding the use of the invariant subspace notion, is via applying a similarity transformation T, bringing the realization above to the form

$$Tx[t + 1] = TAT^{-1}Tx[t] + TBu[t] = \begin{bmatrix} \tilde{A} & 0 \\ \times & \bar{A} \end{bmatrix} Tx[t] + \begin{bmatrix} \tilde{B} \\ \bar{B} \end{bmatrix} u[t], \tag{3.26}$$

where $\tilde{A} \in \mathbb{R}^{\tilde{n} \times \tilde{n}}$ contains all eigenvalues of A that have to be shifted, $\bar{A} \in \mathbb{R}^{(n-\tilde{n}) \times (n-\tilde{n})}$ contains those to be kept untouched, and "$\times$" denotes an irrelevant block. It is readily seen that unreachable modes of $(\tilde{A}, \tilde{B})$ are also unreachable modes of (A, B). An obvious choice of the required state-feedback gain for this realization is $K = \begin{bmatrix} \tilde{K} & 0 \end{bmatrix}$, where $\tilde{K}$ is such that the eigenvalues of $\tilde{A} + \tilde{B}\tilde{K}$ are assigned to required positions.

An important fact is that the resulted control law in the original coordinates,

$$u[t] = \begin{bmatrix} \tilde{K} & 0 \end{bmatrix} Tx[t] = \tilde{K} \begin{bmatrix} I & 0 \end{bmatrix} Tx[t],$$

does not require the whole similarity transformation matrix T, but only its $\tilde{n}$ first rows. An exhaustive characterization of this part of T is given by the following result:

Lemma 3.1. *Let $\sigma_{shift} \subset \mathrm{spec}(A)$ contain all modes of A that we need to shift by feedback. An $\tilde{n} \times n$ matrix $\tilde{T}$ is the first $\tilde{n}$ rows of a nonsingular $T \in \mathbb{R}^{n \times n}$ such that*

$$TAT^{-1} = \begin{bmatrix} \tilde{A} & 0 \\ \times & \bar{A} \end{bmatrix}$$

for some $\tilde{A} \in \mathbb{R}^{\tilde{n} \times \tilde{n}}$ such that $\mathrm{spec}(\tilde{A}) = \sigma_{shift}$ iff

$$\tilde{T}A = \tilde{A}\tilde{T} \quad and \quad \mathrm{rank}\, \tilde{T} = \tilde{n}. \tag{3.27}$$

Proof. The "only if" statement follows from the relation

$$TA = \begin{bmatrix} \tilde{A} & 0 \\ \times & \bar{A} \end{bmatrix} T \quad \Longrightarrow \quad \begin{bmatrix} I_{\tilde{n}} & 0 \end{bmatrix} TA = \begin{bmatrix} I_{\tilde{n}} & 0 \end{bmatrix} \begin{bmatrix} \tilde{A} & 0 \\ \times & \bar{A} \end{bmatrix} T = \tilde{A} \begin{bmatrix} I_{\tilde{n}} & 0 \end{bmatrix} T.$$

To show the "if" statement, assume that there is a full-rank $\tilde{T}$ satisfying (3.27). There is then a full-rank $\bar{T} \in \mathbb{R}^{(n-\tilde{n}) \times n}$ such that $T := \begin{bmatrix} \tilde{T}' & \bar{T}' \end{bmatrix}'$ is nonsingular. In this case $\tilde{T}T^{-1} = \begin{bmatrix} I_{\tilde{n}} & 0 \end{bmatrix}$ and we have that

$$\begin{bmatrix} I_{\tilde{n}} & 0 \end{bmatrix} TAT^{-1} = \tilde{T}AT^{-1} = \tilde{A}\tilde{T}T^{-1} = \begin{bmatrix} \tilde{A} & 0 \end{bmatrix},$$

as required. $\qquad \square$

Thus, all we need is to solve (3.27) in $\tilde{T}$ and $\tilde{A}$, whose spectrum coincides with the part of $\mathrm{spec}(A)$ that is planned to be moved, and implement the control law

$$u[t] = \tilde{K}\tilde{T}x[t]$$

for $\tilde{K}$ assigning the $\tilde{n}$ eigenvalues of $\tilde{A} + \tilde{T}B\tilde{K}$ to desired positions.

Partial pole placement for (3.24)

Now return to the state equation (3.24). We know what part of its dynamics we need to move, so consider the following version of (3.27) for it:

$$
\underbrace{\begin{bmatrix} T_x & T_\tau & \cdots & T_2 & T_1 \end{bmatrix}}_{\tilde{T}}
\begin{bmatrix}
A & B & 0 & \cdots & 0 \\
0 & 0 & I & \cdots & 0 \\
\vdots & \vdots & \vdots & \ddots & \vdots \\
0 & 0 & 0 & \cdots & I \\
0 & 0 & 0 & \cdots & 0
\end{bmatrix}
= \underbrace{\begin{bmatrix} T_x A & T_x B & T_\tau & \cdots & T_2 \end{bmatrix}}_{\tilde{T} A_\tau}
= A \underbrace{\begin{bmatrix} T_x & T_\tau & T_{\tau-1} & \cdots & T_1 \end{bmatrix}}_{\tilde{T}},
$$

where the choice of "$\tilde{A}$" is an educated guess (it has to have the same spectrum as A, but need not be equal A in general). It is not hard to see that this equality is solved by

$$
\begin{bmatrix} T_x & T_\tau & \cdots & T_2 & T_1 \end{bmatrix} = \begin{bmatrix} A^\tau & A^{\tau-1}B & \cdots & AB & B \end{bmatrix}, \tag{3.28}
$$

which has full rank iff (A, B) has no unreachable modes at the origin. By the reachability assumption, the full rank property is thus guaranteed. With this choice, $\tilde{T} B_\tau = B$ and the controller gain $\tilde{K}$ is thus designed for the delay-free pair (A, B). The choices of $\tilde{A}$ and $\tilde{T}$ above are not unique, but they do appear natural and they lead to an interpretable controller.

Remark 3.3 (reachability of (A, B)). The assumption that (A, B) is reachable simplifies the exposition above, in particular, arguments about the assignment of modes of A and the proof that the choice of $\tilde{T}$ as in (3.28) has full rank. However, the result holds even if the milder condition of the stabilizability of (A, B) is assumed. In that case only reachable modes of (A, B) can be assigned, which is obvious. Also, if (A, B) has unreachable modes at the origin, then the matrix in (3.28) has a reduced rank. But this not a problem, as by the design logic those deadbeat modes are not intended to be shifted anyway. ▽

Thus, a version of (3.25) that does not touch the $m\tau$ deadbeat modes of (3.24) is

$$
u[t] = K\left(A^\tau x[t] + \sum_{i=1}^{\tau} A^{i-1} B u[t-i]\right) = K\left(A^\tau x[t] + \sum_{r=t-\tau}^{t-1} A^{t-r-1} B u[r]\right), \tag{3.29}
$$

where K assigns the eigenvalues of $A + BK$ to desired positions, which are the closed-loop eigenvalues of the input-delay system (3.23). It is readily seen that this control law is based on the predicted $x[t+\tau]$. As such, it is the perfect discrete-time counterpart of the prediction-based controller (3.17) under $v = 0$. Just now it is derived by a conventional state-feedback rationale and thus has a solid justification. Namely, the predictive feedback is merely a static state feedback that potentially alters only the poles of the delay-free part of the open-loop system.

The same rationale applies to the continuous-time law (3.17). It is nothing but the static state feedback law, shifting only the finite modes of the open-loop plant, which are the eigenvalues of A in (3.16). This state feedback happens to be a predictor in the single-delay case, but might not be readily interpretable this way for multiple-delay systems.

3.3.2 Gaining insight via discrete-time systems: output feedback

Now consider the system

$$
\begin{aligned}
x[t+1] &= Ax[t] + Bu[t-\tau] \\
y[t] &= Cx[t] + Du[t-\tau]
\end{aligned} \tag{3.30}
$$

in which only a part of the delay-free plant state is measured. We assume that (A, B) is stabilizable and (C, A) is detectable. The state-space realization of this system given by (1.11) on p. 5 assumes that the

system is an operator $u \mapsto y$. This assumption may be natural in analyzing the behavior of y, but does not reflect actual measurement variables. This is because we have also measurements of the last $m\tau$ components of the state variable $x_\tau[t]$ defined in (3.24). Thus, the accurate measurement equation now is

$$
\underbrace{\begin{bmatrix} y[t] \\ \hline u[t-\tau] \\ \vdots \\ u[t-2] \\ u[t-1] \end{bmatrix}}_{y_\tau[t]} = \underbrace{\begin{bmatrix} C & D & \cdots & 0 & 0 \\ \hline 0 & I & \cdots & 0 & 0 \\ \vdots & \vdots & \ddots & \vdots & \vdots \\ 0 & 0 & \cdots & I & 0 \\ 0 & 0 & \cdots & 0 & I \end{bmatrix}}_{C_\tau} \underbrace{\begin{bmatrix} x[t] \\ \hline u[t-\tau] \\ \vdots \\ u[t-2] \\ u[t-1] \end{bmatrix}}_{x_\tau[t]} + \underbrace{\begin{bmatrix} 0 \\ \hline 0 \\ \vdots \\ 0 \\ 0 \end{bmatrix}}_{D_\tau} u[t],
\tag{3.31}
$$

which complements the state equation (3.24). It is straightforward to show that unobservable modes of the pair (C_τ, A_τ) are those of (C, A). Hence, the realization (3.24), (3.31) is detectable.

Equation (3.31) still does not measure the whole state of the system. It is then natural to implement the state-feedback controller (3.29) in combination with a state observer. Moreover, if u can be measured without noise, then it is well justified to consider a *reduced-order observer* [25, Sec. 4.3], reconstructing only the x component of x_τ using n-dimensional dynamics. The structure of A_τ and C_τ facilitates the construction of a reduced-order observer for x directly from (3.30). It is readily verified that

$$
\hat{x}[t+1] = A\hat{x}[t] + Bu[t-\tau] - L(y[t] - C\hat{x}[t] - Du[t-\tau])
$$

yields the following equation for the estimation error $e[t] := x[t] - \hat{x}[t]$:

$$
e[t+1] = (A + LC)e[t].
$$

Thus, the stabilizing controller for (3.30) of the form

$$
\hat{x}[t+1] = A\hat{x}[t] + Bu[t-\tau] - L(y[t] - C\hat{x}[t] - Du[t-\tau])
\tag{3.32a}
$$

$$
u[t] = K\left(A^\tau \hat{x}[t] + \sum_{r=t-\tau}^{t-1} A^{t-r-1} Bu[r] \right),
\tag{3.32b}
$$

results in the closed-loop dynamics with the characteristic equation

$$
\chi_{\tau,\text{cl}}(z) = z^{m\tau} \det(zI - A - BK) \det(zI - A - LC).
$$

This implies that the observer-predictor control law is merely an observer-based feedback, featuring a reduced-order observer (justified by perfect measurements of u) and state feedback keeping $m\tau$ open-loop modes at the origin untouched. This appears to be a well-justified controller architecture.

Remark 3.4 (noisy measurements of u). It might happen that the past control signals used in (3.32b) are corrupted by noise. One may be tempted to expect that in such a situation we need to build a full-order observer instead of (3.32a). However, this is normally not the case. Namely, the optimal *strictly causal* estimator of x_τ under noisy measurements of both y and u is still a reduced-order observer of form (3.32a), whose gain L depends on noise intensities. Moreover, even the optimal *causal* estimator is of this form if if $D = 0$, see [50] for details. ∇

3.3.3 Intermezzo: Fiagbedzi–Pearson reduction for systems with internal delays

The logic above can be used to address the stabilization of a substantially wider and more challenging class of systems. Below we consider the approach of Fiagbedzi and Pearson [13], applied to the general single-delay interconnection of Fig. 1.7 on p. 10, whose dynamics are described by (1.27).

Assume that the whole state of the system, which is $(x(t), \check{z}_t)$, is measurable, so only the "state dynamics" part,

$$\begin{bmatrix} \dot{x}(t) \\ z(t) \end{bmatrix} = \begin{bmatrix} A & B_w \\ C_z & D_{zw} \end{bmatrix} \begin{bmatrix} x(t) \\ z(t-\tau) \end{bmatrix} + \begin{bmatrix} B_u \\ D_{zu} \end{bmatrix} u(t), \tag{3.33}$$

is required. The characteristic function $\chi_\tau(s)$ associated with this equation is given by (2.2) on p. 20. This is a quasi-polynomial with an infinite number of roots. As such, finite spectrum assignment should not be expected, in general. Still, under the already familiar assumption that $\rho(D_{zw}) < 1$, there is only a finite number roots of $\chi_\tau(s)$ in the closed right-hand plane $\bar{\mathbb{C}}_0$. Hence, the ideas of FSA / reduction can be applied only to unstable open-loop poles.

Introduce the $\tilde{n}$-dimensional signal

$$\tilde{x}(t) := Qx(t) + \int_{t-\tau}^t e^{\tilde{A}(t-r)} Rz(r)\,dr$$

for some matrices $\tilde{A} \in \mathbb{R}^{\tilde{n}\times\tilde{n}}$, $Q \in \mathbb{R}^{\tilde{n}\times n}$, and $R \in \mathbb{R}^{\tilde{n}\times m_\tau}$ to be determined. Differentiating this variable and using the Leibniz integral rule (2.24) and the relations of (3.33) for $\dot{x}$ and z, we have that

$$\begin{aligned} \dot{\tilde{x}}(t) &= Q\dot{x}(t) + Rz(t) - e^{\tilde{A}\tau} Rz(t-\tau) + \tilde{A} \int_{t-\tau}^t e^{\tilde{A}(t-r)} Rz(r)\,dr \\ &= Q\big(Ax(t) + B_w z(t-\tau) + B_u u(t)\big) + R(C_z x(t) + D_{zw} z(t-\tau) + D_{zu} u(t)) - e^{\tilde{A}\tau} Rz(t-\tau) \\ &\quad + \tilde{A} \int_{t-\tau}^t e^{\tilde{A}(t-r)} Rz(r)\,dr \\ &= \tilde{A}\tilde{x}(t) + (QB_u + RD_{zu})u(t) + (QA + RC_z - \tilde{A}Q)x(t) + (QB_w + RD_{zw} - e^{\tilde{A}\tau}R)z(t-\tau). \end{aligned}$$

The dependence on x and z can be eliminated if $\tilde{A}$, Q, and R are chosen to satisfy the equation

$$\begin{bmatrix} Q & R \end{bmatrix} \begin{bmatrix} A & B_w \\ C_z & D_{zw} \end{bmatrix} = \begin{bmatrix} \tilde{A}Q & e^{\tilde{A}\tau}R \end{bmatrix}. \tag{3.34}$$

If such matrices exist, then $\tilde{x}$ satisfies the finite-dimensional equation

$$\dot{\tilde{x}}(t) = \tilde{A}\tilde{x}(t) + \tilde{B}u(t),$$

where $\tilde{B} := QB_u + RD_{zu}$.

To understand equation (3.34), pre-multiply both its sides by a left eigenvector $\eta_i \in \mathbb{C}^{\tilde{n}}$ of $\tilde{A}$, corresponding to some $\lambda_i \in \text{spec}(\tilde{A})$. Using the fact that $\eta_i' e^{\tilde{A}\tau} = e^{\lambda_i \tau} \eta_i'$, we then obtain the equality

$$\eta_i' \begin{bmatrix} Q & R \end{bmatrix} \begin{bmatrix} \lambda_i I - A & -B_w e^{-\lambda_i \tau} \\ -C_z & I - D_{zw} e^{-\lambda_i \tau} \end{bmatrix} = 0.$$

Hence, if $\eta_i' \begin{bmatrix} Q & R \end{bmatrix} \neq 0$, then every eigenvalue λ_i of $\tilde{A}$ necessarily satisfies $\chi_\tau(\lambda_i) = 0$, i.e. it is a root of the characteristic function of the open-loop system (3.33). For that reason equation (3.34) is referred to as the *left characteristic matrix equation*. But the relation above implies that (3.34) can be viewed as a counterpart of (3.27). Thus, the control law $u(t) = \tilde{K}\tilde{x}(t) + K_v v(t)$ or, equivalently,

$$u(t) = \tilde{K}\left(Qx(t) + \int_{t-\tau}^t e^{\tilde{A}(t-r)} Rz(r)\,dr \right) + K_v v(t) \tag{3.35}$$

is a state-feedback law assigning only the part of the open-loop spectrum, that of the matrix $\tilde{A}$, to $\tilde{A} + \tilde{B}\tilde{K}$.

This conclusion can be supported by analyzing the closed-loop characteristic function, which can be derived from the relation

$$
\begin{bmatrix}
sI - A & -B_w e^{-\tau s} & -B_u \\
-C_z & I - D_{zw} e^{-\tau s} & -D_{zu} \\
-\tilde{K}Q & -\tilde{K} \int_0^\tau e^{-(sI-\tilde{A})t} \, dt R & I
\end{bmatrix}
\begin{bmatrix}
X(s) \\
Z(s) \\
U(s)
\end{bmatrix}
=
\begin{bmatrix}
0 \\
0 \\
K_v
\end{bmatrix}
V(s),
$$

which represents the system dynamics (3.33) and the control law (3.34) in the Laplace transform domain.

The closed-loop characteristic function for this system is

$$
\chi_{\tau,\text{cl}}(s) = \det
\begin{bmatrix}
sI - A & -B_w e^{-\tau s} & -B_u \\
-C_z & I - D_{zw} e^{-\tau s} & -D_{zu} \\
-\tilde{K}Q & -\tilde{K} \int_0^\tau e^{-(sI-\tilde{A})t} \, dt R & I
\end{bmatrix}.
$$

Using equations (A.5) and the equality

$$
\begin{bmatrix} Q & \int_0^\tau e^{-(sI-\tilde{A})t} \, dt R \end{bmatrix} = (sI - \tilde{A})^{-1} \begin{bmatrix} Q & R \end{bmatrix}
\begin{bmatrix}
sI - A & -B_w e^{-\tau s} \\
-C_z & I - D_{zw} e^{-\tau s}
\end{bmatrix},
$$

which can be verified by straightforward algebra via (3.34), we have:

$$
\chi_{\tau,\text{cl}}(s) = \det\left(
\begin{bmatrix}
sI - A & -B_w e^{-\tau s} \\
-C_z & I - D_{zw} e^{-\tau s}
\end{bmatrix}
-
\begin{bmatrix}
B_u \\
D_{zu}
\end{bmatrix}
\tilde{K}
\begin{bmatrix} Q & \int_0^\tau e^{-(sI-\tilde{A})t} \, dt R \end{bmatrix}
\right)
$$

$$
= \det\left(I -
\begin{bmatrix}
B_u \\
D_{zu}
\end{bmatrix}
\tilde{K}(sI-\tilde{A})^{-1}
\begin{bmatrix} Q & R \end{bmatrix}
\right)
\det
\begin{bmatrix}
sI - A & -B_w e^{-\tau s} \\
-C_z & I - D_{zw} e^{-\tau s}
\end{bmatrix}
$$

$$
= \det(sI - \tilde{A})^{-1} \det
\begin{bmatrix}
I & 0 & B_u \tilde{K} \\
0 & I & D_{zu} \tilde{K} \\
Q & R & sI - \tilde{A}
\end{bmatrix}
\det
\begin{bmatrix}
sI - A & -B_w e^{-\tau s} \\
-C_z & I - D_{zw} e^{-\tau s}
\end{bmatrix}
$$

$$
= \det(sI - \tilde{A} - \tilde{B}\tilde{K}) \frac{\chi_\tau(s)}{\det(sI - \tilde{A})}.
$$

This proves that the closed-loop spectrum under (3.35) differs from the open-loop one only in moving $\tilde{n}$ characteristic roots belonging to $\text{spec}(\tilde{A})$ to $\text{spec}(\tilde{A} + \tilde{B}\tilde{K})$, as expected.

Thus, to stabilize (3.33) we need to solve the left characteristic matrix equation (3.34) for $\tilde{A}$ containing all roots of $\chi_\tau(s)$ that are required to be shifted. This set must clearly include all unstable characteristic roots of (3.33), i.e. those in $\overline{\mathbb{C}}_0$, but might contain additional modes. There are only a finite number of such roots and finding them is currently a well understood numerical problem. The left characteristic matrix equation can also be solved numerically, see [13] and some later developments of the same authors. Note that spectral properties of $\tilde{A}$ effectively define that matrix unambiguously, because any similarity transformation of $\tilde{A}$ just leads to an appropriate scaling of Q and R. If $D_{zw} = 0$, which corresponds to a retarded system, the second column of (3.34) yields the closed-form $R = e^{-\tilde{A}\tau} Q B_w$ and then a simpler version of the first column,

$$
QA + e^{-\tilde{A}\tau} Q B_w C_z = \tilde{A} Q, \tag{3.34'}
$$

to be solved in $\tilde{A}$ and Q, and then $\tilde{B} = Q B_u + e^{-\tilde{A}\tau} Q B_w D_{zu}$. We illustrate the procedure with a simple example, which represents a rare case when analytic solution to the stabilization problem is possible.

Example 3.1. Consider the system

$$
\begin{bmatrix} \dot{x}(t) \\ z(t) \end{bmatrix}
=
\begin{bmatrix} -1 & 1 \\ 1 & 0 \end{bmatrix}
\begin{bmatrix} x(t) \\ z(t-\tau) \end{bmatrix}
+
\begin{bmatrix} 1 \\ 0 \end{bmatrix}
u(t)
$$

(i.e. $\dot{x}(t) = -x(t) + x(t - \tau) + u(t)$ in form (1.29)), whose characteristic function

$$\chi_\tau(s) = \det \begin{bmatrix} s + 1 & -\mathrm{e}^{-\tau s} \\ -1 & 1 \end{bmatrix} = s + 1 - \mathrm{e}^{-\tau s}.$$

First, prove that this quasi-polynomial has no roots in $\mathbb{C}_0$. To this end, note that the magnitude relation corresponding to the characteristic equation $s + 1 = \mathrm{e}^{-\tau s}$ reads $|s + 1| = |\mathrm{e}^{-\tau s}|$. This equality is contradictory in $\mathrm{Re}\, s > 0$ because its left-hand side is larger than 1 and its right-hand side is smaller than 1 there. Regarding pure imaginary roots, the magnitude relation for $s = \mathrm{j}\omega$ reads $|1 + \mathrm{j}\omega| = 1$, which is only solvable for $\omega = 0$. Thus, $\chi_\tau(s)$ can have only unstable roots at the origin. It is easy to verify that $\chi_\tau(0) = 0$ for all τ, indeed. This is a simple root, which can be seen from

$$\lim_{s \to 0} \frac{\chi_\tau(s)}{s} = 1 + \lim_{s \to 0} \frac{1 - \mathrm{e}^{-\tau s}}{s} = 1 + \lim_{s \to 0} \frac{\tau \mathrm{e}^{-\tau s}}{1} = 1 + \tau \neq 0.$$

Thus, to stabilize this system we only need to move its single pole at the origin. This suggests the choice of $\tilde{n} = 1$ and $\tilde{A} = 0$. Because $D_{zw} = 0$ in this case, we only solve (3.34$'$) which reads $-Q + Q = 0$ and is thus solvable by any $Q \neq 0$. This yields $R = Q$ and $\tilde{B} = Q$, so that the reduced system is $\dot{\tilde{x}} = Qu(t)$, which is a plain integrator. This system is stabilizable and the control law $u(t) = -k/Q\tilde{x}(t)$ for $k > 0$ stabilizes it, assigning its pole to $s = -k$. But this implies that the control law

$$u(t) = K_v v(t) - k\left(x(t) + \int_{t-\tau}^{t} x(r)\mathrm{d}r \right)$$

assigns

$$\chi_{\tau,\mathrm{cl}}(s) = (s + k) \frac{s + 1 - \mathrm{e}^{-\tau s}}{s},$$

which is an entire function, although not a finite quasi-polynomial. Note that the control law above is independent of the choice of Q. $\triangledown$

In some special cases, when the open-loop characteristic function $\chi_\tau(s)$ is a plain polynomial, the left characteristic matrix equation can be solved analytically. For instance, if applied to the input-delay system, whose state-space realization was discussed in Example 2.1 on p. 20 and for which $z = u$, it reads

$$\begin{bmatrix} Q & R \end{bmatrix} \begin{bmatrix} A & B \\ 0 & 0 \end{bmatrix} = \begin{bmatrix} \tilde{A}Q & \mathrm{e}^{\tilde{A}\tau}R \end{bmatrix}.$$

If we choose $\tilde{n} = n$, then this equation is obviously solved by $\tilde{A} = A$, $Q = I$, and $R = \mathrm{e}^{-A\tau}B$, so that $\tilde{B} = B$ and we end up with the control law (3.22), as expected.

Another special case with a relatively simple solution is that where $D_{zw} = 0$ and the matrices A and $B_w C_z$ have the following structure:

$$A = \begin{bmatrix} * & * & \cdots & * & * \\ 0 & * & \cdots & * & * \\ \vdots & \vdots & \ddots & \vdots & \vdots \\ 0 & 0 & \cdots & * & * \\ 0 & 0 & \cdots & 0 & * \end{bmatrix} \quad \text{and} \quad A_\tau := B_w C_z = \begin{bmatrix} 0 & * & \cdots & * & * \\ 0 & 0 & \cdots & * & * \\ \vdots & \vdots & \ddots & \vdots & \vdots \\ 0 & 0 & \cdots & 0 & * \\ 0 & 0 & \cdots & 0 & 0 \end{bmatrix},$$

where the asterisk stands for a potentially nonzero element. This class of DDEs is a particular case of retarded systems described by (1.29), where the open-loop characteristic function is still a plain polynomial. We can then always choose $\tilde{n} = n$ and $Q = I$, so that (3.34$'$) reads

$$\tilde{A} - A = \mathrm{e}^{-\tilde{A}\tau} B_w C_z. \tag{3.34$''$}$$
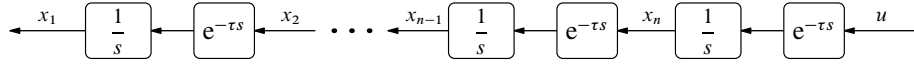
Fig. 3.7: Chain of n integrators with communication delays

This equation can be solved iteratively in an upper-triangular $\tilde{A}$, column by column, starting from the first column. As a matter of fact, this immediately yields that $\tilde{a}_{ii} = a_{ii}$ for all $i \in \mathbb{Z}_{1..n}$. We provide a flavor of this procedure via an example.

Example 3.2. Consider the problem of stabilizing a chain of n integrators connected in series with equal delays in between, see Fig. 3.7. This setup can be viewed as a baby-platooning problem, with no constraints in information exchange between involved vehicles. Assuming that all states of the integrators are measurable, this system can be described by the interconnection in Fig. 1.7 with

$$
G = \begin{bmatrix} J_n/s & e_n \\ I_n/s & 0 \end{bmatrix} = \left[\begin{array}{c|cc} 0 & I_n & 0 \\ \hline J_n & 0 & e_n \\ I_n & 0 & 0 \end{array} \right],
$$

where e_i stands for the ith standard basis of $\mathbb{R}^n$,

$$
J_n := \begin{bmatrix} 0 & e_1 & \cdots & e_{n-1} \end{bmatrix} = \begin{bmatrix} 0 & 1 & \cdots & 0 \\ \vdots & \vdots & \ddots & \vdots \\ 0 & 0 & \cdots & 1 \\ 0 & 0 & \cdots & 0 \end{bmatrix}
$$

is the n-dimensional Jordan block corresponding to the zero eigenvalue, and state components

$$
x(t) = \begin{bmatrix} x_1(t) \\ \vdots \\ x_{n-1}(t) \\ x_n(t) \end{bmatrix} \in \mathbb{R}^n \quad \text{and} \quad z(t) = \begin{bmatrix} x_2(t) \\ \vdots \\ x_n(t) \\ u(t) \end{bmatrix} \in \mathbb{R}^n.
$$

The characteristic function of this system, $\chi_\tau(s) = s^n$, is expectably a plain polynomial.

Equation (3.34″) for this system reads $\tilde{A} = e^{-\tilde{A}\tau} J_n$ and can equivalently be presented as the recursion

$$
\tilde{A} e_1 = 0 \qquad \text{and} \qquad \tilde{A} e_i = e^{-\tilde{A}\tau} e_{i-1}, \quad i \in \mathbb{Z}_{2..n}.
$$

This relation defines an upper-triangular nilpotent $\tilde{A}$, whose ith column coincides with the $(i-1)$th column of its matrix exponential. At the time we evaluate the ith column of $\tilde{A}$ all previous columns are already determined. But the upper-triangular structure of $\tilde{A}$ implies that the first $i-1$ columns of its exponential depend only on its first $i-1$ columns of $\tilde{A}$. Therefore, the recursion above can be implemented.

To illustrate the procedure, consider it in details for $n = 3$. In this case the steps of the recursion above are as follows:

1: $\quad \tilde{A} e_1 = 0 \qquad \Longrightarrow \qquad e^{-\tilde{A}\tau} e_1 = \exp\left(\begin{bmatrix} 0 & \times & \times \\ 0 & \times & \times \\ 0 & \times & \times \end{bmatrix} \tau \right) e_1 = \begin{bmatrix} 1 & \times & \times \\ 0 & \times & \times \\ 0 & \times & \times \end{bmatrix} e_1 = e_1$

2: $\quad \tilde{A} e_2 = e^{-\tilde{A}\tau} e_1 = e_1 \quad \Longrightarrow \quad e^{-\tilde{A}\tau} e_2 = \exp\left(\begin{bmatrix} 0 & -1 & \times \\ 0 & 0 & \times \\ 0 & 0 & \times \end{bmatrix} \tau \right) e_2 = \begin{bmatrix} 1 & -\tau & \times \\ 0 & 1 & \times \\ 0 & 0 & \times \end{bmatrix} e_2 = e_2 - \tau e_1$

3: $\quad \tilde{A} e_3 = e^{-\tilde{A}\tau} e_2 = e_2 - \tau e_1,$

where "×" stands for not yet evaluated elements. Having determined $\tilde{A}$, we can find its matrix exponential

$$
e^{\tilde{A}t} = \exp\left(\begin{bmatrix} 0 & 1 & -\tau \\ 0 & 0 & 1 \\ 0 & 0 & 0 \end{bmatrix} t\right) = \begin{bmatrix} 1 & t & t(t-2\tau)/2 \\ 0 & 1 & t \\ 0 & 0 & 1 \end{bmatrix},
$$

required for

$$
\tilde{B} = e^{-\tilde{A}\tau} B_w D_{zu} = \begin{bmatrix} 1 & -\tau & 3\tau^2/2 \\ 0 & 1 & -\tau \\ 0 & 0 & 1 \end{bmatrix} e_n = \begin{bmatrix} 3\tau^2/2 \\ -\tau \\ 1 \end{bmatrix}
$$

and the matrix function of r

$$
e^{\tilde{A}(t-r)} R = e^{\tilde{A}(t-r-\tau)} B_w = \begin{bmatrix} 1 & t-r-\tau & (t-r-\tau)(t-r-3\tau)/2 \\ 0 & 1 & t-r-\tau \\ 0 & 0 & 1 \end{bmatrix},
$$

which appears in the control law (3.35). As $(\tilde{A}, \tilde{B})$ is controllable, we can find $\tilde{K}$ assigning the eigenvalues of $\tilde{A} + \tilde{B}\tilde{K}$ arbitrarily. Choosing the closed-loop characteristic function as $\chi_{\tau,\mathrm{cl}}(s) = (s+\alpha)^3$ for some $\alpha > 0$, the application of Ackermann's formula yields

$$
\tilde{K} = -\begin{bmatrix} \alpha^3 & \alpha^2(2\tau\alpha + 3) & \alpha((\tau\alpha + 3)^2 - 3)/2 \end{bmatrix}.
$$

The control law (3.35) is then of the form

$$
\begin{aligned}
u(t) = K_v v(t) - \alpha^3 x_1(t) - \alpha^2 &\left((2\tau\alpha + 3)x_2(t) + \alpha \int_{t-\tau}^{t} x_2(r)\,\mathrm{d}r\right) \\
&- \alpha\left(\frac{(\tau\alpha + 3)^2 - 3}{2} x_3(t) - \alpha \int_{t-\tau}^{t} (\alpha r - 3 - \alpha(t+\tau))x_3(r)\,\mathrm{d}r\right) \\
&\qquad - \alpha \int_{t-\tau}^{t} \left(\frac{\alpha^2}{2}r^2 - (3+\alpha t)\alpha r + \frac{(\tau\alpha + 3)^2 - 3}{2}\right) u(r)\,\mathrm{d}r
\end{aligned}
$$

and it assigns all three closed-loop poles to $s = -\alpha$.

For a general n the formulae are more involved, but an analytic form of $\tilde{A}$ and its exponential can still derived. Namely, it can be shown that

$$
\tilde{A}e_1 = 0 \quad \text{and} \quad \tilde{A}e_i = -\sum_{j=1}^{i-1} \frac{(j-i)^{i-j-2}}{(i-j-1)!}\tau^{i-j-1} e_j, \quad i \in \mathbb{Z}_{2..n}
$$

and

$$
e^{\tilde{A}t} e_i = \sum_{j=1}^{i} \frac{t(t - (i-j)\tau)^{i-j-1}}{(i-j)!} e_j, \quad i \in \mathbb{Z}_{1..n}
$$

(mind that $0! = 1$, as customary), which are both Toeplitz.   ▽

3.4   Loop shifting and all stabilizing controllers

In this section another technique is discussed, which shows that the dead-time compensation is actually an intrinsic part of *every* stabilizing controller. This offers further insight into the stabilization of input-delay systems and justification of the DTC architecture.
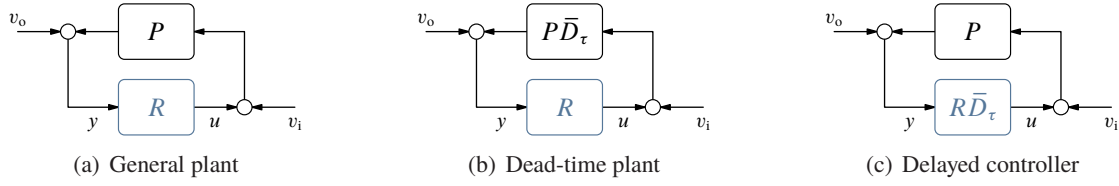
(a) General plant   (b) Dead-time plant   (c) Delayed controller

Fig. 3.8: Internal stability setups

3.4.1 Internal stability and loop shifting

We start with describing some general ideas. Consider the feedback interconnection in Fig. 3.8(a), where P and R are LTI plant and controller, respectively. It defines the relation

$$\begin{bmatrix} I & -P \\ -R & I \end{bmatrix}\begin{bmatrix} y \\ u \end{bmatrix} = \begin{bmatrix} I \\ 0 \end{bmatrix}\begin{bmatrix} I & P \end{bmatrix}\begin{bmatrix} v_o \\ v_i \end{bmatrix}. \tag{3.36}$$

We say that this interconnection is *well posed* if

there is $\alpha > 0$ such that $\|(I - P(s)R(s))^{-1}\| < \infty$ for all $s \in \mathbb{C}_\alpha$.

If both P and R are finite dimensional, then this condition reads as the non-singularity of $I - P(\infty)R(\infty)$. In any case, well posedness requires the properness of $(I - P(s)R(s))^{-1}$ and implies that the transfer function

$$\begin{bmatrix} I & -P(s) \\ -R(s) & I \end{bmatrix}^{-1} = \begin{bmatrix} 0 & 0 \\ 0 & I \end{bmatrix} + \begin{bmatrix} I \\ R(s) \end{bmatrix}(I - P(s)R(s))^{-1}\begin{bmatrix} I & P(s) \end{bmatrix},$$

which can be derived by (A.3), is proper.

The feedback interconnection in Fig. 3.8(a) is said to be *internally stable* if all four systems $\begin{bmatrix} v_o \\ v_i \end{bmatrix} \mapsto \begin{bmatrix} y \\ u \end{bmatrix}$ are stable. The reason for considering all possible closed-loop systems, rather than only one of them, lies in the need to rule out stabilization of certain closed-loop systems via unstable cancellations in the loop. It is readily seen that the system is internally stable iff

$$\begin{bmatrix} I & -P \\ -R & I \end{bmatrix}^{-1}\begin{bmatrix} I \\ 0 \end{bmatrix}\begin{bmatrix} I & P \end{bmatrix} = \begin{bmatrix} I \\ R \end{bmatrix}(I - PR)^{-1}\begin{bmatrix} I & P \end{bmatrix} =: \begin{bmatrix} S_o & T_d \\ T_c & T_i \end{bmatrix} \in H_\infty,$$

where S_o is the output sensitivity, T_i is the input complementary sensitivity, T_d is the disturbance sensitivity, and T_c is the control sensitivity systems, aka the *Gang of Four*. It is worth emphasizing that internal stability requires the system to be well posed (otherwise, S_o cannot be in H_∞) and $R(s)$ to be proper (otherwise, T_c cannot be in H_∞).

Consider now the sequence of block-diagram transformations presented in Fig. 3.9. They transform the system in Fig. 3.8(a) to that in Fig. 3.9(e) by redistributing dynamics between its elements on the basis of a chosen linear Π. The transformation has different effects on the parts of the loop, it adds Π in parallel to the plant P and in feedback to the controller R. Because these manipulations do not alter the loop itself, we can expect that properties of the original setup in Fig. 3.8(a) can be analyzed in terms of the transformed (shifted) setup in Fig. 3.9(e). The hope is that the latter might be easier to analyze for an appropriate choice of Π. This is an old idea, see [82, Sec. 6.2] or [12, Sec. III.6] and the references therein, which has been extensively used in nonlinear control, e.g. to introduce a required degree of passivity to the plant.

Two technical aspects of the loop-shifting technique have to be kept in mind. First, the elements of the shifted loop should themselves be well posed. This is obviously always true for $\tilde P = P + \Pi$, but might require extra attention for the feedback $\tilde R = R(I + \Pi R)^{-1}$. Second, the manipulations in Fig. 3.9 alter

(a) Equivalent of Fig. 3.8(a)   (b) Moving summing and pickoff   (c) $\tilde{y} = y + \Pi u$ and $\tilde{v}_o = v_o - \Pi v_i$

(d) $\tilde{u} = u$ and $\tilde{v}_i = v_i$ (e) Equivalent final loop
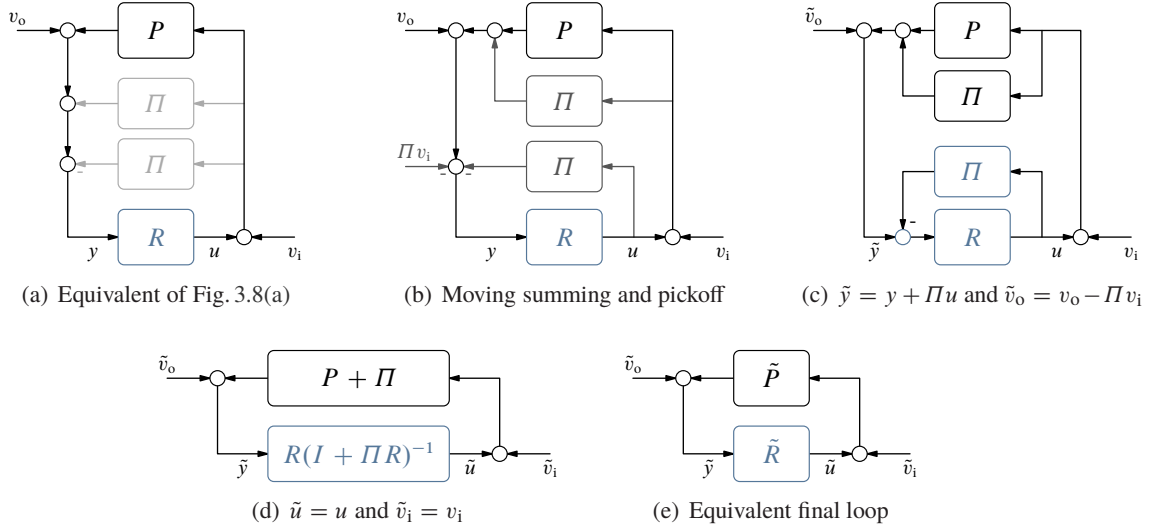
Fig. 3.9: Loop shifting by Π, with $\tilde{P} := P + \Pi$ and $\tilde{R} := R(I + \Pi R)^{-1}$

both exogenous and internal signals of the loop, in the way that the relation between signals of interest in Fig. 3.8(a) and their counterparts in Fig. 3.9(e) are

$$\begin{bmatrix} \tilde{y} \\ \tilde{u} \end{bmatrix} = \begin{bmatrix} I & \Pi \\ 0 & I \end{bmatrix} \begin{bmatrix} y \\ u \end{bmatrix} \quad \text{and} \quad \begin{bmatrix} \tilde{v}_o \\ \tilde{v}_i \end{bmatrix} = \begin{bmatrix} I & -\Pi \\ 0 & I \end{bmatrix} \begin{bmatrix} v_o \\ v_i \end{bmatrix}. \tag{3.37}$$

They follows by standard block-diagram manipulation rules in the transition from Fig. 3.9(b) to Fig. 3.9(c). These relations suggest that Π itself should be kept stable in order to preserve internal stability under loop shifting. But apart from the limitations above, the choice of Π is arbitrary, which renders the method quite flexible in its abilities to affect properties of $\tilde{P}$.

Our interest is to exploit those abilities in the context of dead-time plants of the form $P\bar{D}_\tau$. To be specific, the goal is to construct Π with which $\tilde{P} = P\bar{D}_\tau + \Pi$ is finite dimensional. This idea can be traced back to [8], where it was applied to a wider class of infinite-dimensional systems. Implicitly, it is also related to the earlier dead-time compensation developments in [80] discussed in §3.2.1, cf. (3.15).

3.4.2 Preliminary: truncation and completion operators

Consider a finite-dimensional system G given by its state-space realization $G(s) = D + C(sI - A)^{-1}B$ (not necessarily minimal). Its impulse response is $g(t) = D\delta(t) + Ce^{At}B\mathbb{1}(t)$. By the *FIR truncation operator* $\pi_\tau\{G\}$ associated with this G and a constant $\tau > 0$ we understand the system, whose impulse response is the truncation of $g(t)$ to the interval $[0, \tau]$. This operator can be visualized as the mapping

$$\pi_\tau\{G\} : \quad \text{} \quad \longmapsto \quad \text{}. \tag{3.38}$$

Formally, the impulse response of this system is

$$g(t)\big(\mathbb{1}(t) - \mathbb{1}(t - \tau)\big) = g(t) - Ce^{At}B\mathbb{1}(t - \tau) = g(t) - Ce^{A\tau}e^{A(t-\tau)}B\mathbb{1}(t - \tau).$$

The last term above can be recognized as the impulse response of the dead-time system $\hat{G}\bar{D}_\tau$, where

$$\hat{G}(s) = \left[\begin{array}{c|c} A & B \\ \hline Ce^{A\tau} & 0 \end{array}\right] = \left[\begin{array}{c|c} A & e^{A\tau}B \\ \hline C & 0 \end{array}\right]. \tag{3.39}$$

This immediately yields one possible representation of the transfer function of the truncation operator,

$$\pi_\tau \left\{ \left[\begin{array}{c|c} A & B \\ \hline C & D \end{array} \right] \right\} = G(s) - \hat{G}(s) e^{-\tau s} = \left[\begin{array}{c|c} A & B \\ \hline C & D \end{array} \right] - \left[\begin{array}{c|c} A & B \\ \hline C e^{A\tau} & 0 \end{array} \right] e^{-\tau s} \tag{3.40a}$$

It can be verified by direct substitution that all singularities of the function above, which are the eigenvalues of A, are removable. But the same function can be represented in a different form, where no singularities are present at all. This representation follows directly from the Laplace transform of the impulse response of $\pi_\tau\{G\}$, i.e. $\mathcal{L}\{D\delta(t) + C e^{At} B \mathbb{1}_{[0,\tau]}(t)\}$. Straightforward use of (B.16) yields then

$$\pi_\tau \left\{ \left[\begin{array}{c|c} A & B \\ \hline C & D \end{array} \right] \right\} = D + C \int_0^\tau e^{-(sI-A)t} \, dt \, B. \tag{3.40b}$$

This is an entire function and, because $\|e^{-(sI-A)t}\| < \|e^{At}\|$ for all Re $s > 0$, it is bounded in $\mathbb{C}_0$. Hence, $\pi_\tau\{G\} \in H_\infty$ regardless of the stability property of G.

A dual, in a sense, operator to the truncation is the *FIR completion operator* $\sigma_\tau\{G\bar{D}_\tau\}$, associated with the input-delay alteration of G. It is defined as the truncation of the delay-free system $\tilde{G}$, whose impulse response matches that of $G\bar{D}_\tau$ in the whole interval (τ, ∞), and can be viewed as the mapping

$$\sigma_\tau\{G\bar{D}_\tau\} : \qquad\qquad\qquad \longmapsto \qquad\qquad\qquad . \tag{3.41}$$

This $\tilde{G}$ can be determined from the impulse response equality

$$\tilde{g}(t) = g(t - \tau) = D\delta(t - \tau) + C e^{A(t-\tau)} B \mathbb{1}(t - \tau) = C e^{-A\tau} e^{At} B, \quad \forall t > \tau.$$

A finite-dimensional $\tilde{G}$ satisfying this equality has the transfer function

$$\tilde{G}(s) = \left[\begin{array}{c|c} A & B \\ \hline C e^{-A\tau} & 0 \end{array} \right] = \left[\begin{array}{c|c} A & e^{-A\tau} B \\ \hline C & 0 \end{array} \right]. \tag{3.42}$$

By definition,

$$\sigma_\tau \left\{ \left[\begin{array}{c|c} A & B \\ \hline C & D \end{array} \right] e^{-\tau s} \right\} = \pi_\tau \left\{ \left[\begin{array}{c|c} A & B \\ \hline C e^{-A\tau} & D \end{array} \right] \right\} - (1 - e^{-\tau s})D,$$

so the following two representations follow from (3.40) via the substitution $C \to C e^{-A\tau}$:

$$\sigma_\tau \left\{ \left[\begin{array}{c|c} A & B \\ \hline C & D \end{array} \right] e^{-\tau s} \right\} = \tilde{G}(s) - G(s) e^{-\tau s} = \left[\begin{array}{c|c} A & B \\ \hline C e^{-A\tau} & 0 \end{array} \right] - \left[\begin{array}{c|c} A & B \\ \hline C & D \end{array} \right] e^{-\tau s} \tag{3.43a}$$

$$= C e^{-A\tau} \int_0^\tau e^{-(sI-A)t} \, dt \, B - e^{-\tau s} D \tag{3.43b}$$

and we again have that $\sigma_\tau\{G\bar{D}_\tau\} \in H_\infty$ regardless of the stability of G. Comparing this expression with (3.15), we can conclude that the MSP of Watanabe–Ito is effectively $\sigma_\tau\{P\bar{D}_\tau\}$ for P with a strictly proper transfer function.

As was already discussed in Remark 1.4 on p. 6, the FIR systems $\pi_\tau\{G\}$ and $\sigma_\tau\{G\bar{D}_\tau\}$ are sometimes referred to as distributed-delay systems. Although this terminology is avoided throughout the notes, one can encounter it in the literature.
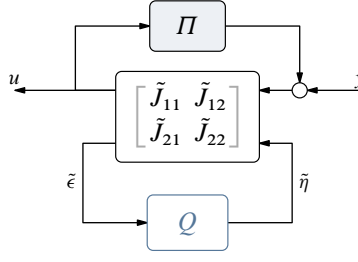
Fig. 3.10: All stabilizing controllers for $P\bar{D}_\tau$

3.4.3 Loop shifting for dead-time systems

Return now to the internal stability problem. Consider the input-delay version of the system presented in Fig. 3.8(a), where the plant is of the form $P\bar{D}_\tau$, see Fig. 3.8(b). With the loop-shifting procedure in mind and a systematic way to produce stable systems $\Pi = \sigma_\tau\{P\bar{D}_\tau\}$ rendering $P\bar{D}_\tau + \Pi$ finite dimensional, the following result can be formulated:

Theorem 3.2. *R internally stabilizes the dead-time system in Fig. 3.8(b) iff*

$$R = \tilde{R}\big(I - \sigma_\tau\{P\bar{D}_\tau\}\tilde{R}\big)^{-1} \tag{3.44}$$

for some $\tilde{R}$ internally stabilizing the finite-dimensional $\tilde{P} = P\bar{D}_\tau + \sigma_\tau\{P\bar{D}_\tau\}$ in the setup of Fig. 3.9(e).

Proof. The result follows from the loop shifting procedure with $\Pi = \sigma_\tau\{P\bar{D}_\tau\}$. Because $\tilde{P}(s)$ constructed according to (3.42) is strictly proper, we have that $\lim_{\alpha\to\infty}\sup_{s\in\mathbb{C}_\alpha}\|\Pi(s)\| = 0$, meaning that the feedback in the interconnection of $\tilde{R}$ is well posed whenever $R(s)$ is proper.

Another, algebraic, way to see the equivalence is via rewriting (3.36) as

$$\begin{bmatrix} I & 0 \\ 0 & I + R\Pi \end{bmatrix}\begin{bmatrix} I & -\tilde{P} \\ -\tilde{R} & I \end{bmatrix}\begin{bmatrix} \tilde{y} \\ \tilde{u} \end{bmatrix} = \begin{bmatrix} I \\ 0 \end{bmatrix}\begin{bmatrix} I & \tilde{P} \end{bmatrix}\begin{bmatrix} \tilde{v}_{\mathrm{o}} \\ \tilde{v}_{\mathrm{i}} \end{bmatrix},$$

where (3.37) and the formula $\tilde{R} = (I + R\Pi)^{-1}R$ are used. It follows from the fact that the chosen $\Pi \in H_\infty$ that the boundedness of y and u for all bounded v_{o} and v_{i} is equivalent to that of their "tilded" versions in (3.37). $\qquad\square$

It is perhaps not surprising now that the controller defined by (3.44) is exactly of the DTC-based form presented in Fig. 3.6, with the primary controller $\tilde{R} = -\tilde{R}$ and the DTC element $\Pi = \sigma_\tau\{P\bar{D}_\tau\}$. However, unlike the clever guesses in Section 3.2 or the use of state-feedback based architectures in Section 3.3, this architecture shows up as an outcome of an abstract procedure, not connected with any particular choice of the controller structure. We thus may claim that every stabilizing controller for the dead-time plant $P\bar{D}_\tau$ can be cast as a dead-time compensator.

This claim is further strengthened by the fact that we can parametrize all stabilizing controllers $\tilde{R}$ for the finite-dimensional $\tilde{P}$. This parametrization, known as the Youla–Kučera parametrization, can be presented in several different forms, see [45, Sec. 6.1] for details. We essentially need only one of them, that given in the result below.

Theorem 3.3 (delay-free Youla–Kučera parametrization). *Consider an LTI plant P, given in terms of its stabilizable and detectable realization $P(s) = C(sI - A)^{-1}B$. A controller R internally stabilizes P iff $R = \mathcal{F}_l(J, Q)$ for*

$$J(s) = \begin{bmatrix} J_{11}(s) & J_{12}(s) \\ J_{21}(s) & J_{22}(s) \end{bmatrix} = \left[\begin{array}{c|cc} A + BK + LC & -L & B \\ \hline K & 0 & I \\ -C & I & 0 \end{array}\right], \tag{3.45}$$
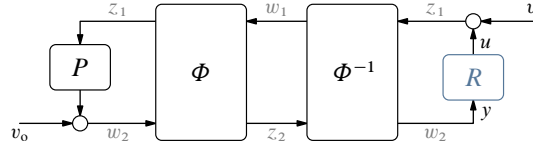
Fig. 3.11: General loop skewing

where K and L are any matrices such that $A + BK$ and $A + LC$ are Hurwitz, and some stable Q.

The application of this result to the dead-time plant $P\bar{D}_\tau$ is straightforward in the light of the result of Theorem 3.2. Indeed, that result establishes that the stabilization of $P\bar{D}_\tau$ reduces to that of the finite-dimensional $\tilde{P}$, whose state-space realization is $\tilde{P}(s) = Ce^{-A\tau}(sI - A)^{-1}B$, as in (3.42). If the original realization of P is stabilizable and detectable, then so is the realization of $\tilde{P}$ above. Hence, the set of all stabilizing controllers for $\tilde{P}$ is $\tilde{R} = \mathcal{F}_l(\tilde{J}, Q)$, where

$$\tilde{J}(s) = \begin{bmatrix} \tilde{J}_{11}(s) & \tilde{J}_{12}(s) \\ \tilde{J}_{21}(s) & \tilde{J}_{22}(s) \end{bmatrix} = \left[\begin{array}{c|cc} A + BK + e^{A\tau}LCe^{-A\tau} & -e^{A\tau}L & B \\ \hline K & 0 & I \\ -Ce^{-A\tau} & I & 0 \end{array} \right]. \tag{3.46}$$

Combining this result with that Theorem 3.2 we end up with a complete parametrization of all stabilizing controllers in the form depicted in Fig. 3.10. This is again a DTC-based controller.

3.4.4 Possible extensions

The loop shifting idea is not limited to the transformations of Fig. 3.9. An obvious alteration is to change the direction of the "Π" blocks in Fig. 3.9(a) or, equivalently, swap P with R and adjust involved signals appropriately. With the now familiar constraints on the stability of Π and the well posedness of the internal feedback loop, such a transformation would again convert the stabilization problem for the system in Fig. 3.8(a) to that in Fig. 3.9(e), but now with

$$\tilde{P} = P(I + \Pi P)^{-1} \quad \text{and} \quad \tilde{R} = R + \Pi.$$

This kind of loop shifting can be advantageous for some classes of systems with internal delays. For example, let $P(s) = 1/(1 - ae^{-\tau s})$ and apply the transformation above with $\Pi(s) = ae^{-\tau s}$, which is obviously stable and for which the feedback loop around the plant is well posed. With this choice $\tilde{P}(s) = 1$ is rational. Of course, the "forward" and "backward" shifts can be combined, by carrying out successively.

Another class of loop transformations are so-called multipliers, see [82, Sec. 6.1] or [12, Sec. VI.9]. Their basic idea is that the cascade MM^{-1} can be introduced at any point of the loop and then split without affecting stability if the multiplier M is bi-stable.

A yet more general transformation is shown in Fig. 3.11. The diagram there is rotated 90° counterclockwise to present the loop in the so-called chain-scattering (implicit) form, for which the formulae are simpler. But now Φ, as well as Φ^{-1}, represents a relation between a mixture of inputs and outputs, rather than the more conventional i/o relation. For instance, the relation

$$\begin{bmatrix} z_1 \\ w_2 \end{bmatrix} = \begin{bmatrix} \Phi_{11} & \Phi_{12} \\ \Phi_{21} & \Phi_{22} \end{bmatrix} \begin{bmatrix} w_1 \\ z_2 \end{bmatrix} \iff \begin{bmatrix} z_1 \\ z_2 \end{bmatrix} = \begin{bmatrix} \Phi_{11} - \Phi_{12}\Phi_{22}^{-1}\Phi_{21} & \Phi_{12}\Phi_{22}^{-1} \\ -\Phi_{22}^{-1}\Phi_{21} & \Phi_{22}^{-1} \end{bmatrix} \begin{bmatrix} w_1 \\ w_2 \end{bmatrix},$$

provided Φ_{22} is square and invertible. The second equality above is the conventional i/o relation. The loop shifting of Fig. 3.9 corresponds in this setting to the choice $\Phi = \begin{bmatrix} I & 0 \\ -\Pi & I \end{bmatrix}$. An example of a nontrivially more general loop skewing is the scattering transformation of [2], popular in bilateral teleoperation. It

involves two sets of transformations of the form presented in Fig. 3.11, at the master and slave sides, both with

$$\Phi = \begin{bmatrix} \sqrt{b/2} & \sqrt{b/2} \\ -1/\sqrt{2b} & 1/\sqrt{2b} \end{bmatrix},$$

where $b > 0$ is the characteristic impedance of the transmission line. This transformation renders delayed transmission lines passive. General stability preservation conditions, as well as relations between original and transformed signals of interest, for the transformation in Fig. 3.11 are more involved though.

3.5   Delay as a constraint: extraction

As if a plethora of ideas presented up to this point were not enough, the chapter is concluded with yet another approach to characterize all stabilizing controllers for dead-time systems. The idea here is to treat the loop delay as a causality constraint imposed upon the controller, rather than a part of the plant. The applicability scope of this approach is thus essentially limited to dead-time systems, where the delay can be moved between the plant and the controller along the loop. At the same time, the approach extends to various optimal control problems in a relatively straightforward manner, which renders it a powerful design tool in many applications.

Before starting to expose the approach, a technical result is required.

Lemma 3.4. *If $G(s)$ is proper, i.e. uniformly bounded on $\mathbb{C}_\alpha$ for a sufficiently large $\alpha > 0$, then*

$$G \in H_\infty \iff G_\tau := G\bar{D}_\tau \in H_\infty.$$

Proof. The implication $G \in H_\infty \implies G_\tau \in H_\infty$ is obvious by the stability of the delay element. To prove the other direction, assume, on the contrary, that $G_\tau \in H_\infty$, whereas G is not. It follows from the relation $G(s) = G_\tau(s)e^{\tau s}$ and the fact that $e^{\tau s}$ is entire that $G(s)$ is holomorphic in $\mathbb{C}_0$ [65, Rem. 10.3]. Because $G(s)$ is proper, there is $\alpha > 0$ such that it is uniformly bounded on $\mathbb{C}_\alpha$. Hence, for $G \notin H_\infty$, the function $G(s)$ must be unbounded in the strip $\mathbb{C}_0 \setminus \mathbb{C}_\alpha$. But in that strip $\|G(s)\| = |e^{\tau s}| \|G_\tau(s)\| \le e^{\alpha \tau} \|G_\tau(s)\|$, which is a contradiction. $\square$

Consider the internal stability setup in Fig. 3.8(c). Strictly speaking, this system is not equivalent to that in Fig. 3.8(b), because the delay element $\bar{D}_\tau$, which is a multiplier moved from one part to another, is not bi-stable. Nonetheless, with mild well-posedness assumptions their stability properties are equivalent. Indeed, it is readily verified that

$$\begin{bmatrix} S_{\text{o},3.8(b)} & T_{\text{d},3.8(b)} \\ T_{\text{c},3.8(b)}\bar{D}_\tau & T_{\text{i},3.8(b)} \end{bmatrix} = \begin{bmatrix} S_{\text{o},3.8(c)} & T_{\text{d},3.8(c)}\bar{D}_\tau \\ T_{\text{c},3.8(c)} & T_{\text{i},3.8(c)} \end{bmatrix}.$$

Thus, if $P(s)$, $R(s)$, and $(I - P(s)R(s)e^{-\tau s})^{-1}$ are proper, the stability of the system in Fig. 3.8(b) is equivalent to that in Fig. 3.8(c) by Lemma 3.4.

The idea of the extraction approach is that the set of all delayed stabilizing controllers $R\bar{D}_\tau$ is a subset of the set of all causal stabilizing controllers, say R_0. Hence, we may start with characterizing the latter set first and then extract from it all τ-delayed controllers. Because P is finite dimensional, Theorem 3.3 yields a complete parametrization of causal stabilizing controllers for it, which is $R_0 = \mathcal{F}_l(J, Q)$ for J given by (3.45) and an arbitrary $Q \in H_\infty$. Thus, all we need is to characterize all stable Q such that $\mathcal{F}_l(J, Q) = R\bar{D}_\tau$ for a causal R, i.e. is a dead-time system.

To this end, let J be an invertible finite-dimensional LTI system having a 2×2 partition with square J_{12} and J_{21} sub-blocks. Define

$$H := J^{-1} = \begin{bmatrix} H_{11} & H_{12} \\ H_{21} & H_{22} \end{bmatrix},$$

where the partition is compatible with that of J, and bring in the decompositions

$$H_{22} = \pi_\tau\{H_{22}\} + \hat{H}_{22}\bar{D}_\tau \quad \text{and} \quad H_{11}\bar{D}_\tau = \tilde{H}_{11} - \sigma_\tau\{H_{11}\bar{D}_\tau\},$$

where $\hat{H}_{22}$ and $\tilde{H}_{11}$ have strictly proper transfer functions and can be obtained by (3.39) and (3.42), respectively. We have then the following key technical result:

Lemma 3.5. *If J is such that J_{12} and J_{21} are invertible, then a causal Q renders $\mathcal{F}_l(J, Q) = R\bar{D}_\tau$ under a causal R iff*

$$Q = \pi_\tau\{H_{22}\} + \tilde{Q}\bar{D}_\tau$$

for a causal $\tilde{Q}$. Moreover, all attainable R's are then in the form shown in Fig. 3.10 with

$$\tilde{J} = \begin{bmatrix} \tilde{H}_{11} & H_{12} \\ H_{21} & \hat{H}_{22} \end{bmatrix}^{-1}$$

and an arbitrary causal $\tilde{Q}$.

Proof. The invertibility of J and its $(1, 2)$ and $(2, 1)$ sub-blocks guarantees [45, Prop. 5.6] that the mapping $Q \mapsto \mathcal{F}_l(J, Q)$ is bijective whenever it is well posed, with $R_0 = \mathcal{F}_l(J, Q) \iff Q = \mathcal{F}_u(J^{-1}, R_0)$. In other words, $R_0 = R\bar{D}_\tau$ iff

$$Q = H_{22} + H_{21}(I - R\bar{D}_\tau H_{11})^{-1}R\bar{D}_\tau H_{12} = H_{22} + H_{21}(I - RH_{11}\bar{D}_\tau)^{-1}RH_{12}\bar{D}_\tau,$$

where the latter equality follows by the time-invariance of H_{11} and H_{12}. It is readily seen that the response of this Q to the impulse applied at every t_c coincides with that of H_{22} in the whole $[t_c, t_c + \tau]$ for every causal R. This suggests that the required Q can be connected with the truncation of H_{22}.

To prove that formally, consider first the system

$$(I - RH_{11}\bar{D}_\tau)^{-1}R = (I + R\sigma_\tau\{H_{11}\} - R\tilde{H}_{11})^{-1}R = (I - \tilde{R}\tilde{H}_{11})^{-1}\tilde{R},$$

where

$$\tilde{R} := (I + R\sigma_\tau\{H_{11}\})^{-1}R$$

By arguments used in §3.4.3, we know that for any causal R the mapping $R \mapsto \tilde{R}$ is bijective and well-posed for all causal R (thus resulting in a causal $\tilde{R}$). Thus, we can equivalently rewrite the relation for Q in terms of $\tilde{R}$ as

$$Q = H_{22} + H_{21}(I - \tilde{R}\tilde{H}_{11})^{-1}\tilde{R}H_{12}\bar{D}_\tau = \pi_\tau\{H_{22}\} + \left(\hat{H}_{22} + H_{21}(I - \tilde{R}\tilde{H}_{11})^{-1}\tilde{R}H_{12}\right)\bar{D}_\tau.$$

The system

$$\tilde{Q} := \hat{H}_{22} + H_{21}(I - \tilde{R}\tilde{H}_{11})^{-1}\tilde{R}H_{12} = \mathcal{F}_u(\tilde{J}^{-1}, \tilde{R})$$

is well posed (because $\tilde{H}_{11}(s)$ is strictly proper) for all causal $\tilde{R}$ and is thus causal whenever so is $\tilde{R}$.

The next step is to show that the mapping $\tilde{R} \mapsto \mathcal{F}_u(\tilde{J}^{-1}, \tilde{R})$ is bijective. To this end, consider the equality

$$\begin{bmatrix} J_{11} & J_{12} \\ J_{21} & J_{22} \end{bmatrix}\begin{bmatrix} H_{11} \\ H_{21} \end{bmatrix} = \begin{bmatrix} I \\ 0 \end{bmatrix}.$$

Its first row yields that $H_{11} = -J_{21}^{-1}J_{22}H_{21}$ and then the second raw—that $H_{21}^{-1} = J_{12} - J_{11}J_{21}^{-1}J_{22}$. Because $J_{12} - J_{11}J_{21}^{-1}J_{22}$ is well defined, by assumption, we conclude that H_{21} is invertible. The invertibility of H_{12} can be shown by similar arguments. But this implies that $\tilde{J}$ possesses the same properties as J itself and the statement follows.

Thus, we showed that every Q rendering $R_0 = R\bar{D}_\tau$ is of the form $\pi_\tau\{H_{22}\} + \tilde{Q}\bar{D}_\tau$ and that any causal $\tilde{Q}$ can be attained by a causal $\tilde{R}$. The result then follows by the relation $R = \tilde{R}(I - \sigma_\tau\{H_{11}\bar{D}_\tau\}\tilde{R})^{-1}$, which represents the system in Fig. 3.10 for $\tilde{R} = \mathcal{F}_l(\tilde{R}, \tilde{Q})$. □

The result of Lemma 3.5 applies to general, possibly time-varying controllers. In the time-invariant case, we just need to consider time-invariant $\tilde{Q}$. Then the result of Lemma 3.4 and the fact that $\pi_\tau\{\hat{H}_{22}\} \in H_\infty$ can be used to prove that $\tilde{Q} \in H_\infty \iff Q \in H_\infty$ and thus that the system in Fig. 6.1(b) characterizes all stabilizing controllers for $P\bar{D}_\tau$.

To conclude, construct a state-space realization of $\tilde{J}$ from that of J given by (3.45). It is readily seen that

$$J^{-1}(s) = \left[\begin{array}{c|cc} A & -B & L \\ \hline -C & 0 & I \\ K & I & 0 \end{array}\right].$$

Hence, by (3.39) we have that

$$H_{22}(s) = \left[\begin{array}{c|c} A & L \\ \hline K & 0 \end{array}\right] \implies \hat{H}_{22}(s) = \left[\begin{array}{c|c} A & e^{A\tau}L \\ \hline K & 0 \end{array}\right]$$

and by (3.42)—that

$$H_{11}(s) = \left[\begin{array}{c|c} A & -B \\ \hline -C & 0 \end{array}\right] = \left[\begin{array}{c|c} A & B \\ \hline C & 0 \end{array}\right] \implies \tilde{H}_{11}(s) = \left[\begin{array}{c|c} A & -B \\ \hline -Ce^{-A\tau} & 0 \end{array}\right].$$

Hence,

$$\left[\begin{array}{cc} \tilde{H}_{11}(s) & H_{12}(s) \end{array}\right] = \left[\begin{array}{c|cc} A & -B & e^{A\tau}L \\ \hline -Ce^{-A\tau} & 0 & I \end{array}\right] \quad\text{and}\quad \left[\begin{array}{cc} H_{21}(s) & \hat{H}_{22}(s) \end{array}\right] = \left[\begin{array}{c|cc} A & -B & e^{A\tau}L \\ \hline K & I & 0 \end{array}\right]$$

where the realization for H_{12} is obtained by a similarity transformation of that in J^{-1}, from which

$$\tilde{J}^{-1}(s) = \left[\begin{array}{c|cc} A & -B & e^{A\tau}L \\ \hline -Ce^{-A\tau} & 0 & I \\ K & I & 0 \end{array}\right].$$

Applying (B.26) we then end up exactly with the realization (3.46), matching the results derived by the loop-shifting approach in §3.4.3.

Chapter 4

Robustness to Delay Uncertainty

U P TO THIS POINT, delays in studied analysis and design problems were mostly assumed to be known and constant. These assumptions might not be realistic. In fact, in all examples considered in Section 1.2 delays vary in course of operation due to fluctuations of system parameters, such as the speed of rolls in Fig. 1.2(a) or the conveyor belt in Fig. 1.2(b), unevenness of communication delays in networked applications, jitter in computation time, et cetera. In some of such cases variations of loop delays can be taken into account in the design process, see e.g. Remark 3.2 on p. 50. But in many situations actual values of delays are unknown, or only known to lie in some interval. In such situations robustness analysis, i.e. the analysis of the sensitivity of a system to uncertainty in its delay element, is the approach to explore.

The setup studied in this chapter is presented in Fig. 4.1(a), where $\tau_0 \geq 0$ is a *nominal delay* and $\tau_\delta \geq -\tau_0$ is a deviation of the delay from τ_0. In most cases we assume that τ_δ is constant, time-varying deviations are discussed briefly in §4.2.5. We assume that the nominal system, that with $\tau_\delta = 0$, is stable and study the sensitivity of the stability property to nonzero τ_δ. In line with the convention to move only "troublesome" elements outside the LFT generator, we normally study the problem in the form presented in Fig. 4.1(a), where the nominal delay element $\bar{D}_{\tau_0}$ is absorbed into G_{zw} and G_{yw} (or, equivalently, into G_{zw} and G_{zu}), i.e. we do not limit G to be finite dimensional. Moreover, our main focus is on the particular case of this setup presented in Fig. 4.1(c). It corresponds to the input-delay case, cf. (1.25), with P interpreted as a plant (may include the nominal delay $\bar{D}_{\tau_0}$) and R as a controller, either fixed or to be designed to reduce the sensitivity of the loop to uncertainty in τ_δ.

4.1 Delay margin

We start with studying the system in Fig. 4.1(c) under a SISO loop $L := PR$. The *delay margin* μ_d is defined as the the smallest τ_δ, i.e. the smallest deviation of the loop delay from nominal value, under which the system becomes unstable. If the system is stable for all $\tau_\delta \in [-\tau_0, \infty)$, then we say that $\mu_d = \infty$ or that the system is *delay-independent stable*.
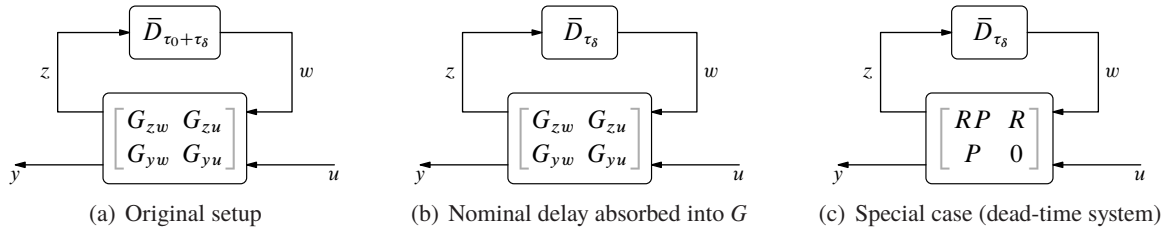

| (a) Original setup | (b) Nominal delay absorbed into G | (c) Special case (dead-time system) |

Fig. 4.1: General single-delay interconnection with uncertain delay
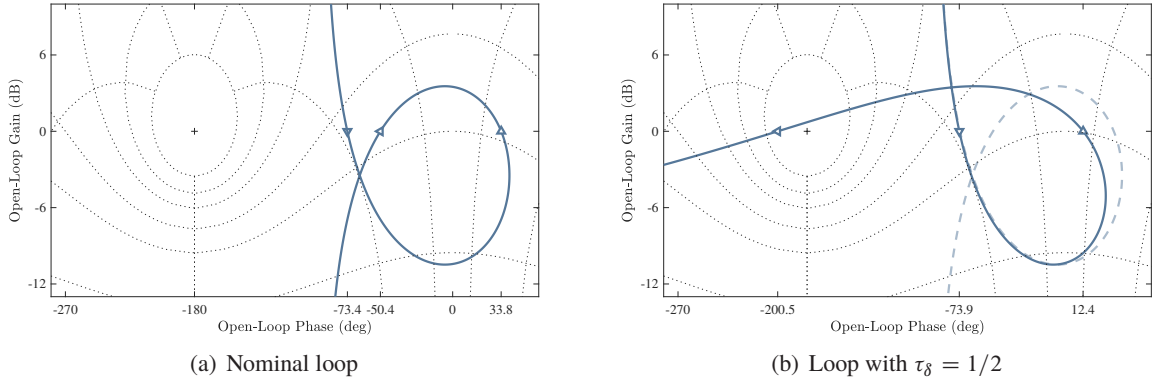
(a) Nominal loop

(b) Loop with $\tau_\delta = 1/2$

Fig. 4.2: Nichols plots of the loop frequency response for $L(s) = 6(s^2 + 0.2s + 0.01)/(s(s+2)^2)$

The delay margin is a classical control notion, sometimes defined in textbooks as

$$\mu_{\mathrm{d}} = \frac{\mu_{\mathrm{ph}}}{\omega_{\mathrm{c}}}, \tag{4.1}$$

where μ_{ph} (in radians) is the phase margin of the loop L and ω_{c} (in radians per time unit) is the crossover frequency, i.e. the frequency ω at which $|L(\mathrm{j}\omega)| = 1$. However, this definition is not always accurate. First, as we already know from the discussion in §2.1.3 on p. 23, if L is finite dimensional and its high-frequency gain $|L(\infty)| > 1$, then the system is unstable for all $\tau_\delta > 0$. Thus, the system with $L(s) = \sqrt{2}s/(s+1)$ has a zero delay margin, even though formula (4.1) in this case would yield $\mu_{\mathrm{d}} = 1.25\pi/1 \approx 3.927$. Second, there are systems with several crossover frequencies, for which the phase margin and the corresponding crossover frequency are not a good indicator of delay tolerance. For example, consider a system with $L(s) = 6(s^2 + 0.2s + 0.01)/(s(s+2)^2)$, whose Nichols plot is shown in Fig. 4.2(a). The phase margin in this case is $\mu_{\mathrm{ph}} \approx 1.86$ [rad], measured at the crossover frequency $\omega_{\mathrm{c},1} \approx 0.015$ (marked by the downward triangle). Formula (4.1) yields then $\mu_{\mathrm{d}} \approx 121.16$. But this is not even close to the smallest destabilizing delay in this case. For example, Fig. 4.2(b) shows the loop gain under $\tau_\delta = 1/2$, which clearly yields an unstable system. The reason is that there are two more crossover frequencies, viz. $\omega_{\mathrm{c},2} \approx 0.746$ (the upward triangle) and $\omega_{\mathrm{c},3} \approx 5.239$ (the leftward triangle). The distances from the critical point at those frequencies are larger than that at $\omega_{\mathrm{c},1}$, so they do not count in the calculation of the phase margin. However, these crossover frequencies, especially $\omega_{\mathrm{c},3}$, are higher than $\omega_{\mathrm{c},1}$. As such, phase lags due to the delay at those crossovers are larger. In particular, the delays at which each one of these points crosses the critical point are $\tau_2 = \mu_{\mathrm{ph},2}/\omega_{\mathrm{c},2} \approx 3.73/0.746 \approx 5$ and $\tau_3 = \mu_{\mathrm{ph},3}/\omega_{\mathrm{c},3} \approx 2.26/5.239 \approx 0.432$. Thus the true delay margin for this system is $\mu_{\mathrm{d}} \approx 0.432$.

By this logic, the delay margin with respect to positive τ_δ should be calculated as

$$\mu_{\mathrm{d}} = \begin{cases} 0 & \text{if } \limsup_{\omega \to \infty} |P(\mathrm{j}\omega)R(\mathrm{j}\omega)| \geq 1 \\ \min_i \dfrac{\mu_{\mathrm{ph},i}}{\omega_{\mathrm{c},i}} & \text{otherwise} \end{cases} \tag{4.2}$$

where $\mu_{\mathrm{ph},i}$ is the angular distance from the critical point in the negative angle direction at the crossover frequency $\omega_{\mathrm{c},i}$. The delay margin with respect to negative τ_δ is calculated similarly, modulo the replacement of the phase margins with angular distances from the critical point in the positive direction, denote them $\tilde{\mu}_{\mathrm{ph},i}$, and the constraint that such delay margin must be lowerbounded by the nominal τ_0.

4.1.1   Bounds on the achievable delay margin

It is of interest not only to define the delay margin notion, but also to understand, what is the maximum μ_{d} attainable by an appropriate choice of R. If $P \in H_\infty$, then the answer is obviously $\mu_{\mathrm{d}} = \infty$. This is

what we get under the choice $R = 0$. The question becomes nontrivial for unstable plants. Bounds on the attainable delay margins for several classes of unstable plants were derived in [40]. Some of these results, as well as ideas behind the proofs, are presented below.

We start with a result, establishing that unstable poles at the origin do not impose limitations on the achievable delay margin.

Proposition 4.1. *If $P(s)$ has no poles in $\bar{\mathbb{C}}_0 \setminus \{0\}$, then any μ_d is attainable by a stabilizing R.*

Proof (outline). It will be shown in §4.2.3 that the delay margin is lowerbounded by the reciprocal of the H_∞-norm of the transfer function $sT(s)$, where T is the complementary sensitivity function corresponding the the zero-delay case. A controller attaining an arbitrarily small H_∞-norm of $sT(s)$ was designed in [40, App. C]. □

Any pole of $P(s)$ in $\bar{\mathbb{C}}_0 \setminus \{0\}$ imposes hard constraints on the attainable delay margin. The result below proves that for a real pole.

Proposition 4.2. *If $P(s)$ has a pole at $s = a > 0$, then*

$$\mu_d < \frac{2}{a}.$$

This bound is tight if this pole is the only pole of $P(s)$ in $\bar{\mathbb{C}}_0$ and $P(s)$ is minimum-phase.

Proof. Consider first the stabilization problem for the system in Fig. 2.5 with $\bar{R}_\alpha(s) := (-s + \alpha)/(s + \alpha)$, under the very same $G_{zw} = PR$. Because $\bar{R}_\alpha(s)|_{\alpha=\infty} = \bar{D}_\tau(s)|_{\tau=0}$, any controller stabilizing this system under $\alpha = \infty$ does that for the system in Fig. 4.1 under $\tau_\delta = 0$. Then, as α decreases, roots of the characteristic polynomial move continuously along corresponding loci. What we know is that at $\alpha = a$ the system is unstable, just because $s = a$ is then a root of its characteristic polynomial no matter what R is (unstable cancellations). Therefore, roots must cross the imaginary axis, say at $s = \pm j\omega_{\text{cross}}$ for some $\omega_{\text{cross}} > 0$, for at least one $\alpha = \alpha_{\text{cross}} > a$ regardless what R stabilizing the system for $\alpha = \infty$ is used. But the arguments of Rekašius, discussed in §2.1.6, imply that there must then exist a minimal delay $\tau_{\text{cross}} > 0$, for which there are pure imaginary roots of the characteristic quasi-polynomial associated with the system in Fig. 4.1 at the very same $s = \pm j\omega_{\text{cross}}$. This corresponding destabilizing delay, cf. (2.13), satisfies

$$\frac{\alpha_{\text{cross}}}{\omega_{\text{cross}}} = \cot \frac{\tau_{\text{cross}}\omega_{\text{cross}}}{2} \quad \Longrightarrow \quad \tau_{\text{cross}} = \frac{2}{\omega_{\text{cross}}} \arctan \frac{\omega_{\text{cross}}}{\alpha_{\text{cross}}} < \frac{2}{\alpha_{\text{cross}}} < \frac{2}{a}$$

(the first upper bound is approached as $\omega_{\text{cross}} \downarrow 0$). This yields the bound of the proposition.

To show that this bound is tight whenever $P(s)$ has no other unstable poles and no nonminimum-phase zeros, write

$$P(s) = \frac{1}{s - a} P_{\text{inv}}(s)$$

for stable and minimum-phase $P_{\text{inv}}(s)$. In this case the controller $R_a(s) = -P_{\text{inv}}^{-1}(s)k_{\text{p}}(T_{\text{d}}s + a)$ renders the stabilization problem equal to that for the first-order $P_a(s) := 1/(s + a)$ and the PD $R_a = -k_{\text{p}}(T_{\text{d}}s + a)$. But this is essentially the stabilization problem studied in §3.1.2. Specifically, it was shown there that a PD controller approaches the upper-bound delay margin $2/a$ as $k_{\text{p}} \downarrow 1$ and $T_{\text{d}} \uparrow 1$. Although this controller is not proper, its slight modification can attain the same bound as well, see [40, Rem. 8]. □

The result below extends this bound for the case of complex and pure imaginary poles.

Proposition 4.3. *If $P(s)$ has poles at $s = (\zeta \pm j\sqrt{1 - \zeta^2})\omega_n$ for some $0 \le \zeta < 1$ and $\omega_n > 0$, then*

$$\mu_d < \frac{\sqrt{1 - \zeta^2}}{\omega_n}\left(\pi + 2\max\left\{\frac{\zeta}{\sqrt{1 - \zeta^2}}, \arctan\frac{\sqrt{1 - \zeta^2}}{\zeta}\right\}\right) = $$

This bound is tight if these poles are the only poles of $P(s)$ in $\bar{\mathbb{C}}_0$ and $P(s)$ is minimum-phase.
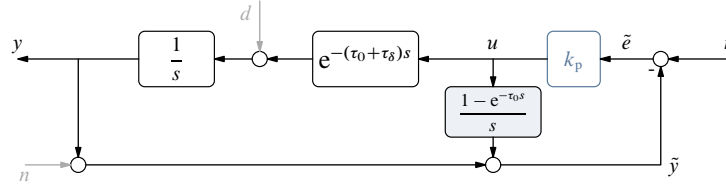
Fig. 4.3: Smith controller with proportional primary controller

Proof (outline). The proof for the case of $\zeta > 0$ follows the ideas of that of Proposition 4.2, just with the rational substitution of the form $\bar{R}_\alpha(s) = (\zeta - j\sqrt{1-\zeta^2} - s/\alpha)/(\zeta + j\sqrt{1-\zeta^2} + s/\alpha)$, which has complex parameters, see [40, Thm. 9] for details. The case of $\zeta = 0$ can be addressed by somewhat simpler arguments. Namely, in this case the loop has an infinite magnitude at $\omega = \omega_n$ and a strictly contractive high-frequency gain under any stabilizing controller. This implies that there is a crossover frequency $\omega_c > \omega_n$ with some $\mu_{ph} \in (0, 2\pi)$. Hence, the delay margin $\mu_d \leq \mu_{ph}/\omega_c < 2\pi/\omega_n$. Finally, controllers approaching the upper bound of the proposition are presented in [40, Sec. IV]. $\square$

It should be emphasized that controllers maximizing the delay margin tend to render the crossover frequency $\omega_c \downarrow 0$. In other words, maximizing μ_d alone, without imposing additional constraints on the crossover frequency or related feedback properties, does not make much engineering sense.

Remark 4.1 (time-varying controllers). Curiously, and perhaps somewhat counterintuitively, there are no constraints on the attainable delay margins, even for an unstable LTI P, if time-varying linear controllers are allowed [41]. Still, the control strategy achieving that, which hinges on the ability to estimate both the state of P and its appropriate prediction in finite time, is not quite practical either. ∇

4.1.2 Delay margins of DTC-based loops: case study and general considerations

Consider now the system in Fig. 4.3, which is an integrator plant controlled by the Smith controller with a proportional primary part. Assume that the actual loop delay is constant yet uncertain, of the form $\tau_0 + \tau_\delta$ for some $\tau_\delta \geq -\tau_0$. This is a particular case of the setup in Fig. 4.1(c) under

$$P(s) = \frac{e^{-\tau_0 s}}{s} \quad \text{and} \quad R(s) = -\frac{k_p s}{s + k_p(1 - e^{-\tau_0 s})} \tag{4.3}$$

(mind negative feedback). As we know from the discussion in §3.2.1, the controller stabilizes this system under the nominal delay iff k_p stabilizes the delay-free integrator. The corresponding characteristic polynomial, $\chi(s) = s + k_p$, is Hurwitz iff $k_p > 0$, which is assumed hereafter. The static gain of R is

$$R(0) = \lim_{s \to 0} \frac{k_p s}{s + k_p(1 - e^{-\tau_0 s})} = \frac{k_p}{1 + \tau_0 k_p} = \frac{r_0}{\tau_0}, \quad \text{where } r_0 := \frac{\tau_0 k_p}{1 + \tau_0 k_p} \in (0, 1).$$

In other words, the low-frequency gain is bounded by $1/\tau_0$ even if k_p grows unbounded, more about this is discussed in Chapter 5. The nominal closed-loop complementary sensitivity function is then

$$T(s) = \frac{k_p}{s + k_p} e^{-\tau_0 s},$$

whose bandwidth $\omega_b = k_p$ is an increasing and unbounded function of k_p.

Consider now stability margins attained in the system in Fig. 4.3 for the actual, not equivalent delay-free, system with the loop transfer function

$$L(s) = P(s)R(s) = \frac{k_p e^{-\tau_0 s}}{s + k_p(1 - e^{-\tau_0 s})} = \frac{r_0 e^{-\tau_0 s}}{(1 - r_0)\tau_0 s + r_0(1 - e^{-\tau_0 s})}.$$

(a) Gain margin, μ_g (b) Phase margin, μ_{ph} (c) Normalized delay margin, μ_d/τ_0
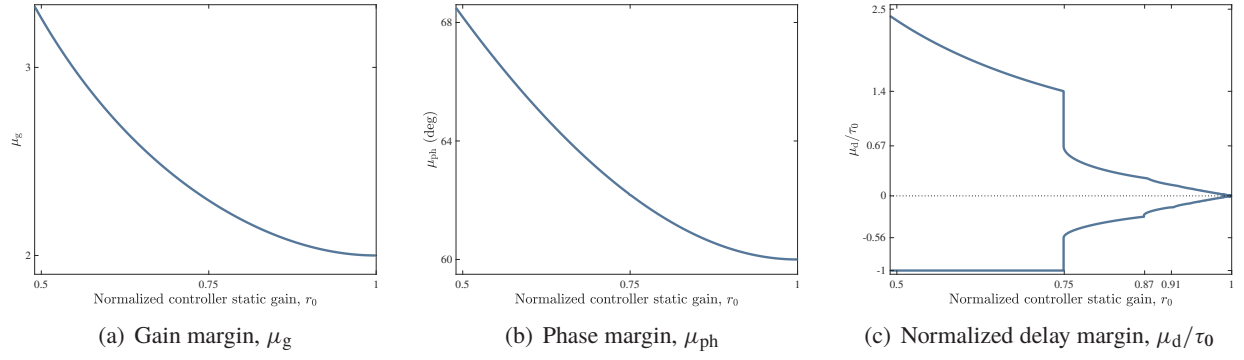
Fig. 4.4: Stability margins as functions of the normalized controller static gain $r_0 = \tau_0 R(0)$

It is convenient to analyze stability margins as functions of the normalized static gain of the controller, r_0, rather than those of k_p, because the range of the former is bounded and because it better reflects the DC properties of the resulted closed-loop system. The gain and phase margins of this loop, shown in Fig. 4.4(a) and 4.4(b), respectively (see [21, App. A] for details of their derivations), are expectably monotonically decreasing and continuous. As a matter of fact, as $r_0 \downarrow 0$, the gain margin grows unbounded and the phase margin approaches 90°, whereas as $r_0 \uparrow 1$, they reduce to the respectable $\mu_g = 2$ and $\mu_{ph} = 60°$. The normalized delay margin, i.e. the maximum normalized deviation τ_δ/τ_0 from the nominal loop delay, is shown in Fig. 4.4(c). It is also a monotonically decreasing function of r_0, unbounded as $r_0 \downarrow 0$. However, it is no longer continuous. For example, at $r_0 \approx 0.75$ the delay margin for positive τ_δ drops from 1.4 to 0.67, i.e. by more than a factor of two, and delay margin for negative τ_δ jumps from its highest value of -1 (for which the delay-free system is also stable with the DTC-based controller) to -0.56. Moreover, the delay margin vanishes as $r_0 \uparrow 1$, which is also qualitatively different from the behavior of μ_g and μ_{ph}.

The rationale behind this behavior of μ_d becomes apparent if we take a look at the loop frequency response around the borderline value $r_0 \approx 0.74902$. At a slightly lower gain of $r_0 = 0.749$, there is only one crossover frequency at $\omega_c \approx 0.774/\tau_0$, see Fig. 4.5(a). Hence, the delay margin is calculated by (4.1) as $\mu_d \approx 1.086/(0.774/\tau_0) = 1.402\tau_0$. But at $r_0 = 0.74902$ another (double) crossover frequency $\omega_{c,2} \approx 5.1075/\tau_0$ pops up, see Fig. 4.5(b). Hence, the delay margin is calculated by (4.2) as

$$\mu_d = \max\left\{\frac{\mu_{ph,1}}{\omega_{c,1}}, \frac{\mu_{ph,2}}{\omega_{c,2}}\right\} \approx \max\left\{\frac{1.086}{0.774/\tau_0}, \frac{3.4089}{5.1075/\tau_0}\right\} \approx 0.667\tau_0$$

(the phase margin and the first crossover frequency are virtually the same as those for $r_0 = 0.749$). As

(a) $r_0 = 0.749$, $\omega_c \approx 0.774/\tau_0$ (b) $r_0 = 0.74902$, $\omega_{c,1} \approx 0.774/\tau_0$, $\omega_{c,2} \approx 5.1075/\tau_0$

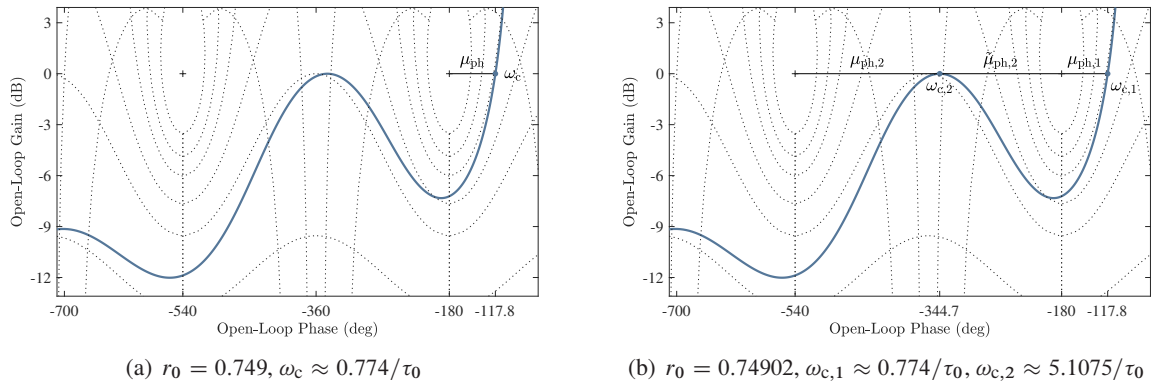Fig. 4.5: Nichols plots of the loop frequency response for the system in Fig. 4.3
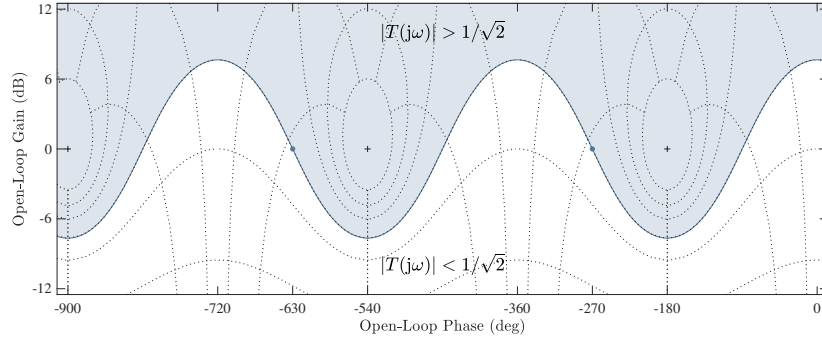
Fig. 4.6: Closed-loop bandwidth contour on the Nichols chart

$\omega_{c,2}$ is larger than $\omega_{c,1}$ by more than a factor of six, this delay margin drops dramatically, even though $\mu_{ph,1} < \mu_{ph,2}$, and we have the jump. Also, instability can now be caused by a decrease of the delay, as the plot can also cross the critical point if a phase lead of $\tilde{\mu}_{ph,2} \approx 2.874\,[\text{rad}]$ is added at the second crossover $\omega_{c,2}$. Note that as r_0 increases towards 1, more and more crossover frequencies pop up, resulting in a further deterioration of the delay margin. In the limit, as $r_0 \uparrow 1$, the loop transfer function approaches

$$L(s) = \frac{e^{-\tau_0 s}}{1 - e^{-\tau_0 s}},$$

which yields the infinite-bandwidth $T(s) = e^{-\tau_0 s}$, but an infinite and unbounded sequence of crossover frequencies $\{\omega_{c,i}\}$ satisfying $\cos(\omega_{c,i}\tau_0) = 1/2$. Consequently, the delay margin of this loop indeed vanishes, even though the gain and phase margins are reasonably high.

A natural question in this respect is whether this kind of behavior, namely the proliferation of the number of crossover frequencies, is representative in the context of dead-time compensation. The answer is yes, if the primary controller attempts to increase the closed-loop bandwidth beyond certain level. Specifically, define the closed-loop bandwidth as the largest ω_b for which $|T(j\omega)| \geq 1/\sqrt{2}$ in the whole frequency range $\omega \in [0, \omega_b]$. The loop frequency response $L(j\omega)$ must then lie in the shaded area of the Nichols chart in Fig. 4.6, determined by the corresponding M-circle, for all $\omega \in [0, \omega_b]$. It is readily seen that if $|T(0)| > 1/\sqrt{2}$ and the closed-loop system is stable, then there is more than one crossover frequency whenever one of the two conditions below holds:

1. the phase lag of the open-loop system exceeds 270° at $\omega = \omega_b$, i.e. $\arg L(j\omega_b) < -3\pi/2$,

2. $L(s)$ has at least two unstable poles, so its frequency response must encircle the critical point.

Moreover, additional phase lag or / and unstable poles increase the number of crossover frequencies. Classical control has some accepted rules of thumb, saying that the presence of a loop delay imposes limitations of the attainable bandwidth, see [19, §8.6.2]. However, such limitations are less visible in DTC-based settings. Indeed, as follows from (3.13) on p. 46, the complementary sensitivity transfer function in a general DTC-based setup, like that in Fig. 3.5, is

$$T(s) = \frac{P(s)}{1 + \tilde{P}(s)\tilde{R}(s)}\, e^{-\tau_0 s} =: T_{\tau_0}(s)\, e^{-\tau_0 s},$$

where T_{τ_0} is assigned by a delay-free design of the primary controller $\tilde{R}$. Thus, the closed-loop bandwidth does not depend on the delay element, as $|T(j\omega)| = |T_{\tau_0}(j\omega)|$, so one might be tempted to increase it without accounting for the phase lag of the plant at ω_b due to the delay. As a result, either the loop has a large phase lag at ω_b or the controller introduces unstable modes to add enough phase lead and compensate for the phase lag introduced by $e^{-j\omega\tau_0}$. In either case, extra crossover frequencies arise and μ_d deteriorates.

(a) System of interest, $\tau_\delta \in [0, \bar{\tau}]$ (b) Covering system, $\bar{D}_{\tau_\delta} \subset \Delta$ for all $\tau_\delta \in [0, \bar{\tau}]$
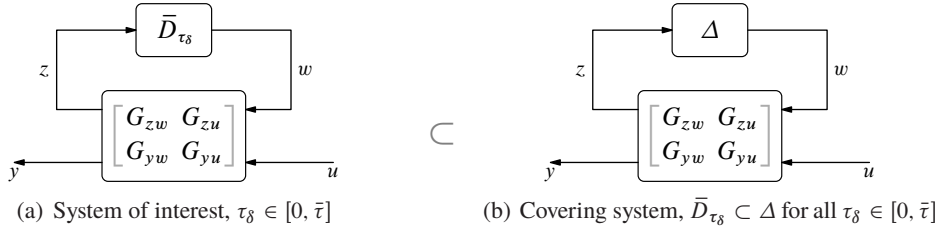
Fig. 4.7: Embedding into a wider class of uncertain systems

Remark 4.2 (closed-loop bandwidth). A moral of the discussion above is that it might be safer to define the closed-loop bandwidth via the gain of the sensitivity function, say as the largest ω_b for which $|S(j\omega)| \leq \mu_b$ in the whole range $\omega \in [0, \omega_b]$ for some $\mu_b \in (0, 1)$. If μ_b is sufficiently small, say $\mu_b \leq 1 - 1/\sqrt{2} \approx 0.293$, then this measure requires not only the gain of T to be close to one (because $1 - \mu_b \leq |T(j\omega)| \leq 1 + \mu_b$, by the triangle inequality), but also its phase to be close to zero. Thinking this way may help to resist the temptation of using an overly aggressive design of the primary controller. ∇

4.2 Embedding uncertain delays into less structured uncertainty classes

The precise, i.e. non-conservative, analysis of the delay margin might not be an easy problem to address and even harder to incorporate into control design methods. A pragmatic alternative is to analyze sensitivity to uncertain delay via general-purpose robustness tools, which are quite well understood and can be embedded into optimization design frameworks. This is especially so for robust stability analyses under unstructured, and sometimes structured, complex uncertainty. In this section methods of the embedding of uncertain delays into wider uncertainty formalisms are studied.

4.2.1 Underlying idea

Let us return to the general case presented in Fig. 4.1(b) and consider the problem of finding conditions, under which the system is stable for all τ_δ from a given interval, i.e. robustly. Without loss of generality, we may assume that this interval is $\tau_\delta \in [0, \bar{\tau}]$ for a given nonzero $\bar{\tau} > 0$. If there is a lower bound $\underline{\tau} \geq -\tau_0$, then the replacement of τ_0 with $\tau_0 + \underline{\tau}$ reduces the problem to the case of $\underline{\tau} = 0$.

Let $\mathbf{\Delta}_{\bar{\tau}}$ be is a class of systems that contains all admissible delay elements, i.e. such that $\bar{D}_{\tau_\delta} \in \mathbf{\Delta}_{\bar{\tau}}$ for every $\tau_\delta \in [0, \bar{\tau}]$. A rather obvious, but nevertheless important, observation is that the system in Fig. 4.7(a) is robustly stable if yet another system, that in Fig. 4.7(b), is stable for every $\Delta \in \mathbf{\Delta}_{\bar{\tau}}$. Replacing the system in Fig. 4.7(a) with that in Fig. 4.7(b) means an expansion of the admissible uncertainty set. The rationale behind such an expansion is that the robust stability problem for the system in Fig. 4.7(b) for $\Delta \in \mathbf{\Delta}_{\bar{\tau}}$ may be easier to analyze than that for $\Delta = \bar{D}_{\tau_\delta}$. The price paid for such a simplification is that any resulting stability condition is only sufficient, i.e. potentially *conservative*. Namely, the robust *in*stability of the system in Fig. 4.7(b) does not imply that of the original system in Fig. 4.7(a).

Thus, the basic idea is to embed a system of interest into a wider class of systems, whose analysis is simpler. A key to the success of this approach is the choice of the uncertainty set $\mathbf{\Delta}_{\bar{\tau}}$. On the one hand, it should cover the original uncertain element $\bar{D}_{\tau_\delta}$ tightly, to reduce conservatism. On the other hand, it should result in a simple, and preferably design-friendly, analysis. The quest for an easily tunable and transparent tradeoff here is perhaps still under way, with no clear winner and a plenty of barely discriminable results [83, §3.3]. It is probably safe to claim that the conservatism can be effectively eliminated by increasing the computational complexity. However, such low-conservatism methods tend to be limited to analysis problems, where the controller is given. Design-friendly approaches normally use simpler
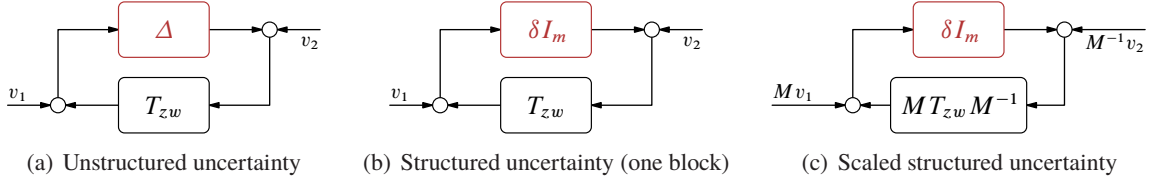
(a) Unstructured uncertainty   (b) Structured uncertainty (one block)   (c) Scaled structured uncertainty

Fig. 4.8: Robust stability setups for $m \times m$ stable Δ and scalar stable δ

uncertainty sets and are more conservative.

4.2.2 Preliminary: robust stability with respect to norm-bounded uncertainty

Arguably, the handiest class of uncertainties is the class of unstructured norm-bounded ones. The simplest such class, which can be used as a building block for more sophisticated extensions, is the unit ball in H_∞,

$$\mathcal{B}_\infty^{m \times m} := \left\{ \Delta \in H_\infty^{m \times m} \mid \|\Delta\|_\infty \leq 1 \right\}$$

(if the dimension is irrelevant of clear from the context, we write $\mathcal{B}_\infty$). In the LTI setting, this set describes stable systems Δ, whose frequency response is contractive at every frequency, i.e. $\|\Delta(\mathrm{j}\omega)\| \leq 1$, $\forall \omega \in \mathbb{R}$. With some abuse of notation, we also use the nomenclature $\mathcal{B}_\infty$ for possibly time-varying or even nonlinear systems, which are stable as operators $L_2 \to L_2$ and whose L_2-induced norm is contractive.

Consider now the internal stability interconnection in Fig. 4.8(a) for a known $m \times m$ LTI system T_{zw} and an uncertainty element Δ, which is only know to belong to $\mathcal{B}_\infty^{m \times m}$.

Theorem 4.4 (Robust Stability Theorem). *The feedback interconnection in Fig. 4.8(a) is internally stable for all $\Delta \in \mathcal{B}_\infty^{m \times m}$ iff $T_{zw} \in H_\infty$ and $\|T_{zw}\|_\infty < 1$.*

Proof. Sufficiency follows by the celebrated Small Gain Theorem, see [82, §4.4.2], [12, Sec. III.2], or [10, Thm. 9.1.7] for example. The stability of T_{zw} is obviously necessary, because $\Delta = 0$ is admissible. To prove the necessity of the norm bound on T_{zw}, assume, on the contrary, that $\|T_{zw}\|_\infty = \gamma \geq 1$. This implies that at least one of the following two conditions holds: (i) $\limsup_{\omega \to \infty} \|T_{zw}(\mathrm{j}\omega)\| = \gamma$ or (ii) there is $\omega_0 \in \mathbb{R}$ such that $\|T_{zw}(\mathrm{j}\omega_0)\| = \gamma$. If the high-frequency gain of T_{zw} is not strictly contractive, the system is destabilized by the admissible $\Delta = \bar{D}_\tau$ for every $\tau > 0$, see §2.1.3. If condition (ii) holds, then there are unitary vectors $u_0, v_0 \in \mathbb{C}^m$ such that $u_0' T_{zw}(\mathrm{j}\omega_0) v_0 = \gamma$ (obtained via SVD). If $\omega_0 = 0$, then u_0 and v_0 are real and choose $\Delta(s) = v_0 u_0'/\gamma$. If $\omega \neq 0$, consider an LTI $\Delta \in H_\infty$ with the transfer function

$$\Delta(s) = \frac{1}{\gamma} \begin{bmatrix} |v_{01}| \mathrm{e}^{-s(\arg \bar{v}_{01})/\omega_0} \\ \vdots \\ |v_{0m}| \mathrm{e}^{-s(\arg \bar{v}_{0m})/\omega_0} \end{bmatrix} \begin{bmatrix} |u_{01}| \mathrm{e}^{-s(\arg u_{01})/\omega_0} & \cdots & |u_{0m}| \mathrm{e}^{-s(\arg u_{0m})/\omega_0} \end{bmatrix},$$

where $\bar{x}$ stands for the complex conjugate of $x \in \mathbb{C}$ and the argument of x is assumed to be nonnegative. In either case $\|\Delta\|_\infty = 1/\gamma \leq 1$, so that Δ is admissible, and $\Delta(\mathrm{j}\omega_0) = v_0 u_0'/\gamma$. Hence, we have that

$$u_0'\big(I - T_{zw}(\mathrm{j}\omega_0)\Delta(\mathrm{j}\omega_0)\big) = u_0' - u_0' T_{zw}(\mathrm{j}\omega_0) v_0 u_0'/\gamma = 0,$$

i.e. $I - T_{zw}(s)\Delta(s)$ has a singularity on the imaginary axis. But this implies that the closed-loop system is unstable as it has a pure imaginary pole. Thus, there is a destabilizing admissible Δ and the system is not robustly stable. □

The result above implies that robust stability with respect to the set of contractive uncertainty elements is equivalent to an H_∞ optimization problem. This renders it a convenient analysis framework. Indeed,

the bound on the H_∞ norm can be verified by several different approaches, such as checking $\|T_{zw}(j\omega)\|$ over a chosen frequency grid, solving an eigenvalue problem associated with a Hamiltonian matrix built from a realization of $T_{zw}(s)$ [45, Prop. 4.17] (if T_{zw} is finite dimensional) or a Linear Matrix Inequality resulting from the KYP lemma [45, Thm. 4.18] (also for a finite-dimensional T_{zw}), et cetera. Moreover, casting the problem as a bound on the H_∞-norm of a known ("certain") system facilitates casting robust design as a standard H_∞ problem of the form presented in Fig. 6.1(a) on p. 98, just remove the "Δ" block from the system in Fig. 4.7(b) and connect u with y via a controller R.

We may add more structure into the uncertainty set by considering the setup in Fig. 4.8(b) for a scalar $\delta \in \mathcal{B}_\infty^{1\times1}$. Such a configuration is a particular case of the general μ (structured singular values) framework, where structured uncertainty is described by block-diagonal elements [56]. The case of only one "repeated scalar" block is sufficient for our purposes as it fits well the embedding procedure of §4.2.1 in the single-delay case, when the signals z and w in Fig. 4.7(a) are not scalar.

First, it should be clear that $\delta I_m \in \mathcal{B}_\infty^{m\times m}$ for all $\delta \in \mathcal{B}_\infty^{1\times1}$. Hence, Theorem 4.4 can be used to end up with sufficient robust stability conditions. However, such conditions might be arbitrarily conservative, as illustrated by the example below.

Example 4.1. Consider the system in Fig. 4.8(b) for the static

$$T_{zw}(s) = \begin{bmatrix} \alpha & \beta \\ 0 & \alpha \end{bmatrix}, \quad \text{for } \alpha, \beta \in \mathbb{R}$$

and an LTI $\delta \in \mathcal{B}_\infty^{1\times1}$. Standard imaginary-axis crossing arguments yield that the closed-loop system is stable iff $I_2 - \delta(j\omega)T_{zw}(j\omega)$ is nonsingular for all $\omega \in \mathbb{R}$. This, in turn, is equivalent to the condition that $|\alpha| < 1$, which does not depend on β. At the same time, Theorem 4.4 yields the robust stability condition

$$\left\| \begin{bmatrix} \alpha & \beta \\ 0 & \alpha \end{bmatrix} \right\| < 1 \quad \Longleftrightarrow \quad \frac{\sqrt{4\alpha^2 + \beta^2} + |\beta|}{2} < 1 \quad \Longleftrightarrow \quad |\alpha| < \sqrt{1 - |\beta|}.$$

This condition is non-conservative only if $\beta = 0$. The degree of conservatism of this condition, i.e. the gap between it and the actual condition $|\alpha| < 1$, increases with $|\beta|$ and the problem becomes unsolvable at all if $|\beta| \geq 1$. ▽

Conservatism can be reduced by noticing that $\delta I = M^{-1}(\delta I)M$ for all LTI and nonsingular M. If M is bi-stable, then the internal stability of the system in Fig. 4.8(b) is equivalent to that in Fig. 4.8(c). The freedom in the choice of the multiplier M (cf. the discussion in §3.4.4) can then be used to reduce the H_∞ norm of $MT_{zw}M^{-1}$. The following result, which is a particular case of the general μ theory [56], holds:

Proposition 4.5. *The following statements are equivalent:*

1. *The feedback interconnection in Fig. 4.8(b) is internally stable for all $\delta \in \mathcal{B}_\infty^{1\times1}$.*
2. *$T_{zw} \in H_\infty$ and there is $M \in H_\infty^{m\times m}$ such that $M^{-1} \in H_\infty^{m\times m}$ and $\|MT_{zw}M^{-1}\|_\infty < 1$.*
3. *$T_{zw} \in H_\infty$ and $\rho(T_{zw}(j\omega)) < 1$ for all $\omega \in \mathbb{R}$.*

In the SISO case, i.e. if $m = 1$, the conditions of Proposition 4.5 clearly reduce to that of Theorem 4.4.

Example 4.2. Return to Example 4.1. The third condition of Proposition 4.5 obviously reads $|\alpha| < 1$. To apply the second condition, let us select $M = \begin{bmatrix} \mu & 0 \\ 0 & 1 \end{bmatrix}$, which is obviously bi-stable for all $\mu \in \mathbb{R} \setminus \{0\}$. The stability condition reads then

$$\left\| \begin{bmatrix} \mu & 0 \\ 0 & 1 \end{bmatrix} \begin{bmatrix} \alpha & \beta \\ 0 & \alpha \end{bmatrix} \begin{bmatrix} 1/\mu & 0 \\ 0 & 1 \end{bmatrix} \right\| = \left\| \begin{bmatrix} \alpha & \mu\beta \\ 0 & \alpha \end{bmatrix} \right\| < 1 \quad \Longleftrightarrow \quad |\alpha| < \sqrt{1 - |\mu\beta|}.$$

As μ is almost arbitrary (nonzero), the quantity $|\mu\beta|$ can be made arbitrarily small, so we can recover the non-conservative condition $|\alpha| < 1$, again. ▽

The scaling in Proposition 4.5 requires dynamic systems in general. Finding such a system is normally a matter of using a finite number of matrix parameters over a chosen frequency grid. This is not particularly elegant and might lead to rather high-order conditions. However, if only static scaling parameters M are used, the contractiveness of $MT_{zw}M^{-1}$ can be cast as a standard LMI (as a matter of fact, the use of only static scaling is enough if δ is allowed to be time varying [68]).

Proposition 4.6. *Let $T_{zw}(s) = D + C(sI - A)^{-1}B$ for a Hurwitz A be an $m \times m$ transfer function. There is $M \in \mathbb{R}^{m \times m}$ such that $\|MT_{zw}M^{-1}\|_\infty < 1$ iff there are $X, Y > 0$ such that*

$$\begin{bmatrix} A'X + XA + C'YC & XB + C'YD \\ B'X + D'YC & D'YD - Y \end{bmatrix} < 0. \tag{4.4}$$

Proof. Because

$$MT_{zw}(s)M^{-1} = \left[\begin{array}{c|c} A & BM^{-1} \\ \hline MC & MDM^{-1} \end{array} \right],$$

the condition $\|MT_{zw}M^{-1}\|_\infty < 1$ is equivalent [45, §4.3.4] to the existence of $X = X' > 0$ such that

$$\begin{bmatrix} A'X + XA + C'M'MC & XBM^{-1} + C'M'MDM^{-1} \\ M^{-'}B'X + M^{-'}D'M'MC & M^{-'}D'M'MDM^{-1} - I \end{bmatrix} < 0.$$

This condition does no change it its left-hand side is pre-multiplied by $\begin{bmatrix} I & 0 \\ 0 & M' \end{bmatrix}$ and post-multiplied by $\begin{bmatrix} I & 0 \\ 0 & M \end{bmatrix}$ (as M is nonsingular). This yields (4.4) by denoting $Y = M'M > 0$. □

Return now to the uncertainty set $\mathcal{B}_\infty$. It might appear that in most situations this is a rather rough description of uncertain elements. Indeed, it is hard to imagine a realistic uncertain element, whose frequency response lies in the unit disk in the complex plane in all frequencies. A finer model should accommodate different modeling mismatch sizes over different frequencies, like having smaller errors over low frequencies and larger—over high. Moreover, in many situations uncertain elements are not centered at the origin, but rather at some nonzero nominal value, which might also drift with the frequency.

It happens, however, that the set $\mathcal{B}_\infty$ can generate such models as well. In a sense, $\mathcal{B}_\infty$ serves a base for many more sophisticated, and more realistic, uncertainty models, whose properties are shaped by frequency-dependent *weights*. A general, albeit quite abstract, model for such uncertain sets is

$$\mathcal{F}_u(W, \mathcal{B}_\infty^{m \times m}) := \left\{ \Delta \mid \exists \Delta_0 \in \mathcal{B}_\infty^{m \times m} \text{ such that } \Delta = \mathcal{F}_u(W, \Delta_0) \right\} \tag{4.5}$$

for a given weight W, provided $\mathcal{F}_u(W, \mathcal{B}_\infty^{m \times m}) \in H_\infty$. Likewise, the set $\mathcal{F}_u(W, \mathcal{B}_\infty^{1 \times 1} I_m)$ can be used for structured uncertainty elements. Several concrete simple examples of weight, which are more tangible than the abstract model, are presented below:

Constant scaling: the choice

$$W = \begin{bmatrix} 0 & \alpha I \\ I & 0 \end{bmatrix} \quad \Longrightarrow \quad \mathcal{F}_u(W, \mathcal{B}_\infty) = \mathcal{B}_\infty \alpha,$$

which is merely a uniform scaling of the uncertain element by $\alpha > 0$. In the SISO case, frequency responses of elements from this set lie in a disk of the radius α centered at the origin at all frequencies, i.e. in $\alpha \bar{\mathbb{D}}$.

Frequency-dependent scaling: the choice

$$W = \begin{bmatrix} 0 & W_\alpha \\ I & 0 \end{bmatrix} \quad \Longrightarrow \quad \mathcal{F}_u(W, \mathcal{B}_\infty) = \mathcal{B}_\infty W_\alpha,$$

which scales it by a frequency dependent weight W_α. In the SISO case, frequency responses of elements from this set at each frequency ω lie in a disk of the radius $|W_\alpha(j\omega)|$ centered at the origin, i.e. in $|W_\alpha(j\omega)| \bar{\mathbb{D}}$. Also, $\mathcal{F}_u(W, \mathcal{B}_\infty) \in H_\infty \iff W \in H_\infty$, which is silently assumed hereafter.
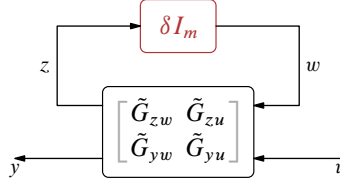
Fig. 4.9: Embedded robustness setup for Fig. 4.1(b) with $\delta \in \mathcal{B}_\infty^{1\times 1}$ and $\tilde{G} = W \star G$

Shifted frequency-dependent scaling: the choice

$$W = \begin{bmatrix} 0 & W_\alpha \\ I & W_\varkappa \end{bmatrix} \quad \implies \quad \mathcal{F}_\mathrm{u}(W, \mathcal{B}_\infty) = W_\varkappa + \mathcal{B}_\infty W_\alpha,$$

which effectively assumes the "nominal model" of the uncertain element at $W_\varkappa$ and scales the deviation from this nominal model by a dynamic, i.e. frequency dependent, weight $W_\alpha \in H_\infty$. In the SISO case, frequency responses of elements from this set at each frequency ω lie in a disk of the radius $|W_\alpha(\mathrm{j}\omega)|$ centered at $W_\varkappa(\mathrm{j}\omega)$, i.e. in $W_\varkappa(\mathrm{j}\omega) + |W_\alpha(\mathrm{j}\omega)|\,\bar{\mathbb{D}}$.

In general, the mapping $\Delta \mapsto \mathcal{F}_\mathrm{u}(W, \Delta)$ can be viewed as a Möbius transformation, which maps the unit disk $\bar{\mathbb{D}}$ into yet another disk on the complex plane $\mathbb{C}$, provided $|W_{11}(\mathrm{j}\omega)| < 1$ for all ω. The latter condition just says that $1 \notin W_{11}(\mathrm{j}\omega)\bar{\mathbb{D}}$. If it does not hold, then a disk may be transformed to a half plane or to the exterior of a disk. If $W_{11} \neq 0$, the transformed disk may be rotated and warped, in the sense that the distance between points is not preserved under the transformation (these properties can perhaps be exploited to reduce the conservatism of the approach, although I am not aware of such results).

The analysis of systems with the uncertainty model (4.5) is not conceptually different from that of systems with the plain unit disk model. Indeed, the feedback connection of T_{zw} and $\mathcal{F}_\mathrm{u}(W, \Delta)$ is equivalent to the feedback connection of $\mathcal{F}_\mathrm{l}(W, T_{zw})$ and Δ. Thus, we return to the setup studied earlier and can use Theorem 4.4, just for $\mathcal{F}_\mathrm{l}(W, T_{zw})$ instead of T_{zw}. Structured uncertainty from the set $\mathcal{F}_\mathrm{u}(W, \mathcal{B}_\infty^{1\times 1} I_m)$ can be treated in the same vein. Thus, taking into account that $\mathcal{F}_\mathrm{u}(G_1, \mathcal{F}_\mathrm{u}(G_2, \Delta)) = \mathcal{F}_\mathrm{u}(G_2 \star G_1, \Delta)$, where "$\star$" stands for the Redheffer start product, the uncertain delay setup in Fig. 4.7(a) can be embedded into the system in Fig. 4.9 under $\tilde{G} = W \star G$.

In what follows, we are interested in this setup for W as in the shifted frequency-dependent scaling model above and the generator G as in Fig. 4.1(c), which corresponds to the input delay system. In this case

$$\tilde{G} = \begin{bmatrix} 0 & W_\alpha \\ I & W_\varkappa \end{bmatrix} \star \begin{bmatrix} RP & R \\ P & 0 \end{bmatrix} = \begin{bmatrix} W_\alpha R \\ I \end{bmatrix} (I - PW_\varkappa R)^{-1} \begin{bmatrix} P & I \end{bmatrix}, \tag{4.6}$$

whose

$$T_{zw} = W_\alpha R(I - PW_\varkappa R)^{-1}P = \mathcal{F}_\mathrm{l}\left(\begin{bmatrix} 0 & W_\alpha \\ P & PW_\varkappa \end{bmatrix}, R \right) \tag{4.7}$$

is assumed to be stable.

4.2.3 Covering models for the uncertain delay element

Having acquired tools to handle problems with unstructured and structured norm-bounded uncertainty, consider now their use in the robust stability analysis of systems with delay uncertainty in Fig. 4.1(b). Our goal is to embed the uncertain delay element $\bar{D}_{\tau_\delta}$ into a family of stable systems, whose frequency responses lie in disks in the complex plane and include those of $\bar{D}_{\tau_\delta}$ for all $\tau_\delta \in [0, \bar{\tau}]$. This, in turn, embed the problem into the robust stability setup in Fig. 4.9.

To construct such families, consider the areas in the complex plane $\mathbb{C}$, which are covered by the uncertain frequency response $e^{-j\omega\tau_\delta}$ for $\tau_\delta \in [0, \bar{\tau}]$. At every frequency ω this is a circular arc of the unit radius, centered at the origin and subtending the angle $\bar{\tau}\omega$ [rad] in the clockwise direction starting from 1 (for $\tau_\delta = 0$). Some of these arcs are presented below:

$$\bar{\tau}\omega = 0 \qquad \bar{\tau}\omega = 1 \qquad \bar{\tau}\omega = 2 \qquad \bar{\tau}\omega = \pi \qquad \bar{\tau}\omega = 4 \qquad \bar{\tau}\omega \geq 2\pi \tag{4.8}$$
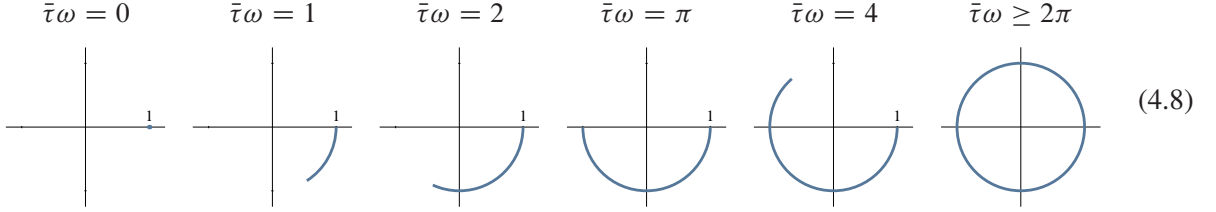
The arc reduces to a single point, 1, at $\omega = 0$ and increases with ω, until it becomes the whole unit circle $\mathbb{T}$ for all $\omega \geq 2\pi/\bar{\tau}$. Our goal is to cover these arcs by tightest disks of the form $\varkappa(\omega) + \alpha(\omega)\bar{\mathbb{D}}$, where $\varkappa(\omega) \in \mathbb{C}$ is a center and $\alpha(\omega) \geq 0$ is a radius, at each frequency. This task clearly depends on the choice of the disk center $\varkappa(\omega)$, so consider several possible choices for it below.

Covering with the center in $\varkappa(\omega) = 0$

Perhaps the simplest choice is to place the center to the origin for all frequencies, which yields the closed unit disk $\bar{\mathbb{D}}$ as the frequency-independent covering, see Fig. 4.10(a). This implies that the system in Fig. 4.1(b) for every τ_δ is covered by the the system in Fig. 4.9 and $\tilde{G} = G$. By Proposition 4.5, the system in Fig. 4.9 is robustly stable iff

$$\tilde{G}_{zw} \in H_\infty \quad \text{and} \quad \exists M, M^{-1} \in H_\infty \text{ such that } \|M\tilde{G}_{zw}M^{-1}\bar{D}_\tau\|_\infty = \|M\tilde{G}_{zw}M^{-1}\|_\infty < 1.$$

Hence, the conditions above also guarantee the stability of the system in Fig. 4.1(b) for all $\tau_\delta \geq -\tau_0$, i.e. the system is delay-independent stable. In the particular case of the standard feedback control system with a plant P, a controller R, and $\tau_0 = 0$, we have that $\tilde{G}_{zw} = PR$ is the loop gain (cf. (1.25)) and the closed-loop system is stable for every constant loop delay if loop gain is stable and its peak frequency-response gain is strictly contractive. In the SISO case, i.e. for $m = 1$, this recovers Tsypkin's criterion [75].

Covering with the center in $\varkappa(\omega) = 1$

Delay-dependent conditions can be obtained by choosing $\varkappa(\omega) \neq 0$. The best studied choice is apparently $\varkappa(\omega) = 1$, which effectively assumes the nominal value $\tau_\delta = 0$. The tightest covering disk for this choice does depend on $\bar{\tau}$, see Figs. 4.10(b) and 4.10(c). The radii of such disks at each frequency are derived as

$$\alpha(\omega) = \max_{\tau_\delta \in [0,\bar{\tau}]}\{|1 - e^{-j\omega\tau_\delta}|\} = \begin{cases} |1 - e^{-j\bar{\tau}\omega}| & \text{if } \bar{\tau}\omega \in [0, \pi] \\ |1 - e^{-j\pi}| = 2 & \text{otherwise} \end{cases}.$$

Taking into account that $|1 - e^{-j\bar{\tau}\omega}|^2 = 2(1 - \cos(\bar{\tau}\omega)) = 4\sin^2(\bar{\tau}\omega/2)$, we end up with $\alpha(\omega) = \alpha_1(\bar{\tau}\omega)$, where

$$\alpha_1(\omega) := \begin{cases} 2\sin(\omega/2) & \text{if } \omega \in [0, \pi] \\ 2 & \text{otherwise} \end{cases} = \quad \text{} \tag{4.9}$$

(this formula was apparently first derived by Owens and Raya in [55]). The function $\alpha_1(\omega)$ is monotonically increasing, vanishing as $\omega \downarrow 0$. This agrees with the intuition that the uncertainty level of this element decreases at low frequencies. Moreover, the range of frequencies, in which the uncertainty radius $\alpha_1(\bar{\tau}\omega)$ is small, increases as $\bar{\tau}$ decreases, which is also intuitive.

(a) $\varkappa(\omega) = 0$

(b) $\varkappa(\omega) = 1$ for $\bar{\tau}\omega = 1$

(c) $\varkappa(\omega) = 1$ for $\bar{\tau}\omega = 4$

(d) $\varkappa(\omega) = \mathrm{e}^{-\mathrm{j}\bar{\tau}\omega/2}$ for $\bar{\tau}\omega = 2$

(e) $\varkappa(\omega) = \mathrm{e}^{-\mathrm{j}\bar{\tau}\omega/2}$ for $\bar{\tau}\omega = 4$

(f) disks comparison for $\bar{\tau}\omega = 2$

(g) $\varkappa(\omega) = \varkappa_3(\bar{\tau}\omega)$ from (4.13) for $\bar{\tau}\omega = 2$

(h) $\varkappa(\omega) = \varkappa_3(\bar{\tau}\omega)$ from (4.13) for $\bar{\tau}\omega = 4$
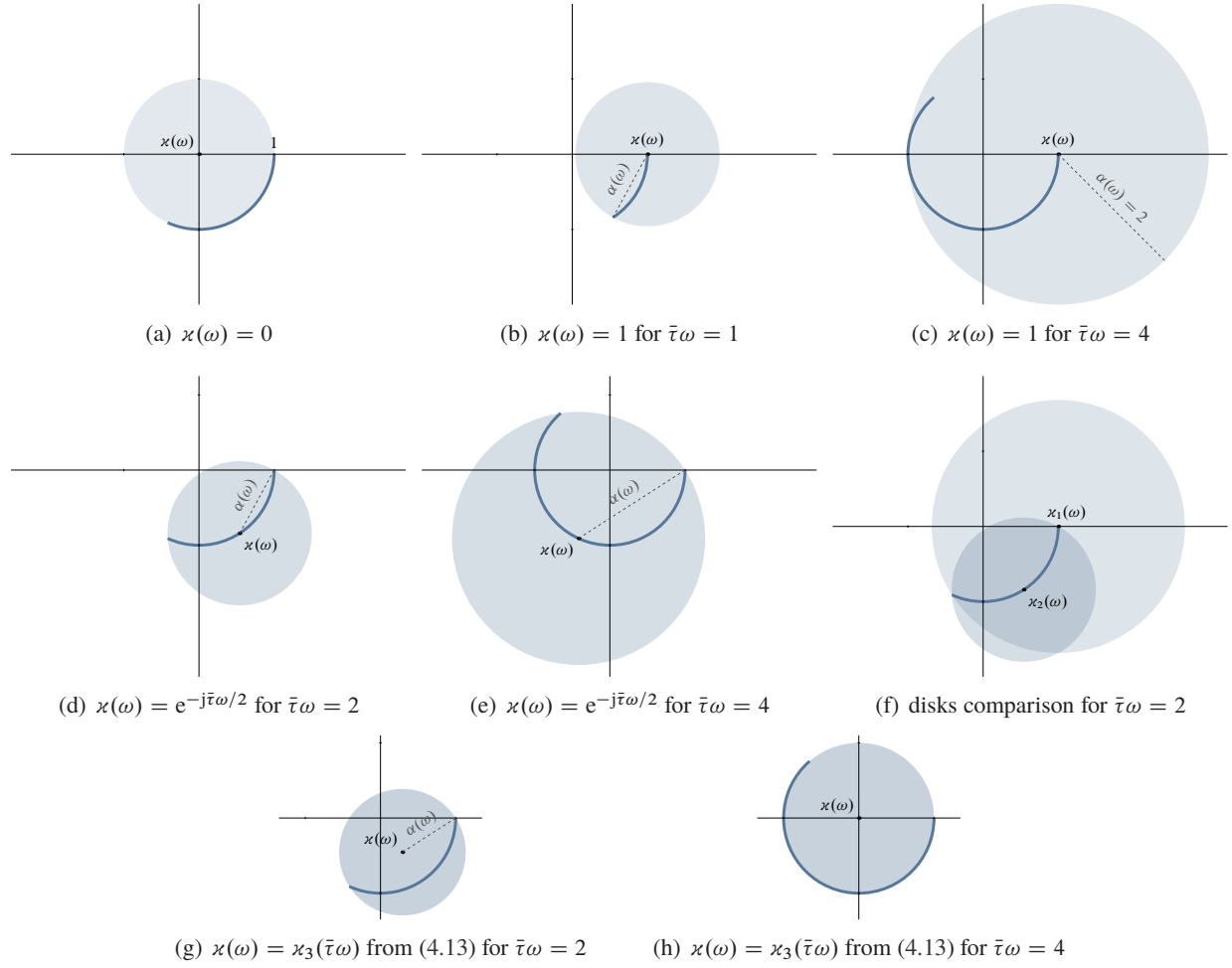
Fig. 4.10: Covering disks for uncertain delays

The use of α_1 as the uncertainty radius for the system in Fig. 4.9 is hampered by the fact that this is not a real-rational function of jω, i.e. it cannot be the frequency response of a finite-dimensional system with real parameters. So we shall approximate $\alpha_1(\omega)$ by the frequency response of a rational transfer function $W_{\alpha 1}(s)$ such that $|W_{\alpha 1}(\mathrm{j}\omega)| \geq \alpha_1(\omega)$. Possible choices are

$$W_{\alpha 1,0}(s) := s, \quad W_{\alpha 1,1}(s) := \frac{2\sqrt{3}\,s}{s + 2\sqrt{3}}, \quad \text{and} \quad W_{\alpha 1,3}(s) := \frac{2.007\,s}{s + 2}\frac{s^2 + 3.695s + 5.56}{s^2 + 3.026s + 5.56}, \quad (4.10)$$

see Fig. 4.11(a). We can see that the use of $W_{\alpha 1,3}$ yields a close approximation of α_1, so further increase of the approximation order is normally not required. It should be emphasized that $|W_{\alpha 1,1}(\mathrm{j}\omega)| < |W_{\alpha 1,0}(\mathrm{j}\omega)|$ for all $\omega \neq 0$, which means that the approximation with $W_{\alpha 1,1}$ always yields less conservative results than that with $W_{\alpha 1,0}$. At the same time, the gain of $W_{\alpha 1,3}$ is not always smaller than that of $W_{\alpha 1,1}$, so there might be situations when the use of this third-order covering leads to more conservative results than for the first-order covering.

With finite-dimensional and stable $W_\varkappa$ and W_α selected according to

$$W_\varkappa(s) = 1 \quad \text{and} \quad W_\alpha(s) = W_{\alpha 1}(\bar{\tau}s)$$

(mind scaling the Laplace variable in W_α), we can embed the robust stability problem for the system in Fig. 4.1(b) into the robust stability problem for the system in Fig. 4.9 with $W = \begin{bmatrix} 0 & I \\ W_\alpha & I \end{bmatrix}$. For the problem

(a) $\alpha_1(\omega)$ from (4.9) for $\varkappa(\omega) = 1$

(b) $\alpha_3(\omega)$ from (4.15) for $\varkappa(\omega) = W_{\varkappa 3}(j\bar{\tau}\omega)$ from (4.14)

Fig. 4.11: Rational approximations of radii of tightest covering disks

with an uncertain loop delay this yields $\tilde{G}$ as in (4.6). The controlled system in (4.7) reads then

$$T_{zw} = W_\alpha (I - RP)^{-1} RP = W_\alpha T,$$

i.e. it is the weighted complementary sensitivity. Thus, by Proposition 4.5 the system in Fig. 4.1(b) is stable for all $\tau_\delta \in [0, \bar{\tau}]$ if $T \in H_\infty$ and there is $M, M^{-1} \in H_\infty$ such that $\|MW_\alpha T M^{-1}\|_\infty < 1$. In the SISO case, this reduces to the condition $\|W_\alpha T\|_\infty < 1$.
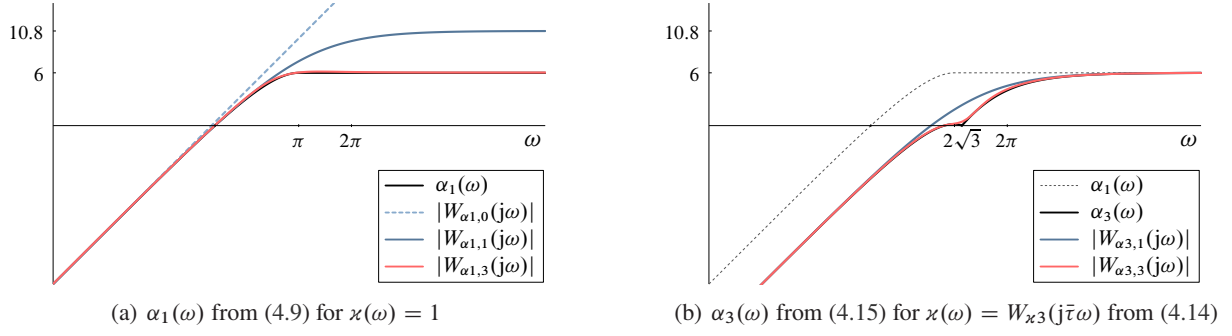
With the choice $W_\alpha(s) = W_{\alpha 1,0}(\bar{\tau}s) = \bar{\tau}s$, the condition above reads as the strict contractiveness of the H_∞-norm of $\bar{\tau}sT(s)$. Thus, the delay margin is lowerbounded by the reciprocal of the H_∞-norm of a system with the transfer function $sT(s)$. Even though this condition is based on the loosest upper bound on $\alpha_1(\omega)$, it is might be useful, see the proof of Proposition 4.1. The reason is that it is a closed-form expression, independent of $\bar{\tau}$ itself, unlike conditions produced from the other bounds in (4.10).

Example 4.3. Consider a SISO plant P, whose only unstable pole is located at $s = a > 0$. The problem addressed in this example is to find conditions under which a stabilizing R exists such that $\|W_\alpha T\|_\infty < 1$. This would yield a (conservative) guarantee on the attainable delay margin μ_d, which is yet another take on the problem studied in §4.1.1. It is not hard to see that $T(a) = -1$ for all stabilizing controllers. Therefore, we have that $\|W_\alpha T\|_\infty \geq |W_\alpha(a)|$. In fact, in the case of a single unstable pole this bound can be approached arbitrarily closely by stabilizing controllers, see [14, Sec. 6.1]. Thus, we have that the system can be robustly stabilized iff

$$|W_{\alpha 1}(\bar{\tau}a)| < 1 \tag{4.11}$$

If $W_\alpha(s) = W_{\alpha 1,0}(\bar{\tau}s) = \bar{\tau}s$, then condition (4.11) results in the feasibility of the robust stability problem whenever $\bar{\tau} < 1/a$. If $W_\alpha(s) = W_{\alpha 1,1}(\bar{\tau}s)$ from (4.9), then we have $\bar{\tau} < 2(6 + \sqrt{3})/(11a) \approx 1.406/a$, while if $W_\alpha(s) = W_{\alpha 1,3}(\bar{\tau}s)$, then all $\bar{\tau} < 1.702/a$ can be attained. All these bounds are more conservative than the upper bound $2/a$ from Proposition 4.2, although the conservatism level decreases as the approximation accuracy increases. $\triangledown$

Covering with the center in $\varkappa(\omega) = e^{-j\bar{\tau}\omega/2}$

Another seemingly natural choice is to place the center to the middle of the uncertain arc at each frequency, i.e. at $\varkappa(\omega) = e^{-j\bar{\tau}\omega/2}$. This effectively assumes the nominal value of the delay at $\tau_\delta = \bar{\tau}/2$. The tightest disks for this choice, see Figs. 4.10(d) and 4.10(e), have the radii

$$\alpha(\omega) = \max_{\tau_\delta \in [0,\bar{\tau}]} \{|e^{-j\bar{\tau}\omega/2} - e^{-j\omega\tau_\delta}|\} = \max_{\tau_\delta \in [0,\bar{\tau}]} \{|1 - e^{-j\omega(\tau_\delta - \bar{\tau}/2)}|\} = \begin{cases} |1 - e^{-j\bar{\tau}\omega/2}| & \text{if } \bar{\tau}\omega \in [0, 2\pi] \\ |1 - e^{-j\pi}| = 2 & \text{otherwise} \end{cases}.$$

Thus, $\alpha(\omega) = \alpha_1(\bar{\tau}\omega/2)$ for $\alpha_1(\omega)$ defined by (4.9) and we can use all its finite-dimensional approximations from (4.10). It is readily seen that $\alpha_1(\bar{\tau}\omega/2) < \alpha_1(\bar{\tau}\omega)$ for all $\omega \in (0, 2\pi)$. Hence, covering disks in this case have smaller radii than those for $\varkappa(\omega) = 1$ for all $\bar{\tau}\omega \in (0, 2\pi)$.

With the use of

$$W_\varkappa(s) = \mathrm{e}^{-\bar{\tau}s/2} \quad \text{and} \quad W_\alpha(s) = W_{\alpha 1}(\bar{\tau}s/2)$$

for the input-delay problem, we end up with (4.6), which includes the nonzero loop delay $\bar{D}_{\bar{\tau}/2}$. This delay can be compensated by the standard MSP though, so its presence does not hamper the design of controllers minimizing $\|T_{zw}\|_\infty$.

Example 4.4. Consider the problem studied in Example 4.3, where a SISO plant has only one unstable pole at $s = a$. The delay margin $\mu_\mathrm{d} = \bar{\tau}$ is guaranteed if there is a stabilizing R such that $\|T_{zw}\|_\infty < 1$, where $T_{zw} = W_\alpha P R/(1 - P W_\varkappa R)$. Because $T_{zw}(a) = |W_\alpha(a)|/|W_\varkappa(a)|$ for every stabilizing R, we have that $\|T_{zw}\|_\infty \geq |W_\alpha(a)|/|W_\varkappa(a)| = \mathrm{e}^{\bar{\tau}a/2}|W_\alpha(a)|$ and this bound can be approached. Hence, the system is robustly stable iff

$$\mathrm{e}^{\bar{\tau}a/2}|W_{\alpha 1}(\bar{\tau}a/2)| < 1. \tag{4.12}$$

For the rational approximations of $\alpha(\omega)$ given by (4.10), inequality (4.12) results in the stability conditions $\bar{\tau} < 1.134/a$, $\bar{\tau} < 1.259/a$, and $\bar{\tau} < 1.305/a$. The first one of them, corresponding to the cover with $W_{\alpha 1,0}(s) = s$, is less conservative than the corresponding condition in Example 4.3. The second and third conditions are actually more conservative, even though the uncertainty disks have smaller radii. $\qquad \triangledown$

The outcome of Example 4.4, in that a smaller covering disk might yield a more conservative bound, might appear counterintuitive at first sight. Yet it is actually not, as explained in [79]. To understand why, compare the disks for $\varkappa(\omega) = 1$ and $\varkappa(\omega) = \mathrm{e}^{-\mathrm{j}\bar{\tau}\omega/2}$ at $\bar{\tau}\omega = 2$, which are shown in Fig. 4.10(f). These disks cover different areas and the smaller disk is not inscribed in the larger one. Consequently, it might happen that the worst uncertainty δ belongs to the area in the smaller disk, but not in the larger one.

Covering with a center motivated by the smallest covering disks

Neither $\varkappa(\omega) = 1$ nor $\varkappa(\omega) = \mathrm{e}^{-\mathrm{j}\bar{\tau}\omega/2}$ results in the smallest disks, i.e. those having the smallest radii, covering the arcs in (4.8). The smallest disks are obtained by placing the center to the midpoint of the chord connecting the end points of the arc for every frequency until the arc becomes a semi-circle, and at the origin afterwards, see Figs. 4.10(g) and 4.10(h). Algebraically, such centers satisfy $\varkappa(\omega) = \varkappa_3(\bar{\tau}\omega)$, where

$$\varkappa_3(\omega) := \frac{1 + \mathrm{e}^{-\mathrm{j}\omega}}{2} \mathbb{1}_{[0,\pi]}(\omega) = \begin{cases} (1 + \mathrm{e}^{-\mathrm{j}\omega})/2 & \text{if } \omega \in [0, \pi] \\ 0 & \text{otherwise} \end{cases} \tag{4.13}$$

The radii of such disks are

$$\alpha(\omega) = \max_{\tau_\delta \in [0,\bar{\tau}]} \left\{ \left| \frac{1 + \mathrm{e}^{-\mathrm{j}\bar{\tau}\omega}}{2} - \mathrm{e}^{-\mathrm{j}\omega\tau_\delta} \right| \right\} = \frac{|1 - \mathrm{e}^{-\mathrm{j}\bar{\tau}\omega}|}{2} = \sin\frac{\bar{\tau}\omega}{2}$$
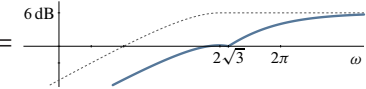
if $\bar{\tau}\omega \in [0, \pi]$ and $\alpha(\omega) = 1$ if $\bar{\tau}\omega \geq \pi$. Thus, we end up with $\alpha(\omega) = \alpha_1(\bar{\tau}\omega)/2$, where $\alpha_1(\omega)$ is given by (4.9). Moreover, the resulting disks are always inscribed in the disks corresponding to the choice $\alpha(\omega) = 1$. This implies that centering disks in (4.13) would never result in more conservative results than for disks centered at $\alpha(\omega) = 1$.

However, the use of (4.13) in robust control problems is not easy. What we need is a causal system $W_\varkappa$, whose frequency response coincides with that of $\varkappa(\omega)$. The finite support of $\varkappa(\omega)$, which bears some resemblance to the ideal low-pass filter, makes this problem vain. But motivated by the "optimal" choice above, consider placing the center at $\varkappa(\omega) = W_{\varkappa 3}(\mathrm{j}\bar{\tau}\omega)$, where

$$W_{\varkappa 3}(s) = \frac{s^2 + 12}{s^2 + 6s + 12}, \tag{4.14}$$

which is the $[2, 2]$-Padé approximant of $(1 + e^{-s})/2$. The radii of covering disks for this choice, derived in [1], are given in the following result.

Lemma 4.7. *The tightest covering disks for* $\varkappa(\omega) = W_{\varkappa 3}(\mathrm{j}\bar{\tau}\omega)$ *have the radii* $\alpha(\omega) = \alpha_3(\bar{\tau}\omega)$, *where*

$$\alpha_3(\omega) := \sqrt{2 - 2\frac{18\omega^2 + (12 - \omega^2)\beta(\omega)}{\omega^4 + 12\omega^2 + 144}} \qquad\qquad (4.15)$$

where

$$\beta(\omega) = \begin{cases} \dfrac{(12 - \omega^2)\cos\omega + 6\omega\sin\omega}{\sqrt{\omega^4 + 12\omega^2 + 144}} & \text{if } \omega \in [0, 2\sqrt{3}] \\ & \\ \text{otherwise} \end{cases}.$$

Proof. Without loss of generality assume that $\bar{\tau} = 1$. Denote

$$\epsilon(\tau) := |e^{-\mathrm{j}\omega\tau} - W_{\varkappa 3}(\mathrm{j}\omega)|^2 = 2 - 2\frac{18\omega^2 + (12 - \omega^2)((12 - \omega^2)\cos(\omega\tau) + 6\omega\sin(\omega\tau))}{\omega^4 + 12\omega^2 + 144}$$

for $\tau \in \mathbb{R}_+$ and analyze its maximum for $\tau \in [0, 1]$. This is a periodic continuous function of τ with

$$\frac{\mathrm{d}\epsilon}{\mathrm{d}\tau} = \frac{2\omega(\omega^2 - 12)(6\omega\cos(\omega\tau) + (\omega^2 - 12)\sin(\omega\tau))}{\omega^4 + 12\omega^2 + 144}$$

and $\dot{\epsilon}(\tau) = 0$ at every

$$\tau = \tau_k := \frac{1}{\omega}\arctan\frac{6\omega}{12 - \omega^2} + \frac{\pi}{\omega}k, \quad k \in \mathbb{Z}.$$

If $\omega^2 < 12$, then τ_0 is a decreasing function of ω, starting from 0.5 at $\omega = 0$ and approaching $\pi/(4\sqrt{3}) \approx 0.45$ as $\omega \uparrow \sqrt{12}$. In this frequency range $\pi/\omega \geq \pi/\sqrt{12} > 0.9$, we have that $\tau_k > 1$ if k is positive and $\tau_k < 0$ if k is negative. Thus, so the only $\tau_k \in [0, 1]$ is τ_0. It can be verified that $\tau = \tau_0$ is a local minimum point. Hence, the maximum, required for calculating $\alpha(\omega)$, is achieved either at $\tau = 0$ or at $\tau = 1$. Direct calculations show that for all $\omega \in [0, 2\sqrt{3}]$ we should pick the latter, so that $\alpha_3(\omega) = \sqrt{\epsilon(1)}$.

If $\omega^2 > 12$, then $\tau_0 < 0$ and τ_1 is a decreasing function of ω lying in $(0, \pi/(4\sqrt{3}))$. Moreover, τ_k is a local maximum point for all odd k. Because for all odd k

$$(12 - \omega^2)\cos(\omega\tau_k) + 6\omega\sin(\omega\tau_k) = \sqrt{\omega^4 + 12\omega^2 + 144}$$

is independent of k and $\tau_1 \in [0, 1]$ for all $\omega > 2\sqrt{3}$, we may always take $\alpha_3(\omega) = \sqrt{\epsilon(\tau_1)}$. $\qquad\square$

Similarly to the procedure for $\varkappa(\omega) = 1$, it is possible to approximate the function $\alpha_3(\omega)$ by the magnitude frequency response of rational transfer functions. Two possible choices are

$$W_{\alpha 3,1}(s) := \frac{2s}{s + 4} \quad \text{and} \quad W_{\alpha 3,3}(s) := W_{\alpha 3,1}(s)\frac{s^2 + 1.92s + 12.781}{s^2 + 2.393s + 12.781}, \qquad (4.16)$$

see Fig. 4.11(b) on p. 82. This first-order approximation, $|W_{\alpha 3,1}(\mathrm{j}\omega)|$, is tight at both low and high frequencies. This is in contrast to $|W_{\alpha 1,1}(\mathrm{j}\omega)|$, which is loose at high frequencies. In fact, it can be verified, numerically, that

$$W_{\varkappa 3}(\mathrm{j}\omega) + |W_{\alpha 3,1}(\mathrm{j}\omega)|\,\bar{\mathbb{D}} \subset 1 + |W_{\alpha 1,1}(\mathrm{j}\omega)|\,\bar{\mathbb{D}}$$

for all ω. Hence, covering the uncertain delay $\bar{D}_{\tau_\delta}$ with disks centered at $W_{\varkappa 3}$ and having the radius $|W_{\alpha 3,1}(\mathrm{j}\omega)|$ is less conservative than covering with those centered at 1 and having the radius $|W_{\alpha 1,1}(\mathrm{j}\omega)|$. Also, it is readily seen that $|W_{\alpha 3,1}(\mathrm{j}\omega)| > |W_{\alpha 3,2}(\mathrm{j}\omega)|$ for all $\omega > 0$, so the third-order upper bound is always less conservative than the first-order one in this case. This observation is confirmed by the example below.

Example 4.5. Returning to the system in Examples 4.3 and 4.4. Now the problem is solved for

$$W_\varkappa(s) = W_{\varkappa 3}(\bar{\tau}s) \quad \text{and} \quad W_\alpha(s) = W_{\alpha 3}(\bar{\tau}s).$$

By the arguments already used in Example 4.4, the problem is solvable if

$$|W_{\alpha 3}(\mathrm{j}\bar{\tau}a)| < |W_{\varkappa 3}(\mathrm{j}\bar{\tau}a)|.$$

This yields the conditions $\bar{\tau} < 1.691/a$ and $\bar{\tau} < 1.769/a$ under $W_{\alpha 3} = W_{\alpha 3,1}$ and $W_{\alpha 3} = W_{\alpha 3,1}$, respectively. These conditions are less conservative than those in both Example 4.3 and Example 4.4, under compatible dimensions of W_α. In fact, the condition $\bar{\tau} < 1.769/a$ is only about 88% of the upper bound in Proposition 4.2, which is not bad for a conservative covering. $\qquad \triangledown$

4.2.4 Case study

Return to the system studied in §4.1.2, where a proportional primary controller was designed for the plain integrator with a nominal delay τ_0, see Fig. 4.3. Consider again its delay margin, i.e. the minimal destabilizing $\tau_\delta = \bar{\tau} > 0$ (for the sake of simplicity, only the increase of the loop delay is addressed below). But unlike the analysis in §4.1.2, where the actual delay margin was calculated, the problem is now analyzed from the general uncertainty embedding point of view. To this end, consider the system T_{zw} from (4.7) for P and R as in (4.3). Given stable $W_\varkappa(s)$ and $W_\alpha(s)$, the resulting T_{zw} has the transfer function

$$T_{zw}(s) = -\frac{W_\alpha(s)\mathrm{e}^{-\tau_0 s}}{s/k_\mathrm{p} + 1 - \mathrm{e}^{-\tau_0 s} + W_\varkappa(s)\mathrm{e}^{-\tau_0 s}} =: -T_0(s)W_\alpha(s)\mathrm{e}^{-\tau_0 s}.$$

The robust stability condition reads then $\|T_0 W_\alpha\|_\infty < 1$. As a matter of fact, the latter condition in this case is equivalent to $T_0 \in H_\infty$ and $|T_0(\mathrm{j}\omega)| < 1/|W_\alpha(\mathrm{j}\omega)|$ for all ω. Because this is not a design problem, we can use the actual disk radius function $\alpha(\omega)$ rather than its rational approximation $|W_\alpha(\mathrm{j}\omega)|$, so the condition to verify is

$$T_0 \in H_\infty \quad \text{and} \quad |T_0(\mathrm{j}\omega)| < \frac{1}{\alpha(\omega)}, \quad \forall \omega \in \mathbb{R}. \tag{4.17}$$

A brute-force search over a chosen frequency grid can then be used to check the second condition above. It can be shown, via the use of the Poisson integral formula, that an H_∞ function, actually outer, $W_\alpha(s)$ exists such that $|W_\alpha(\mathrm{j}\omega)| = \alpha(\omega)$, see [58, Eqn. (1.7)]. Hence, the replacement above is well justified.

First, consider the covering under $W_\varkappa(s) = 1$. With this choice the delay is eliminated from $T_0(s)$, yielding the rational

$$T_0(s) = \frac{k_\mathrm{p}}{s + k_\mathrm{p}},$$

which is clearly stable for all $k_\mathrm{p} > 0$. With $\alpha(\omega) = \alpha_1(\bar{\tau}\omega)$ defined by (4.9), condition (4.17) reads

$$\frac{1}{\sqrt{1 + \omega^2/k_\mathrm{p}^2}} < \frac{1}{2}\begin{cases} 1/\sin(\bar{\tau}\omega/2) & \text{if } \bar{\tau}\omega \in [0, \pi] \\ 1 & \text{otherwise} \end{cases}$$

In fact, because the left-hand side above is a strictly decreasing function of ω, we may only check the condition in the frequency range $\bar{\tau}\omega \in [0, \pi]$. The stability condition is then

$$2\sin(\bar{\tau}\omega/2) < \sqrt{1 + \omega^2/k_\mathrm{p}^2}, \quad \forall \bar{\tau}\omega \in [0, \pi]$$

or, equivalently,

$$\bar{\tau} < \min_{\omega \in [0, \sqrt{3}k_\mathrm{p}]} \frac{2}{\omega}\arcsin\frac{\sqrt{1 + \omega^2/k_\mathrm{p}^2}}{2} = \min_{\tilde{\omega} \in [0, \sqrt{3}]} \frac{2}{\tilde{\omega}k_\mathrm{p}}\arcsin\frac{\sqrt{1 + \tilde{\omega}^2}}{2} \approx \frac{1.4775}{k_\mathrm{p}} = \frac{1.4775(1 - r_0)\tau_0}{r_0},$$
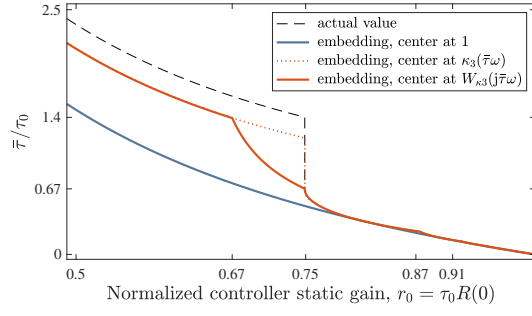
Fig. 4.12: Normalized delay margins calculated via embedding

where $r_0 = \tau_0 R(0) \in (0, 1)$ is the normalized static gain of the controller. Thus, we end up with the condition

$$\frac{\bar{\tau}}{\tau_0} < 1.4775 \frac{1 - r_0}{r_0},$$

which is easy to verify. This bound is presented in Fig. 4.12 by cyan-blue line (the actual margin from Fig. 4.4(c) is shown by the dashed black line now). It is quite conservative for $r_0 < 0.75$, but becomes very accurate after the first jump at $r_0 \approx 0.749$. However, the approach does not capture the discontinuity of the actual delay margin in this case.

Now, let us choose $W_\varkappa(s) = W_{\varkappa 3}(\bar{\tau} s)$ from (4.14). In this case

$$T_0(s) = \frac{1}{s/k_{\mathrm{p}} + 1 - (1 - W_\varkappa(\bar{\tau} s)) e^{-\tau_0 s}} = \frac{1}{s/k_{\mathrm{p}} + 1 - V(\bar{\tau} s) e^{-\tau_0 s}},$$

where $V(s) := 6s/(s^2 + 6s + 12)$. This transfer function is actually stable for all admissible parameters. Indeed, this transfer function can result from the feedback interconnection of $k_{\mathrm{p}}/(s + k_{\mathrm{p}})$ and $V(\bar{\tau} s) e^{-\tau_0 s}$. Both these transfer functions are stable and have contractive frequency responses. Moreover, the first one has the unit magnitude only at $\omega = 0$, whereas the second—only at $\bar{\tau} \omega = 2\sqrt{3} > 0$. Hence, the loop gain is strictly contractive at all frequencies and $T_0 \in H_\infty$ for all $\tau_0 \geq 0$ and $\bar{\tau} > 0$ by the Small Gain Theorem.

The second condition of (4.17) is more involved that that for the choice $\varkappa(\omega) = 1$ and there is probably no analytic solution to it. Still, it is readily verified numerically, resulting in the bound shown in Fig. 4.12 by red solid line. It is visibly less conservative than the previous bound for $r_0 < 0.749$ and is virtually indistinguishable from the precise margin for $r_0 > 0.749$. It also does capture the discontinuity of the delay margin.

As a matter of fact, the small-gain arguments used to prove the stability of T_0 above can also be applied in the case when the actual $\varkappa_3$ from (4.13) (or, more accurately, its outer extension) is used instead of $W_{\varkappa 3}$. The resulting bound is shown by the red dotted line in Fig. 4.12. This curve is almost the same as the solid red line, except for the interval $r_0 \in (0.673, 0.749)$.

4.2.5   Time-varying delays

Time-varying delays can also be embedded into the general robustness setup in Fig. 4.9, now with a potentially time-varying uncertainty element $\delta \in \mathcal{B}_\infty^{1 \times 1}$. As already discussed at the beginning of §4.2.2, by this unit ball we understand then the set of all stable systems, whose $L_2(\mathbb{R})$-induced norm is contractive.

Covering time-varying delays is a more delicate, and less visual, task. The fact that the time-varying delay operator $\bar{D}_{\tau(t)}$ might be unstable, see Remark 1.2 on p. 3, adds even more complications. Nonetheless, covering norm-bounded uncertainty sets can be found and the following two results, which should be apparently attributed to [20, §8.6.1], are instrumental toward this end.

Lemma 4.8. *If $\tau(t) \in [0, \bar{\tau}]$ and $|\dot{\tau}(t)| \leq \upsilon < 1$, then $\bar{D}_{\tau(t)}$ is a bounded operator on $L_2(\mathbb{R}_+)$, with*

$$\|\bar{D}_{\tau(t)}\|_{L_2(\mathbb{R}_+) \to L_2(\mathbb{R}_+)} = \frac{1}{\sqrt{1-\upsilon}} > 1.$$

Proof. Let $\theta(t) := t - \tau(t)$. Because $\dot{\theta}(t) \geq 1 - \upsilon > 0$, the function $\phi(t) := \theta^{-1}(t)$ is well defined with $t \leq \phi(t) \leq t + \bar{\tau}$ and $0 < \dot{\phi}(t) \leq 1/(1-\upsilon)$. Now, if $w = \bar{D}_{\tau(t)}z$, then we have that

$$\|w\|_2^2 = \int_0^\infty [z(t - \tau(t))]^2 \, dt \Big|_{t=\phi(s)} = \int_{-\tau(0)}^\infty [z(s)]^2 \dot{\phi}(s) \, ds = \int_0^\infty [z(s)]^2 \dot{\phi}(s) \, ds$$

$$\leq \frac{1}{1-\upsilon} \int_0^\infty [z(s)]^2 \, ds = \frac{1}{1-\upsilon} \|z\|_2^2$$

(the facts that $t = \phi(s) \iff s = \theta(t)$ and $z(t) = 0$ whenever $t < 0$ were used). Now it only remains to prove that the bound is tight. To this end, let

$$z(t) = \mathbb{1}_{[0,(1/\upsilon-1)\bar{\tau}]}(t) \quad \text{and} \quad \tau(t) = \begin{cases} \upsilon t & \text{if } 0 \leq t \leq \bar{\tau}/\upsilon, \\ \bar{\tau} & \text{otherwise} \end{cases},$$

for which $w(t) = \mathbb{1}_{[0,\bar{\tau}/\upsilon]}(t)$ and

$$\frac{\|w\|_2^2}{\|z\|_2^2} = \frac{\bar{\tau}/\upsilon}{(1/\upsilon - 1)\bar{\tau}} = \frac{1}{1-\upsilon}.$$

This is what we need. $\qquad \square$

The second result was also independently shown in [26]:

Lemma 4.9. *If $\tau(t) \in [0, \bar{\tau}]$, then the system $\Delta_{\bar{\tau}} : z \mapsto w$ such that*

$$w(t) = \int_{t-\tau(t)}^t z(s) \, ds = \int_{-\tau(t)}^0 z(t+s) \, ds$$

is a bounded operator on $L_2(\mathbb{R}_+)$ with $\|\Delta_{\bar{\tau}}\|_{L_2(\mathbb{R}_+) \to L_2(\mathbb{R}_+)} = \bar{\tau}$.

Proof. By the Cauchy–Schwarz inequality,

$$w^2(t) = \left(\int_{-\tau(t)}^0 z(t+s) \, ds\right)^2 \leq \left(\int_{-\tau(t)}^0 1^2 \, ds\right)\left(\int_{-\tau(t)}^0 z^2(t+s) \, ds\right) = \tau(t) \int_{-\tau(t)}^0 z^2(t+s) \, ds$$

$$\leq \bar{\tau} \int_{-\bar{\tau}}^0 z^2(t+s) \, ds$$

for every t, so that (mind that it is assumed that $z(t) = 0$ whenever $t < 0$)

$$\|w\|_2^2 \leq \int_0^\infty \bar{\tau} \int_{-\bar{\tau}}^0 z^2(t+s) \, ds \, dt = \bar{\tau} \int_{-\bar{\tau}}^0 \int_0^\infty z^2(t+s) \, dt \, ds = \bar{\tau} \int_{-\bar{\tau}}^0 \|z\|_2^2 \, ds$$

Thus, $\|w\|_2^2 \leq \bar{\tau}^2 \|z\|_2^2$. This bound is tight because in the particular case of $\tau(t) \equiv \bar{\tau}$ the system $\Delta_{\bar{\tau}}$ is actually the LTI system with the transfer function $(1 - e^{-\bar{\tau}s})/s$, whose H_∞-norm equals $\bar{\tau}$. $\qquad \square$

Lemma 4.8 is readily applicable to the problem of finding stability conditions under uncertain varying delays assumed to satisfy $|\dot{\tau}_\delta(t)| \leq \upsilon$ for a given $0 \leq \upsilon < 1$. The procedure is almost identical then to the use of disks with centers at the origin in the LTI case, like that in Fig. 4.10(a). The only deviation is a different scaling, i.e. we need the static $W_\alpha = 1/\sqrt{1-\upsilon} \geq 1$ instead of $W_\alpha = 1$ now. This would lead to delay-independent results in terms of the size of $\tau_\delta(t)$, requiring $\tilde{G}_{zw} = 1/\sqrt{1-\upsilon} RP\bar{D}_{\tau_0}$ to be stable and strictly contractive, which reads $\|PR\|_\infty < \sqrt{1-\upsilon} \leq 1$.

The use of Lemma 4.9 is also similar to the LTI case. To see this, observe that the operator $\Delta_{\bar{\tau}}$ defined in the lemma can be viewed as $1 - \bar{D}_{\tau(t)}$ acting on the integrated signal z. In other words,

$$\Delta_{\bar{\tau}} = \mathcal{F}_l\left(\begin{bmatrix} -G_{\text{int}} & 1 \\ G_{\text{int}} & 0 \end{bmatrix}, \bar{D}_{\tau(t)}\right),$$

where G_{int} is the integrator element having the transfer function $G_{\text{int}}(s) = 1/s$. But this implies that

$$\bar{D}_{\tau(t)} = \mathcal{F}_u\left(\begin{bmatrix} 0 & G_{\text{int}}^{-1} \\ 1 & 1 \end{bmatrix}, \Delta_{\bar{\tau}}\right) = \mathcal{F}_u\left(\begin{bmatrix} 0 & W_\alpha \\ 1 & W_\varkappa \end{bmatrix}, \Delta_{\bar{\tau}}/\bar{\tau}\right),$$

where $W_\varkappa(s) = 1$ and $W_\alpha(s) = \bar{\tau}s$, exactly as the approximation of α_1 for the very same $W_\varkappa(s) = 1$, see (4.9), by the rational bound $W_{\alpha 1,0}(s)$ from (4.10). Because $\Delta_{\bar{\tau}}/\bar{\tau} \in \mathcal{B}_\infty$ by Lemma 4.9, we have that

$$\bar{D}_{\tau(t)} \in \mathcal{F}_u\left(\begin{bmatrix} 0 & W_\alpha \\ 1 & W_\varkappa \end{bmatrix}, \mathcal{B}_\infty\right), \quad \forall \tau(t) \in [0, \bar{\tau}]$$

and the rest is by now standard. For example, this means that the result of Example 4.3 under this W_α, which says that any system whose only unstable pole is at $s = a$ is stable for all $\tau_\delta \le \bar{\tau}$ if $\bar{\tau} < 1/a$, remains valid for arbitrary time-varying $\tau_\delta(t)$. In fact, it should be less conservative in the time-varying case.

4.2.6   Beyond simple coverings

So far, only approaches directly leading to (scaled) Small Gain Theorem applications have been discussed. Advantage of this kind of results are their relative simplicity and suitability for off-the-shelf design methods, like the H_∞ optimization. However, they might result in rather conservative results. Conservatism can be expected to be reduced if more sophisticated covering options are used.

One trick toward this end is the use of multiple covering areas. To grasp the idea, let us take a look at Fig. 4.13. It illustrates covering uncertain delays by two convex regions, a disk and a half-plane. The darkest region in each of these plots is the tightest convex region in $\mathbb{C}$ containing uncertain constant delays, so we may expect it to be less conservative that each of the covering methods in Fig. 4.10. Both involved areas, the unit disk and a half-plane, can be generated by quadratic forms in the frequency domain and thus falls into the general IQC (integral quadratic constraint) framework introduced in [37]. The use of integral quadratic constraints in the context of the analysis of the robustness of delay systems can be found in [27], where various bounds are found and the conservatism is shown to be reduced. However, IQCs, and even more so those with non-rational weights, are not quite easy to incorporate into design procedures. Still, some approaches of doing that are available, see [77] and the references therein.
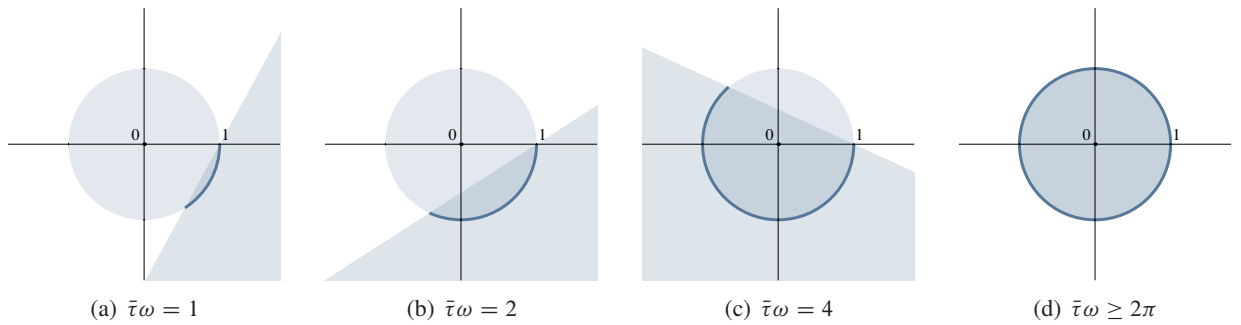

(a) $\bar{\tau}\omega = 1$ (b) $\bar{\tau}\omega = 2$ (c) $\bar{\tau}\omega = 4$ (d) $\bar{\tau}\omega \ge 2\pi$

Fig. 4.13: Covering uncertain delays by multiple areas

4.3 Analysis based on Lyapunov–Krasovskii methods

Lyapunov's direct method studied in Section 2.2 can also be used to analyze the robustness of systems to delay uncertainty. The literature on this subject is monstrous, with a great variety of results and not always clear differentiation between them. Both Lyapunov–Krasovskii and Lyapunov–Razumikhin functions are used. Below only a flavor of the use of the Lyapunov–Krasovskii approach is provided.

Consider the DDE

$$\dot{x}(t) = Ax(t) + A_\tau x(t - \tau), \quad \check{x}_0 = 0 \tag{4.18}$$

for $A \in \mathbb{R}^{n \times n}$ and $A_\tau \in \mathbb{R}^{n \times n}$. This is a version of (2.18) under zero initial conditions. Our goal is to characterize conditions under which this DDE is stable for all $\tau \in [0, \bar{\tau}]$ for some $\bar{\tau} \geq 0$. A typical modus operandi is to transform the system equation into a Lyapunov–Krasovskii-friendly form, then choose a structure of the Lyapunov–Krasovskii functional, and then analyze its derivative along the trajectories of the system via upper-bounding cross terms. Each one of these stages has a plenty of options to play with. The model transformation stage appears to be abandoned in more modern treatments, but exploring that direction goes beyond the scope of this text. The choice of an appropriate Lyapunov–Krasovskii functional is normally a tradeoff between treatability and conservatism. The general functional of the form (2.23) might be too much to digest, it does not appear to lead to manageable robustness formulations. Bounding cross-terms might not be quite intuitive, but this is where several clever and helpful tricks were introduces.

So we start with rewriting DDE (4.18) in the form

$$\dot{x}(t) = (A + A_\tau)x(t) - A_\tau\big(x(t) - x(t - \tau)\big) = (A + A_\tau)x(t) - A_\tau \int_{-\tau}^{0} \dot{x}(t + s)\,\mathrm{d}s. \tag{4.19}$$

It turns out to be advantageous (the idea is from [16]) to rewrite this equation in descriptor form

$$\underbrace{\begin{bmatrix} I & 0 \\ 0 & 0 \end{bmatrix}}_{\tilde{E}} \underbrace{\begin{bmatrix} \dot{x}(t) \\ \dot{y}(t) \end{bmatrix}}_{\dot{\tilde{x}}(t)} = \underbrace{\begin{bmatrix} 0 & I \\ A + A_\tau & -I \end{bmatrix}}_{\tilde{A}} \underbrace{\begin{bmatrix} x(t) \\ y(t) \end{bmatrix}}_{\tilde{x}(t)} - \underbrace{\begin{bmatrix} 0 \\ A_\tau \end{bmatrix}}_{\tilde{B}} \int_{-h}^{0} y(t + \theta)\,\mathrm{d}\theta$$

by adding the auxiliary variable

$$\dot{x}(t) =: y(t) = \underbrace{\begin{bmatrix} 0 & I \end{bmatrix}}_{\tilde{C}} \tilde{x}(t).$$

Choose now a Lyapunov–Krasovskii functional of the form

$$V(t) = V_1(t) + V_2(t) := \tilde{x}'(t)P'\tilde{E}\tilde{x}(t) + \int_{-\tau}^{0}\int_{t+s}^{t} y'(r)Ry(r)\,\mathrm{d}r\,\mathrm{d}s$$

for $R > 0$ and

$$P = \begin{bmatrix} P_1 & 0 \\ P_2 & P_3 \end{bmatrix}, \quad P_1 > 0. \tag{4.20}$$

Because $\tilde{x}'(t)P'\tilde{E}\tilde{x}(t) = x'(t)P_1x(t) \geq \lambda_{\min}(P_1)\|x(t)\|^2$, this V satisfies the condition of Theorem 2.5 with $\alpha(\|x(t)\|) = \lambda_{\min}(P_1)\|x(t)\|^2$, which is an unbounded function of $\|x(t)\|$. The derivatives are

$$\dot{V}_1(t) = 2\tilde{x}'(t)P'\tilde{E}\dot{\tilde{x}}(t) = 2\tilde{x}'(t)P'\left(\tilde{A}\tilde{x}(t) - \tilde{B}\int_{-\tau}^{0} y(t+s)\,\mathrm{d}s\right)$$

$$= \tilde{x}'(t)\big(P'\tilde{A} + \tilde{A}'P\big)\tilde{x}(t) - 2\int_{-h}^{0} \tilde{x}'(t)P'\tilde{B}y(t+s)\,\mathrm{d}s$$

and, using the Leibniz integral rule (2.24),

$$\dot{V}_2(t) = \int_{-\tau}^{0} \left(y'(t)Ry(t) - y'(t+s)Ry(t+s) \right) ds = \tau \tilde{x}'(t)\tilde{C}'R\tilde{C}\tilde{x}(t) - \int_{-\tau}^{0} y'(t+s)Ry(t+s)ds.$$

Taking into account that $\tau \leq \bar{\tau}$, we have:

$$\dot{V}(t) \leq \tilde{x}'(t)\left(P'\tilde{A} + \tilde{A}'P + \bar{\tau}\tilde{C}'R\tilde{C} \right)\tilde{x}(t) - \int_{-\tau}^{0} y'(t+s)Ry(t+s)ds - 2\int_{-\tau}^{0} \tilde{x}'(t)P'\tilde{B}y(t+s)ds.$$

The last term in the right-hand side above is the cross term to be bounded. To handle that, note that for all $Q > 0$ and vectors v_1 and v_2, we have that $0 \leq (v_1 + Q^{-1}v_2)'Q(v_1 + Q^{-1}v_2) = v_1'Qv_1 + v_2'Q^{-1}v_2 + 2v_2'v_1$ or, equivalently, that

$$-2v_2'v_1 \leq v_1'Qv_1 + v_2'Q^{-1}v_2. \tag{4.21}$$

Thus

$$-2\int_{-\tau}^{0} \tilde{x}'(t)P'\tilde{B}y(t+s)ds \leq \int_{-\tau}^{0} \left(\tilde{x}'(t)P'\tilde{B}Q^{-1}\tilde{B}'P\tilde{x}'(t) + y'(t+s)Qy(t+s) \right) ds$$

$$\leq \bar{\tau}\tilde{x}'(t)P'\tilde{B}Q^{-1}\tilde{B}'P\tilde{x}'(t) + \int_{-\tau}^{0} y'(t+s)Qy(t+s)ds,$$

which is true for all $Q > 0$, in particular, for $Q = R$. Thus,

$$\dot{V}(t) \leq \tilde{x}'(t)\left(P'\tilde{A} + \tilde{A}'P + \bar{\tau}\tilde{C}'R\tilde{C} + \bar{\tau}P'\tilde{B}R^{-1}\tilde{B}'P \right)\tilde{x}(t)$$

and $\dot{V}(t) \leq -\beta(\|x(t)\|)$ for $\beta(\|x(t)\|) = \lambda_{\min}(-P'\tilde{A} - \tilde{A}'P - \bar{\tau}\tilde{C}'R\tilde{C} - \bar{\tau}P'\tilde{B}R^{-1}\tilde{B}'P)\|x(t)\|^2$, which is strictly positive for all $\tilde{x} \neq 0$ if

$$P'\tilde{A} + \tilde{A}'P + \bar{\tau}\tilde{C}'R\tilde{C} + \bar{\tau}P'\tilde{B}R^{-1}\tilde{B}'P < 0.$$

Equivalently, using (A.6) we can end up with the asymptotic stability condition if the LMI

$$\begin{bmatrix} P'\tilde{A} + \tilde{A}'P + \bar{\tau}\tilde{C}'R\tilde{C} & \bar{\tau}P'\tilde{B} \\ \bar{\tau}\tilde{B}'P & -\bar{\tau}R \end{bmatrix} < 0 \tag{4.22}$$

is solvable in $0 < R \in \mathbb{R}^{n \times n}$ and $P \in \mathbb{R}^{2n \times 2n}$ as in (4.20). This condition is readily verifiable for a fixed $\bar{\tau}$ and can be used as a base for a parametric search over the scalar $\bar{\tau}$ to maximize the delay margin.

Remark 4.3 (connections with embedding). Equation (4.18) can be presented as the feedback interconnection of the uncertain delay $\bar{D}_\tau$ with a system having the transfer function $C_z(sI - A)^{-1}B_w$, where C_z and B_w are any matrices in the rank decomposition $A_\tau = B_wC_z$. Choosing now covering with $W_x(s) = 1$ and $W_\alpha(s) = \bar{\tau}s$, the robust stability problem converts to the form presented in Fig. 4.8(b) for

$$T_{zw}(s) = \mathcal{F}_l\left(\begin{bmatrix} 0 & \bar{\tau}sI \\ I & I \end{bmatrix}, C_z(sI - A)^{-1}B_w \right) = \bar{\tau}sC_z(sI - A - B_wC_z)^{-1}B_w$$

$$= \bar{\tau}C_zB_w + \bar{\tau}C_z(sI - A - A_\tau)^{-1}(A + A_\tau)B_w,$$

which is a standard system. We can then apply Propositions 4.5 and 4.6 to end up with the LMI condition

$$\begin{bmatrix} (A + A_\tau)'X + X(A + A_\tau) + \bar{\tau}^2 C_z'YC_z & X(A + A_\tau)B_w + \bar{\tau}^2 C_z'YC_zB_w \\ B_w'(A + A_\tau)'X + \bar{\tau}^2 B_w'C_z'YC_z & \bar{\tau}^2 B_w'C_z'YC_zB_w - Y \end{bmatrix} < 0, \tag{4.23}$$

which is simpler, i.e. has less decision variables with $X \in \mathbb{R}^{n \times n}$ and $Y \in \mathbb{R}^{\text{rank } A_\tau \times \text{rank } A_\tau}$, than (4.22). But now ignore the possibility to exploit a potential rank deficiency of A_τ and choose $C_z = I$ and $B_w = A_\tau$. Also, consider an alternative, descriptor, representation of T_{zw} above, namely

$$T_{zw}(s) = \bar{\tau} \begin{bmatrix} 0 & I \end{bmatrix} \left(s \begin{bmatrix} I & 0 \\ 0 & 0 \end{bmatrix} - \begin{bmatrix} 0 & I \\ A + A_\tau & -I \end{bmatrix} \right)^{-1} \begin{bmatrix} 0 \\ A_\tau \end{bmatrix} = \bar{\tau} \tilde{C} (s \tilde{E} - \tilde{A})^{-1} \tilde{B},$$

which can be verified by straightforward algebra. It can then be shown, using the LMI characterization of the H_∞ norm of descriptor systems from [35], that finding whether there is M such that $\| M T_{zw} M^{-1} \|_\infty < 1$ is equivalent to solving the very LMI (4.22). In other words, (4.23) is merely a more economical version of (4.22). It should also be emphasized that the covering disks chosen in the derivation of (4.23) are not the tightest ones. ▽

Note that inequality (4.21) can be made less conservative, e.g. if replaced with Park's inequality [57]

$$-2v_2' v_1 \leq \begin{bmatrix} v_1' & v_2' \end{bmatrix} \begin{bmatrix} Q & QS \\ S'Q & (I + S'Q)Q^{-1}(I + QS) \end{bmatrix} \begin{bmatrix} v_1 \\ v_2 \end{bmatrix},$$

which follows from (4.21) via the substitution $v_1 \to v_1 + S v_2$. The additional variable S, whose choice as $S = 0$ gives (4.21), can be used to tighten the bound. Then, LMI conditions resulting from such a replacement, can again be shown to be equivalent to those resulting with the embedding approach [84].

There are then more directions for refining the analysis using Lyapunov–Krasovskii functionals, like the use of functionals with more design parameters, exploiting Jensen's, Wirtinger's, Bessel's inequalities, et cetera, see surveys [83, 67, 85] and the references therein. Still, the vast majority of these methods apply only to the analysis problem, where a controller, actually a finite-dimensional one, is given and the stability is verified. But in such situations, it might be easier to use graphical tests, like the Nyquist criterion, to estimate the delay margin in a system. The real need in analytical methods is in *design* problems, where a controller is to be constructed to satisfy certain performance requirements, including robustness. It appears that Lyapunov-based methods are not there yet. They also appear to be less transparent in revealing conservatism sources than methods based on embedding delay uncertainty into general-purpose robustness problems.

Chapter 5

Performance: Disturbance Attenuation by Industrial Controllers

Although stability is a crucial property, it is seldom the ultimate goal of control design. Rather, control systems are supposed to impose a required behavior on controlled systems, like good command following, a sufficient disturbance attenuation level, required transient characteristics, et cetera. These properties are collectively known as *control performance*. There are zillions of ways to express performance of control systems, from classical loop-shaping and pole-placement ideas to more modern quantitative characteristics based on system norms or Lyapunov-based decay estimates. It is obviously impossible to expose all these approaches in the notes. As such, the discussion in the coming two chapters is focused mainly on two aspects of "performance" considerations. These are disturbance attenuation analysis in first-order-plus-time-delay (FOPTD) attainable by PID-based controllers and general-purpose optimization-based design methods, which reflects my personal preferences.

Time delays are integral parts of (chemical) process models used in numerous processes control applications. It is not surprising then that various aspects of the control performance in time-delay systems are extensively studied in the process control literature, see [53] and the references therein. In fact, the very idea of the dead-time compensation originated among the process control community, in [70]. At the same time, process control models are frequently not too complex, with monotonic frequency responses, controllers used there are relatively simple, with a small number of tuning parameters, and mathematical tools used in the analysis of such systems are not overly sophisticated. These factors make the analysis of such systems an ideal starting point in studying the performance of DTC-based systems.

5.1 The setup

Consider the unity feedback setup in Fig. 5.1, where d_i and d_o are input (load) and output disturbances, respectively, n is a measurement noise, and r is a reference signal. The plant contains the delay element, with a delay $\tau > 0$, and a finite-dimensional part P, which is assumed to be a first-order system with the transfer function

$$P(s) = \frac{k}{Ts + 1}$$

for some static gain $k \neq 0$ and a time constant $T > 0$. This plant is said to be *balanced* if $\tau/(\tau + T) \approx 1/2$, meaning that the loop delay and the finite-dimensional part of the plant have comparable effects on the dynamics of the plant. In situations when $\tau/(\tau + T) \downarrow 0$ the plant is called *lag dominant*, whereas *delay-dominant* dynamics correspond to $\tau/(\tau + T) \uparrow 1$. Delay-dominant plants behave more like pure delay elements and are considered harder to control, while lag-dominant plants are closer to first-order systems
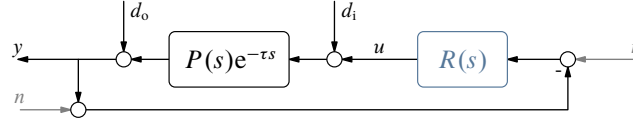
Fig. 5.1: Process control unity-feedback setup

and are considered as easier to control. However, these conclusions should be taken with a grain of salt, as effects of the loop delay depend on the intended crossover region of the system.

Signals of interest in this closed-loop system, the plant output y and the control input u, are connected with the exogenous signals mentioned above as

$$\begin{bmatrix} y \\ u \end{bmatrix} = \begin{bmatrix} S & T_d \\ -T_c & -T \end{bmatrix} \begin{bmatrix} d_o \\ d_i \end{bmatrix} + \begin{bmatrix} T \\ T_c \end{bmatrix} r - \begin{bmatrix} T \\ T_c \end{bmatrix} n,$$

where the four closed-loop systems (aka GoF)—sensitivity S, complementary sensitivity T, disturbance sensitivity T_d, and control sensitivity T_c—have the transfer functions

$$\begin{bmatrix} S(s) & T_d(s) \\ T_c(s) & T(s) \end{bmatrix} := \frac{1}{1 + C(s)P(s)e^{-\tau s}} \begin{bmatrix} 1 \\ C(s) \end{bmatrix} \begin{bmatrix} 1 & P(s)e^{-\tau s} \end{bmatrix}. \tag{5.1}$$

These relations show that the response to input and output disturbances captures all aspects of closed-loop dynamics. This justifies, in a sense, the omission of the analysis of noise and reference responses below. Moreover, the response to r can be addressed independently of those to d_i, d_o, and n via the use of 2-degree-of-freedom configurations and is thus less informative for studying feedback control architectures for dead-time systems.

5.1.1 Control goals

A popular performance measure in process control applications is the so-called IAE (integral absolute error) cost, normally calculated for responses to step exogenous signals [4]. In our case, two quantities of interest are

$$\text{IAE}_i := \int_0^\infty |y_i(t)| dt \quad \text{and} \quad \text{IAE}_o := \int_0^\infty |y_o(t)| dt, \tag{5.2}$$

where y_i and y_o are the responses of the system in Fig. 5.1 to the unit steps in d_i and d_o, respectively. This reflects common situations in process control. At the same time, the quantities in (5.2) equal the L_∞-induced norms of the closed-loop systems $\dot{d}_i \mapsto y$ and $\dot{d}_o \mapsto y$, whose transfer functions are $T_d(s)/s$ and $S(s)/s$, respectively. Thus, IAE_i and IAE_o can also be thought of as the peak magnitudes of $y(t)$ over all input and output disturbances, respectively, with unity peak derivatives.

It should be emphasized that attenuating IAE_i and IAE_o might require different control strategies. Because y_o depends only on the product $P(s)C(s)e^{-\tau s}$, canceling the stable pole of $P(s)$ at $s = -1/T$ is never harmful, it does not show up in $S(s)$ anyway. This is not the case for y_i, as the canceled plant pole remains the pole of $T_d(s)$. This slows down the response to d_i when T is not sufficiently small (a lag dominant plant). Thus, whereas it may be advantageous from the IAE_o viewpoint to cancel the plant pole by the controller even in the lag-dominant case, this is not a good idea for reducing IAE_i. At the same time, attenuating IAE_i does not require any effort at frequencies well above the bandwidth of P, because they are filtered out by the plant. But this is not the case for attenuating the output disturbance, low loop gain renders $|S(j\omega)| \approx 1$ at the corresponding frequencies and contributes to an increase of IAE_o. For these reasons, it is more representative to analize some mixture of the cost functions on (5.2), for instance their linear combination

$$\lambda_i \text{IAE}_i + \lambda_o \text{IAE}_o$$

for some positive λ_i and λ_o, whose choice will be justified below.

Reducing each quantity in (5.2) requires high-gain feedback and results in loops with high crossover frequencies, see Section 5.2 below for details. The price of that is normally large control effort, as well as excessive sensitivity to measurement noise and high-frequency modeling uncertainty. Hence, analyzing the IEA performance of the plant output alone would lead to one-sided conclusions. A remedy, which is standard in feedback control, is to counterbalance (5.2) by some other performance measure(s) penalizing high controller gains. There are plenty of options to chose to that end, like penalizing the control signal, taking measurement noise into account, including various robustness considerations, et cetera. Robustness analysis appears to be dominant in process control, so this direction is also pursued below. Also in this directions options are numerous. Classical gain μ_g and phase μ_{ph} margins are used sometimes. A wider accepted choice is the *modulus margin* $\mu_m := \inf_\omega |1 + C(j\omega)P(j\omega)e^{-j\omega\tau}| = 1/\|S\|_\infty$, which is the Euclidean distance of the loop frequency response from the critical point on the Nyquist plane. A potential disadvantage of these options, which are based on the loop gain, is that they do not penalize high-frequency gains of the loop or the controller itself. As a result, high sensitivity to loop delay mismatches is not captured by them, see Section 4.1. A way to account for such mismatches is to add the delay margun μ_d to the picture explicitly or to .

It might not be immediate from the definitions above, but all these measures implicitly impose limitations on the attainable crossover frequency

5.1.2 Controller architectures

The term "industrial controller" is historically reserved to the PI and PID controller architectures, which are simple, robust, and relatively easy to tune. In the presence of loop delays such controllers may be complemented by a dead-time compensation (DTC) part, like the classical Smith predictor introduced in §3.2.1. These are controllers studied in this chapter.

The PI structure is exactly that defined by (3.3) on p. 42, i.e.

$$C(s) = C_{PI}(s) := k_p\left(1 + \frac{1}{T_i s}\right) \tag{5.3}$$

for some proportional gain k_p and integral time (constant) T_i. The ideal PID structure is

$$C(s) = C_{PID}(s) := k_p\left(1 + \frac{1}{T_i s} + T_d s\right) \tag{5.4}$$

for a derivative time (constant) T_d. However, the transfer function $C_{PID}(s)$ above is not proper, with all consequences of this (non-implementable, sensitive to high-frequency noise and modeling inaccuracies, etc). For this reason, its implementable form is

$$C(s) = C_{PID,\gamma}(s) := k_p\left(1 + \frac{1}{T_i s} + \frac{T_d s}{(T_d/\gamma)s + 1}\right) \tag{5.5}$$

for some[1] γ, which is the high-frequency gain of its D part. This controller is virtually the same as C_{PID} at low frequencies, but deviates at high frequencies, approaching $k_p(1 + \gamma)$ instead of infinity. The latter property renders $C_{PID,\gamma}$ a more practical alternative to C_{PID}. Yet having an additional, fourth, parameter could complicate the tuning of $C_{PID,\gamma}$. For that reason, γ is frequently kept prespecified, say as a constant in the range $\gamma \in [2, 20]$, see [4, Sec. 3.3].

A typical design procedure for such systems is to fix the DTC element (often, as the classical Smith predictor) and then to design a fixed-structure (often, PI) primary controller for a delay-free equivalent

---

[1]This constant is frequently denoted by "N" in the literature, the symbol "γ" is adopted below mainly for aesthetic reasons.

plant. An important requirement to this separated design procedure is its transparency, namely the ability of the resulted closed-loop system to inherit properties of the delay-free loop, for which $\tilde{C}$ is designed. The choice of Π is a key for a successful design towards this end. So in the discussion below the main emphasis is placed on the effect of the DTC element on the design transparency. Also, because these kinds of methods are seldom analytical, the ideas are introduces via simple examples.

5.2   Attainable disturbance attenuation

5.2.1   Response to the output disturbance

5.2.2   Response to the load disturbance

5.3   Robustness measure and its attainable level

Chapter 6

Performance: Optimization-Based Design

O PTIMIZATION-BASED methods constitute an important class of design approaches. Their idea is express requirements to the behavior of controlled variables in terms of a size a cost function, which is them minimized by a control signal under standard constraints of system dynamics and the internal stability. This chapter studies H_2 and H_∞ formulations of optimization-based control design in dead-time systems. The choice of performance measures is mostly motivated by my own preferences. Some preliminary familiarity with optimization-based control is expected, albeit the exposition attempts to avoid getting too deep into solution technicalities. Rather, the main emphasis is placed on effects of loop delays on the controller structure and on attainable performance levels.

6.1 Standard H_2 and H_∞ problems

The standard problem corresponds to the lower LFT configuration depicted in Fig. 6.1(a). The system G there is known as the generalized plant and R is referred to as the controller. The goal is then to design R to reduce the effect of w on z in the system $T_{zw} := \mathcal{F}_l(G, R) : w \mapsto z$. The generalized plant has two inputs, w and u, and two outputs, z and y, whose meaning is spelled out below.

w is dubbed the *exogenous input* and contains all exogenous signals, whose effect is important for the problem at hand. These may be a reference signal, a load disturbance, measurement noise, et cetera. In many cases these are fictitious (normalized) signals forming the actual signals of interest.

z is dubbed the *regulated output* and contains signals that are required to be kept "small" (in whatever sense). These may be deviations from a required behavior, like tracking or estimation errors, actuator signals and suchlike, weighted to focus their relative importance and important aspects of them.

y is the *measured output*, through which the controller acquires the information about the effect of w on the system behavior.

u is the *control input*, which is the signal generated by the controller and through which the effect of w on z can be affected.

The generalized plant G contains then dynamics of a controlled plant itself, sensors, and actuators (all, normally, in its $u \mapsto y$ part), as well as weighing functions, and even some fixed parts of the controller (e.g. the integral action). For more details and examples see [45, Ch. 7].

The reduction of the effect of w on z can be quantified by a norm of T_{zw}. Below we consider the H_2 and H_∞ system norms for this purpose.

- The H_2-norm of a causal LTI system $G : u \mapsto y$, whose impulse response $g(t)$ is square integrable,

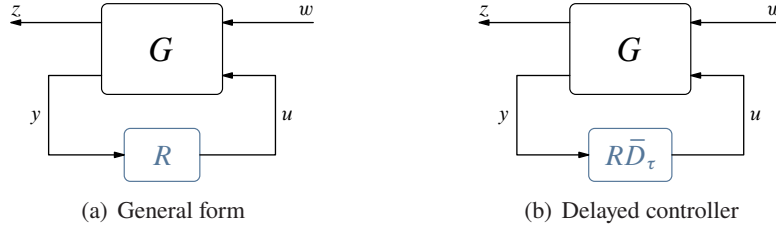(a) General form   (b) Delayed controller

Fig. 6.1: The standard problem setup

equals

$$\|G\|_2 = \left(\frac{1}{2\pi} \int_{\mathbb{R}} \|G(j\omega)\|_F^2 \, d\omega\right)^{1/2} = \left(\int_{\mathbb{R}_+} \|g(t)\|_F^2 \, dt\right)^{1/2}, \tag{6.1}$$

where $\|\cdot\|_F$ denotes the Frobenius matrix norm. It has also a stochastic interpretation: if $u(t)$ is a unit-intensity white Gaussian process, then $\|G\|_2^2$ equals the steady-state variance of $y(t)$. The space of all $p \times m$ systems with a bounded H_2-norm is known as $H_2^{p \times m}$ (the dimensions are frequently skipped). It comprises all causal systems with square-summable impulse responses. This is a Hilbert space, with the inner product

$$\langle G_1, G_2\rangle_2 := \frac{1}{2\pi} \int_{\mathbb{R}} \operatorname{tr}\left([G_2(j\omega)]' G_1(j\omega)\right) d\omega = \int_{\mathbb{R}_+} \operatorname{tr}\left([g_2(t)]' g_1(t)\right) dt. \tag{6.2}$$

The H_2-norm normally fits applications where properties of exogenous signals are known sufficiently well. Examples of the standard H_2 problem are the infinite-horizon LQG and steady-state Kalman–Bucy filtering problems.

- The H_∞-norm of a causal LTI system $G : u \mapsto y$, whose transfer function $G \in H_\infty$ as defined by (B.17), equals

$$\|G\|_\infty = \operatorname*{ess\,sup}_{\omega \in \mathbb{R}} \|G(j\omega)\|,$$

which is the peak gain of the frequency response of G. Its time-domain interpretation is the induced $L_2(\mathbb{R}_+)$-gain of G, i.e. $\|G\|_\infty = \sup_{0 \neq u \in L_2(\mathbb{R}_+)} \|y\|_2 / \|u\|_2$, where $\|\cdot\|_2$ stands for the $L_2(\mathbb{R}_+)$-norm (the square root of its energy) of a signal. This norm fits applications where properties of exogenous signals are unknown, as well as robust stability problems. Examples of the standard H_2 problem are the weighted- and mixed-sensitivity problems and the gap optimization.

It should be emphasized that H_∞ is the stability space of LTI system, so the H_∞ formulation clicks well with the stability requirement. At the same time, not all systems with a finite H_2 norm are stable (although this is the case for finite-dimensional systems). That implies that some care should be taken for in the stability analysis of H_2 problems for infinite-dimensional systems.

An important property of both H_2 and H_∞ standard problems is that there are complete parametrizations of all their suboptimal solutions. In both of these cases, the parametrizations can be expressed in the form

$$R = \mathcal{F}_l(J, Q) \tag{6.3}$$

for some LTI generator of all suboptimal controllers J, which depends on the problem data, and a free parameter Q, which is only limited to be stable and norm bounded. The bound on $\|Q\|$ depends on the performance that we expect to attain. Moreover, the generator J is square and invertible, with square and invertible $(1, 2)$ and $(2, 1)$ sub-systems. As we already saw in Section 3.5, these properties assure that the mapping $Q \mapsto R$ is bijective. This is a key property for solving delayed versions of the problem, which is presented in Fig. 6.1(b).

6.1.1 State-space formulae

If the generalized plant G in Fig. 6.1(a) is finite dimensional, solutions can be developed in terms of its state-space realization. Below such solutions are presented.

Standard assumptions

We assume that G is be given in terms of its state-space realization representing the joint dynamics of its components, i.e. as

$$G(s) = \begin{bmatrix} G_{zw}(s) & G_{zu}(s) \\ G_{yw}(s) & G_{yu}(s) \end{bmatrix} = \left[\begin{array}{c|cc} A & B_w & B_u \\ \hline C_z & D_{zw} & D_{zu} \\ C_y & D_{yw} & D_{yu} \end{array}\right], \tag{6.4}$$

where the input and output partitions are compatible with those in Fig. 6.1(a). It is conventional then to impose the following assumptions on its parameters:

$\mathcal{A}_5$: the pair (A, B_u) is stabilizable,

$\mathcal{A}_6$: the pair (C_y, A) is detectable,

$\mathcal{A}_7$: the realization (A, B_u, C_z, D_{zu}) has no invariant zeros in $j\mathbb{R}$ and $D'_{zu} D_{zu} > 0$,

$\mathcal{A}_8$: the realization (A, B_w, C_y, D_{yw}) has no invariant zeros in $j\mathbb{R}$ and $D_{yw} D'_{yw} > 0$.

Assumptions $\mathcal{A}_{5,6}$ are necessary and sufficient conditions for the existence of an internally stabilizing controller, so they are naturally required. Assumptions $\mathcal{A}_{7,8}$ are technical and are required to guarantee the solvability of two involved algebraic Riccati equations. The constraints that they impose on the corresponding feedthrough terms just say that all components of the control input u are penalized in the cost function (the full column rank of D_{zu}) and that all measurement channels are corrupted by noise (the full row rank of D_{yw}). Normally, although still not always, assumptions $\mathcal{A}_{7,8}$ are necessary for the corresponding optimization problems to be well defined.

All H_2 suboptimal solutions for finite-dimensional generalized plants

The standard H_2 problem for the system in Fig. 6.1 can be posed as the design on an internally stabilizing R, which minimizes $\|T_{zw}\|_2$. Its solution is based on the following two algebraic Riccati equations:

$$A'X + XA + C'_z C_z - (XB_u + C'_z D_{zu})(D'_{zu} D_{zu})^{-1}(B'_u X + D'_{zu} C_z) = 0 \tag{6.5a}$$

and

$$AY + YA' + B_w B'_w - (YC'_y + B_w D'_{yw})(D_{yw} D'_{yw})^{-1}(C_y Y + D_{yw} B'_w) = 0, \tag{6.5b}$$

whose solutions X and Y are said to be stabilizing if $A + B_u K_u$ and $A + L_y C_y$ are Hurwitz, respectively, where

$$K_u := -(D'_{zu} D_{zu})^{-1}(B'_u X + D'_{zu} C_z) \quad \text{and} \quad L_y := -(YC'_y + B_w D'_{yw})(D_{yw} D'_{yw})^{-1}. \tag{6.6}$$

If $\mathcal{A}_{5\text{-}8}$ hold true, then stabilizing solutions always exist, are unique, and such that $X = X' \geq 0$ and $Y = Y' \geq 0$. Furthermore, $X > 0$ iff (A, B_u, C_z, D_{zu}) has no invariant zeros in $\mathbb{C} \setminus \bar{\mathbb{C}}_0$ and $Y > 0$ iff (A, B_w, C_y, D_{yw}) has no invariant zeros in $\mathbb{C} \setminus \bar{\mathbb{C}}_0$.

Theorem 6.1. *Let $\mathcal{A}_{5\text{-}8}$ hold true and $D_{zw} = 0$. If all stabilizing controllers are presented in the form $R = \mathcal{F}_l(J_2, Q)$, where*

$$J_2(s) = \left[\begin{array}{c|cc} A + B_u K_u + L_y C_y + L_y D_{yu} K_u & -L_y & B_u + L_y D_{yu} \\ \hline K_u & 0 & I \\ -C_y - D_{yu} K_u & I & -D_{yu} \end{array}\right] \tag{6.7}$$

with K_u and L_y as in (6.6), then $\|T_{zw}\|_2^2 = \|\mathcal{F}_l(G, R)\|_2^2 = \gamma_0 + \|D_{zu} Q D_{yw}\|_2^2$, where

$$\gamma_0 := \operatorname{tr}(B_w' X B_w) + \operatorname{tr}(C_z Y C_z') + \operatorname{tr}(XAY + YA'X). \tag{6.8}$$

The central controller, corresponding to $Q = 0$, is then the unique optimal controller, attaining γ_0.

Some remarks are in order:

Remark 6.1 (solution properties). The optimal R above is an observer-based controller comprised of the LQR state feedback with the gain K_u and the Kalman–Bucy filter with the gain L_y. This separation is remarkable and not quite obvious. At the same time, the optimal cost is not just a sum of the LQR (the first term in the expression for γ_0) and the Kalman–Bucy (the second term) costs. It also contains the coupling term $\operatorname{tr}(XAY + YA'X)$, which might be both positive and negative, depending of properties of A. To explain this fact, rewrite the optimal cost as

$$\gamma_0 = \operatorname{tr}(B_w' X B_w) + \operatorname{tr}(D_{zu} K_u Y K_u' D_{zu}').$$

The first term above is still the LQR cost. The second term is the cost of estimating the signal $v(t) = D_{zu} K_u x(t)$ from the measured $y(t)$. The signal v is nothing but the LQR control law, normalized by the its penalty in the cost function.   ▽

All H_∞ suboptimal solutions for finite-dimensional generalized plants

The standard H_∞ problem for the system in Fig. 6.1 can be posed as the design on an internally stabilizing R, which renders $\|T_{zw}\|_\infty < \gamma$ for a given $\gamma > 0$. Its solution is based on two algebraic Riccati equations too, now of the form

$$A'X + XA + C_z'C_z - \left(X \begin{bmatrix} B_w & B_u \end{bmatrix} + C_z' \begin{bmatrix} D_{zw} & D_{zu} \end{bmatrix}\right)$$
$$\times \begin{bmatrix} D_{zw}'D_{zw} - \gamma^2 I & D_{zw}'D_{zu} \\ D_{zu}'D_{zw} & D_{zu}'D_{zu} \end{bmatrix}^{-1} \left(\begin{bmatrix} B_w' \\ B_u' \end{bmatrix} X + \begin{bmatrix} D_{zw}' \\ D_{zu}' \end{bmatrix} C_z\right) = 0 \tag{6.9a}$$

and

$$AY + YA' + B_w B_w' - \left(Y \begin{bmatrix} C_z' & C_y' \end{bmatrix} + B_w \begin{bmatrix} D_{zw}' & D_{yw}' \end{bmatrix}\right)$$
$$\times \begin{bmatrix} D_{zw}D_{zw}' - \gamma^2 I & D_{zw}D_{yw}' \\ D_{yw}D_{zw}' & D_{yw}D_{yw}' \end{bmatrix}^{-1} \left(\begin{bmatrix} C_z \\ C_y \end{bmatrix} Y + \begin{bmatrix} D_{zw} \\ D_{yw} \end{bmatrix} B_w'\right) = 0, \tag{6.9b}$$

whose solutions are said to be stabilizing if $A + B_w K_w + B_u K_u$ and $A + L_z C_z + L_y C_y$ are Hurwitz, where

$$\begin{bmatrix} K_w \\ K_u \end{bmatrix} := -\begin{bmatrix} D_{zw}'D_{zw} - \gamma^2 I & D_{zw}'D_{zu} \\ D_{zu}'D_{zw} & D_{zu}'D_{zu} \end{bmatrix}^{-1} \left(\begin{bmatrix} B_w' \\ B_u' \end{bmatrix} X + \begin{bmatrix} D_{zw}' \\ D_{zu}' \end{bmatrix} C_z\right) \tag{6.10a}$$

and

$$\begin{bmatrix} L_z & L_y \end{bmatrix} := -\left(Y \begin{bmatrix} C_z' & C_y' \end{bmatrix} + B_w \begin{bmatrix} D_{zw}' & D_{yw}' \end{bmatrix}\right) \begin{bmatrix} D_{zw}D_{zw}' - \gamma^2 I & D_{zw}D_{yw}' \\ D_{yw}D_{zw}' & D_{yw}D_{yw}' \end{bmatrix}^{-1}. \tag{6.10b}$$

Assumptions $\mathcal{A}_{5\text{-}8}$ are necessary for the solvability of these equations, but might not be sufficient if γ is not sufficiently large. Moreover, even if AREs (6.9) do admit stabilizing solutions, these solutions might not be positive semi-definite, also depending on γ. At the same time, null spaces of X and Y do not depend on γ. We still have that $\det(X) \neq 0$ iff (A, B_u, C_z, D_{zu}) has no invariant zeros in $\mathbb{C} \setminus \bar{\mathbb{C}}_0$ and $\det(Y) \neq 0$ iff (A, B_w, C_y, D_{yw}) has no invariant zeros in $\mathbb{C} \setminus \bar{\mathbb{C}}_0$. Also, the AREs in (6.9) reduce to the corresponding H_2 AREs in (6.5) as $\gamma \to \infty$.

Theorem 6.2. *If $\mathcal{A}_{5\text{-}8}$ hold true and $\|D_{zw}\| < \gamma$, then the standard H_∞ problem is solvable iff the following conditions hold:*

(a) there is a stabilizing solution X to ARE (6.9a) such that $X = X' \geq 0$,

(b) there is a stabilizing solution Y to ARE (6.9b) such that $Y = Y' \geq 0$,

(c) $\rho(XY) < \gamma^2$.

In such a case, all γ-suboptimal, possibly infinite-dimensional, controllers are given by $R = \mathcal{F}_l(J_\infty, Q)$, where

$$J_\infty(s) = \left[\begin{array}{c|cc} A_\gamma & -Z_\gamma L_y & Z_\gamma(B_u + L_z D_{zu} + L_y D_{yu}) \\ \hline K_u & 0 & I \\ -C_y - D_{yw}K_w - D_{yu}K_u & I & -D_{yu} - D_\gamma \end{array} \right], \qquad (6.11)$$

for any $Q \in H_\infty$ such that $\|(I - \gamma^{-2}D_{zw}D'_{zw})^{-1/2}D_{zu}QD_{yw}(I - \gamma^{-2}D'_{zw}D_{zw})^{-1/2}\|_\infty < \gamma$, where

$$A_\gamma := A + B_w K_w + B_u K_u + Z_\gamma L_y(C_y + D_{yw}K_w + D_{yu}K_u),$$

$D_\gamma := D_{yw}D'_{zw}(\gamma^2 I - D_{zw}D'_{zw})^{-1}D_{zu}$, *and* $Z_\gamma := (I - \gamma^{-2}YX)^{-1}$.

Some remarks are in order:

Remark 6.2 (solution properties). Although this fact is less evident than in the H_2 case, the central suboptimal controller, that corresponding to $Q = 0$, is also observer based. The resulting control signal is also the H_∞ suboptimal estimate of the H_∞ state feedback control signal $u = K_u x$ (which would be admissible under measuring the whole state of the plant iff condition (a) of Theorem 6.2 holds). In contrast to the H_2 (Kalman–Bucy) case, parameters of the H_∞ estimator do depend on the signal it estimates, so the formulae are more involved and nontrivial transformations are required to decouple the estimator ARE, which depends on the state-feedback gain, from K_u. The coupling condition (c) of Theorem 6.2 is actually a remnant of this procedure. ▽

Remark 6.3 (simplifications). The formulae of Theorem 6.2 are greatly simplified in the case when $D_{zw} = 0$. Indeed, in this case the AREs (6.9) read

$$A'X + XA + C'_z C_z - (XB_u + C'_z D_{zu})(D'_{zu}D_{zu})^{-1}(B'_u X + D'_{zu}C_z) + \gamma^{-2}XB'_w B_w X = 0 \qquad (6.9a')$$

$$AY + YA' + B_w B'_w - (YC'_y + B_w D'_{yw})(D_{yw}D'_{yw})^{-1}(C_y Y + D_{yw}B'_w) + \gamma^{-2}YC_z C'_z Y = 0, \qquad (6.9b')$$

control and estimation gains are

$$K_u = -(D'_{zu}D_{zu})^{-1}(B'_u X + D'_{zu}C_z) \quad \text{and} \quad K_w = \gamma^{-2}B'_w X, \qquad (6.10a')$$

$$L_y = -(YC'_y + B_w D'_{yw})(D_{yw}D'_{yw})^{-1} \quad \text{and} \quad L_z = \gamma^{-2}YC'_z, \qquad (6.10b')$$

and $D_\gamma = 0$. Still, the assumption $D_{zw} = 0$ does not fit such important cases as the mixed and balanced sensitivity problems. ▽

6.1.2 Design case study

To illustrate the use of the formulae above and the implication of the choice of the generalized plant on properties of the resulted closed-loop system, in this subsection we study a simple academic design example and analyze the design of H_2 and H_∞ controllers for it.

Consider the simple single-loop control system shown in Fig. 6.2. The plant there is a plain integrator, subject to load disturbances $d(t)$. To compensate the effect of d on the controlled output y_c, a feedback loop is introduced on the basis of a measured version of the controlled output, $y_m = y_c + n$, where $n(t)$ is
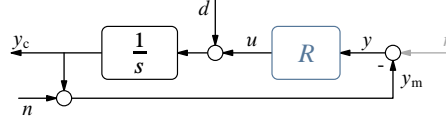
Fig. 6.2: System for optimal control design examples (delay-free case)

a measurement noise signal. Our goal is to design a stabilizing controller R, which attenuates the effect of the load disturbances on the controlled output, while not amplifying the effect of the measurement noise on it. Also, we would like to achieve both these goals by a "reasonable" control effort.

The first step in constructing the generalized plant for this problem is to form the exogenous input and regulated output the signals. The former is naturally taken of the form

$$w(t) = \begin{bmatrix} d(t) \\ n(t)/\varsigma \end{bmatrix},$$

where the weight ς reflects the relative size of the measurement noise and the load disturbance. It is tuned so that d and n/ς have comparable intensities. As a result, a decrease of ς implies putting more weight on the load disturbance, while an increase of ς renders the measurement noise more dominant. The regulated signal of choice is

$$z(t) = \begin{bmatrix} y_c(t) \\ \varrho u(t) \end{bmatrix},$$

whose L_2-norm $\|z\|_2^2 = \|y_c\|_2^2 + \varrho^2 \|u\|_2^2$. In other words, we penalize both the increase of y_c and that of u, where the weight ϱ serves as a tuning parameter, trading off disturbance attenuation and control effort. which justifies the introduction of the control signal u to regulated output. The measured output is obviously $y = -y_m = -y_c - n$ and the control input is u. With these choices, the generalized plant

$$G(s) = \left[\begin{array}{ccc|cc} 0 & 1 & 0 & 1 \\ \hline 1 & 0 & 0 & 0 \\ 0 & 0 & 0 & \varrho \\ \hline -1 & 0 & -\varsigma & 0 \end{array} \right].$$

It is readily seen that it satisfies all assumptions $\mathcal{A}_{5\text{-}8}$ whenever $\varsigma > 0$ and $\varrho > 0$.

Another way to interpret the generalized plant is via the relation

$$\begin{bmatrix} y_c \\ u \end{bmatrix} = \begin{bmatrix} T_d & -T \\ T & -T_c \end{bmatrix} \begin{bmatrix} d \\ n \end{bmatrix},$$

from which

$$z = \begin{bmatrix} 1 & 0 \\ 0 & \varrho \end{bmatrix} \begin{bmatrix} y_c \\ u \end{bmatrix} = \begin{bmatrix} 1 & 0 \\ 0 & \varrho \end{bmatrix} \begin{bmatrix} T_d & -T \\ T & -T_c \end{bmatrix} \begin{bmatrix} 1 & 0 \\ 0 & \varsigma \end{bmatrix} w = \begin{bmatrix} T_d & -\varsigma T \\ \varrho T & -\varrho \varsigma T_c \end{bmatrix} w = T_{zw} w.$$

Thus, the closed-loop system T_{zw} includes the disturbance sensitivity, twice the complementary sensitivity weighted by ϱ and by ς, and the control sensitivity weighted by $\varrho \varsigma$.

H_2 design

Consider first the H_2 performance measure. To use Theorem 6.1, we need the stabilizing solutions to the Riccati equations (6.5a),

$$0 \cdot X + X \cdot 0 + 1 - X \cdot 1 \cdot \varrho^{-2} \cdot 1 \cdot X = 0 \implies X = \varrho$$

(a) Disturbance sensitivity   (b) Control sensitivity   (c) Complementary sensitivity
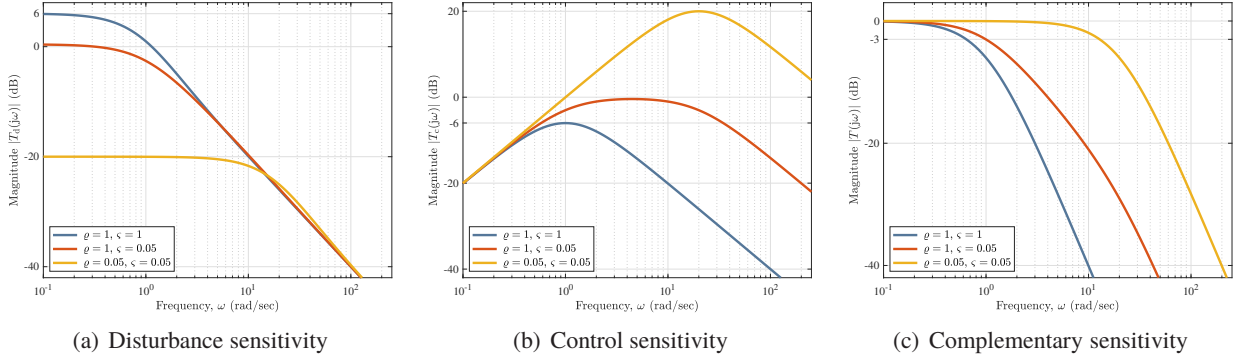
Fig. 6.3: Closed-loop frequency-response plots

(the stabilizing solution must be non-negative), and (6.5b),

$$Y \cdot 0 + 0 \cdot Y + 1 - Y \cdot (-1) \cdot \varsigma^{-2} \cdot (-1) \cdot Y = 0 \implies Y = \varsigma.$$

The resulting gains are then

$$K_u = -\frac{1}{\varrho} \quad \text{and} \quad L_y = \frac{1}{\varsigma},$$

for which $A + B_u K_u = -1/\varrho$ and $A + L_y C_y = -1/\varsigma$ are indeed Hurwitz. Expectably, the state-feedback gain K_u increases as the control penalty decreases. Likewise, the Kalman filter gain L_y increases as the measurement noise weight decreases.

The optimal controller

$$R(s) = \mathcal{F}_l(J_2, 0) = \left[\begin{array}{c|c} -1/\varrho - 1/\varsigma & -1/\varsigma \\ \hline -1/\varrho & 0 \end{array} \right] = \frac{1}{\varrho\varsigma s + \varrho + \varsigma}$$

then. It is stable for all $\varrho > 0$ and $\varsigma > 0$, its static gain is a decreasing function of both ϱ and ς, and its time constant $\varrho\varsigma/(\varrho + \varsigma)$ is an increasing function of both these parameters. In other words, the decrease of either one of these tuning parameter increases both the static gain and the bandwidth of the optimal R.

Consider now the four closed-loop systems (GoF) resulted from this design. We have that

$$\begin{bmatrix} T_d(s) & S(s) \\ T(s) & T_c(s) \end{bmatrix} = \frac{1}{1 + P(s)R(s)} \begin{bmatrix} 1 \\ R(s) \end{bmatrix} \begin{bmatrix} P(s) & 1 \end{bmatrix} = \frac{1}{(\varrho s + 1)(\varsigma s + 1)} \begin{bmatrix} \varrho\varsigma s + \varrho + \varsigma \\ 1 \end{bmatrix} \begin{bmatrix} 1 & s \end{bmatrix}.$$

The closed-loop poles are at $s = -1/\varrho$ and $s = -1/\varsigma$, which is consistent with the separation arguments for observer-based controllers.

The disturbance sensitivity magnitude

$$|T_d(j\omega)|^2 = \frac{\varrho^2\varsigma^2\omega^2 + (\varrho + \varsigma)^2}{(\varrho^2\omega^2 + 1)(\varsigma^2\omega^2 + 1)},$$

which is a monotonically decreasing function of ω with its peak $\|T_d\|_\infty = \varrho + \varsigma$ attained at $\omega = 0$, see Fig. 6.3(a) for three choices. Clearly, the increase of either ϱ or ς increases $\|T_d\|_\infty$, which is expectable as both these constants aim at trading off the disturbance response with other closed-loop properties. At the same time, the high-frequency gain of $T_d(s)$, which equals 1, is independent of tuning parameters.

The control sensitivity magnitude

$$|T_c(j\omega)|^2 = \frac{\omega^2}{(\varrho^2\omega^2 + 1)(\varsigma^2\omega^2 + 1)}.$$

This function vanishes at both very small and very high frequencies, peaking at $\omega = 1/\sqrt{\varrho\varsigma}$ with the value $\|T_\text{c}\|_\infty = 1/(\varrho + \varsigma) = 1/\|T_\text{d}\|_\infty$, see Fig. 6.3(b). Thus, the increase of either ϱ or ς clearly decreases $\|T_\text{c}\|_\infty$. But the decrease of either one of these parameters does not necessarily increases the peak of the control sensitivity, to that end both ϱ and ς have to be decreased.

The magnitude of the complementary sensitivity, which is the last function that we penalize in T_{zw},

$$|T(\text{j}\omega)|^2 = \frac{1}{(\varrho^2\omega^2 + 1)(\varsigma^2\omega^2 + 1)}.$$

This is a monotonically decreasing function of ω, attaining its maximum $\|T\|_\infty = 1$ at $\omega = 0$, see Fig. 6.3(c). This value does not depend on tuning parameters, which is because the gain of the plant at this frequency is infinite. But tuning parameters affect the time constants of this system and thus its bandwidth, which is

$$\omega_\text{b} = \sqrt{\frac{1}{2}\left(\sqrt{\frac{1}{\varrho^4} + \frac{6}{\varrho^2\varsigma^2} + \frac{1}{\varsigma^4}} - \frac{1}{\varrho^2} - \frac{1}{\varsigma^2}\right)}.$$

If both ϱ and ς decrease, the bandwidth of $T(\text{j}\omega)$ increases.

As a matter of fact, the sensitivity magnitude,

$$|S(\text{j}\omega)|^2 = \frac{(\varrho^2\varsigma^2\omega^2 + (\varrho + \varsigma)^2)\omega^2}{(\varrho^2\omega^2 + 1)(\varsigma^2\omega^2 + 1)},$$

is contractive, i.e. smaller than or equal to 1, iff $\omega \le 1/\sqrt{2\varrho\varsigma}$. This implies that as either ϱ or ς decreases, the frequency range in which $|S(\text{j}\omega)| \le 1$ increases. This range of frequencies, in which the feedback is effective, is a way to define the closed-loop bandwidth. This bandwidth increases faster if ϱ and ς decrease simultaneously.

6.2 H_2 design for dead-time systems

This section studies the H_2 (LQG) problem for the system in Fig. 6.1(b), for which $T_{zw} = \mathcal{F}_\text{l}(G, R\bar{D}_\tau)$. We impose the same assumptions on the generalized plant G as in the delay-free case, i.e. suppose that $\mathcal{A}_{5\text{-}8}$ hold.

6.2.1 Extraction of optimal dead-time controllers

The main idea discussed in this subsection is essentially the same as that in §3.5. Namely, the starting point is the recognition of the fact that no delayed controller can attain a performance level below that attainable by its delay-free counterpart, γ_0, just because delay imposes additional constraints on the controller. We thus start with the parametrization of all sub-optimal causal controllers in Theorem 6.1 and then seek for conditions to be imposed on its free Q-parameter to render the overall controller of the form $R\bar{D}_\tau$.

Two facts are instrumental towards this end. First, the performance attainable by any controller of the form $R = \mathcal{F}_\text{l}(J_2, Q)$ for J_2 given by (6.7) is $\|T_{zw}\|_2^2 = \gamma_0^2 + \|D_{zu}QD_{yw}\|_2^2$. Because γ_0 given by (6.8) is fixed, we shall be concerned only with the second term above. Second, the generator of all suboptimal controllers satisfies the assumptions of Lemma 3.5, so all Q's rendering $\mathcal{F}_\text{l}(J_2, Q)$ a dead-time system for a given τ must be of the form $Q = \pi_\tau\{H_{2,22}\} + \tilde{Q}\bar{D}_\tau$, where

$$\begin{bmatrix} H_{2,11}(s) & H_{2,12}(s) \\ H_{2,21}(s) & H_{2,22}(s) \end{bmatrix} := J_2^{-1}(s)\left[\begin{array}{c|cc} A & B_u & -L_y \\ \hline C_y & D_{yu} & I \\ -K_u & I & 0 \end{array}\right],$$
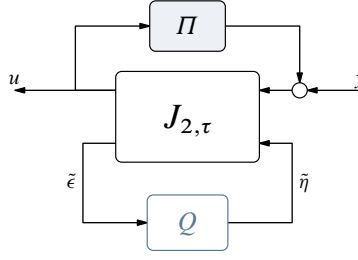
Fig. 6.4: All H_2 suboptimal controllers for the standard problem in Fig. 6.1(b)

for some stable and causal $\tilde{Q}$. Thus, the H_2 optimization problem reduces to the problem of finding a stable and causal $\tilde{Q}$ minimizing $\|Q_0 + Q_\tau \bar{D}_\tau\|_2$, where

$$Q_0 := D_{zu}\pi_\tau\{H_{2,22}\}D_{yw} \quad \text{and} \quad Q_\tau := D_{zu}\tilde{Q}D_{yw}.$$

A key observation about the expression above is that the two terms (systems) in the decomposition $Q_0 + Q_\tau \bar{D}_\tau$ have non-overlapping impulse responses. This implies that they are *orthogonal* in H_2 (provided $\tilde{Q} \in H_2$, of course). Indeed, let $q_0(t)$ and $q_\tau(t)$ be the impulse responses of Q_0 and Q_τ, respectively. By definition, q_0 has support in $[0, \tau]$, while q_τ—in $\mathbb{R}_+$. The impulse response of $Q_\tau\bar{D}_\tau$ is then $q_\tau(t - \tau)$ and it has support in $[\tau, \infty)$, see the discussion on p. 4. It then follows from (6.2) that

$$\langle Q_0, Q_\tau\rangle_2 = \int_{\mathbb{R}_+} \text{tr}\big([q_\tau(t - \tau)]'q_0(t)\big)\,\mathrm{d}t = \int_0^\tau \text{tr}\big(\underbrace{[q_\tau(t - \tau)]'q_0(t)}_{=0}\big)\,\mathrm{d}t + \int_{\mathbb{R}_+} \text{tr}\big(\underbrace{[q_\tau(t)]'q_0(t + \tau)}_{=0}\big)\,\mathrm{d}t = 0.$$

Hence, by Pythagoras and the fact that a shift does not affect the H_2-norm, we have that

$$\|Q_0 + Q_\tau\bar{D}_\tau\|_2^2 = \|Q_0\|_2^2 + \|Q_\tau\bar{D}_\tau\|_2^2 = \|Q_0\|_2^2 + \|Q_\tau\|_2^2,$$

which clearly implies that the norm is minimal under $Q_\tau = 0$. By $\mathcal{A}_{7,8}$, the matrices D_{zu} and D_{yw} are left and right invertible, respectively, so that $Q_\tau = 0 \iff \tilde{Q} = 0$. This yields the optimal $Q = Q_0$ for the dead-time system and the following result:

Theorem 6.3. *Let $\mathcal{A}_{5\text{-}8}$ hold true and $D_{zw} = 0$. If all stabilizing controllers are presented in the form shown in Fig. 6.4, where (K_u and L_y below are as in (6.6), again)*

$$J_{2,\tau}(s) = \left[\begin{array}{c|cc} A + B_uK_u + \mathrm{e}^{A\tau}L_yC_y\mathrm{e}^{-A\tau} + \mathrm{e}^{A\tau}L_yD_{yu}K_u & -\mathrm{e}^{A\tau}L_y & B_u + \mathrm{e}^{A\tau}L_yD_{yu} \\ \hline K_u & 0 & I \\ -C_y\mathrm{e}^{-A\tau} - D_{yu}K_u & I & -D_{yu} \end{array}\right] \quad (6.12)$$

and

$$\Pi = \sigma_\tau\{G_{yu}\} = \sigma_\tau\left\{\left[\begin{array}{c|c} A & B_u \\ \hline C_y & D_{yu} \end{array}\right]\right\},$$

then $\|T_{zw}\|_2^2 = \|\mathcal{F}_l(G, R\bar{D}_\tau)\|_2^2 = \gamma_0 + \gamma_{DT}(\tau) + \|D_{zu}QD_{yw}\|_2^2$, where the delay-free optimal performance γ_0 is given by (6.8) and

$$\gamma_{DT}(\tau) := \int_0^\tau \|D_{zu}K_u\mathrm{e}^{At}L_yD_{yw}\|_F^2\,\mathrm{d}t. \quad (6.13)$$

The central controller, corresponding to $Q = 0$, is the unique optimal controller, attaining $\gamma_0 + \gamma_{DT}(\tau)$.

Proof. As the structure in Fig. 6.4 is the same as that in Fig. 3.10, it is only remained to show that $\|Q_0\|_2^2 = \gamma_{DT}(\tau)$. To this end, note that the impulse response of Q_0 is $q_0(t) = D_{zu}K_u\mathrm{e}^{At}L_yD_{yw}\mathbb{1}_{[0,\tau]}(t)$. The result then follows by the second equality in (6.1). $\qquad\square$

Some remarks are in order:

Remark 6.4 (H_2 cost of delay). The quantity $\gamma_{\mathrm{DT}}(\tau)$ defined in (6.13) is the increment of γ_0 due to the presence of the loop delay in the setup of Fig. 6.1(b). Thus, it can be viewed as the cost of delay from the H_2 perspective. This is obviously a nonnegative quantity. It is also a nondecreasing quantity, just because

$$\int_0^{\tau+\delta} \|D_{zu} K_u e^{At} L_y D_{yw}\|_{\mathrm{F}}^2 dt = \int_0^\tau \|D_{zu} K_u e^{At} L_y D_{yw}\|_{\mathrm{F}}^2 dt + \int_0^\delta \|D_{zu} K_u e^{A(t+\tau)} L_y D_{yw}\|_{\mathrm{F}}^2 dt,$$

where the last term in the right-hand side is nonnegative for all $\delta > 0$. There might be situations though, in which $\gamma_{\mathrm{DT}}(\tau) = 0$. As D_{zu} and D_{yw} are left and right invertible, respectively, this happens iff $K_u e^{At} L_y = 0$ for all $t \in [0, \tau]$. This, in turn, happens iff $K_u(sI - A)^{-1} L_y = 0$, which follows directly from the Gramian-based controllability and observability test [45, Thm. 4.1]. Now, it can be verified that

$$\left[\begin{array}{c|c} A & L_y \\ \hline K_u & 0 \end{array} \right] = 0 \quad \Longleftrightarrow \quad \left[\begin{array}{c|c} A + B_u K_u + L_y C_y + L_y D_{yu} K_u & L_y \\ \hline K_u & 0 \end{array} \right] = \mathcal{F}_{\mathrm{l}}(J_2(s), 0) = 0.$$

The last equality takes place iff the optimal controller for the delay-free H_2 problem is zero. This can happen, but it is clearly not quite a typical situation. Hence, we may conclude that the cost of delay is normally nonzero and is a strictly increasing function of τ. $\triangledown$

Remark 6.5 (sampled-data vs. delayed feedback). It can be shown [44, §V.A] that the optimal attainable H_2 performance under a sampled-data controller with the sampling period $h > 0$ is $\gamma_0 + \gamma_{\mathrm{SD}}(h)$, where

$$\gamma_{\mathrm{SD}}(h) := \frac{1}{h} \int_0^h \int_0^{h-t} \|D_{zu} K_u e^{At} L_y D_{yw}\|_{\mathrm{F}}^2 dt\, ds$$

(assuming that its A/D and D/A parts are also design parameters). Because

$$\frac{1}{h} \int_0^h \int_0^{h-t} f(t)\, dt\, ds \leq \frac{1}{h} \int_0^h \int_0^h f(t)\, dt\, ds = \frac{1}{h} \int_0^h \int_0^h f(t)\, ds\, dt = \int_0^h f(t)\, dt$$

for any bounded $f(t) \geq 0$ (moreover, the equality holds iff $f(t) = 0$ for all $t \in [0, h]$), we have that

$$\gamma_{\mathrm{SD}}(h) \leq \gamma_{\mathrm{DT}}(h),$$

with the equality iff $\mathcal{F}_{\mathrm{l}}(J_2, 0) = 0$. In other words, the cost of delay normally exceeds the cost of sampling in the H_2 case if the sampling period h coincides with the loop delay τ. $\triangledown$

Remark 6.6 (controller structure). The H_2 (sub) optimal controllers in Fig. 6.4 are clearly dead-time compensator, with the modifies Smith predictor (MSP) DTC block, exactly like that introduced by Watanabe–Ito. This provides an additional justification of the DTC controller configuration. $\triangledown$

6.2.2 Loop shifting solution

Another way to treat the H_2 optimization for time-delay systems is an extension of the loop-shifting idea discussed in Section 3.4. Such an extension might not be simple for general delay systems, even though it applies to a general stabilization problem. The reason is that loop transformations, like those discussed in §3.2.3 and §3.3.3, do not necessarily preserve the structure of the cost function, which is the regulated signal z in Fig. 6.1. Still, in the case of dead-time plants there is a workaround proposed in [47], which is outlined below.

Consider the setup in Fig. 6.5(a), which is exactly that in Fig. 6.1(b) modulo moving the delay from the input of the controller to its output (so the controller is supposed to be time invariant). The first step
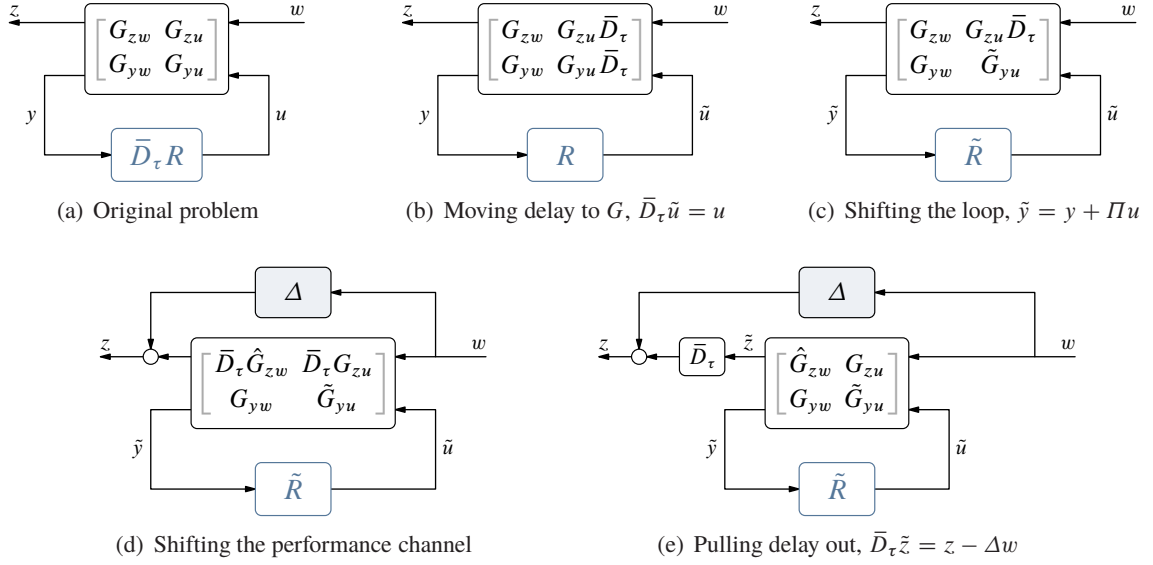
(a) Original problem (b) Moving delay to G, $\bar{D}_\tau \tilde{u} = u$ (c) Shifting the loop, $\tilde{y} = y + \Pi u$

(d) Shifting the performance channel (e) Pulling delay out, $\bar{D}_\tau \tilde{z} = z - \Delta w$

Fig. 6.5: Loop shifting in the general problem setup; here $\tilde{G}_{yu} = \Pi + G_{yu}\bar{D}_\tau$, $\tilde{R} = R(I + \Pi R)^{-1}$, and $G_{zw} = \Delta + \hat{G}_{zw}\bar{D}_\tau$

is to move that delay from the controller to the generalized plant as shown in Fig. 6.5(b). This adds the delay element $\bar{D}_\tau$ to two sub-blocks of G. The new "control input" $\tilde{u}$ is then the τ-previewed version of u. Next, the loop-shifting procedure of Section 3.4 with a stable Π is applied, resulting in the block-diagram in Fig. 6.5(c) with $\tilde{G}_{yu} = \Pi + G_{yu}\bar{D}_\tau$ and $\tilde{R} = R(I + \Pi R)^{-1}$. And, as we already saw, with the choice $\Pi = \sigma_\tau\{G_{yu}\bar{D}_\tau\}$ the system $\tilde{G}_{yu}$ is finite dimensional. The problem is that the generalized plant in Fig. 6.5(c) still contains a delayed sub-block, that from $\tilde{u}$ to z. So some more shifts are required. To this end, select any $\Delta \in H_\infty$ such that $G_{zw} = \Delta + \hat{G}_{zw}\bar{D}_\tau$ for a finite-dimensional $\hat{G}_{zw}$. In this case, the system can be equivalently presented in the form depicted in Fig. 6.5(d), in which both systems in the upper raw are delayed. As a result, the delay element can be pulled out of the system, as shown in Fig. 6.5(e). The signal $\tilde{z}$ there is related to the original regulated signal via $z = \bar{D}_\tau \tilde{z} + \Delta w$.

The transformations above decomposes the closed-loop system $T_{zw} = \mathcal{F}_l(G, R\bar{D}_\tau)$ as

$$T_{zw} = \Delta + \bar{D}_\tau T_{\tilde{z}w}, \tag{6.14}$$

where $T_{\tilde{z}w} = \mathcal{F}_l(\tilde{G}, \tilde{R})$ for

$$\tilde{G} := \begin{bmatrix} \hat{G}_{zw} & G_{zu} \\ G_{yw} & \tilde{G}_{yu} \end{bmatrix}.$$

By the stability of Δ and Lemma 3.4, $T_{zw} \in H_\infty \iff T_{\tilde{z}w} \in H_\infty$, i.e. the transformation preserves stability. In light of the discussion preceding Theorem 6.3, it would make sense to separate the impulse responses of the two terms in the right-hand side of (6.14). This is always the case with the choice $\Delta = \pi_\tau\{G_{zw}\}$, for which the impulse response of Δ has support in $[0, \tau]$ and thus

$$\|T_{zw}\|_2^2 = \|\Delta\|_2^2 + \|T_{\tilde{z}w}\bar{D}_\tau\|_2^2 = \|\Delta\|_2^2 + \|T_{\tilde{z}w}\|_2^2.$$

This implies that the problem reduces to the standard finite-dimensional H_2 problem for the generalized plant $\tilde{G}$, which can be solved by Theorem 6.3. In fact, as the "zu" and "yw" parts of G and $\tilde{G}$ coincide, assumptions $\mathcal{A}_{5\text{-}8}$ hold for G iff they hold for $\tilde{G}$.

To see the structure of the equivalent problem, bring in the realizations

$$\hat{G}_{zw}(s) = \left[\begin{array}{c|c} A & e^{A\tau}B_w \\ \hline C_z & 0 \end{array}\right] \quad \text{and} \quad \tilde{G}_{yu}(s) = \left[\begin{array}{c|c} A & B_u \\ \hline C_y e^{-A\tau} & 0 \end{array}\right]$$

(by (3.39) and (3.42), respectively), so that

$$\tilde{G}(s) = \left[\begin{array}{c|cc} A & e^{A\tau}B_w & B_u \\ \hline C_z & 0 & D_{zw} \\ C_y e^{-A\tau} & D_{yw} & 0 \end{array}\right] = \left[\begin{array}{c|cc} A & B_w & e^{-A\tau}B_u \\ \hline C_z e^{A\tau} & 0 & D_{zw} \\ C_y & D_{yw} & 0 \end{array}\right]. \tag{6.15}$$

Because the realization of the "zu" part above is the same as that in G, the control ARE (6.5a) and the corresponding LQR gain K_u for $\tilde{G}$ are the same as those for G. The realization of the "yw" part of $\tilde{G}$ is similar to that of G, with the similarity matrix $e^{A\tau}$. As a result, the filtering ARE (6.5b) for $\tilde{G}$ is solved by $e^{A\tau}Y e^{A'\tau}$, where Y is the corresponding solution for G, with the Kalman filter gain $e^{A\tau}L_y$ for L_y defined in (6.6) for G. Therefore, applying the formulae of Theorem 6.3 to $\tilde{G}$ we end up with the controllers in Theorem 6.3.

The optimal cost is for the finite-dimensional problem for $\tilde{G}$ can be expressed as (cf. Remark 6.1)

$$\begin{aligned} \tilde{\gamma}_0 &= \text{tr}(B_w' e^{A'\tau} X e^{A\tau} B_w) + \text{tr}(D_{zu} K_u e^{A\tau} Y e^{A'\tau} K_u' D_{zu}') \\ &= \gamma_0 + \text{tr}\big(B_w'(e^{A'\tau} X e^{A\tau} - X)B_w\big) + \text{tr}\big(D_{zu} K_u(e^{A\tau} Y e^{A'\tau} - Y)K_u' D_{zu}'\big), \end{aligned}$$

where γ_0 is the optimal cost for G. Now, it can be verified that if W satisfies the equation $A'W + WA = V$ for some V, then

$$e^{A'\tau} W e^{A\tau} - W = \int_0^\tau e^{A't} V e^{At}\, dt.$$

Applying this expression to the AREs in (6.5), we have:

$$\begin{aligned} \tilde{\gamma}_0 &= \gamma_0 + \text{tr}\left(B_w' \int_0^\tau e^{A't}(K_u' D_{zu}' D_{zu} K_u - C_z' C_z)e^{At}\, dt\, B_w\right) \\ &\quad + \text{tr}\left(D_{zu} K_u \int_0^\tau e^{At}(L_y D_{yw} D_{yw}' L_y - B_w B_w')e^{A't}\, dt\, K_u' D_{zu}'\right) \\ &= \gamma_0 - \text{tr}\left(B_w' \int_0^\tau e^{A't} C_z' C_z e^{At}\, dt\, B_w\right) + \text{tr}\left(\int_0^\tau D_{zu} K_u e^{At} L_y D_{yw} D_{yw}' L_y e^{A't} K_u' D_{zu}'\, dt\right) \\ &= \gamma_0 - \|\Delta\|_2^2 + \gamma_{\text{DT}}(\tau), \end{aligned}$$

where $\gamma_{\text{DT}}(\tau)$ is defined by (6.13) and the expression for $\|\Delta\|_2^2$ follows by the second equality of (6.1). Thus, we end up with $\|T_{zw}\|_2^2 = \|\Delta\|_2^2 + \tilde{\gamma}_0 = \gamma_0 + \gamma_{\text{DT}}(\tau)$, exactly as in Theorem 6.3.

6.2.3 Design case study

Return to the problem studied in §6.1.2. Because $A = 0$ in this case, we have that $e^{A\tau} = 1$ for all τ and the central controller in Theorem 6.3 is the same as that in Theorem 6.1 and does not depend on the loop delay. Yet there is always a DTC block with the transfer function $\Pi(s) = (1 - e^{-\tau s})/s$ present, resulting in the overall controller

$$R(s) = \frac{s}{(\varrho s + 1)(\varsigma s + 1) - e^{-\tau s}},$$

whose static gain, $R(0) = 1/(\varrho + \varsigma + \tau)$, decreases as τ grows. The controller in this case is stable for all τ, which can be seen by the fact that the frequency-response gain of $1/((\varrho s + 1)(\varsigma s + 1))$ is strictly contractive for all positive frequencies. We already saw, in §3.2.1, that the use of the MSP dead-time compensator renders the control sensitivity the same as in the delay-free case and the complementary sensitivity—a delayed version of its delay-free counterpart. Thus, the magnitude plots in Figs. 6.3(b) and 6.3(c) remain unchanged and we can see the effect of the loop delay only via the disturbance sensitivity.

The plots in Fig. 6.6 present $|T_{\text{d}}(j\omega)|$ for various combinations of the weights ϱ and ς and for three loop delays, namely for $\tau \in \{0, 1, 2\}$. The case of $\varrho = 1$ and $\varsigma = 1$, which resulted in a cautious design with the

(a) $\varrho = 1$ and $\varsigma = 1$ (b) $\varrho = 1$ and $\varsigma = 0.05$ (c) $\varrho = 0.05$ and $\varsigma = 0.05$
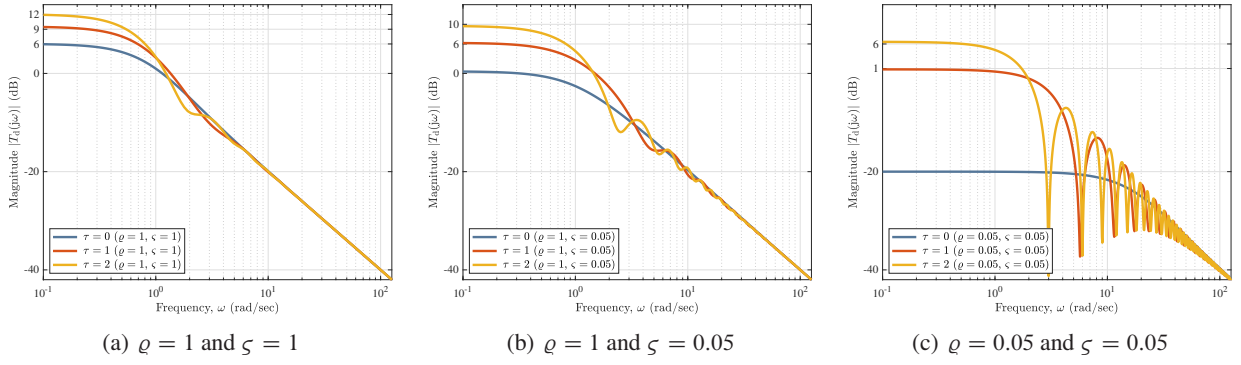
Fig. 6.6: Closed-loop disturbance sensitivity frequency-response plots

narrowest bandwidth and smallest static gain of the controller, is presented in Fig. 6.6(a). We can see that the increase of the loop delay increases $|T_d(j\omega)|$ for low frequencies, although this increase is relatively small. The effect of the loop delay becomes more visible as we decrease the weights. This is most visible in the plot in Fig. 6.6(c), which corresponds to the "aggressive" choice of $\varrho = 0.05$ and $\varsigma = 0.05$. The increase of the delay from zero to 1 increase the sensitivity to step load disturbances by a factor of 11, i.e. by more than 20 dB. These observations agree with the understanding that the effect of loop delays is more harmful for systems with higher loop gains and, consequently, higher crossovers.

6.2.4 Extensions to systems with multiple loop delays

It is not hard to imagine a situations where different input and output channels have different delays, cf. Remark 1.3 on p. 5. We already saw that several stabilization methods studied in Chapter 3 extend to systems with multiple delays seamlessly, see Remark 3.1 on p. 49 for example. It happens that this is not quite the case for performance-oriented methods. In this subsection we touch upon involved difficulties and possible workarounds.

Consider first the apparently simplest nontrivial extension of the single-delay setup in Fig. 6.1(b) to the multiple delay case. Namely, assume that there are two, possibly vector, control input channels, one of which is delay free and another one is delayed by $\tau > 0$. In other words, we assume that

$$u = \begin{bmatrix} u_0 \\ u_\tau \end{bmatrix} = \begin{bmatrix} u_0 \\ \bar{D}_\tau \bar{u}_\tau \end{bmatrix} = \begin{bmatrix} I & 0 \\ 0 & \bar{D}_\tau \end{bmatrix} Ry =: \bar{D}_{\{0,\tau\}} Ry.$$

Such a delay element is referred to[1] as the *input adobe delay* element. This situation corresponds to the setup in Fig. 6.7(a) or, equivalently, in Fig. 6.7(b). In principle, we can now shift the feedback loop in this system, similarly to what was done in Fig. 6.5(c). This step requires only minor alterations to the single-delay case:

$$G_{yu}\bar{D}_{\{0,\tau\}} = \begin{bmatrix} G_{yu,0} & G_{yu,\tau}\bar{D}_\tau \end{bmatrix} = \overbrace{\begin{bmatrix} G_{yu,0} & \tilde{G}_{yu,\tau} \end{bmatrix}}^{\tilde{G}_{yu}} + \overbrace{\begin{bmatrix} 0 & \sigma_\tau\{G_{yu,\tau}\bar{D}_\tau\} \end{bmatrix}}^{\Pi}$$

for the respective partitioning of G_{yu}. But this appears to be a dead end in general. The main obstacle is that the adobe delay element does not commute with G_{zu}, unless this system is block-diagonal. It is thus not clear how to pool the delay out of the generalized plant via the "z" channel, as done in the single-delay case in Fig. 6.5(e).

To gain insight into this issue, let us simplify the problem even more. Assume for the time being that

$$G_{zu} = \begin{bmatrix} G_{zu,0} & G_{zu,0\tau} \\ 0 & G_{zu,\tau} \end{bmatrix}, \tag{6.16}$$

---

[1] The term was coined in [38], where it was used as a building block (an adobe brick) in solving more general cases.

(a) Original problem   (b) Moving delay to G, $\bar{D}_{\{0,\tau\}}\tilde{u} = u$ (c) Swapping adobe delay with G_{zu}

(d) Pre-shifting the loop and decomposing G_{zw} (e) Final setup, $\tilde{y} = y + \Pi_y\tilde{u}$ and $\Psi_z\tilde{z} = z - \Delta w$
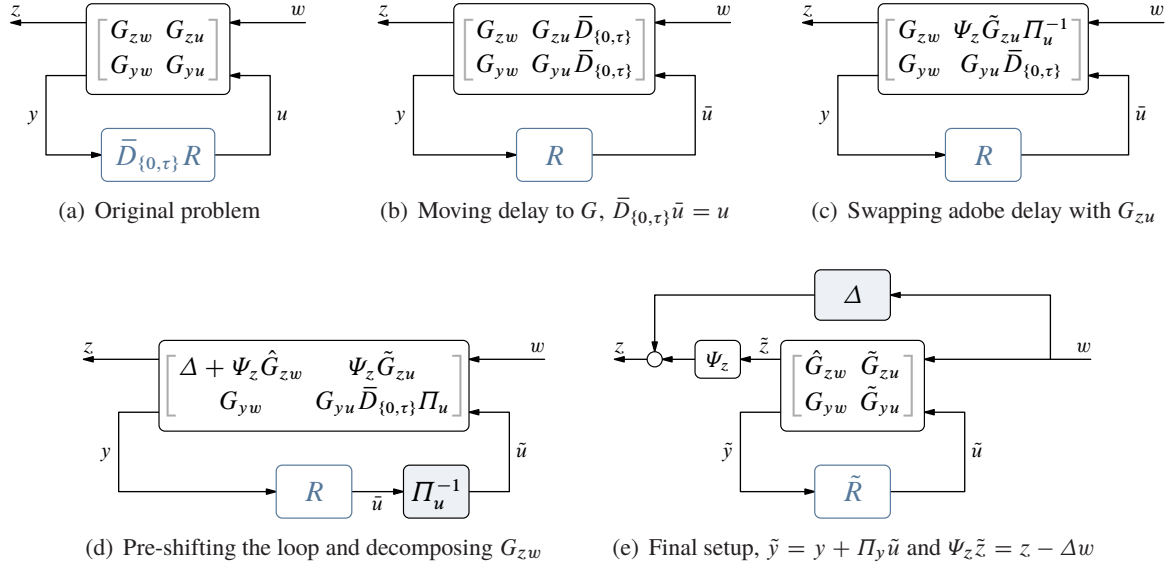
Fig. 6.7: H_2 loop shifting for input adobe delay, with $\tilde{R} = \Pi_u^{-1}R(I + \Pi_y R)^{-1}$

for a square and invertible $G_{zu,0}$, where the input partition is compatible with that in $\bar{D}_{\{0,\tau\}}$. Consider the signal

$$z_u := G_{zu}u = \begin{bmatrix} G_{zu,0} & G_{zu,0\tau}\bar{D}_\tau \\ 0 & G_{zu,\tau}\bar{D}_\tau \end{bmatrix}\begin{bmatrix} u_0 \\ \tilde{u}_\tau \end{bmatrix} = \begin{bmatrix} G_{zu,0}(u_0 + G_{zu,0}^{-1}G_{zu,0\tau}\bar{D}_\tau\tilde{u}_\tau) \\ \bar{D}_\tau G_{zu,\tau}\tilde{u}_\tau \end{bmatrix}$$

and split

$$G_{zu,0}^{-1}G_{zu,0\tau}\bar{D}_\tau = \tilde{G}_{\mathrm{a}} - \sigma_\tau\{G_{zu,0}^{-1}G_{zu,0\tau}\bar{D}_\tau\} =: \tilde{G}_{\mathrm{a}} - \Pi_{u,0\tau} \tag{6.17}$$

as in (3.43a). Denoting $\tilde{G}_{zu,0\tau} := G_{zu,0}\tilde{G}_{\mathrm{a}}$, which is finite dimensional, we end up with the relation

$$z_u = \begin{bmatrix} I & 0 \\ 0 & \bar{D}_\tau \end{bmatrix}\begin{bmatrix} G_{zu,0} & \tilde{G}_{zu,0\tau} \\ 0 & G_{zu,\tau} \end{bmatrix}\begin{bmatrix} I & -\Pi_{u,0\tau} \\ 0 & I \end{bmatrix}\begin{bmatrix} u_0 \\ \tilde{u}_\tau \end{bmatrix} =: \Psi_z\tilde{G}_{zu}\Pi_u^{-1}\tilde{u}. \tag{6.18}$$

The system Ψ_z is also an adobe delay element in this case, just with potentially different dimensions of the delayed block in it ($G_{zu,\tau}$ is not necessarily square). This yields the system in Fig. 6.7(c).

The rest is quite technical, albeit straightforward. Because Π_u is bi-stable, we can use it as a multiplier and shift to the controller side as shown in Fig. 6.7(d). Partitioning the output of G_{zw} according the the partition of Ψ_z and using the decomposition in (3.40a), we can write

$$\begin{bmatrix} G_{zw,0} \\ G_{zw,\tau} \end{bmatrix} = \begin{bmatrix} G_{zw,0} \\ \pi_\tau\{G_{zw,\tau}\} + \bar{D}_\tau\hat{G}_{zw,\tau} \end{bmatrix} = \begin{bmatrix} 0 \\ \pi_\tau\{G_{zw,\tau}\} \end{bmatrix} + \begin{bmatrix} I & 0 \\ 0 & \bar{D}_\tau \end{bmatrix}\begin{bmatrix} G_{zw,0} \\ \hat{G}_{zw,\tau} \end{bmatrix} =: \Delta + \Psi_z\hat{G}_{zw},$$

see the generalized plant in Fig. 6.7(d). The impulse response of this Δ still does not overlap that of $\Psi_z T$ for every causal T, so it can be handled by already familiar approaches.

It is thus only left to eliminate the infinite-dimensional part in the "G_{yu}" part of the generalized plant. To this end, note that

$$G_{yu}\bar{D}_{\{0,\tau\}}\Pi_u^{-1} = \begin{bmatrix} G_{yu,0} & G_{yu,\tau}\bar{D}_\tau - G_{yu,0}\Pi_{u,0\tau} \end{bmatrix} = \begin{bmatrix} G_{yu,0} & \bar{G}_{yu,0\tau}\bar{D}_\tau - G_{yu,0}\tilde{G}_{\mathrm{a}} \end{bmatrix},$$

where (6.17) is used to decompose $\Pi_{u,0\tau}$ and $\bar{G}_{yu,0\tau} := G_{yu,\tau} + G_{yu,0}G_{zu,0}^{-1}G_{zu,0\tau}$ is finite dimensional. Decomposing

$$\bar{G}_{yu,0\tau}\bar{D}_\tau = \tilde{G}_{yu,0\tau} - \sigma_\tau\{\bar{G}_{yu,0\tau}\bar{D}_\tau\} =: \tilde{G}_{yu,0\tau} - \Pi_{y,\tau},$$
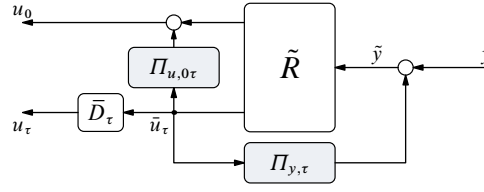
Fig. 6.8: Feedforward action Smith predictor (FASP)

we end up with

$$G_{yu}\bar{D}_{\{0,\tau\}}\Pi_u^{-1} = \begin{bmatrix} G_{yu,0} & \tilde{G}_{yu,0\tau} - G_{yu,0}\tilde{G}_{\mathrm{a}} \end{bmatrix} - \begin{bmatrix} 0 & \Pi_{y,\tau} \end{bmatrix} =: \tilde{G}_{yu} - \Pi_y \tag{6.19}$$

for a finite-dimensional $\tilde{G}_{yu}$, which is ready for applying the loop shifting from §3.4.1. Thus, the final setup is as shown in Fig. 6.7(e) with

$$\tilde{R} := \Pi_u^{-1}R(I + \Pi_y\Pi_u^{-1}R)^{-1} = \Pi_u^{-1}R(I + \Pi_y R)^{-1} \tag{6.20}$$

(because $\Pi_y\Pi_u^{-1} = \Pi_y$). Taking into account the orthogonality of Δ and $\bar{D}_\tau T_{\tilde{z}w}$, the H_2 problem again reduces to a finite-dimensional H_2 standard problem, which can be solved by Theorem 6.1.

Now return to the structure of G_{zu} assumed in (6.16). The structure itself is quite special and should not be expected to hold true in many applications. Nonetheless, the ideas presented above do extend to a general G_{zu} under the mild condition that the feedthrough term $G_{zu}(\infty)$ has full column rank. The most technically nontrivial part of the general solution is the factorization

$$G_{zu}\bar{D}_{\{0,\tau\}} = \Psi_z\tilde{G}_{zu}\Pi_u^{-1} \tag{6.21}$$

for a finite-dimensional $\tilde{G}_{zu}$, inner (i.e. stable and energy preserving) Ψ_z, and a bi-stable Π_u. In fact, this factorization results in $\tilde{G}_{zu}$ having the same "A" matrix as G_{zu} and in block upper triangular Π_u with static invertible diagonal elements. Moreover, it is then always possible to decompose $G_{zw} = \Delta + \Psi_z\hat{G}_{zw}$ with orthogonal Δ and $\Psi_z T_{\tilde{z}w}$ for all $T_{\tilde{z}w} \in H_2$ and a finite-dimensional $\hat{G}_{zw}$ having the same "A" matrix as G_{zw}. Details, which are rather technical, can be found in [46, §III-B]. The input adobe delay result extends then to the output adobe delay case, where there are delay-free and delayed measurements channels, and eventually to systems with general multiple input and output delays by running a recursion of adobe delay problems. In all these cases delayed H_2 problems reduce to equivalent delay-free H_2 problems. Details go beyond the scope of the notes though.

Remark 6.7 (FASP architecture). The controller structure induced by (6.20) is of a special interest. The mapping $R \mapsto \tilde{R}$ defined by that relation is bijective, with $R = \Pi_u\tilde{R}(I - \Pi_y\tilde{R})^{-1}$ for a finite-dimensional "primary controller" $\tilde{R}$ designed for a finite-dimensional H_2 problem. Taking into account the structure of the "Π" elements from (6.18) and (6.19), which is preserved in the case of a general G_{zu}, the controller above corresponds to the block-diagram in Fig. 6.8. It has a "conventional" DTC FIR element $\Pi_{y,\tau}$ as its internal feedback, although only from the delayed control channel. On top of that, there is also the "interchannel" DTC FIR element $\Pi_{u,0\tau}$, which, in a sense, compensates for the delay in the performance channel. This unorthodox structure is known as the FASP (*feedforward-action Smith predictor*).

Curiously, nothing similar to FASP has appeared in the classical literature, where DTC architectures are typically ad hoc. In fact, the question of a proper extension of the DTC architecture to systems with multiple delays was for long considered an open problem, because stabilization-induced structures produced rather poor feedback performance, see the discussion in the beginning of [24]. It was even suggested by Jerome and Ray in [24] that in many situations artificial delays should be added to channels with smaller delays to equalize loop delays, which is conceptually flawed. Only the advent of transparent solutions to optimal

control problems revealed the FASP architecture. This was done for the first time in [38], as a technical by-product of the H_∞ optimization procedure for systems with multiple loop delays. The arguments above are from [46] and are somewhat more transparent. ∇

It should be emphasized that the discrepancy between stability- and performance-induced DTC architectures discussed above shows up only in problems with multiple i/o delays. It is not unreasonable to expect that a similar discrepancy exists in more general multiple delay systems, like that discussed in Remark 3.1 on p. 49. But studies of such architectures are yet to be carried out.

6.3 H_∞ design for dead-time systems

Let us turn now to the H_∞ problem for the system in Fig. 6.1(b). We again impose the same delay-free assumptions on the generalized plant G, i.e. suppose that $\mathcal{A}_{5\text{-}8}$ hold. To simplify the formulae, we also assume throughout this section that $D_{zw} = 0$, so that the formulae of Remark 6.3 on p. 101 can be used.

6.3.1 Extraction of γ-suboptimal dead-time controllers

The logic here follows that in §6.2.1, just this time we use Theorem 6.2 as the starting point. The generator of all suboptimal controllers in Theorem 6.2 satisfies the assumptions of Lemma 3.5 too, so all Q's rendering $\mathcal{F}_l(J_\infty, Q)$ a dead-time system for a given τ must be of the form $Q = \pi_\tau\{H_{\infty,22}\} + \tilde{Q}\bar{D}_\tau$, where $H_\infty := J_\infty^{-1}$ with

$$
\begin{bmatrix} H_{\infty,11}(s) & H_{\infty,12}(s) \\ H_{\infty,21}(s) & H_{\infty,22}(s) \end{bmatrix} = \left[\begin{array}{c|cc} A + B_w K_w - \gamma^{-2} Z_\gamma Y (X B_u + C_z' D_{zu}) K_u & Z_\gamma (B_u + L_z D_{zu}) & -Z_\gamma L_y \\ C_y + D_{yw} K_w & D_{yu} & I \\ -K_u & I & 0 \end{array} \right],
$$

for some stable and causal $\tilde{Q}$, i.e. such that its transfer function $\tilde{Q} \in H_\infty$. Thus, the H_∞ optimization problem reduces to the problem of finding whether a $\tilde{Q} \in H_\infty$ exists such hat $\|Q_0 + Q_\tau \bar{D}_\tau\|_\infty < \gamma$, where

$$
Q_0 := D_{zu}\pi_\tau\{H_{\infty,22}\}D_{yw} \quad \text{and} \quad Q_\tau := D_{zu}\tilde{Q}D_{yw}.
$$

Although this problem looks similar to the corresponding problem in the H_2 case, the elegant H_2 projection reasonings do not apply here. H_∞ is not a Hilbert space, so there is no orthogonality notion on it. As such, the separation of the norms of Q_0 and Q_τ exploited in the H_2 case does no longer hold. In fact, zeroing $\tilde{Q}$, similarly to the optimal strategy for the H_2 case, is not the right course of action in general. This is illustrated by the following simple example:

Example 6.1. Let
$$
Q_0(s) = \pi_\tau\left\{\frac{1}{s}\right\} = \frac{1 - e^{-\tau s}}{s}
$$

and consider the problem of minimizing $\|Q_0 + Q_\tau \bar{D}_\tau\|_\infty$ by a causal Q_τ. First, in an attempt to imitate the H_2 solution, choose $Q_\tau = 0$. With this choice the attained norm is

$$
\|Q_0\|_\infty = \sup_{\omega \in \mathbb{R}} \frac{|1 - e^{-j\tau\omega}|}{\omega} = \left.\frac{|1 - e^{-j\tau\omega}|}{\omega}\right|_{\omega=0} = \tau.
$$

Choose now
$$
Q_\tau(s) = \frac{1}{s} - \frac{(2\tau)^2 s^2 + \pi^2}{\pi s(2\tau s + \pi e^{-\tau s})}
$$

(an educated guess). This is an H_∞ function. Indeed, it is clearly proper, so bounded on $\mathbb{C}_\alpha$ for a sufficiently large α. Its singularities are at the origin and roots of the quasi-polynomial $p(s) = 2\tau s + \pi e^{-\tau s}$. The singularity at $s = 0$ is removable, because

$$\lim_{s \to 0} Q_\tau(s) = \lim_{s \to 0} \frac{\pi(2\tau s + \pi e^{-\tau s}) - (2\tau)^2 s^2 + \pi^2}{\pi s(2\tau s + \pi e^{-\tau s})} = -\frac{\pi - 2}{\pi}\tau.$$

Roots of $p(s)$ can be analyzed via the Nyquist criterion for $\pi e^{-\tau s}/(2\tau s)$. Its crossover frequency is $\omega_c = \pi/(2\tau)$ and its phase at this frequency is

$$\arg \frac{\pi}{j2\tau\omega_c} e^{-j\tau\omega_c} = -\frac{\pi}{2} - \tau\omega_c = -\pi.$$

This implies that the quasi-polynomial $p(s)$ has all its roots in the left-half plane $\mathbb{C} \setminus \bar{\mathbb{C}}_0$ except the pair at $\pm j\omega_c$. But at those roots we have that

$$\lim_{s \to \pm j\omega_c} Q_\tau(s) = \lim_{s \to \pm j\omega_c} \frac{\pi(2\tau s + \pi e^{-\tau s}) - (2\tau)^2 s^2 + \pi^2}{\pi s(2\tau s + \pi e^{-\tau s})} = \frac{-16 \pm j\, 2(\pi - 2)^2}{\pi(\pi^2 + 4)}\tau,$$

i.e. these singularities are also removable.

Now,

$$Q_0(s) + Q_\tau(s)e^{-\tau s} = \frac{2\tau}{\pi} \frac{\pi - 2\tau s e^{-\tau s}}{2\tau s + \pi e^{-\tau s}} = \frac{2\tau}{\pi}e^{-\tau s}\frac{p(-s)}{p(s)}.$$

We already know that this is an H_∞ function, so

$$\|Q_0 + Q_\tau \bar{D}_\tau\|_\infty = \sup_{\omega \in \mathbb{R}} \frac{2\tau}{\pi}|e^{-j\tau\omega}|\frac{|p(-j\omega)|}{|p(j\omega)|} = \frac{2}{\pi}\tau < \tau = \|Q_0\|_\infty.$$

Thus, it is possible to improve the $\|Q_0\|_\infty$ bound by at least a factor of $\pi/2 \approx 1.57$ in this case by an appropriate choice of Q_τ, even though the impulse responses of Q_0 and $Q_\tau \bar{D}_\tau$ do not overlap. $\triangledown$

The problem of finding functions $Q_\tau \in H_\infty$ such that $\|Q_0 + Q_\tau \bar{D}_\tau\|_\infty < \gamma$ is known as the Nehari extension problem, named after Zeev Nehari. It is known that this problem is solvable iff the Hankel norm of $Q_0' \bar{D}_\tau$ is smaller than γ, where Q_0' is the adjoint operator, on $L_2(\mathbb{R})$, of Q_0, i.e. the system whose impulse response is $[q_0(-t)]'$, and the Hankel norm is the induced norm as an operator $L_2(\mathbb{R}_-) \to L_2(\mathbb{R}_+)$.

The following result from [42], presented here without proof, gives a verifiable solvability condition for the required Hankel norm to be smaller than γ and parametrizes all solutions to the problem.

Lemma 6.4 (Nehari problem for delayed systems). *Let*

$$G_0(s) = \left[\begin{array}{c|c} A_0 & B_0 \\ \hline C_0 & 0 \end{array}\right].$$

There is $Q_\tau \in H_\infty$ such that $\|\pi_\tau\{G_0\} + Q_\tau \bar{D}_\tau\|_\infty < \gamma$ iff $\det \Sigma_{22}(t) \neq 0$ for all $t \in [0, \tau]$, where

$$\begin{bmatrix} \Sigma_{0,11}(t) & \Sigma_{0,12}(t) \\ \Sigma_{0,21}(t) & \Sigma_{0,22}(t) \end{bmatrix} := \exp\left(\begin{bmatrix} A_0 & B_0 B_0' \\ -\gamma^{-2}C_0'C_0 & -A_0' \end{bmatrix} t\right).$$

If this condition holds, then all solutions of the problem can be presented in the form

$$\pi_\tau\{G_0\} + Q_\tau \bar{D}_\tau = \left(\Phi_{12} + (\Phi_{11} - \bar{D}_\tau I)Q_{NEP}\right)(I + \Phi_{22} + \Phi_{21}Q_{NEP})^{-1},$$

where

$$
\begin{bmatrix} \Phi_{11}(s) & \Phi_{12}(s) \\ \Phi_{21}(s) & \Phi_{22}(s) \end{bmatrix} = \pi_\tau \left\{ \left[\begin{array}{cc|cc} A_0 & B_0 B_0' & 0 & B_0 \\ -\gamma^{-2}C_0'C_0 & -A_0' & -\gamma^{-2}\Sigma_{0,22}^{-1}(\tau)C_0' & -\Sigma_{0,22}^{-1}(\tau)\Sigma_{0,21}(\tau)B_0 \\ \hline C_0 & 0 & 0 & 0 \\ 0 & B_0' & 0 & 0 \end{array} \right] \right\}
$$

and $Q_{NEP} \in H_\infty$ is such that $\|Q_{NEP}\|_\infty < \gamma$ but otherwise arbitrary.

Example 6.2. Return to the problem studies in Example 6.1, in which $G_0(s) = 1/s$. For this system

$$
\begin{bmatrix} \Sigma_{0,11}(t) & \Sigma_{0,12}(t) \\ \Sigma_{0,21}(t) & \Sigma_{0,22}(t) \end{bmatrix} := \exp\left(\begin{bmatrix} 0 & 1 \\ -\gamma^{-2} & 0 \end{bmatrix} t \right) = \begin{bmatrix} \cos(t/\gamma) & \gamma\sin(t/\gamma) \\ -\gamma^{-1}\sin(t/\gamma) & \cos(t/\gamma) \end{bmatrix},
$$

so that the problem is solvable iff $\gamma > 2\tau/\pi$. This is exactly what the choice of Q_τ in Example 6.1 attains. The "central" Q_τ, the one obtained by setting $Q_{NEP} = 0$, attains

$$
Q(s) = \frac{\cos(\tau/\gamma)s - \gamma^{-1}\sin(\tau/\gamma) - (\cos(2\tau/\gamma)s - \gamma^{-1}\sin(2\tau/\gamma))e^{-\tau s}}{(\cos(\tau/\gamma)s - \gamma^{-1}\sin(\tau/\gamma))s + (\gamma^{-1}\sin(2\tau/\gamma)s + \cos(2\tau/\gamma))e^{-\tau s}} \xrightarrow{\gamma \to 2\tau/\pi} \frac{2\tau}{\pi}\frac{\pi - 2\tau s e^{-\tau s}}{2\tau s + \pi e^{-\tau s}},
$$

which leads to

$$
Q_\tau(s) = \left(\frac{2\tau}{\pi}\frac{\pi - 2\tau s e^{-\tau s}}{2\tau s + \pi e^{-\tau s}} - \frac{1}{s} + \frac{e^{-\tau s}}{s} \right)e^{\tau s} = \frac{1}{s} - \frac{(2\tau)^2 s^2 + \pi^2}{\pi s(2\tau s + \pi e^{-\tau s})}
$$

exactly as that in Example 6.1. Thus, the "educated guess" there was actually the optimal solution.   ▽

The result of Lemma 6.4 is instrumental in the solution to the standard H_∞ problem for the system in Fig. 6.1(b). To formulate this solution, define the matrix functions

$$
\Sigma(t) := \exp\left(\begin{bmatrix} A & B_w B_w' \\ -\gamma^{-2}C_z'C_z & -A' \end{bmatrix} t \right).
$$

and the matrices

$$
B_\tau := \begin{bmatrix} Y & I \end{bmatrix} \Sigma'(\tau) \begin{bmatrix} \gamma^{-2}C_z'D_{zu} \\ B_u \end{bmatrix} \quad \text{and} \quad C_\tau := \begin{bmatrix} -D_{yw}B_w' & C_y \end{bmatrix} \Sigma(\tau)' \begin{bmatrix} -\gamma^{-2}X \\ I \end{bmatrix}.
$$

The result below if the counterpart of Theorem 6.2 for dead-time systems:

Theorem 6.5. *If $\mathcal{A}_{5-8}$ hold true and $D_{zw} = 0$, then the standard H_∞ problem is solvable iff the following conditions hold:*

(a) *there is a stabilizing solution X to ARE (6.9a) such that $X = X' \geq 0$,*

(b) *there is a stabilizing solution Y to ARE (6.9b) such that $Y = Y' \geq 0$,*

(c) *$Z_\gamma(t)$ is well defined for all $t \in [0, \tau]$, where*

$$
Z_\gamma(t) := \left(\begin{bmatrix} Y & I \end{bmatrix} \Sigma'(t) \begin{bmatrix} -\gamma^{-2}X \\ I \end{bmatrix} \right)^{-1}
$$

In such a case, all γ-suboptimal controllers are given as the system in Fig. 6.9, where

$$
J_{\infty,\tau}(s) = \left[\begin{array}{c|cc} A + B_w K_w + B_u K_u + Z_\gamma(\tau)L_yC_\tau & -Z_\gamma(\tau)L_y & Z_\gamma(\tau)B_\tau \\ \hline K_u & 0 & I \\ -C_\tau & I & 0 \end{array} \right] \tag{6.22}
$$
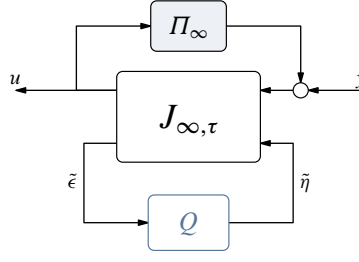
Fig. 6.9: All H_∞ suboptimal controllers for the standard problem in Fig. 6.1(b)

and

$$\Pi_\infty(s) = \sigma_\tau\{\mathcal{F}_u(G(s), \gamma^{-2}[G_{zw}(-s)]')e^{-\tau s}\} = \sigma_\tau\left\{\left[\begin{array}{cc|c} A & B_w B_w' & B_u \\ -\gamma^{-2}C_z'C_z & -A' & -\gamma^{-2}C_z'D_{zu} \\ \hline C_y & D_{yw}B_w' & D_{yu} \end{array}\right]e^{-\tau s}\right\} \quad (6.23)$$

for any $Q \in H_\infty$ such that $\|D_{zu}QD_{yw}\|_\infty < \gamma$.

Proof. Follows by plugging the conditions and the parametrization of Lemma 6.4 to the parametrization of Theorem 6.2. Technical details are quite involved and can be found in [42]. □

Some remarks are in order:

Remark 6.8 (H_∞ cost of delay). It is readily seen that $Z_\gamma(0)$ in Theorem 6.5 equals $Z_\gamma = (I - \gamma^{-2}YX)^{-1}$ from Theorem 6.2. This implies that the solvability conditions for the dead-time H_∞ problem cover those of its delay-free counterpart, which is expectable. The addition is expressed in Theorem 6.5 in terms of the matrix function $Z_\tau(t)$. Equivalently, it can be shown that the delay problem is solvable iff the delay-free problem is solvable and, in addition, the solution to the differential Riccati equation

$$\dot{P}_X(t) = P_X(t)A + A'P_X(t) + C_z'C_z + \gamma^{-2}P_X(t)B_w B_w'P_X(t) = 0, \quad P_X(0) = X$$

exists $\forall t \in [0, \tau]$ and is such that $\rho(YP_X(\tau)) < \gamma^2$. Yet another version is that the solution to the differential Riccati equation

$$\dot{P}_Y(t) = P_Y(t)A + A'P_Y(t) + B_w B_w' + \gamma^{-2}P_Y(t)C_z'C_z P_Y(t) = 0, \quad P_Y(0) = Y$$

exists $\forall t \in [0, \tau]$ and is such that $\rho(P_Y(0)X) < \gamma^2$. Moreover, both $P_X(t)$ and $P_Y(t)$ are non-decreasing functions of t, in the sense that $\dot{P}_X(t) \geq 0$ and $\dot{P}_Y(t) \geq 0$ for all $t \geq 0$. Normally, the performance level attainable in the delay-free case is attainable for no $\tau > 0$. But there might be situations, and not only those in which the delay-free suboptimal controller $R = 0$, in which the addition of a finite delay does not harm the attainable performance. ▽

Remark 6.9 (sampled-data vs. delayed feedback). An interesting observation is that the solvability conditions for the dead-time H_∞ problem discussed in Remark 6.8 coincide with the solvability conditions for the sampled-data H_∞ problem for the same generalized plant, see [44, §V.B]. In other words, the cost of delay equals the cost of sampling in the H_∞ case if the sampling period coincides with the loop delay, which is different from the H_2 case. This fact is somewhat surprising, because causality constraints imposed on the controller by sampling are less restrictive than those imposed by the delay. Nonetheless, the disturbance is capable to "outsmart" the controller, which acts in open loop during each intersample interval, in this situation. ▽

Remark 6.10 (controller structure). The H_∞ suboptimal controllers in Fig. 6.9 are dead-time compensator, again. Yet the DTC block Π_∞ given by (6.23) is quite different from the modifies Smith predictor (unless $G_{zw} = 0$ or $\gamma = \infty$). It is intriguing to understand the rationale behind this structure. To this end, write

$$\mathcal{F}_{\mathrm{u}}(G, \gamma^{-2}G'_{zw}) = G_{yu} + G_{yw}(\gamma^2 I - G'_{zw}G_{zw})^{-1}G'_{zw}G_{zu},$$

where G'_{zw} denotes the adjoint operator over $L_2(\mathbb{R})$. Thus, the relation $y = \mathcal{F}_{\mathrm{u}}(G, \gamma^{-2}G'_{zw})u$ can be presented in the form

$$y = G_{yw}w_\star + G_{yu}u,$$

where the exogenous input is generated as

$$w_\star = (\gamma^2 I - G'_{zw}G_{zw})^{-1}G'_{zw}G_{zu}u \iff w_\star = \gamma^{-2}G'_{zw}(G_{zw}w_\star + G_{zu}u) = \gamma^{-2}G'_{zw}z.$$

It can be shown that this signal is the worst-case disturbance in the open-loop setting, viz. the signal that maximizes $\|z\|_2^2 - \gamma^2\|w\|_2^2$ for any given u. Thus, the H_∞ DTC element compensates the loop delay under the worst-case open-loop scenario. The rationale behind this is well founded. Indeed, the whole H_∞ design methodology is effectively a game where u plays against w, trying to minimize $\|z\|_2^2 - \gamma^2\|w\|_2^2$. But the effect of the control signal on z delays with respect to that of w, so in the "prediction" part we can only act in open loop. The DTC form of the H_∞ controller was first recognized by Meinsma and Zwart in [39] for the mixed-sensitivity problem and then derived, and interpreted, for the general case in [42].   ▽

6.3.2   Loop shifting approach

The loop-shifting procedure of Fig. 6.5 is not quite helpful in the H_∞ case, just because systems with non-overlapping impulse responses can still alter the effect of each other, cf. Example 6.1. But there is one special case where the procedure can still be used in the H_∞ context. This is the case where $G_{zw} = 0$, for which we can take $\Delta = 0$ and end up with the relation $\mathcal{F}_{\mathrm{l}}(G, R\bar{D}_\tau) = \mathcal{F}_{\mathrm{l}}(\tilde{G}, \tilde{R})\bar{D}_\tau$. Because the delay does not affect the magnitude of the frequency response, we have that

$$\|\mathcal{F}_{\mathrm{l}}(G, R\bar{D}_\tau)\|_\infty = \|\mathcal{F}_{\mathrm{l}}(\tilde{G}, \tilde{R})\|_\infty,$$

which implies that the problem reduces to a finite-dimensional H_∞ problem for $\tilde{G}$ given by (6.15) and the DTC element is the standard MSP, like that in the H_2 case.

H_∞ problems with $G_{zw} = 0$ are actually important. Several robust stability problems fall into this category. For example, consider a plant P, described as $P = P_0(I + W_2\Delta_{\mathrm{IM}}W_1)$ for known nominal plant P_0 and weights $W_1, W_2 \in RH_\infty$ and an uncertain element Δ_{IM}, of which we only know that $\Delta_{\mathrm{IM}} \in H_\infty$ and $\|\Delta_{\mathrm{IM}}\|_\infty \leq \alpha$ for some $\alpha > 0$ known as the *uncertainty radius*. This is the so-called *input multiplicative* modeling uncertainty model. It follows from small-gain arguments that a controller R robustly stabilizes this plant, i.e. stabilizes all P of this form, iff $\|\mathcal{F}_{\mathrm{l}}(G, R)\|_\infty < 1/\alpha$, where the generalized plant

$$G = \begin{bmatrix} 0 & W_1 \\ P_0W_2 & P_0 \end{bmatrix}$$

has a zero "G_{zw}" part. Likewise, the generalized plants for the *output multiplicative* uncertainty model $P = (I + W_2\Delta_{\mathrm{OM}}W_1)P_0$ and for the *additive* uncertainty model $P = P_0 + W_2\Delta_{\mathrm{AD}}W_1$ are

$$G = \begin{bmatrix} 0 & W_1P_0 \\ W_2 & P_0 \end{bmatrix} \quad \text{and} \quad G = \begin{bmatrix} 0 & W_1 \\ W_2 & P_0 \end{bmatrix},$$

respectively, and both have zero "G_{zw}" parts.

A consequence of this is that the MSP is actually a part of the optimal robust controller, i.e. the controller stabilizing P under the maximum uncertainty radius. This might sound surprising, taking into account that the dead-time compensation procedure is intrinsically open loop. Moreover, if P_0 is stable, then we can always choose $\Pi = P_0(1 - \bar{D}_\tau)$ in the loop-shifting procedure in Fig. 6.5, resulting in the classical Smith predictor as the optimal controller. With this choice, $\tilde{G}_{yu} = G_{yu} = P_0$ and we conclude that the Smith controller has the very same robustness level for a dead-time plant as its primary controller has for the delay-free version of the plant, with respect to either multiplicative or additive uncertainty (in fact, even with respect to some classes of structural uncertainty). This conclusion is not that obvious.

Chapter 7

Implementation of DTC-based Controllers

$\mathbf{W}$E SAW IN PREVIOUS CHAPTERS that dead-time compensation (DTC) architectures are intrinsic to stabilization and optimal control problems for time-delay systems. In the heart of these architectures are DTC elements, which are normally infinite-dimensional FIR systems of the form

$$\Pi(s) = \sigma_\tau \left\{ \left[\begin{array}{c|c} A & B \\ \hline C & D \end{array} \right] e^{-\tau s} \right\} = \left[\begin{array}{c|c} A & e^{-A\tau}B \\ \hline C & 0 \end{array} \right] - \left[\begin{array}{c|c} A & B \\ \hline C & D \end{array} \right] e^{-\tau s} = \left[\begin{array}{c|cc} A & e^{-A\tau}B & -B \\ \hline C & 0 & -D \end{array} \right] \left[\begin{array}{c} I \\ e^{-\tau s}I \end{array} \right] \quad (7.1a)$$

$$= C \int_0^\tau e^{-(sI-A)t} \, dt \, e^{-A\tau}B - De^{-\tau s} \quad (7.1b)$$

(cf. (3.43) on p. 63). Such elements are only parts of overall controllers, like those presented in Fig. 3.10 on p. 64 or Fig. 6.8 on p. 111. However, their delayed parts do not blend easily with finite-dimensional primary controllers and their finite-dimensional parts, like $C(sI - A)^{-1}e^{-A\tau}B$ above, cannot be separated from Π for DTC elements must be stable themselves. For these reasons, DTC elements are implemented separately from primary controllers, as FIR systems. This chapter discusses related implementation issues.

7.1 General observations

The last equality in (7.1a) suggests that $\Pi : u \mapsto y_\Pi$ can be implemented as the following dynamics:

$$\begin{cases} \dot{x}_\Pi(t) = Ax_\Pi(t) + e^{-A\tau}Bu(t) - Bu(t - \tau) \\ y_\Pi(t) = Cx_\Pi(t) + Du(t - \tau) \end{cases} \quad (7.2)$$

The only infinite-dimensional element required for this implementation is a buffer to realize the delay line for having access to the past u, which is a relatively simple element. However, this implementation does not always work, as can be seen in the example below.

Example 7.1. Consider the system presented in Fig. 7.1, which is an implementation of controller (3.22)
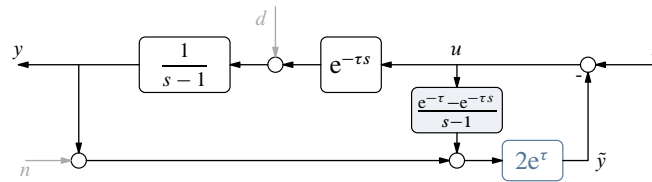

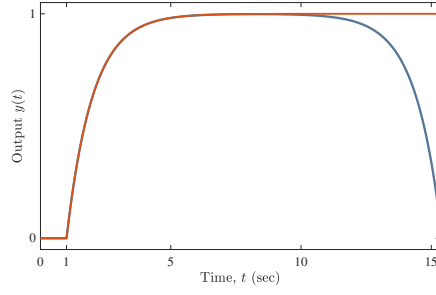Fig. 7.1: Benchmark system for DTC implementation

Fig. 7.2: DTC element in Fig. 7.1 implemented via (7.2), solid line

on p. 50 for the plant with $A = 1$ and $B = 1$ and for $K = -2$. It should result in the closed-loop system $T_{yr} : r \mapsto y$ with the transfer function

$$T_{yr}(s) = \frac{e^{-\tau s}}{s + 1},$$

which is readily verifiable. The expected response of the closed-loop system to the unit-step $r(t) = \mathbb{1}(t)$ is $y(t) = (1 - e^{\tau - t})\mathbb{1}(t - \tau)$, which is presented in Fig. 7.2 by the red line. Yet implementing the DTC part of the controller according to (7.2) leads to an unstable closed-loop response, as shown by the cyan-blue line in Fig. 7.2. The simulations producing this are carried out in Simulink with the variable-step ode45 solver under a maximal step size of 0.0001, which should be small enough for this closed-loop time constant (and the results do not improve under smaller steps).   ▽

The results of Example 7.1 can be understood by noticing that the representation of Π via (7.1a) actually cancels all modes of A. If A is not Hurwitz, as in Example 7.1, these *cancellations are unstable*. As a result, inaccuracies in performing those cancellations, say due to roundoff errors, might be disastrous. Indeed, the output of Π in this case is not y_Π generated by (7.2), but rather $\tilde{y}_\Pi$ generated by

$$\begin{cases} \dot{x}_\Pi(t) = A x_\Pi(t) + e^{-A\tau} B u(t) - B u(t - \tau) + \epsilon_{\text{roff}}(t) \\ \tilde{y}_\Pi(t) = C x_\Pi(t) + D u(t - \tau) \end{cases} \tag{7.3}$$

where ϵ_{roff} represents roundoff errors in solving the differential equation for x_Π (accounting for errors in the second equation is not quite important here). Assuming zero initial conditions, $(x_\Pi(0), \check{u}_0) = 0$,

$$\tilde{y}_\Pi(t) = C \int_0^t e^{A(t-s)} \big(e^{-A\tau} B u(s) - B u(s - \tau) + \epsilon_{\text{roff}}(s)\big) ds + D u(t - \tau)$$

$$= \left(C \int_{t-\tau}^t e^{A(t-s-\tau)} B u(s) ds + D u(t - \tau) \right) + C \int_0^t e^{A(t-s)} \epsilon_{\text{roff}}(s) ds =: y_\Pi(t) + \epsilon_\Pi(t) \tag{7.4}$$

for all $t \geq 0$. The error signal ϵ_Π is the response of a system with the transfer function $C(sI - A)^{-1}$ to ϵ_{roff}. If the matrix A is not Hurwitz, which is what we have in Example 7.1, this response diverges and we end up with the unstable behavior like that in Fig. 7.2.

7.2   Implementation via reset mechanism

An elegant workaround for handling unstable cancellations in (7.2) was proposed by Tam and Moore in [73] in the context of fixed-lag smoothing, which also involves an analog FIR part. The idea is to reset dynamics (7.2) periodically to avoid the error signal ϵ_Π in (7.4) to grow up unbounded. A mechanical reset (7.2) would obviously result in a different response from that of Π. But because Π is FIR, i.e. has a finite memory, such deviations would last only for τ time units after the reset. This fact can be exploited

by introducing two clones of Π, which run in parallel and reset at odd and even multiples of the delay τ, respectively. In this scheme, while the first system generates the signal y_Π, the second one accumulates right initial conditions. After τ time units the second system is ready to generate the correct y_Π, so at this point the first system is reset and the roles are interchanged.

To be specific, consider (7.3) and assume that its state $(x_\Pi(t), \breve{u}_t)$ is reset to zero at $t = t_c$. In this case

$$
\begin{aligned}
x_\Pi(t) &= \int_{t_c}^t e^{A(t-s)} \big(e^{-A\tau} Bu(s) - Bu(s-\tau)\mathbb{1}(s - t_c - \tau) + \epsilon_{\text{roff}}(s) \big) \, ds \\
&= \int_{t_c}^t e^{A(t-s-\tau)} Bu(s)\,ds - \int_{\min\{t_c+\tau,t\}}^t e^{A(t-s)} Bu(s-\tau)\,ds + \int_{t_c}^t e^{A(t-s)}\epsilon_{\text{roff}}(s)\,ds \\
&= \int_{t_c}^t e^{A(t-s-\tau)} Bu(s)\,ds - \int_{\min\{t_c,t-\tau\}}^{t-\tau} e^{A(t-s-\tau)} Bu(s)\,ds + \int_{t_c}^t e^{A(t-s)}\epsilon_{\text{roff}}(s)\,ds \\
&= \int_{t-\tau}^t e^{A(t-s-\tau)} Bu(s)\,ds - \int_{\min\{t_c,t-\tau\}}^{t_c} e^{A(t-s-\tau)} Bu(s)\,ds + \int_{t_c}^t e^{A(t-s)}\epsilon_{\text{roff}}(s)\,ds
\end{aligned}
$$

for all $t \geq t_c$. Thus, $\tilde{y}_\Pi(t) = y_\Pi(t) + y_\delta(t) + \epsilon_\Pi(t)$, where the error caused by (potentially wrong) zero initial conditions,

$$
y_\delta(t) := -C \int_{\min\{t_c,t-\tau\}}^{t_c} e^{A(t-s-\tau)} Bu(s)\,ds,
$$

vanishes after $t = t_c + \tau$, when the system forgets all wrong initial conditions. The term ϵ_Π due to roundoff errors still tends to diverge under non-Hurwitz A, but if the system resets every T time units, then it remains uniformly bounded. In fact, in this case [12, Sec. II.6]

$$
\|\epsilon_\Pi\|_\infty \leq \int_0^T \|Ce^{At}\|_\infty \, dt \, \|\epsilon_{\text{roff}}\|_\infty, \tag{7.5}
$$

where the ∞-norm of a matrix / vector M is $\|M\|_\infty := \max_i \sum_j |M_{ij}|$ and the $L_\infty(\mathbb{R}_+)$-norm of a signal ξ is $\|\xi\|_\infty := \sup_{t\in\mathbb{R}_+} \|\xi(t)\|_\infty$.

Thus, the implementation of $\Pi : u \mapsto y_\Pi$ by the time-varying dynamics

$$
\begin{cases}
\dot{x}_1(t) = Ax_1(t) + e^{-A\tau} Bu(t) - \varsigma_t Bu(t-\tau), & x_1(0) = x_1((2k+1)\tau) = 0 \\
\dot{x}_2(t) = Ax_2(t) + e^{-A\tau} Bu(t) - (1-\varsigma_t)Bu(t-\tau), & x_2(2k\tau) = 0 \\
y_\Pi(t) = \varsigma_t Cx_1(t) + (1-\varsigma_t)Cx_2(t) + Du(t-\tau)
\end{cases} \tag{7.6a}
$$

for all $k \in \mathbb{Z}_+$ and the switching function

$$
\varsigma_t = \begin{cases}
1 & \text{if } t \in [2k\tau, (2k+1)\tau) \\
0 & \text{if } t \in [(2k+1)\tau, (2k+2)\tau)
\end{cases} \tag{7.6b}
$$

results in a stable system, in the sense that the error ϵ_Π caused by roundoff errors is uniformly bounded by (7.5), with $T = 2\tau$ (provided the roundoff errors are the same for each clone). The implementation of equations (7.6) is straightforward, with relatively low computational expenses and standard tools applicable.

At the same time, there is not much we can do to improve the accuracy of the method. It is always a matter of how large 2τ vis-à-vis unstable modes of A. In principle, it is possible to implement more than two clones of (7.2) in parallel, with a round-robin scheduling. But even in this case the run time of each clone between resets is lower-bounded by τ, which is the time required to accumulate the right initial condition. Thus, if there are $\nu \in \mathbb{N} \setminus \{1\}$ clones, the horizon in the error bound in (7.5) decreases only to $T = \tau\nu/(\nu-1) > \tau$, which might still be insufficient if the delay is too large.
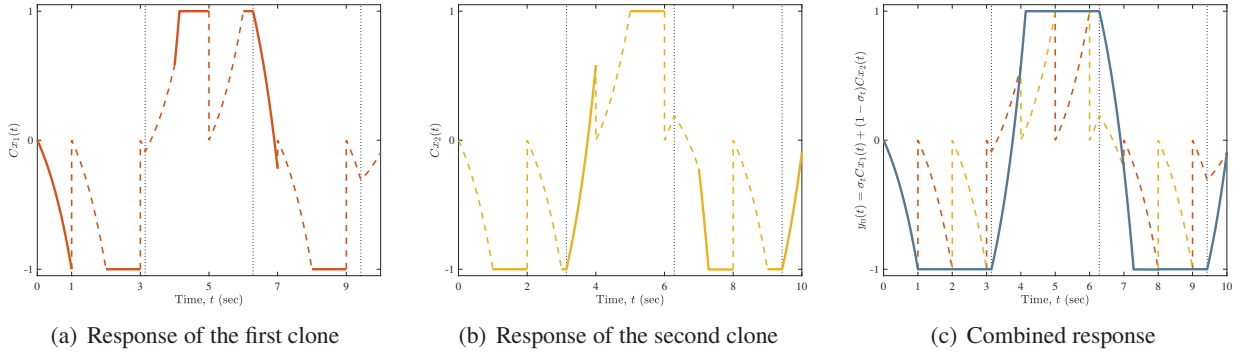
(a) Response of the first clone   (b) Response of the second clone   (c) Combined response

Fig. 7.3: Response of Π implemented by (7.6) to a square wave of period 2π and amplitude $\mathrm{e}/(\mathrm{e}-1)$

Example 7.2. Return to the problem studied in Example 7.1 and consider its DTC element, whose transfer function

$$\Pi(s) = \frac{\mathrm{e}^{-\tau} - \mathrm{e}^{-\tau s}}{s - 1}$$

and the static gain $\Pi(0) = 1 - \mathrm{e}^{-\tau}$. Fig. 7.3 presents the response of this Π to a square wave with the frequency 2π [sec] and the amplitude $1/\Pi(0) = \mathrm{e}^{\tau}/(\mathrm{e}^{\tau}-1)$ under $\tau = 1$. The responses of each one of two clones to the same input are depicted in Figs. 7.3(a) and 7.3(b). The dashed lines there represent intervals, where proper initial conditions are accumulated after each reset and solid lines represent intervals in which the corresponding output is used as the actual y_{Π}. They then combine into the solid line in Fig. 7.3(c), which is bounded and virtually coincides in this case with the expected response. The response of the closed-loop system in Fig. 7.1 is then indistinguishable from the ideal response $y(t) = (1 - \mathrm{e}^{\tau-t})\mathbb{1}(t - \tau)$, which is shown by the red line in Fig. 7.2. ∇

7.3 Rational approximations

Another direction in implementing Π given by (7.1) is to approximate it by a finite-dimensional system. This would put the DTC element on an equal footing with the primary controller, so that the overall controller can be implemented as one block, by standard tools. Several approaches to finite-dimensional approximations are outlined below.

7.3.1 Naïve Padé

The "laziest" approach is just to replace the delay element in (7.1a) with its $[n, n]$-Padé approximant studied in §1.3.1. This results in

$$\Pi_{\mathrm{naïveP},n}(s) = \left[\begin{array}{c|c} A & \mathrm{e}^{-A\tau} B \\ \hline C & 0 \end{array} \right] - \left[\begin{array}{c|c} A & B \\ \hline C & D \end{array} \right] R_{n,n}(s)$$

and requires only standard technical and numerical tools. But this approach does not work in the case when A is not Hurwitz, at least it does not work off the shelf. Indeed, nothing guarantees that unstable modes of A are canceled in the expression above. In fact, they generally are not. For example, for the DTC element in Fig. 7.1 we have that

$$\Pi_{\mathrm{naïveP},n}(s) = \frac{\mathrm{e}^{-1} - R_{n,n}(s)}{s - 1} = \begin{cases} -\dfrac{0.632121(s-\mathbf{1.00148})(s-11.9822)}{(s-1)(s^2+6s+12)} & \text{if } n = 2 \\[3mm] \dfrac{1.36788(s-\mathbf{0.99998969})(s^2-4.54542s+55.4546)}{(s-1)(s+4.64437)(s^2+7.35563s+25.8377)} & \text{if } n = 3 \quad (7.7) \\[3mm] -\dfrac{0.632121(s-\mathbf{1.00000004})(s-39.8821)(s^2-2.39698s+42.1242)}{(s-1)(s^2+8.41516s+45.9512)(s^2+11.5848s+36.5605)))} & \text{if } n = 4 \end{cases}$$

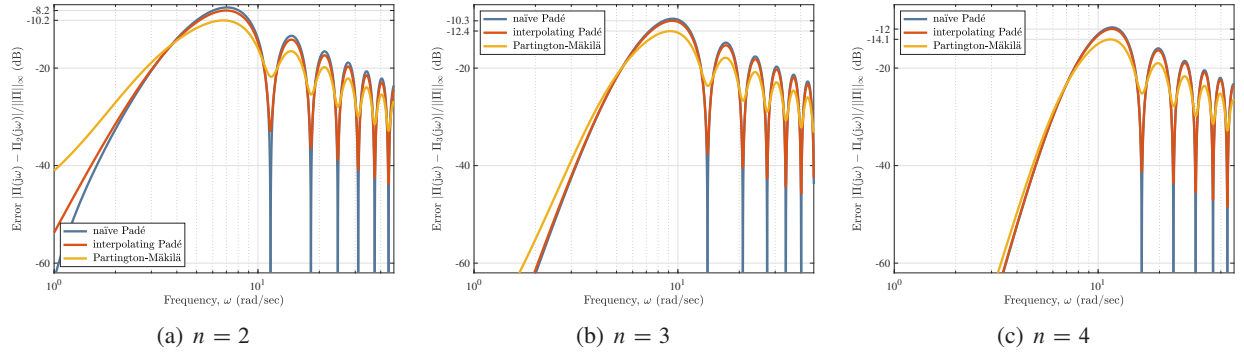(a) $n = 2$ (b) $n = 3$ (c) $n = 4$

Fig. 7.4: Normalized approximation errors for rational approximations of $\Pi(s) = (e^{-1} - e^{-s})/(s - 1)$

are all unstable, which is not what we need. Still, as can be seen from the formulae above, their unstable pole at $s = 1$ is quite close to a zero and can thus be canceled without impairing the frequency response of the resulted approximation much. Thus, the approach might be a handy tool for a quick approximation if accompanied by a manual cancellation of all unstable poles of the result. This works well for the approximation in (7.7), whose approximation errors are presented in Fig. 7.4 by cyan-blue lines for the approximant degrees $n = 2, 3, 4$. In canceling close pole and zero there, the static gain of the approximant was kept equal to $\Pi_{\text{naïveP},n}(0) = \Pi(0)$. However, this approach is simple only in the SISO case and might fail if the resulting transfer functions have relatively distant poles and zeros in $\overline{\mathbb{C}}_0$.

7.3.2 Padé with interpolation constraints

The problem above can be fixed by adding extra interpolation constraints to the Padé approximant of $e^{-\tau s}$ so that

$$R_{n,n}(\lambda_i) = e^{-\tau \lambda_i} \tag{7.8}$$

at all eigenvalues of A in $\overline{\mathbb{C}}_0 \setminus \{0\}$ (eigenvalues at the origin are already handled by the Padé approximant). If the algebraic multiplicity of an eigenvalue is larger than 1, then additional constraints on derivatives of the approximant at that point must be added. This ensures that all such eigenvalues are canceled in the approximant. Such approximants are special cases of so-called *multipoint* Padé approximants, where an approximant is designed to match a function and its derivatives at several points.

Adding constraints like (7.8) to the procedure described in §1.3.1 is a matter of replacing the last rows of (1.33) on p. 15 with appropriate linear constraints. Taking into account that (1.33) approximates e^s, each constraint (7.8) should be recast as $R_{n,n}(-\lambda_i \tau) = e^{-\lambda_i / \tau}$, which results in the linear constraints

$$\begin{bmatrix} 1 & -\lambda_i \tau & \cdots & (-1)^n (\lambda_i \tau)^n & -e^{\lambda_i \tau} & e^{\lambda_i \tau} \lambda_i \tau & \cdots & -(-1)^n e^{\lambda_i \tau} (\lambda_i \tau)^n \end{bmatrix} \begin{bmatrix} 1 \\ q_1 \\ \vdots \\ q_n \\ p_0 \\ p_1 \\ \vdots \\ p_n \end{bmatrix} = 0.$$

The rest is technical. If the number of interpolation points does not exceed the number of parameters, which is $2n + 1$, then the resulting problem can be solved by inverting the last $2n + 1$ columns of the counterpart of the matrix in the left-hand side of (1.33).
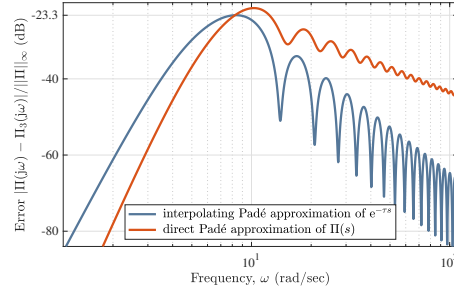
Fig. 7.5: Rational approximations of $\Pi(s) = \sigma_\tau\{2e^{-s}/(2s^2 - 3s + 1)\}$

For the DTC element in Fig. 7.1 this approach yields

$$\Pi_{\text{intP},n}(s) = \begin{cases} -\dfrac{0.451471(s-15.28403)}{s^2+5.6387s+10.9161} & \text{if } n = 2 \\[2mm] \dfrac{1.23504(s^2-4.29253s+57.3393)}{(s+4.51376)(s^2+7.08771s+24.8196)} & \text{if } n = 3 \\[2mm] -\dfrac{0.527108(s-45.0554)(s^2-2.36514s+42.3681)}{(s^2+8.20247s+45.0126)(s^2+11.3775s+35.3632)} & \text{if } n = 4 \end{cases} \qquad (7.9)$$

These transfer functions are stable, so no fine tuning at the end of the procedure is needed. However, the derivations require extra effort and numerical calculations become problematic for large n (they fail for $n = 8$ for the example above). The approximation errors are presented in Fig. 7.4 by red lines for the approximant degrees $n = 2, 3, 4$. The H_∞-norm of the errors under all three n are a bit below of what we have with the naïve approximation, although in this case the gain is not quite substantial.

7.3.3   Direct Padé

Another conceptually straightforward approach is to derive the Padé approximant directly to the function $\Pi(s)$, without the use of the delay element as the approximation agent. If $D = 0$ in (7.1), then it would make sense to use strictly proper Padé approximants, i.e. to select $m < n$ in the procedure of §1.3.1.

As a matter of fact, applying to the DTC element in Fig. 7.1 under $m = n - 1$, this produces the same approximant as that given by (7.9). However, in general these two methods result in different approximants. For example, if $\Pi(s) = \sigma_\tau\{2e^{-s}/(2s^2 - 3s + 1)\}$, then the interpolating Padé and direct Padé result in

$$-\frac{0.4773(s^2 + 9.428s + 70.1)}{(s + 4.444)(s^2 + 6.946s + 24.32)} \quad \text{and} \quad -\frac{0.68479(s^2 + 5.264s + 87.82)}{(s + 5.472)(s^2 + 8.994s + 35.49)},$$

respectively. The corresponding error magnitudes are presented in Fig. 7.5. The interpolating Padé produces a smaller H_∞-norm of the approximation error, 0.0685 vs. 0.0849 for the direct approximation. But the latter method produces better approximations in low frequencies, namely for $\omega \leq 8.256$.

7.3.4   Approach of Partington–Mäkilä

Yet another approach to construct finite-dimensional approximations of DTC elements was proposed by Partington and Mäkilä in [60]. Its key observation is that the function $\Pi(s)$ defined by (7.2) can be equivalently expressed as

$$\Pi(s) = C\phi([sI - A])e^{-A\tau}B, \quad \text{where } \phi(s) := \frac{1 - e^{-\tau s}}{s} = \pi_\tau\left\{\frac{1}{s}\right\}. \qquad (7.1c)$$

Thus, we can approximate $\Pi(s)$ via approximating the scalar function $\phi(s)$ by its $[n - 1, n]$-Padé approximant $R_{n-1,n}(s)$, or whatever other method, and then using

$$\Pi_{\text{PaMä},n}(s) = CR_{n-1,n}([sI - A])e^{-A\tau}B \qquad (7.10)$$

as a rational approximation of $\Pi(s)$. In fact, $R_{n-1,n}(s)$ can be calculated analytically via the $[n, n]$-Padé approximant of $e^{-\tau s}$ as

$$R_{n-1,n}(s) = \tau \frac{P_{n-1}(\tau s)}{Q_n(\tau s)},$$

where the degree-n polynomial $Q_n(s)$ is given by (1.35) on p.16 and the degree-$2\lfloor (n-1)/2 \rfloor$ polynomial

$$P_{n-1}(s) = \frac{Q(s) - Q(-s)}{s} = \sum_{i=0}^{\lfloor (n-1)/2 \rfloor} 2 \binom{n}{2i+1} \frac{(2n - 2i - 1)!}{(2n)!} s^{2i},$$

where $\lfloor \cdot \rfloor$ stands for the floor function. It should be emphasized that the dimension of the transfer function $\Pi_{\text{PaMä},n}(s)$ in (7.10) is $n \dim(A)$, rather than n, in general. Consequently, the order of this approximation may be quite high even if n is chosen to be small.

For $\Pi(s)$ as in Example 7.2 this approach yields (in this case A is scalar, so the order of this approximant is exactly n)

$$\Pi_{\text{PaMä},n}(s) = \begin{cases} \frac{4.41455}{s^2 + 4s + 7} & \text{if } n = 2 \\[2mm] \frac{0.735759(s^2 - 2s + 61)}{(s + 3.64437)(s^2 + 5.35563s + 19.4821)} & \text{if } n = 3 \\[2mm] \frac{14.7152(s^2 - 2s + 43)}{(s^2 + 6.41516s + 38.536)(s^2 + 9.58484s + 25.9757)} & \text{if } n = 4 \end{cases} \tag{7.11}$$

whose magnitude approximation errors are presented in Fig. 7.4 by yellow lines. In all three cases of n these approximation produces the lowest H_∞-norm of the approximation error. But it also produces larger approximation errors in low frequencies. Thus, the comparison can be regarded as indecisive.

Remark 7.1 (stability of approximants). It should be emphasized that no general stability results for approximation methods presented in this whole section appears to be available. As such, the stability of the resulting approximants is not guaranteed even when all unstable eigenvalues of A are canceled in the approximant, as additional poles in $\overline{\mathbb{C}}_0$ might appear. An exception is the analysis in [60] for the case where the function $\phi(s)$ in (7.1c) is approximated via some alternatives of the $[n-1, n]$-Padé. For example, if

$$e^{-s} \approx \left(\frac{-s + 2n}{s + 2n} \right)^n \quad \Longrightarrow \quad \phi(s) \approx \frac{(\tau s + 2n)^n - (-\tau s + 2n)^n}{s(\tau s + 2n)^n},$$
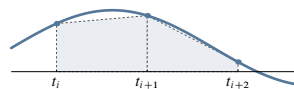
then the approximant in (7.11) is stable whenever $n > \left(\max_{s \in \text{spec}(A)} \text{Re } s \right) \tau / 2$. $\triangledown$

7.4   Lumped-delay approximations (LDA)

The third direction that we study is motivated by the integral form of Π in (7.1b) and the Newton–Cotes quadrature (numerical integration) rules. A general Newton–Cotes formula of degree $v \in \mathbb{N}$, which estimates a definite integral using a piecewise-polynomial approximation of the integrand, is of the form

$$\int_a^b f(t)\,dt \approx \sum_{i=0}^{v} \phi_i f(t_i), \quad \text{where } t_i := a + i(b - a)/v \tag{7.12}$$

for some sequence $\{\phi_i\}_{i=0}^{v}$, which depends on the specific approximation of f. Examples of popular approximation schemes are the trapezoidal rule, in which $f(t)$ is approximated by piecewise-linear functions connecting the points $f(t_i)$ and $f(t_{i+1})$ and for which

$$\Longrightarrow \quad \phi_i = \frac{b - a}{2v} \begin{cases} 2 & \text{if } i = 1, \dots, v - 1 \\ 1 & \text{if } i = 0, v \end{cases}$$

(a) Closed-loop time response
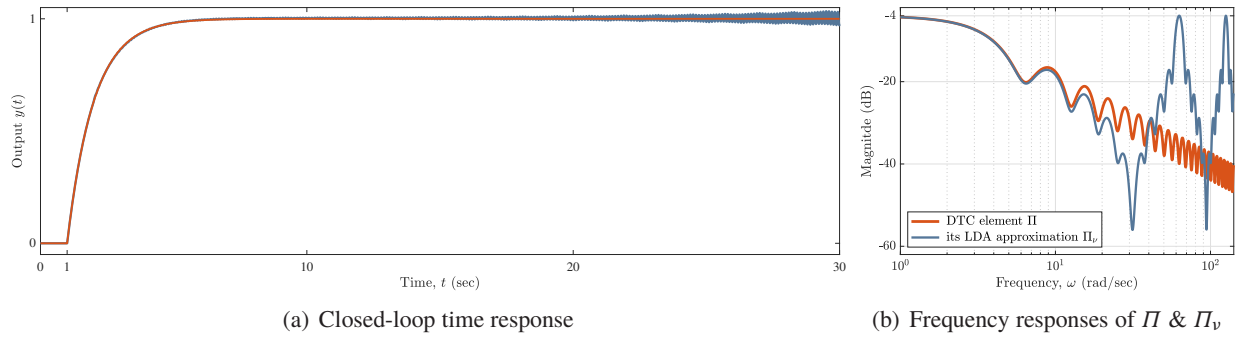

(b) Frequency responses of Π & Π_ν

Fig. 7.6: DTC element in Fig. 7.1 implemented via (7.13)

and Simpson's rule (ν should be even), in which $f(t)$ is approximated by piecewise-quadratic functions connecting the points $f(t_{2i})$, $f(t_{2i+1})$, and $f(t_{2i+2})$ and for which

 $\implies$ $\phi_i = \dfrac{b-a}{6\nu} \begin{cases} 1 & \text{if } i = 0, \nu \\ 2 & \text{if } i \text{ even but neither } 0 \text{ nor } \nu \\ 4 & \text{if } i \text{ odd} \end{cases}$

Applications of Newton–Cotes formulae to (7.1b) lead to easily implementable and stable approximants, although certain care should be taken to keep system-theoretic common sense in place.

7.4.1 Naïve use of Newton–Cotes formulae

Let us start with applying formula (7.12) to the integral term in (7.1b) mechanically. To this end, write the integrand as $f(t) = Ce^{-(sI-A)t}e^{-A\tau}B = Ce^{A(t-\tau)}Be^{-ts}$, for which

$$\Pi(s) \approx \Pi_\nu(s) := \sum_{i=0}^{\nu} \phi_i Ce^{A(\tau_i-\tau)}Be^{-\tau_i s} - De^{-\tau_\nu s}, \quad \text{where } \tau_i := \frac{\tau}{\nu}i. \tag{7.13}$$

This function is a train of (lumped) delays $e^{-\tau_i s}$, so Π_ν is referred to as a *lumped-delay approximation* (LDA) of Π. Obviously, if ϕ_i are all bounded, then $\Pi_\nu \in H_\infty$ for all ν, meaning that we have stability as an intrinsic property of this approximation method.

Example 7.3. Apply the approach presented above to the system studied in Example 7.1 for $\tau = 1$ and the trapezoidal integration rule. The LDA (7.13) yields then the approximant

$$\Pi_\nu(s) = \frac{\tau e^{-\tau}}{2\nu} + \sum_{i=1}^{\nu-1} \frac{\tau e^{-(1-i/\nu)\tau}}{\nu}e^{-(\tau i/\nu)s} + \frac{\tau}{2\nu}e^{-\tau s},$$

which is sufficiently simple. Yet simulating the system in Fig. 7.1 for this choice and $\nu = 10$ results in a slowly diverging oscillatory response, shown in Fig. 7.6(a), rather than in the expected red line. As a matter of fact, increasing the number of partitions of the integration interval, ν, does not result in a stable closed-loop response (oscillations just become faster). A change of the numerical integration rule also does not change this behavior qualitatively [76].   ▽

Although the closed-loop behavior in the example above might appear counter-intuitive at first sight, it can in fact be easily explained from system-theoretic perspectives. To this end, it is important to remember that we approximate an operator, or a function of s in terms of its transfer function. Because $\Pi_\nu(s)$ always

remains an H_∞-function, we may be only concerned with its behavior on the imaginary axis, i.e. with the frequency response $\Pi_\nu(j\omega)$. And this behavior does not have bounded derivatives, e.g. the first time derivative, which satisfies[1]

$$\|\dot{f}(t)\|_F^2 = \|Ce^{A(t-\tau)}(A - j\omega I)Be^{-j\omega t}\|_F^2 = \|Ce^{A(t-\tau)}AB\|_F^2 + \omega^2\|Ce^{A(t-\tau)}B\|_F^2,$$

is unbounded as a function of ω unless $Ce^{A(t-\tau)}B \equiv 0$, which is only the case if $\Pi = 0$. As a result, $\Pi_\nu(j\omega)$ does not converge to $\Pi(j\omega)$ as $\nu \to \infty$. In more classical control-engineering terms, the LDA as in (7.13) attempts to approximate a system with a vanishing high-frequency gain (the integral term in (7.1b)) by a system with a non-decaying high-frequency gain (the sum in (7.13)). For instance, the magnitude frequency responses of Π (in red) and Π_ν (in cyan-blue) for the system in Example 7.3, presented in Fig. 7.6(b), show clearly that the LDA approximation there is not a good fit for $\Pi(j\omega)$ at high frequencies. It can actually be shown that

$$\limsup_{\omega \to \infty} |\Pi_\nu(j\omega)| = \Pi_\nu(0) = \frac{\tau(1 - e^{-\tau})(e^{\tau/\nu} + 1)}{2\nu(e^{\tau/\nu} - 1)} \xrightarrow{\nu \to \infty} 1 - e^{-\tau} = \Pi(0)$$

in this case. Because the high-frequency gain of Π vanishes, we have that $\|\Pi - \Pi_\nu\|_\infty \geq \Pi_\nu(0) > 1 - e^{-\tau}$ in this example as well.

It should be emphasized that the lack of convergence of the approximation error to zero cannot explain the unstable response in Fig. 7.6(a) alone. Instability in this example is actually a result of a lethal combination of non-zero high-frequency gain of the approximation error $\Delta_\Pi = \Pi - \Pi_\nu$ and a poor robustness of the system in Fig. 7.1 to high-frequency uncertainty [43]. Indeed, by presenting the implemented $\Pi_\nu = \Pi - \Delta_\Pi$, the loop in Fig. 7.1 can be rearranged as the feedback interconnection of Δ_Π and the control sensitivity, whose transfer function $T_c(s) = 2e^\tau(-s + 1)/(s + 1)$ and the high-frequency gain is $\lim_{\omega \to \infty} |T_c(j\omega)| = 2e^\tau$. The high-frequency gain of this loop equals then $2(e^\tau - 1) \approx 3.4366$. This gain is not strictly contractive, implying that the loop is extremely sensitive to high-frequency modeling errors, viz. infinitesimal high-frequency modeling uncertainties, like loop delays, cause its instability (cf. the discussion on p. 23 for the case of $\rho(D_{zw}) > 1$). This is exactly what happens in Example 7.3. A more robust system, e.g. that with a strictly proper control sensitivity, would be less sensitive to the high-frequency approximation inaccuracy.

7.4.2 Proper use of Newton–Cotes formulae

Having understood the reason for the failure of approximation (7.13), we can come up with a remedy, which turns out to be quite simple. All we need is to find a way to keep the high-frequency gain of an approximation zero. To this end, note that

$$s \int_0^\tau e^{-(sI-A)t}\,dt = -\int_0^\tau e^{At}\left(\frac{d}{dt}e^{-st}\right)dt = -e^{-(sI-A)t}\Big|_0^\tau + \int_0^\tau \left(\frac{d}{dt}e^{At}\right)e^{-st}\,dt$$

$$= I - e^{A\tau}e^{-\tau s} + \int_0^\tau e^{-(sI-A)t}\,dt\,A,$$

where the second equality in the first line is obtained via integration by parts. Using the obvious equality $\Pi(s) = (s\Pi(s) + \alpha\Pi(s))/(s + \alpha)$, representation (7.1b) can be *equivalently* rewritten as

$$\Pi(s) = \frac{1}{s + \alpha}Ce^{-A\tau}B + \frac{1}{s + \alpha}\int_0^\tau Ce^{A(t-\tau)}(\alpha I + A)Be^{-ts}\,dt - \left(D + \frac{1}{s + \alpha}CB\right)e^{-\tau s} \qquad (7.1d)$$

for every $\alpha \in \mathbb{R}$. Moreover, if $\alpha > 0$, this representation does not involve unstable cancellations and can thus be used casually.

---

[1] The Frobenius norm is chosen for convenience. As all matrix norms are equivalent, this choice does not affect conclusions.

(a) Impulse response of Π (b) Frequency response of Π (c) Trapezoidal rule, $\alpha = 7.8$ & $\nu = 64$
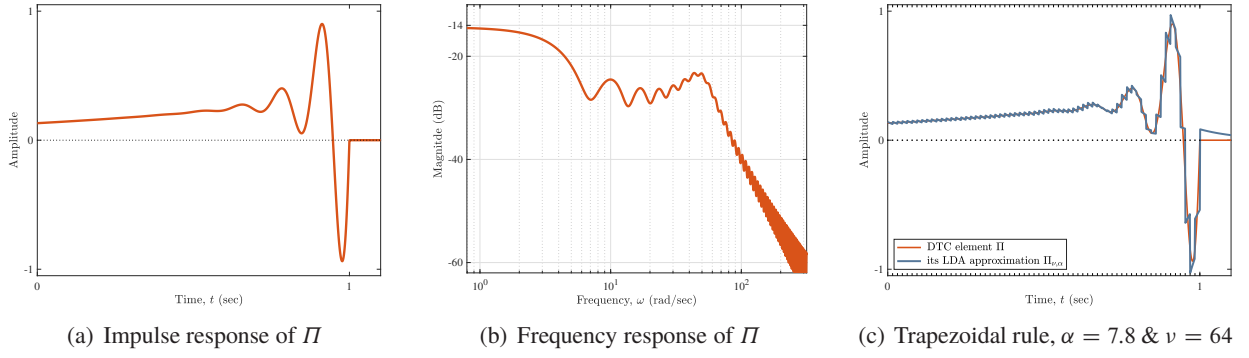
Fig. 7.7: LDA for Example 7.4 (trapezoidal rule, $F(s) = 1/(s + 7.8)$, $\nu = 64$)

The second term in the right-hand side of (7.1d) still contains an integral of the same form as that in (7.1b). But now this term is always postfiltered by the low-pass filter $1/(s + \alpha)$. Hence, a high-frequency mismatch in its approximating is filtered out. A general LDA formula for (7.1d) reads then as follows:

$$\Pi_{\nu,\alpha}(s) = \frac{1}{s + \alpha} C e^{-A\tau} \big(I + (\alpha I + A)\phi_0\big) B$$

$$+ \frac{1}{s + \alpha} \sum_{i=1}^{\nu-1} \phi_i C e^{A(\tau_i - \tau)} (\alpha I + A) B e^{-\tau_i s}$$

$$- \left(D + \frac{1}{s + \alpha} C \big(I - (\alpha I + A)\phi_\nu\big) B \right) e^{-\tau s} \quad (7.14)$$

for a sequence $\{\phi_i\}_{i=0}^{\nu}$ determined by the concrete approximation scheme and with $\tau_i := i\tau/\nu$, like in (7.13). The only term of (7.14) that does not vanish at high frequencies is $D e^{-\tau s}$, which originates in a non-vanishing term of (7.1b). But this term is not an approximation, so it does not affect the approximation error.

Not surprisingly, the use of (7.14) instead of (7.13) for the system in Example 7.3 results in an accurate approximation. For the very same $\nu = 10$ as in Example 7.3, the approximation error $\|\Pi - \Pi_{\nu,\alpha}\|_\infty$ is reduced by more than a factor of 30, to about 0.02 with $\alpha = 1$. Moreover, the approximation error vanishes at high frequencies. The plots of Π and $\Pi_{\nu,\alpha}$, as well as the closed-loop step responses under those choices, are then virtually indistinguishable. Moreover, the impulse responses of Π and $\Pi_{\nu,\alpha}$ for this system are

$$\pi(t) = \quad\text{[graph]}\qquad \text{and} \qquad \pi_{\nu,\alpha}(t) = \quad\text{[graph]}$$

(for $\nu = 10$ and $\alpha = 1$). Note that although the impulse response of $\Pi_{\nu,\alpha}$ appears to vanish for $t \geq \tau$, it actually does not. The system $\Pi_{\nu,\alpha}$ is not FIR in general and its impulse response approaches zero only asymptotically.

Example 7.4. The example considered throughout this chapter so far is quite simple, so any studied method could be relatively easily applied. Consider now a more challenging problem of approximating

$$\Pi(s) = \sigma_\tau \left\{ \frac{80s + 808}{(s - 1)(s^2 - 25s + 2500)} e^{-s} \right\}. \quad (7.15)$$

The impulse and magnitude frequency responses of this system are shown in Figs. 7.7(a) and 7.7(b), respectively. Oscillatory behavior and three unstable poles make these responses more complex and harder to approximate than those of $\sigma_\tau\{e^{-\tau s}/(s-1)\}$, indeed. In fact, rational approximations fail on this example,

in the sense that if accuracy requirements are relatively demanding, like those in (7.16) below, the order of rational approximants is high and off-the-shelf numerics no longer work.

Our goal here is to approximate this Π by the LDA as in (7.14) with the trapezoidal rule so that

$$\|\Pi - \Pi_{\nu,\alpha}\|_\infty \le 0.05 \, \|\Pi\|_\infty \tag{7.16}$$

under the minimal possible number of lumped delays ν. The filter crossover frequency α is then manually tuned, by a trial-and-error search, to end up with the smallest ν. The best results are obtained then for $\alpha = 7.8$, in which case the minimal $\nu = 64$. The impulse response of the approximation is presented in Fig. 7.7(c) by the cyan-blue line. It is now visibly non-FIR. As a result, α should be sufficiently large to provide sufficiently fast decay in $t > \tau$. $\qquad\qquad\qquad\nabla$

7.4.3   Beyond Newton–Cotes

Although numerical integration schemes appear natural in the context of approximating (7.1b) and (7.1d) by lumped delays, we do not have to apply them literally. It might be conceptually cleaner to start with a rather general LDA of the form

$$\Pi_\nu(s) = F(s) \sum_{i=0}^{\nu} \bar\Pi_i e^{-\tau_i s} - D e^{-\tau s} \tag{7.17}$$

for $\nu \in \mathbb{N}$, a sequence $\{\tau_i\}$ such that $0 = \tau_0 < \tau_1 < \cdots < \tau_{\nu-1} < \tau_\nu = \tau$, a strictly proper and stable $F(s)$, and matrix-valued coefficients $\bar\Pi_i$, $i \in \mathbb{Z}_{0,\nu}$. In this formulation the low-pass filter is not constrained to be of the form $F(s) = 1/(s + \alpha)$ as in (7.14), the delays τ_i are not constrained to be equidistant, and the parameters $\bar\Pi_i$ are not constrained to be equal to $\phi_i C e^{A(\tau_i - \tau)} B$ for some scalar ϕ_i. Ideally, we would then like to determine these F, τ_i, and $\bar\Pi_i$, for all $i \in \mathbb{Z}_{0,\nu}$, so that this approximation is close to Π given by (7.1) in whatever meaningful sense. However, such a goal might be overly ambitious and not easily attainable. Still, several directions, in which only a part of the parameter set is designed can be exploited and they are briefly outlined below.

First, fix the number of delays in (7.17) and the filter F and assume that the delays $\tau_i = i\tau/\nu$, i.e. equidistant. As the design goal consider then the choice of $\bar\Pi_i$ minimizing the H_2-norm

$$\|\Pi - \Pi_\nu\|_2. \tag{7.18}$$

This problem can be solved [74] and in some situations (if F has a square "B" matrix) it can be solved analytically. In particular, if $F(s) = 1/(s + \alpha)$ for some $\alpha > 0$, then the optimal choice is

$$\bar\Pi_0 = \frac{2\alpha}{1 - e^{-2\alpha\tau/\nu}} C(A - \alpha I)^{-1} (e^{(A-\alpha I)\tau/\nu} - I) e^{-A\tau} B, \tag{7.19a}$$

$$\bar\Pi_i = 2\alpha C(A - \alpha I)^{-1} \left(\frac{e^{A\tau/\nu} + e^{-A\tau/\nu} - 2e^{-\alpha\tau/\nu} I}{e^{\alpha\tau/\nu} - e^{-\alpha\tau/\nu}} - I \right) e^{A\tau(i-\nu)/\nu} B, \quad \text{for all } i \in \mathbb{Z}_{1..\nu-1} \tag{7.19b}$$

and

$$\bar\Pi_\nu = \frac{2\alpha e^{-\alpha\tau/\nu}}{1 - e^{-2\alpha\tau/\nu}} C(A - \alpha I)^{-1} (I - e^{(A-\alpha I)\tau/\nu}) e^{-A\tau/\nu} B, \tag{7.19c}$$

This choice always results in an FIR approximant, which is attained by an appropriate choice of $\bar\Pi_\nu$.

Example 7.5. Return to the system studied in Example 7.4 and the approximation criterion (7.16). Now, try to attain it with the H_2-optimal choice of $\bar\Pi_i$ from (7.19). It turned out that the best results are obtained for $\alpha = 3.5$, in which case the smallest $\nu = 58$. This is about 10% below of what we have with the trapezoidal rule in Example 7.4 and the resulting Π_ν, whose impulse response is shown in Fig. 7.8(a), has

(a) Uniform $\{\tau_i\}$, $\alpha = 3.5$ and $\nu = 58$ (b) Varying $\{\tau_i\}$, $\alpha = 0.2$ and $\nu = 14$ (c) Varying $\{\tau_i\}$, $\alpha = 3.5$ and $\nu = 8$
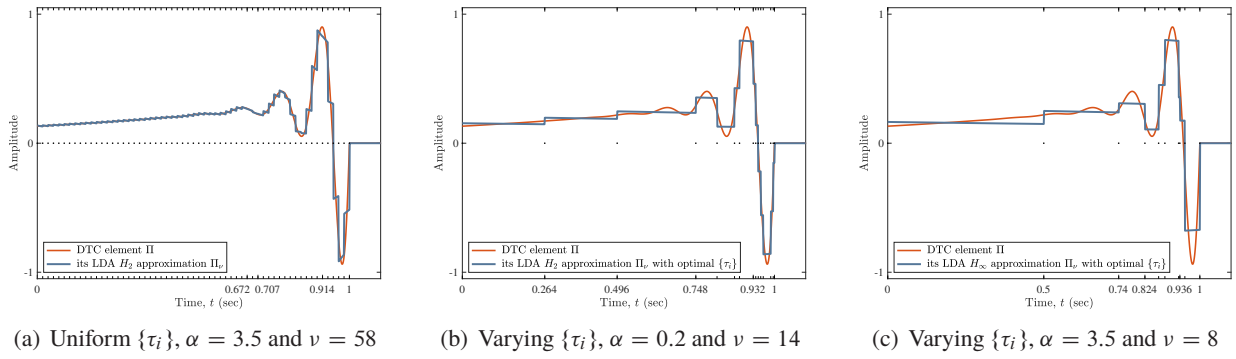
Fig. 7.8: Impulse responses for the general LDA in (7.17)

the same structure from the implementation point of view. In other words, the gain purely due to the use of problem-oriented tuning algorithm, which is better suited for the problem than general-purpose Newton–Cotes schemes. $\triangledown$

The next step is to optimize the delays pattern $\{\tau_i\}$. Benefits of using a nonuniform split are visible already in Fig. 7.8(a). Indeed, it can be seen that at three points, namely for $\tau_i \in \{0.672, 0.707, 0.914\}$, the jumps in the impulse response are virtually invisible. This indicates that the corresponding $\bar{\Pi}_i$'s are close to zero, so these delays, whose indices are 39, 41, and 53, can be eliminated without affecting the approximation performance.

It turns out that optimizing the delay pattern can be done rather efficiently if those delays are restricted to the finite set $\{i\,\tau/\varkappa\}_{i=0}^{\varkappa}$ for a given $\varkappa \in \mathbb{N}$. This does not entail any practical loss of generality, because the grid can be made arbitrarily dense and the implementation of (7.17) would be more efficient in this case anyway. We may then pose the problem of minimizing cost (7.18) under the constraint that the number of delays $\nu \ll \varkappa$ is fixed. A combinatorial search over all possible sets of $\nu - 1$ "internal" delays (i.e. excluding 0 and τ) would require $\binom{\varkappa-1}{\nu-1}$ combinations to be checked, which is not quite practical. Yet in the case when the "B" matrix of $F(s)$ is square, there is an approach that requires only $O(\nu\varkappa^2/2)$ checks, see [74] for details.

Example 7.6. Let us discuss the application of the approach outlined above to the problem studied in Examples 7.4 and 7.5. It turns out that the choice $\alpha = 0.2$ is better in this case. Consider the case of $\varkappa = 250$, meaning that the minimal distance between two delays is set to 0.004. This results in $\nu = 14$, still maintaining (7.16), see Fig. 7.8(b) for the corresponding impulse response. Comparing this result with the uniform split results of Example 7.5, we can see a clear advantage of splitting the interval $[0, \tau]$ non-uniformly. In our example this yields a more than fourfold improvement. This is easy to explain from the form of the impulse response of Π in Fig. 7.7(a). During the first three quarters of the interval $[0, \tau]$ the variations of $\pi(t)$ are relatively minor, so it is sufficient to have only three jumps in that interval. In the final quarter of $[0, \tau]$, the impulse response $\pi(t)$ is considerably more oscillatory, so a more dense grid is required. $\triangledown$

Another possible direction is to minimize directly the H_∞-norm of the approximation error, together with the delay pattern $\{\tau_i\}$. Going this direction drifts us even further from the analytic solution. It is possible to address the problem by numerical optimization methods. Although the problem is not even convex, some trick, known as the ℓ^1-norm heuristic [7], can be used and the result can be seen in Fig. 7.8(c). Going this way we end up with $\nu = 8$, which is the eightfold improvement over the direct Newton–Cotes approach accompanied by the trapezoidal rules, with which we started in Example 7.4.

7.5 Coda

Out ultimate goal is to approximate the controller, so we should be less concerned with the accuracy of approximating Π and more with the accuracy of approximating the whole controller. And even more so with the ability to reproduce the closed-loop properties that were provided by the original DTC element.

One day it should be written . . .

Chapter 8

Exploiting Delays

T HE DELAY ELEMENT HAS SOME FAVORABLE PROPERTIES, which might be exploited in certain situations. A handful of those ideas are outlined in this chapter. It should be emphasized that the delay element has very rich dynamics. For that reason, possible side effects of its use, which might not be immediately visible, should be taken into account. It is therefore well advised to be extra cautious in using such methods, especially when delays are introduced into feedback loops.

8.1 Dead-beat open-loop control

Apparently the safest use of delays is in generating or processing reference signals, as these operations are done outside of feedback loops and are therefore a relatively safe matter, in the worst case only accuracy is lost, not stability. So we start with exposing several such methods, assuming scalar inputs for simplicity.

8.1.1 Posicast control

Consider a cart with a pendulum mounted on it, which is capable of moving in one dimension, say along the x-axis. The control input is supposed to be the position of the cart $x(t)$ itself. The problem is to move the cart from its equilibrium at $x = 0$ to another equilibrium, say at $x = x_f \neq 0$, quickly, but without exciting oscillations in the pendulum. This problem can be motivated by the task of moving a gantry crane with a payload from a pick-up point to a drop-off point without causing oscillations of the payload.

The *posicast control* strategy[1] for such a system, proposed by Otto J. M. Smith in [71], is illustrated by the control sequence depicted in Fig. 8.1. It assumes that the cart movements do not apply longitudinal forces to the pendulum end (i.e. a linearized behavior) and that there is no friction. The cart first leaps half

---

[1]It abbreviates the "positive-cast," because anglers drop their baits in the water at the maximum-position-zero-velocity instant.
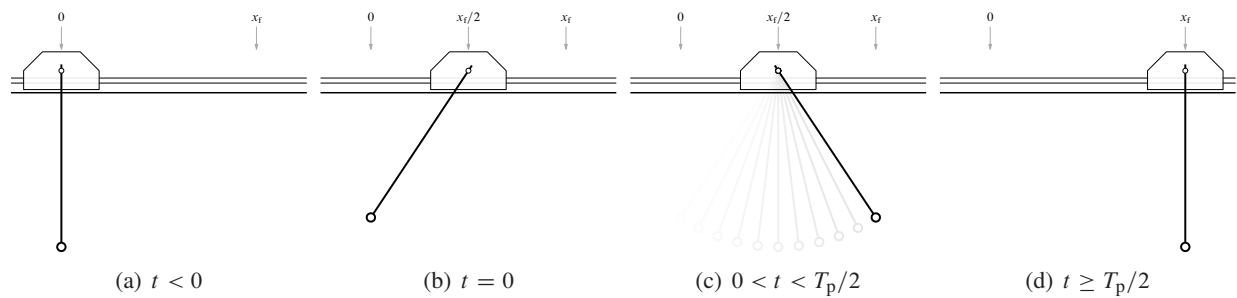

| (a) $t < 0$ | (b) $t = 0$ | (c) $0 < t < T_p/2$ | (d) $t \geq T_p/2$ |

Fig. 8.1: Posicast control of a cart with a pendulum with the period T_p

a way, to the point $x_f/2$, as shown in Fig. 8.1(b), and then waits there for a half of the pendulum period. During this wait time the pendulum swings forth to the rightmost point, whose angle coincides with that at the beginning of the swing and thus having its x-axis position exactly at x_f with the zero velocity, see Fig. 8.1(c). At this moment the cart leaps to the destination point x_f, where the pendulum already stands still, thus bringing the whole system to its required equilibrium. This sequence of actions corresponds to the control signal

$$x(t) = \left(\mathbb{1}(t) + \mathbb{1}(t - T_p/2)\right)x_f/2 = \quad$$

where T_p denotes the pendulum period. In other words, the solution is the response of the open-loop controller

$$R_{\text{pcast}}(s) = \frac{1 + e^{-T_p s/2}}{2}, \tag{8.1}$$

connected in series with the plant, to the scaled step $x_f \mathbb{1}(t)$.

The intuition above can be expressed in control-theoretic terms as well. Assuming that the pendulum is a point mass located at the distance l from its pivot point, the linearized model of the system in Fig. 8.1(a) from the cart position x to the pendulum angle θ is

$$P(s) = \frac{s^2}{ls^2 + g},$$

where g is the standard gravity. Its poles at $s = \pm j\sqrt{g/l}$ cause undamped oscillations if excited. Hence, we should avoid exciting them by a required maneuver. The only way to prevent such oscillations in the open-loop architecture is to cancel these poles by zeros of the controller (ignoring internal instability problems produced by this for a while). This can be done in various ways, one of which is the posicast controller in (8.1). Indeed, its zeros are at $j(2i + 1)\pi/T_p$ for all $i \in \mathbb{Z}$. The period of the pendulum is $T_p = 2\pi\sqrt{l/g}$, so these zeros include the poles of $P(s)$. In fact, the function $P(s)R_{\text{pcast}}(s)$ has no poles and its step response

$$\theta(t) = \mathcal{L}^{-1}\left\{\frac{s(1 + e^{-T_p s/2})}{2(ls^2 + g)}\right\} = \frac{1}{2l}\cos\left(\frac{2\pi}{T_p}t\right)\mathbb{1}_{[0,T_p/2]}(t) = \quad$$

has a finite duration, known as being *dead-beat*.

The approach is readily extendible to damped pendulums, with transfer functions of the form

$$P(s) = \frac{s^2}{ls^2 + 2cs + g} \tag{8.2}$$

for some $c^2 < gl$ (i.e. the response is assumed to be underdamped). This transfer function has a pair of stable poles at $s = -\sigma \pm j\omega$, where

$$\sigma := \frac{c}{l} \quad \text{and} \quad \omega := \sqrt{\frac{g}{l} - \sigma^2} = \frac{2\pi}{T_p}, \tag{8.3}$$

where T_p is still the period of the pendulum and σ can be interpreted as the decay ratio of its oscillations. We consider a controller of the form

$$R_{\text{pcast}}(s) = \phi_0 + \phi_1 e^{-\tau s}, \tag{8.4}$$

with the goal to design its three *real* parameters ϕ_0, ϕ_1, and τ, guaranteeing that $R_{\text{pcast}}(0) = 1$, to have the required steady-state x, and $R_{\text{pcast}}(-\sigma \pm j\omega) = 0$, to have an FIR PR_{pcast}, whose oscillations vanish in finite time. The first requirement yields $\phi_0 + \phi_1 = 1$ and the second one reads

$$\phi_0 + \phi_1 e^{\tau\sigma}e^{\mp j\tau\omega} = \phi_0 + \phi_1 e^{\tau\sigma}\cos(\tau\omega) \mp j\phi_1 e^{\tau\sigma}\sin(\tau\omega) = 0.$$

Obviously, $\phi_1 \neq 0$, so the condition above is solvable in real variables iff $\sin(\tau\omega) = 0$ or, equivalently, iff $\tau = k\pi/\omega$ for some $k \in \mathbb{Z}$. It is justified to choose the smallest τ solving this equality. The choice $\tau = 0$ yields $\phi_0 + \phi_1 = 0$, which contradicts the requirement on the static gain above. The next smallest

$$\tau = \frac{\pi}{\omega} = \frac{T_p}{2},$$

which yields the following linear relation for ϕ_0 and ϕ_1:

$$\begin{bmatrix} 1 & 1 \\ 1 & -e^{\tau\sigma} \end{bmatrix} \begin{bmatrix} \phi_0 \\ \phi_1 \end{bmatrix} = \begin{bmatrix} 1 \\ 0 \end{bmatrix} \quad \implies \quad \begin{bmatrix} \phi_0 \\ \phi_1 \end{bmatrix} = \begin{bmatrix} e^{\sigma T_p/2} \\ 1 \end{bmatrix} \frac{1}{1 + e^{\sigma T_p/2}}.$$

With these choices, the controller has the transfer function

$$R_{\text{pcast}}(s) = \frac{e^{\sigma T_p/2} + e^{-T_p s/2}}{1 + e^{\sigma T_p/2}} \tag{8.5}$$

and results in the following step response of PR_{pcast}:

$$\theta(t) = \frac{1}{1 + e^{-\sigma T_p/2}} \frac{\beta}{l} e^{-\sigma t} \cos\left(\frac{2\pi}{T_p} t + \arccos \frac{1}{\beta}\right) \mathbb{1}_{[0, T_p/2]}(t) = \quad \quad,$$

where $\beta := \sqrt{1 + (\sigma T_p)^2/(2\pi)^2} = 1/\sqrt{1 - c^2/(gl)} \geq 1$. Note that $\phi_0 > \phi_1$ for all $\sigma > 0$, i.e. the first leap of the cart is always larger than the second one for a damped pendulum. The overall time needed for settling at the required equilibrium also increases if the damping is nonzero. This is intuitive, taking into account that the period of the pendulum increases with damping.

Of course, in realistic situations we should not expect the match between zeros of the controller and poles of the plant to be perfect. The response is no longer FIR then, there are residual oscillations of the pendulum. For example, assume that the period of the pendulum T_p is known, but its decay ratio σ used in the controller design is different from the actual $\tilde{\sigma}$, which is realistic. In this case the residual oscillations, which can be derived via the residues of the response $P(s)R_{\text{pcast}}(s)/s$ at $s = -\tilde{\sigma} \pm \mathrm{j}2\pi/T_p$, are

$$\theta_{\text{res}}(t) = \frac{1 - e^{(\tilde{\sigma}-\sigma)T_p/2}}{1 + e^{-\sigma T_p/2}} \theta_{\text{step}}(t),$$

where $\theta_{\text{step}}(s)$ is the step response of the uncontrolled P. The maximum amplitude of this response decays linearly with the mismatch $|\tilde{\sigma} - \sigma|$ if the latter is sufficiently small.

8.1.2 Generating continuous-time FIR responses by a chain of delays

The problem of selecting parameters of the posicast controller in (8.4) can be seen as particular cases of a more general problem of finding a chain of ν delay elements,

$$R = \sum_{i=0}^{\nu} \phi_i \bar{D}_{\tau_i}, \quad 0 = \tau_0 < \tau_1 < \cdots < \tau_\nu, \tag{8.6}$$

for a given finite-dimensional P so that PR is an FIR system, whose impulse response has support in $[0, \tau_\nu]$. The problem may be considered for a given delay sequence $\{\tau_i\}$, when only parameters $\phi_i \in \mathbb{R}^{m \times q}$ are to be found, or in a completely general setting, when delays can also be chosen freely. Sometimes, additional constraints on R, e.g. on its static gain $R(0)$, are incorporated. Such constraints normally also rule out the trivial solution $\phi_i = 0$, for all $i \in \mathbb{Z}_{0..\nu}$.

The following result characterizes solutions to this problem.

Lemma 8.1. *If the realization $P(s) = D + C(sI - A)^{-1}B$ is observable and R is as in (8.6), then PR is FIR iff*

$$\begin{bmatrix} e^{A\tau_\nu}B & \cdots & e^{A(\tau_\nu - \tau_{\nu-1})}B & B \end{bmatrix} \Phi = 0, \tag{8.7}$$

where $\Phi := \begin{bmatrix} \phi_0' & \cdots & \phi_{\nu-1}' & \phi_\nu' \end{bmatrix}'$, and then the impulse response of PR is zero for all $t > \tau_\nu$.

Proof. Decompose

$$P\phi_i \bar{D}_{\tau_i} = \left(\pi_{\tau_\nu - \tau_i}\{P\} + \hat{P}_i \bar{D}_{\tau_\nu - \tau_i}\right)\phi_i \bar{D}_{\tau_i} = \pi_{\tau_\nu - \tau_i}\{P\}\phi_i \bar{D}_{\tau_i} + \hat{P}_i \phi_i \bar{D}_{\tau_\nu},$$

where the truncation operator is defined in §3.4.2 on p. 62 and $\hat{P}_i(s) = C(sI - A)^{-1}e^{A(\tau_\nu - \tau_i)}B$, cf. (3.39). Hence,

$$PR = \sum_{i=0}^{\nu} \pi_{\tau_\nu - \tau_i}\{P\}\phi_i \bar{D}_{\tau_i} + \sum_{i=0}^{\nu} \hat{P}_i \phi_i \bar{D}_{\tau_\nu}.$$

The first term in the right-hand side above is an FIR system, whose impulse response has support in $[0, \tau_\nu]$. The second term is a τ_ν-delayed system. If its finite-dimensional part $\sum_i \hat{P}_i \phi_i \neq 0$, the impulse response of this system has support in (τ_ν, ∞) and PR cannot be FIR. Thus, the FIR property holds iff

$$\sum_{i=0}^{\nu} \hat{P}_i(s)\phi_i = \left[\begin{array}{c|c} A & \sum_{i=0}^{\nu} e^{A(\tau_\nu - \tau_i)}B\phi_i \\ \hline C & 0 \end{array}\right] = 0.$$

Condition (8.7), which reads $\sum_{i=0}^{\nu} e^{A(\tau_\nu - \tau_i)}B\phi_i = 0$, is then clearly sufficient and its necessity follows by the observability of (C, A). □

If P is n-dimensional, then there are nontrivial solutions to (8.7) iff the rank of

$$M_\tau := \begin{bmatrix} e^{A\tau_\nu}B & \cdots & e^{A(\tau_\nu - \tau_{\nu-1})}B & B \end{bmatrix} \in \mathbb{R}^{n \times \nu+1}$$

is smaller than $\nu + 1$. In other words, there must exist a nontrivial kernel of M_τ and then every $\Phi \in \ker M_\tau$ is admissible. This condition holds true whenever $\nu \geq n$, which is a sufficient condition for the existence of a required R. Nevertheless, there might also be situations when (8.7) is solvable by $\Phi \neq 0$ even if $\nu < n$.

To see that, return to the plant with the transfer function (8.2). Its minimal realization is

$$P(s) = \frac{1}{l}\left[\begin{array}{cc|c} -\sigma & \omega & 0 \\ -\omega & -\sigma & 1 \\ \hline \sigma^2/\omega - \omega & -2\sigma & 1 \end{array}\right].$$

Choosing $\nu = n = 2$ we obtain

$$M_\tau = \begin{bmatrix} e^{-\tau_2\sigma}\sin(\tau_2\omega) & e^{-(\tau_2-\tau_1)\sigma}\sin((\tau_2-\tau_1)\omega) & 0 \\ e^{-\tau_2\sigma}\cos(\tau_2\omega) & e^{-(\tau_2-\tau_1)\sigma}\cos((\tau_2-\tau_1)\omega) & 1 \end{bmatrix}.$$

Thus, unless $\sin(\tau_2\omega) = \sin((\tau_2 - \tau_1)\omega) = 0$, this is a rank-two matrix with

$$\ker M_\tau = \operatorname{Im} \begin{bmatrix} \sin((\tau_2 - \tau_1)\omega) \\ -e^{-\tau_1\sigma}\sin(\tau_2\omega) \\ e^{-\tau_2\sigma}\sin(\tau_1\omega) \end{bmatrix} \implies \begin{bmatrix} \phi_0 \\ \phi_1 \\ \phi_2 \end{bmatrix} = \begin{bmatrix} \sin((\tau_2 - \tau_1)\omega) \\ -e^{-\tau_1\sigma}\sin(\tau_2\omega) \\ e^{-\tau_2\sigma}\sin(\tau_1\omega) \end{bmatrix}\alpha$$

for an arbitrary $\alpha \neq 0$. If we pick $\tau_1 = \pi/\omega$ now, then $\sin(\tau_1\omega) = 0$ and we have that $\phi_2 = 0$, i.e. that effectively $\nu = 1$. Because with this choice $\sin((\tau_2 - \tau_1)\omega) = -\sin(\tau_2\omega)$, we then recover the posicast controller (8.5) under $\alpha = -\csc(\tau_2\omega)/(1 + e^{-\pi\sigma/\omega})$.
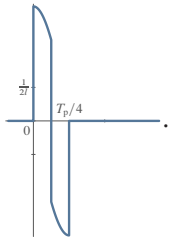
If in the example above τ_1 is such that $\sin(\tau_1\omega) \neq 0$, then two delays are used and the end point can be reached faster. For example, let $\tau_1 = \pi/(4\omega)$ and $\tau_2 = \pi/(2\omega)$. In this case $\phi_0 = \alpha/\sqrt{2}$, $\phi_1 = -e^{-\pi\sigma/(4\omega)}\alpha$, and $\phi_2 = e^{-\pi\sigma/(2\omega)}\alpha/\sqrt{2}$. The condition $R(0) = 1$ reads then

$$\alpha = \frac{\sqrt{2}}{1 - \sqrt{2}e^{-\pi\sigma/(4\omega)} + e^{-\pi\sigma/(2\omega)}} = \frac{\sqrt{2}}{(1 - e^{-\pi\sigma/(4\omega)})^2 + (2 - \sqrt{2})e^{-\pi\sigma/(4\omega)}}.$$

To simplify the expressions, assume the undamped case, i.e. that $\sigma = 0$. The controller is then

$$R(s) = \left(1 + \frac{1}{\sqrt{2}}\right)\left(1 - \sqrt{2}\,e^{-T_\mathrm{p}s/8} + e^{-T_\mathrm{p}s/4}\right)$$

and its step response $x(t) \approx 1.707 \cdot \mathbb{1}(t) - 2.414 \cdot \mathbb{1}(t - T_\mathrm{p}/8) + 1.707 \cdot \mathbb{1}(t - T_\mathrm{p}/4)$. Thus, the cart position first overshoots by about 71% at $t = 0$, then undershoots by about 71% at $t = T_\mathrm{p}/8$, and finally settles at the steady state value at $t = T_\mathrm{p}/4$. This produces the following response of the pendulum:

$$\theta(t) = \frac{2 + \sqrt{2}}{2l}\left(\cos\left(\frac{2\pi}{T_\mathrm{p}}t\right)\mathbb{1}_{[0,T_\mathrm{p}/8]}(t) - \sin\left(\frac{2\pi}{T_\mathrm{p}}t\right)\mathbb{1}_{[T_\mathrm{p}/8,T_\mathrm{p}/4]}(t)\right) = \text{}.$$

which settles twice as fast as in the posicast controller case. The price is higher amplitudes of both the cart and the pendulum.

8.1.3 Input shaping

The idea behind posicast control became popular in numerous *input shaping* schemes, where the control input is the convolution of a reference signal, like a step, with shaping impulses, see [69] for an overview of related techniques. Those shaping impulses can be seen as generated by an array of delays, exactly as in (8.6). Thus, the posicast controller (8.5) can be seen as a special case of an input shaper.

Apart from canceling nominal lightly damped poles, input shapers are also endeavoured to be less sensitive to the location of those poles, i.e. be robust. There are several approaches to improve robustness, normally at the expense of a more involved controller and a longer settling to the final equilibrium. They thus typically use an increased number of delay elements in the controller, like (8.6) for $\nu = 2$ for plant (8.2) instead of $\nu = 1$ as in (8.4). The extra parameters are then used to bring in additional properties, reducing the sensitivity of the scheme to uncertain resonance parameters.

As an example of robustifying ideas, consider the ZVD (zero vibration and derivative) approach. Its key idea is to require from the canceling zeros of the transfer function of the controller to have a higher multiplicity than that of the canceled plant poles. To illustrate this approach, return to the damped pendulum (8.2) and consider the choice of parameters in controller (8.6) under $\nu = 2$ for it. Additional zeros at $s = -\sigma \pm j\omega$ imply the requirement $R'(-\sigma \pm j\omega) = 0$, where $R'(s) := \mathrm{d}R(s)/\mathrm{d}s$. This requirement can be accounted for either explicitly, via adding the constraint

$$\begin{bmatrix} 0 & -\tau_1 e^{\tau_1\sigma}e^{\mp j\tau_1\omega} & -\tau_2 e^{\tau_2\sigma}e^{\mp j\tau_2\omega} \end{bmatrix}\Phi = 0$$

to $M_\tau\Phi = 0$, or implicitly, via solving the problem for the fourth-order $P(s)/(ls^2 + 2cs + g)$. In either case, the problem is solvable iff $\sin(\tau_1\omega) = \sin(\tau_2\omega) = 0$. For instance, the solution for $\tau_1 = \pi/\omega$ and $\tau_1 = 2\pi/\omega$ is

$$R_{\mathrm{ZVD}}(s) = \left(\frac{e^{\sigma T_\mathrm{p}/2} + e^{-T_\mathrm{p}s/2}}{1 + e^{\sigma T_\mathrm{p}/2}}\right)^2. \tag{8.8}$$

The step response of PR_{ZVD} is then

$$\theta(t) = \frac{1}{(1 + e^{-\sigma T_{\mathrm{p}}/2})^2} \frac{\beta}{l} e^{-\sigma t} \cos\left(\frac{2\pi}{T_{\mathrm{p}}}t + \arccos\frac{1}{\beta}\right)\left(\mathbb{1}_{[0,T_{\mathrm{p}}/2]}(t) - \mathbb{1}_{[T_{\mathrm{p}}/2,T_{\mathrm{p}}]}(t)\right) =$$

where $\beta := \sqrt{1 + (\sigma T_{\mathrm{p}})^2/(2\pi)^2}$. This algorithm takes twice the time required by the standard posicast to move to the final point. What we gain is a lower sensitivity to modeling inaccuracies. To see that, assume again that the decay ratio is uncertain, namely, its value σ used to calculate (8.8) is different from its actual value $\tilde{\sigma}$. In this case the poles at $s = -\tilde{\sigma} \pm j\omega$ are not canceled and there are residual oscillations. For controller (8.8) they are

$$\theta_{\mathrm{res}}(t) = \left(\frac{1 - e^{(\tilde{\sigma}-\sigma)T_{\mathrm{p}}/2}}{1 + e^{-\sigma T_{\mathrm{p}}/2}}\right)^2 \theta_{\mathrm{step}}(t),$$

where $\theta_{\mathrm{step}}(s)$ is the step response of the uncontrolled P. Their maximum amplitude decays now quadratically with the mismatch for small deviations, i.e. as $(\tilde{\sigma} - \sigma)^2$. Such a function has a slower grow than a linear function of the error and is thus less sensitive to uncertainty.

Another possible direction of improving the robustness of input shaping algorithms is to place zeros of controller (8.6) not exactly at each lightly-damped pole of the nominal plant, but rather at two different points nearby. For example, we may consider the problem for

$$P(s) = \frac{s^2}{(ls^2 + 2(c + c_\delta)s + g)(ls^2 + 2(c - c_\delta)s + g)}$$

for a small $c_\delta > 0$. By doing this, we sacrifice the nominal response, which will exhibit small residual oscillations, but can guarantee a low gain of the controller in a wider neighborhood of this lightly-damped pole.

Input-shaping ideas extend to systems with multiple flexible modes. *Multi-mode* shapers can be constructed either via the series interconnection of input shapers for each of those modes or by choosing parameters of (8.6) directly. The former approach is simpler from the design point of view, as each factor can be chosen to be of standard forms, like (8.5) or (8.8). The latter approach has a potential advantage in that it may produce more economic controllers, with faster responses. But parameters of (8.6) is typically harder to tune to satisfy (8.7) for general systems. State-of-the-art methods appear to use various numerical optimization schemes.

Remark 8.1 (why dead-beat). An intriguing question is why input-shaping solutions endeavor to reach a dead-beat response from a controlled signal? In principle, lightly-damped modes can also be canceled by finite-dimensional controllers. For example, we can use

$$R(s) = \frac{ls^2 + 2cs + g}{g(Ts + 1)^2}$$

for some $T > 0$ or whatever other denominator polynomial, whose order is at least 2, instead of (8.5), to control a system with the transfer function (8.2). This would yield $P(s)R(s) = s^2/(g(Ts + 1)^2)$, whose step response decays aperiodically, with a faster decay for a smaller T. Such a controller might be easier to design, especially in the multi-mode case, and it might be less sensitive to modeling mismatches. But a finite-dimensional R normally has a slower settling under comparable magnitudes of involved signals. Still, it appears that a comprehensive comparison of these approaches is yet to be carried out. ∇

8.1.4 Time-optimal control

Another related approach to generate reference signals, in terms of the structure of resulted signals, is the use of time-optimal strategy under constraints on the various process variables. Specifically, this is the

case for the problem of steering the state of the n-dimensional system

$$\dot{x}(t) = Ax(t) + Bu(t)$$

from a given initial condition $x(0) = x_0$ to a given final state $x(t_f) = x_f$ in minimum possible time t_f under the constraint that $|u(t)| \leq 1$ for all t. We assume that both x_0 and x_f are admissible equilibria of the system, i.e. are such that $Ax_0 + Bu_0 = Ax_f + Bu_f = 0$ for some $|u_0| \leq 1$ and $|u_f| \leq 1$. This problem is well defined iff (A, B) is controllable and the optimal solution is of the *bang-bang* form, i.e. the optimal $u(t)$ takes values only from the set $\{-1, 1\}$, with a finite number of switches between $u(t) = -1$ and $u(t) = 1$, see [5, Sec. 6.5] for details. Moreover, if all eigenvalues of A are real, then the number of switches is upperbounded by $n - 1$.

It is readily seen that the bang-bang strategy for $t \geq 0$ can be expressed as the step response of (8.6) for $|\phi_0| = 1$ and $\phi_i = (-1)^i 2\phi_0$ for all $i \in \mathbb{Z}_{1..\nu-1}$. We can thus still use (8.7), now for effectively a given Φ and the delays τ_i as the parameters to determine, together with the constraint

$$\lim_{s \to 0} (sI - A)^{-1}(sx_0 + BR(s)) = x_f,$$

which guarantees that $\lim_{t \to \infty} x(t) = x_f$.

To illustrate this procedure, consider the time-optimal control of a DC motor connected to a rigid mechanical load, having the moment of inertia J and the viscous friction coefficient f. Its dynamics can be described as

$$\begin{bmatrix} \dot{\theta}_m(t) \\ \dot{\omega}_m(t) \end{bmatrix} = \begin{bmatrix} 0 & 1 \\ 0 & -a \end{bmatrix} \begin{bmatrix} \theta_m(t) \\ \omega_m(t) \end{bmatrix} + \begin{bmatrix} 0 \\ b \end{bmatrix} u(t),$$

where θ_m is the angle of the shaft, ω_m is its angular velocity, u is the normalized input voltage (so that its maximal peak corresponds to ± 1), $a = (Rf + K_m^2)/(RJ) > 0$, and $b = K_m/(RJ) > 0$, where R is the armature resistance and K_m is the torque constant of the motor. Assume that the initial condition is $\theta_m(0) = \omega_m(0) = 0$ and the goal is to steer the shaft to the equilibrium $\theta_m(t_f) = \theta_f$ and $\omega_m(t_f) = 0$. Both these equilibria correspond to $u = 0$, i.e. they are admissible. As both poles of the system are real, we know that there might be at most one switch in $(0, f)$. Hence, consider (8.6) for $\nu = 2$. Because

$$\exp\left(\begin{bmatrix} 0 & 1 \\ 0 & -a \end{bmatrix} t\right) = \begin{bmatrix} 1 & (1 - e^{-at})/a \\ 0 & e^{-at} \end{bmatrix},$$

condition (8.7) reads

$$b \begin{bmatrix} (1 - e^{-at_f})/a & (1 - e^{-a(t_f - t_s)})/a & 0 \\ e^{-at_f} & e^{-a(t_f - t_s)} & 1 \end{bmatrix} \begin{bmatrix} \phi_0 \\ -2\phi_0 \\ \phi_2 \end{bmatrix} = b \begin{bmatrix} 1/a & -e^{-at_f}/a \\ 0 & e^{-at_f} \end{bmatrix} \begin{bmatrix} 1 & 1 & 1 \\ 1 & e^{at_s} & e^{at_f} \end{bmatrix} \begin{bmatrix} \phi_0 \\ -2\phi_0 \\ \phi_2 \end{bmatrix} = 0$$

for $|\phi_0| = 1$ and the final value condition reads

$$\lim_{s \to 0} \begin{bmatrix} s & -1 \\ 0 & s + a \end{bmatrix}^{-1} \begin{bmatrix} 0 \\ b \end{bmatrix} R(s) = \begin{bmatrix} \theta_f \\ 0 \end{bmatrix} \implies \begin{cases} R'(0) = a\theta_f/b \\ R(0) = 0 \end{cases}.$$

Note that the first row of this version of (8.7) also reads $R(0) = 0$, so one of these conditions is redundant. In any case, from that condition we have that $\phi_2 = \phi_0$ and therefore end up with two inequalities,

$$1 - 2e^{at_s} + e^{at_f} = 0 \quad \text{and} \quad (2t_s - t_f)\phi_0 = a\theta_f/b. \tag{8.9}$$

The first of them reads $e^{at_s} = (e^{at_f} + 1)/2$ and, as the function e^t is strictly convex, implies that $2t_s - t_f > 0$. The second equality of (8.9) yields then that $\phi_0 = \text{sign}\,\theta_f$ and $2t_s - t_f = a|\theta_f|/b$ or, equivalently, that $t_f = 2t_s - a|\theta_f|/b$. Substituting this value to the first equality of (8.9) we get the quadratic equation

$$e^{-a^2|\theta_f|/b}e^{2at_s} - 2e^{at_s} + 1 = 0 \implies e^{at_s} = e^{a^2|\theta_f|/b}\left(1 \pm \sqrt{1 - e^{-a^2|\theta_f|/b}}\right).$$
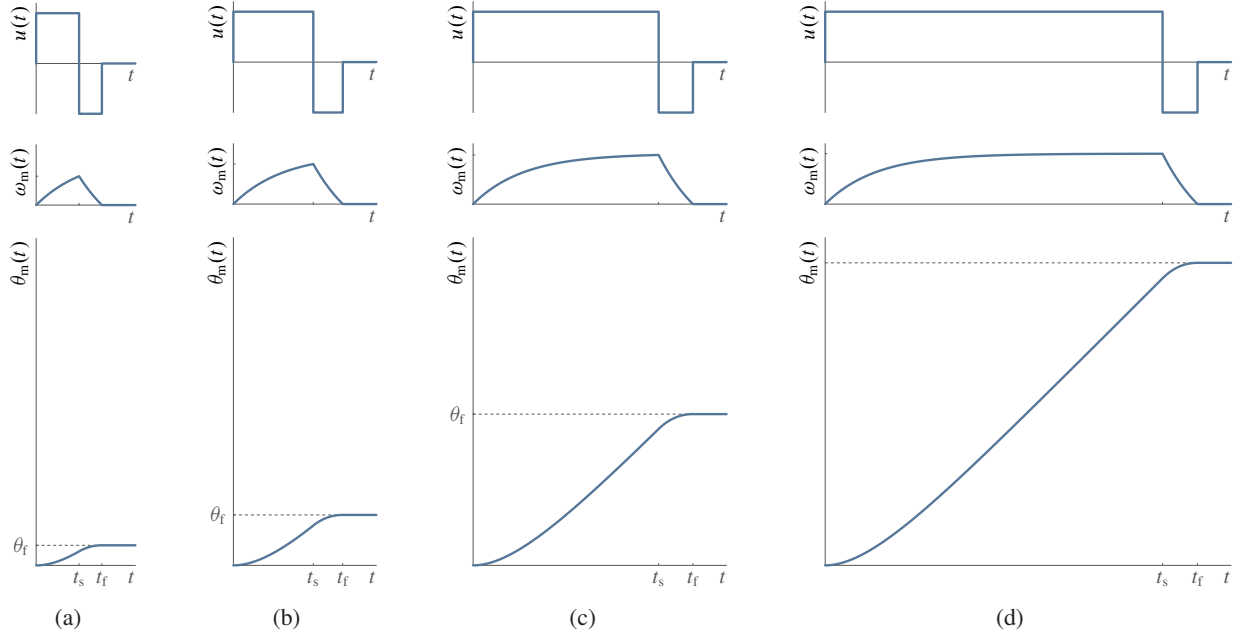
Fig. 8.2: Time-optimal trajectories for a DC motor

We are interested in the "+" solution, as this is the only one for which $t_s < t_f$. Thus, we end up with

$$t_s = \frac{a}{b}\,|\theta_f| + \frac{1}{a}\,\ln\!\left(1 + \sqrt{1 - e^{-a^2|\theta_f|/b}}\right) \quad \text{and} \quad t_f = \frac{a}{b}\,|\theta_f| + \frac{2}{a}\,\ln\!\left(1 + \sqrt{1 - e^{-a^2|\theta_f|/b}}\right).$$

Expectably, these are monotonically increasing functions of $|\theta_f|$. The resulted trajectories of $u(t)$, $\omega_m(t)$, and $\theta_m(t)$ for various θ_f are presented in Fig. 8.2.

Time-optimal trajectories may provide an implicit justification for the input-shaping strategy. In fact, time-optimal trajectories can be used as possible input shapers. However, they are hard to derive in general and are known to be quite sensitive to modeling uncertainty.

8.1.5 Generating continuous-time FIR responses by general FIR systems

The controller architecture (8.6) is not the only possible one to produce an FIR PR for a finite-dimensional P. This goal can be attained by various other structures of controllers. In this subsection we study such kind of problems in a general setting, namely, as a general tracking setup.

A general open-loop tracking problem can be formulated as the two-block model-matching problem, where the error system to be reduced is of the form

$$G_e = G_w + G_u R, \tag{8.10}$$

where G_w and G_u are finite-dimensional systems, given by their joint state-space realization

$$\begin{bmatrix} G_w(s) & G_u(s) \end{bmatrix} = \left[\begin{array}{c|cc} A & B_w & B_u \\ \hline C & D_w & D_u \end{array}\right] \tag{8.11}$$

and R is a controller to find. In the particular case of $G_w = I$ and $G_u = -P$ this error system generates the tracking error $e = r - y$ in the standard open-loop setting, where $R : r \mapsto u$ and the goal is to render the plant output y close to a measured reference signal r. We may add a weighing function W_e to emphasize important frequency ranges for the reduction of the tracking error or to account for a priori information

about properties of r. In such a case $G_w = W_e$ and $G_u = -W_e P$. It is also possible to include the control signal u, maybe shaped by yet another weight W_u, as a part of the error signal. This yields

$$G_w = \begin{bmatrix} W_e \\ 0 \end{bmatrix} \quad \text{and} \quad G_u = \begin{bmatrix} -W_e P \\ W_u \end{bmatrix}$$

and use weights to trade-off tracking performance and control efforts. In some situations, disturbance attenuation problems under measured disturbances can also be cast in the form (8.10).

The general tracking setup is often used to pose tracking problems as optimization problems, with the requirement to minimize a norm, e.g. H_2 or H_∞, of G_e. Any such problem should start with a suitable definition of the class of admissible controllers R. Normally, admissibility is understood as the stability of the controller itself, viz. as $R \in H_\infty$, and of the error system, viz. as $G_e \in H_\infty$. But in some situations, we might also required to strengthen requirements on the controller and the error system by requiring them to be FIR, with the support of its impulse response in a given interval $[0, \tau]$. The stability of both these systems is then guaranteed if the impulse response of R is bounded, which is easy to see.

All such admissible solutions are characterized in the following result:

Lemma 8.2. *If (C, A) in realization (8.11) is observable, then there is an FIR R with the impulse response $r(t)$ supported in $[0, \tau]$ such that G_e is also FIR with the same support iff*

$$B_w + \int_0^\tau e^{-As} B_u r(s) \, ds = 0. \tag{8.12}$$

Proof. If R is FIR, then the impulse response of the error systems is

$$g_e(t) = D_w \delta(t) + C e^{At} B_w \mathbb{1}(t) + D_u r(t) + C \int_0^t e^{A(t-s)} B_u r(s) \, ds \tag{8.13}$$

$$= D_w \delta(t) + C e^{At} B_w \mathbb{1}(t) + D_u r(t) \mathbb{1}_{[0,\tau]}(t) + C \int_0^{\min\{t,\tau\}} e^{A(t-s)} B_u r(s) \, ds.$$

We require $g_e(t) = 0$ for all $t > \tau$, which reads then

$$g_e(t) = C e^{At} \left(B_w + \int_0^\tau e^{-As} B_u k(s) \, ds \right) = 0, \quad \forall t > \tau.$$

Equality (8.12) is obviously sufficient for that and its necessity follows by the observability of (C, A). $\square$

Rewriting condition (8.12)

$$-e^{A\tau} B_w = \int_0^\tau e^{A(t-s)} B_u r(s) \, ds,$$

it can be interpreted in terms of attaining the state $x(\tau) = -e^{A\tau} B_w$ from the zero initial conditions by the system $\dot{x} = Ax + B_u u$, with the resulted u taken as the impulse response of the controller R. This is essentially the controllability question. If it is solvable, which is always the case if (A, B_u) is controllable, there are infinitely many solutions. This degree of freedom can be exploited in different ways. For example, if the final state is supposed to be attained in minimum time under amplitude constraints on u, we end up with the time-optimal solution discussed in §8.1.4. Another possibility is to endeavor to attain the final point with the minimum-energy u:

Proposition 8.3. *If (A, B_u) in (8.11) is controllable, then*

$$r(t) = r_{ME}(t) := -B_u' e^{-A't} \left(\int_0^\tau e^{-As} B_u B_u' e^{-A's} \, ds \right)^{-1} B_w \mathbb{1}_{[0,\tau]}(t)$$

has the minimum energy among all solutions to (8.12).

Proof. If (A, B_u) is controllable, then r_{ME} is well defined and satisfies (8.12), which can be shown by direct substitution. Assume that $r = r_{\text{ME}} + r_\delta$ solves (8.12) as well. This necessarily implies that r_δ satisfies the equation

$$\int_0^\tau e^{-As} B_u r_\delta(s) \, ds = 0.$$

Hence,

$$\|r\|_2^2 = \|r_{\text{ME}}\|_2^2 + \|r_\delta\|_2^2 + 2\langle r_\delta, r_{\text{ME}}\rangle = \|r_{\text{ME}}\|_2^2 + \|r_\delta\|_2^2 + 2\int_0^\tau [r_{\text{ME}}(t)]' r_\delta(t) \, dt$$

$$= \|r_{\text{ME}}\|_2^2 + \|r_\delta\|_2^2 + 2B_w' \left(\int_0^\tau e^{-As} B_u B_u' e^{-A's} \, ds\right)^{-1} \int_0^\tau e^{-At} B_u r_\delta(t) \, dt = \|r_{\text{ME}}\|_2^2 + \|r_\delta\|_2^2.$$

Thus, $\|r_{\text{ME}}\|_2 \leq \|r\|_2$ for every k satisfying (8.12) and the equality holds iff $r_\delta = 0$.   □

To illustrate the minimum-energy algorithm of Proposition 8.3, return to the pendulum on the cart problem presented in Fig. 8.1. To formulate it as a general tracking problem, consider a step reference signal $\mathbb{1}$ for the cart position x and choose as regulated signals the tracking error $\mathbb{1} - x$ and the pendulum angle θ. The systems $w \mapsto \begin{bmatrix} \mathbb{1}-x \\ \theta \end{bmatrix}$, where $w(t) = \delta(t) = \dot{\mathbb{1}}(t)$, has the transfer function

$$\begin{bmatrix} G_w(s) & G_u(s) \end{bmatrix} = \begin{bmatrix} 1/s & -1/s \\ 0 & P(s)/s \end{bmatrix} = \left[\begin{array}{ccc|cc} 0 & 0 & 0 & 1 & -1 \\ 0 & -\sigma & \omega & 0 & 0 \\ 0 & -\omega & -\sigma & 0 & 1 \\ \hline 1 & 0 & 0 & 0 & 0 \\ 0 & -\sigma/(l\omega) & 1/l & 0 & 0 \end{array}\right],$$

where $P(s)$ is given by (8.2) and σ and ω are defined by (8.3). The pair (A, B_u) in the realization above is controllable, so the formulae of Lemma 8.2 apply. To compare them with the response of the posicast control, choose $\tau = \pi/\omega = T_p/2$, so that the response settles in the very same $T_p/2$. This choice yields

$$r_{\text{ME}}(t) = \gamma\left(\frac{1 - e^{\sigma T_p/2}}{\sigma T_p} + \frac{2}{\pi} e^{\sigma t} \sin\left(\frac{2\pi}{T_p} t\right)\right) \mathbb{1}_{[0, T_p/2]}(t),$$

where $\gamma := 2\sigma(\sigma^2 T_p^2 + 4\pi^2)/(8\sigma T_p(1 + e^{\sigma T_p/2}) + (\sigma^2 T_p^2 + 4\pi^2)(1 - e^{\sigma T_p/2}))$, which corresponds to the transfer function

$$R_{\text{ME}}(s) = \gamma\left(\frac{e^{\sigma T_p/2} - 1}{\sigma} \frac{1 - e^{-T_p s/2}}{s} - \frac{4(1 + e^{\sigma T_p/2} e^{-T_p s/2})}{(s - \sigma)^2 + 4\pi^2/T_p^2}\right) \xrightarrow{\sigma \downarrow 0} \frac{16\pi^2}{\pi^2 - 8}\left(\frac{1 - e^{-T_p s/2}}{8T_p s} - \frac{1 + e^{-T_p s/2}}{T_p^2 s^2 + 4\pi^2}\right)$$

rather than (8.5). To simplify the formulae, consider now the undamped pendulum, i.e. assume that $\sigma = 0$. The cart position evolves then as

$$x(t) = x_f + \frac{4x_f}{\pi^2 - 8}\left(1 - \frac{\pi^2}{4}\left(1 - \frac{2}{T_p} t\right) + \cos\left(\frac{2\pi}{T_p} t\right)\right) \mathbb{1}_{[0, T_p/2]}(t) = \; \text{[figure]}$$

instead of two posicast steps and the step response of PR_{ME} is

$$\theta(t) = \frac{\pi}{(\pi^2 - 8)l}\left(1 - \frac{4}{T_p} t\right) \sin\left(\frac{2\pi}{T_p} t\right) \mathbb{1}_{[0, T_p/2]}(t) = \; \text{[figure]}.$$

Both x and θ above are smoother than the corresponding signals for the posicast (bang-bang) case. This is especially important regarding x, as the movements of the card should be feasible under actuator limitations.

Yet another direction to exploit the freedom of the choice of R satisfying (8.12) is consider the H_2 (quadratic) optimization problem associated with the model-matching setup (8.10). The result below presents the solution to this problem.

(a) Cart position, $x(t)$

(b) Pendulum angle, $\theta(t)$
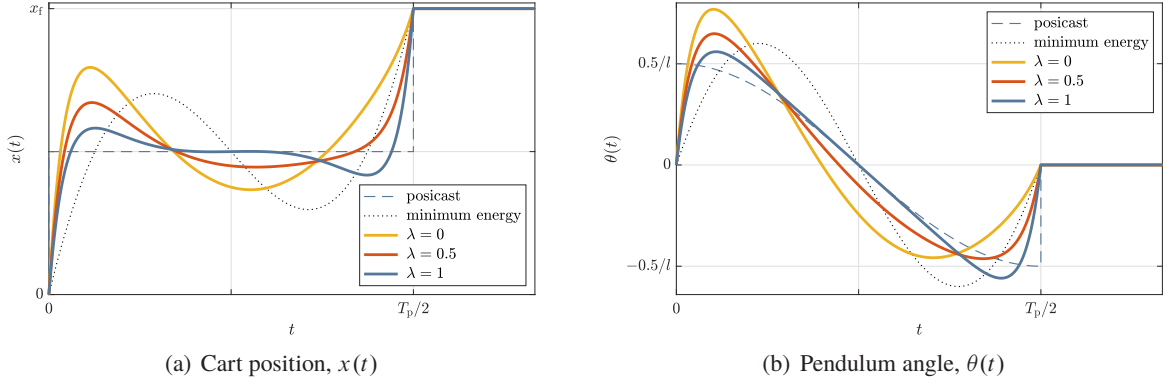
Fig. 8.3: H_2-optimal FIR control of the pendulum on cart system in Fig. 8.1 under $\varrho = 1/500$

Proposition 8.4. *If (A, B_u) in (8.11) is controllable, $D_w = 0$, and D_u has full column rank, then*

$$r(t) = -(D_u' D_u)^{-1} \begin{bmatrix} D_u' C & B_u' \end{bmatrix} e^{Ht} \left(\begin{bmatrix} I & 0 \\ 0 & 0 \end{bmatrix} + \begin{bmatrix} 0 & 0 \\ I & 0 \end{bmatrix} e^{H\tau} \right)^{-1} \begin{bmatrix} B_w \\ 0 \end{bmatrix} \mathbb{1}_{[0,\tau]}(t),$$

where

$$H := \begin{bmatrix} A & 0 \\ -C'C & -A' \end{bmatrix} - \begin{bmatrix} B_u \\ -C'D_u \end{bmatrix} (D_u' D_u)^{-1} \begin{bmatrix} D_u' C & B_u' \end{bmatrix},$$

is the impulse response of the unique FIR controller rendering G_e FIR and minimizing its H_2 norm. The optimal cost

$$\|G_e\|_2^2 = \mathrm{tr}\left(B_w' \begin{bmatrix} 0 & I \end{bmatrix} \left(\begin{bmatrix} I & 0 \\ 0 & 0 \end{bmatrix} + \begin{bmatrix} 0 & 0 \\ I & 0 \end{bmatrix} e^{H\tau} \right)^{-1} \begin{bmatrix} I \\ 0 \end{bmatrix} B_w \right).$$

Moreover, the solution in the case of $C = 0$ and $D_u' D_u = I$ recovers that of Proposition 8.3.

Proof. Follows by applying the Projection Theorem [33, Sec. 3.3] under a barrier associated with (8.12). Details, which are quite technical, can be found in [49] (it corresponds to the case of $\rho = 0$ there). $\square$

To illustrate this approach, consider again the problem studied throughout this section and define the error system as the mapping

$$w \mapsto \begin{bmatrix} \sqrt{1-\lambda}\,(\mathbb{1} - x) \\ \sqrt{\lambda}\,\theta \\ \sqrt{\varrho}\,\dot{x} \end{bmatrix},$$

where $w(t) = \delta(t) = \dot{\mathbb{1}}(t)$, the weight $\lambda \in [0, 1]$ serves to reach a required balance between settling the cart position and oscillations of the pendulum and the weight $\varrho > 0$ is used to regularize the problem ($\varrho = 0$ would render $D_u = 0$). An alternative for such a regularization might be the use of $\dot{\theta}$ instead of $\dot{x}$, as the transfer function of the system $w \mapsto \dot{\theta}$ is also bi-proper. This yields the following

$$\begin{bmatrix} G_w(s) & G_u(s) \end{bmatrix} = \begin{bmatrix} \sqrt{1-\lambda}/s & -\sqrt{1-\lambda}/s \\ 0 & \sqrt{\lambda}P(s)/s \\ 0 & \sqrt{\varrho} \end{bmatrix} = \left[\begin{array}{ccc|cc} 0 & 0 & 0 & 1 & -1 \\ 0 & -\sigma & \omega & 0 & 0 \\ 0 & -\omega & -\sigma & 0 & 1 \\ \hline \sqrt{1-\lambda} & 0 & 0 & 0 & 0 \\ 0 & -\sqrt{\lambda}\,\sigma/(l\omega) & \sqrt{\lambda}/l & 0 & 0 \\ 0 & 0 & 0 & 0 & \sqrt{\varrho} \end{array} \right]. \quad (8.14)$$

The optimal solutions for several choices of λ and $\varrho = 0.002$ are presented in Fig. 8.3. The choice of $\lambda = 1$ penalizes only the pendulum angle. In this case the response, shown by cyan-blue lines, becomes close to

that of the posicast control (dashed lines). The other extreme, $\lambda = 0$, penalizes only the deviation of the cart position from its destination. It yields a smaller error energy, but larger pendulum oscillations, see the yellow lines in Fig. 8.3.

The solution of Proposition 8.4 might not be numerically stable, as the matrix H typically has eigenvalues in $\mathbb{C}_0$. As a result, coefficients of its matrix exponential grow rapidly as τ increases. For instance, the computations in the example above fail for $\varrho \le 10^{-3}$ because one eigenvalue of H grows above 30 in this case, leading to the presence of terms $O(e^{30\tau})$ in $e^{H\tau}$. Nonetheless, this hurdle can be overcame by exploiting the Hamiltonian structure of the matrix H. Namely, bring in the algebraic Riccati equation

$$A'X + XA + C'C - (XB_u + C'D_u)(D_u'D_u)^{-1}(B_u'X + D_u'C) = 0, \tag{8.15}$$

which is the same as (6.5a) on p. 99, modulo notational differences. If the realization (A, B_u, C, D_u) has no pure imaginary invariant zeros, then [45, Sec. B.2] this ARE has a unique stabilizing solution $X = X' \ge 0$ such that $A + B_u K$ is Hurwitz, where $F := -(D_u'D_u)^{-1}(B_u X + D_u'C)$. We also need the matrix Lyapunov equation

$$(A + B_u K)W + W(A + B_u K)' + B_u(D_u'D_u)^{-1}B_u' = 0, \tag{8.16}$$

whose solution $W > 0$ because $(A + B_u K, B_u(D_u'D_u)^{-1/2})$ is controllable, which follows from the controllability of (A, B_u).

Proposition 8.5. *If (A, B_u) in (8.11) is controllable, $D_w = 0$, D_u has full column rank, and (A, B_u, C, D_u) has no pure imaginary invariant zeros, then*

$$R(s) = \pi_\tau\left\{\left[\begin{array}{c|c} A + B_u K & V_\tau B_w \\ \hline F & 0 \end{array}\right]\right\} - \sigma_\tau\left\{\left[\begin{array}{c|c} -(A + B_u K)' & W^{-1}e^{(A+B_u K)\tau}V_\tau B_w \\ \hline FW + (D_u'D_u)^{-1}B_u' & 0 \end{array}\right]e^{-\tau s}\right\}, \tag{8.17}$$

where $V_\tau := (I - We^{(A+B_u K)'\tau}W^{-1}e^{(A+B_u K)\tau})^{-1}$, is the unique FIR controller rendering G_e FIR and minimizing its H_2 norm. The optimal cost

$$\|G_e\|_2^2 = \text{tr}\left(B_w'(X + W^{-1}(V_\tau - I))B_w\right).$$

Proof (outline). It can be verified that

$$H = \left[\begin{array}{cc} I & -W \\ X & I - XW \end{array}\right]\left[\begin{array}{cc} A + B_u K & 0 \\ 0 & -A' - F'B_u' \end{array}\right]\left[\begin{array}{cc} I - WX & W \\ -X & I \end{array}\right],$$

so that

$$e^{Ht} = \left[\begin{array}{cc} I & -W \\ X & I - XW \end{array}\right]\left[\begin{array}{cc} e^{(A+B_u K)t} & 0 \\ 0 & e^{-(A+B_u K)'t} \end{array}\right]\left[\begin{array}{cc} I - WX & W \\ -X & I \end{array}\right].$$

The formulae of the proposition follow then from those of Proposition 8.4 by a routine use of (A.3b). $\square$

Proposition 8.5 offers a numerically stable alternative to the formulae of Proposition 8.4. Indeed, the impulse response of the controller in (8.17),

$$r(t) = Fe^{(A+B_u K)t}V_\tau B_w \mathbb{1}_{[0,\tau]}(t) - (FW + (D_u'D_u)^{-1}B_u')e^{(A+B_u K)'(\tau-t)}W^{-1}e^{(A+B_u K)\tau}V_\tau B_w \mathbb{1}_{[0,\tau]}(t),$$

has the matrix exponential $e^{(A+B_u K)\theta}$ and its transpose only for positive values of θ. Because the matrix $A + B_u K$ is Hurwitz, these exponentials do not tend to have growing components. Moreover, as τ grows unbounded, the second term in the right-hand side of (8.17) vanishes and we end up with the IIR controller $R(s) = F(sI - A - B_u K)^{-1}B_w$. The optimal $\|G_e\|_2$ is a monotonically decreasing function of τ, approaching $\text{tr}(B_w'XB_w)$ as $\tau \to \infty$.

8.2 Preview control

There are situations, where delays are actually our allies, rather than foes. This happens, for example, in applications where *previewed* information about reference or disturbance signals is available. Just think of a frequently encountered situation of handling road potholes or speed bumps while driving, where the ability to see those disturbances ahead of their effect is of a great help. Questions associated with exploiting previewed information arise in many applications, such as signal processing, automotive control, robotics, control of wind turbines, and so on and so forth. From the analysis viewpoint, it might be convenient to treat such problems via introducing time delays into regulated signals, which renders them a natural subject of these notes.

We again consider the general tracking setting introduced in §8.1.5, but now with the error system $G_e : w \mapsto e$ of the form

$$G_e = G_w \bar{D}_\tau + G_u R, \tag{8.18}$$

where G_w and G_u are finite-dimensional systems given by (8.11) and $\tau > 0$ is the preview. The goal is to design a causal and stable controller R to minimize a size of G_e. The term "preview tracking" becomes apparent in the case when $G_w = I$ and $G_u = -P$. The error system in this case, $G_e = \bar{D}_\tau - PR$, defines the error signal as $e(t) = w(t - \tau) - y(t)$. This implies that the plant output y is expected to track a past reference, which was available at the controller side τ time units ago. In other words, the controller has a previewed version of the reference signal w.

A key fact on addressing energy-based preview problems is that the L_2-norm of the error signal generated by (8.18) is equivalent to the L_2-norm of the output of another system having no preview for every exogenous input w. To formulate this result, we need to the matrix

$$H = \begin{bmatrix} H_{11} & H_{12} \\ H_{21} & H_{22} \end{bmatrix} := \begin{bmatrix} A & 0 \\ -C'C & -A' \end{bmatrix} - \begin{bmatrix} B_u \\ -C'D_u \end{bmatrix} (D_u'D_u)^{-1} \begin{bmatrix} D_u'C & B_u' \end{bmatrix} \tag{8.19}$$

(we already saw it in Proposition 8.4) and its exponential

$$\Sigma = \begin{bmatrix} \Sigma_{11} & \Sigma_{12} \\ \Sigma_{21} & \Sigma_{22} \end{bmatrix} := \exp\left(\begin{bmatrix} H_{11} & H_{12} \\ H_{21} & H_{22} \end{bmatrix} \tau \right),$$

in which $\det \Sigma_{22} \neq 0$, see [48, Prop. 3.1]. We also need the matrices

$$\tilde{B}_w := \Sigma_{22}' B_w + \Sigma_{12}' C' D_w \quad \text{and} \quad \tilde{C} := C + D_u(D_u'D_u)^{-1}(D_u'C(\Sigma_{22}' - I) - B_u'\Sigma_{21}').$$

The following lemma, whose proof can be found in [46], is a key technical result towards handling preview tracking problems:

Lemma 8.6. *Given G_w and G_u as in (8.11) with a full column rank D_u, consider yet another error system $\tilde{G}_e : w \mapsto \tilde{e}$ such that $\tilde{G}_e = \tilde{G}_w + \tilde{G}_u(R - \Pi)$, where*

$$\begin{bmatrix} \tilde{G}_w(s) & \tilde{G}_u(s) \end{bmatrix} = \left[\begin{array}{c|cc} A & \tilde{B}_w & B_u \\ \hline \tilde{C}\,\Sigma_{22}^{-\prime} & D_w & D_u \end{array} \right] \tag{8.20a}$$

and

$$\Pi(s) = (D_u'D_u)^{-1} \left(\sigma_\tau \left\{ \left[\begin{array}{cc|c} H_{11} & H_{12} & B_w - B_u(D_u'D_u)^{-1}D_u'D_w \\ H_{21} & H_{22} & -C'(I - (D_u'D_u)^{-1}D_u')D_w \\ \hline D_u'C & B_u' & D_u'D_w \end{array} \right] e^{-\tau s} \right\} - D_u'D_w \right). \tag{8.20b}$$

If R is such that $G_e \in H_\infty$, then so is $\tilde{G}_e$ and, moreover, $\|G_e w\|_2 = \|\tilde{G}_e w\|_2$ for all $w \in L_2(\mathbb{R}_+)$.

Lemma 8.6 fits both H_2 and H_∞ optimization settings. Consider the H_2 case first. As follows from (6.1), the squared H_2-norm of the error system equals the sum of the squared $L_2(\mathbb{R}_+)$-norms of its responses to Dirac δ-impulses applied in each input direction. By Lemma 8.6, $\|G_e e_i \delta\|_2 = \|\tilde{G}_e e_i \delta\|_2$ for every i and every controller, so that $\|G_e\|_2 = \|\tilde{G}_e\|_2$ for all R. Hence, a controller minimizing $\|G_e\|_2$ does that for $\|\tilde{G}_e\|_2$ as well. In the H_∞ case, the cost equals the $L_2(\mathbb{R}_+)$-norm of the output of the error system under a worst-case unit-energy exogenous signal w. Because the $L_2(\mathbb{R}_+)$-norms of $G_e w$ and $\tilde{G}_e w$ coincide for every w and every R, they also coincide for a worst-case w. This implies that $\|G_e\|_\infty = \|\tilde{G}_e\|_\infty$ for every R, so that the H_∞ problems for G and $\tilde{G}$ are equivalent.

One day it should be written . . .

8.3   Stabilizing delays

We saw, see e.g. discussions in Section 2.1, that loop delays normally have destabilizing effects on feedback loops. Nevertheless, there is a number of examples in the literature, demonstrating that added delays may have stabilizing effect on control loops. We consider one of them below.

Example 8.1. This example apparently originates in an SNL report of 1991, which was later on published as [64]. Consider an undamped mass-spring system $u \mapsto y$ having the transfer function

$$P(s) = \frac{1}{ms^2 + k},$$

for some known mass $m > 0$ and spring coefficient $k > 0$. Obviously, this system cannot be stabilized by any proportional controller. But it can be stabilized by a delayed feedback of the form $u(t) = -k_p y(t - \tau)$ for $k_p \neq 0$. Indeed, in this case the characteristic quasi-polynomial is

$$\chi_\tau(s) = ms^2 + k + k_p e^{-\tau s},$$

which is of the form (2.7). Let us use the delay sweeping method studied in §2.1.5 in its analysis. Assumptions $\mathcal{A}_{1\text{-}4}$ on p. 28 hold iff $k_p \neq -k$ and the delay-free is always unstable. The magnitude relation (2.8a) in this case has the form $|m\omega^2 - k| = |k_p|$, which is solved by

$$\omega^2 = \frac{k \pm |k_p|}{m}.$$

If $|k_p| \geq k$, then there is one nonzero crossing frequency and it is always a switch. Hence, this k_p is stabilizing for none τ. If $0 < |k_p| < k$, then there are two positive crossing frequencies,

$$\omega_1 = \sqrt{\frac{k + |k_p|}{m}} \quad \text{and} \quad \omega_2 = \sqrt{\frac{k - |k_p|}{m}},$$

so that $m\omega_1^2 > k$ and $m\omega_2^2 < k$ for all k_p. The corresponding phase relation (2.8b) reads

$$\tau\omega = \arg k_p - \arg(k - m\omega^2) + (2i - 1)\pi, \quad i \in \mathbb{Z}.$$

This leads then to crossing delays

$$\tau_{1i} = \frac{2\pi}{\omega_1} i + \frac{1}{\omega_1} \begin{cases} \pi & \text{if } k_p < 0 \\ 0 & \text{if } k_p > 0 \end{cases} \quad \text{and} \quad \tau_{2i} = \frac{2\pi}{\omega_2} i + \frac{1}{\omega_2} \begin{cases} 0 & \text{if } k_p < 0 \\ \pi & \text{if } k_p > 0 \end{cases}$$

for all $i \in \mathbb{Z}_+$, where τ_{1i} correspond to switches and τ_{2i} correspond to reversals. Because the zero-delay system is unstable and the step in the switches is always smaller than that in reversals, there are stabilizing

k_{p}'s only if $\tau_{20} < \tau_{10}$. This is always the case if $k_{\mathrm{p}} < 0$ and never the case if $k_{\mathrm{p}} > 0$. Thus, we must have $k_{\mathrm{p}} \in (-k, 0)$, which implies positive feedback. And then we have the following chain of crossing delays

$$\tau_j = \left\{ 0, \frac{\pi \sqrt{m}}{\sqrt{k - k_{\mathrm{p}}}}, \frac{2\pi \sqrt{m}}{\sqrt{k + k_{\mathrm{p}}}}, \frac{3\pi \sqrt{m}}{\sqrt{k - k_{\mathrm{p}}}}, \frac{4\pi \sqrt{m}}{\sqrt{k + k_{\mathrm{p}}}}, \frac{5\pi \sqrt{m}}{\sqrt{k - k_{\mathrm{p}}}}, \dots \right\}$$

(gray elements mark reversals). As far as there is one reversal between two subsequent switches, the system becomes stable at each reversal. This alternation of stabilizing and destabilizing delay intervals ends at the point where $\tau_{2i} \geq \tau_{1i}$ or, equivalently, where

$$\frac{2i\pi \sqrt{m}}{\sqrt{k + k_{\mathrm{p}}}} \geq \frac{(2i + 1)\pi \sqrt{m}}{\sqrt{k - k_{\mathrm{p}}}} \quad \Longleftrightarrow \quad i \geq \left\lceil \frac{\sqrt{1 + k_{\mathrm{p}}/k}}{2(\sqrt{1 - k_{\mathrm{p}}/k} - \sqrt{1 + k_{\mathrm{p}}/k})} \right\rceil .$$

Thus, the system can always be stabilized by a (positive) delayed feedback. $\qquad \nabla$

There are other examples in the literature, where loop delays are introduced to feedback loops to control finite-dimensional systems. It appears that there are essentially two classes of problems for which such approaches are considered.

1. One use of delayed feedback is in problems of feedback dampening lightly damped systems, like that considered in Example 8.1 above. It is known, at least since [81, 64], that it might be advantageous to add a *phase lag* into the feedback loop in such problems, cf. the loops in Fig. 2.3 on p. 26. A skillful use of this approach can yield superior closed-loop performance, as demonstrated by the solutions to the ECC'95 benchmark problem [52, 29], where finite-dimensional lag elements are used. Delays can also provide such lags. An example of that is the concept of *delayed resonators*, introduced in [54]. Still, it is not quite clear to me what advantage such delays can have over more orthodox rational lag elements. The analysis of delayed systems is more complex and phase lag introduced by the delay element grows unbounded, which might boomerang at high frequencies. Finite-dimensional lags are less prone to such problems, as they can be analyzed by conventional tools and their lags are bounded.

2. Another direction may be associated with the use of delays in approximating derivative terms, essentially as

$$s \approx \Delta_\tau(s) := \frac{1 - \mathrm{e}^{-\tau s}}{\tau} \tag{8.21}$$

for a sufficiently small $\tau > 0$. This is done either explicitly, like in the problem of stabilizing a chain of of integrators in [51], or implicitly, e.g. in the proportional-minus-delay controller, proposed in [72] as an alternative to PD. But it is not clear to me, again, what are advantages of this approximation over more conventional solutions, like a rational approximation of the form

$$s \approx \Delta_{\mathrm{r},T}(s) := \frac{s}{Ts + 1} \tag{8.22}$$

for a sufficiently small $T > 0$. For example, let us compare the accuracy of these approximations over a given low-frequency range, say $[0, \tilde{\omega}]$. To render such a comparison fair, assume that both approximations have equal high-frequency gain, i.e. that $\limsup_{\omega \to \infty} |\Delta_\tau(\mathrm{j}\omega)| = \lim_{\omega \to \infty} |\Delta_{\mathrm{r},T}(\mathrm{j}\omega)|$. This requirement yields the relation $2/\tau = 1/T$ or, equivalently, $T = \tau/2$. As the measure of the approximation accuracy consider then the quantifies

$$\epsilon_\tau(\tilde{\omega}) := \max_{\omega \in [0, \tilde{\omega}]} \left| 1 - \frac{\Delta_\tau(\mathrm{j}\omega)}{\mathrm{j}\omega} \right| \quad \text{and} \quad \epsilon_{\mathrm{r},\tau/2}(\tilde{\omega}) := \max_{\omega \in [0, \tilde{\omega}]} \left| 1 - \frac{\Delta_{\mathrm{r},\tau/2}(\mathrm{j}\omega)}{\mathrm{j}\omega} \right| .$$

The plots of these functions of the $\tilde{\omega}$ are presented in Fig. 8.4. It is clear that from this point of view the rational approximation (8.22) is a better choice than (8.21) for all frequency ranges and all τ. And, on top of this, adding delays into feedback loop renders their analysis more involved.
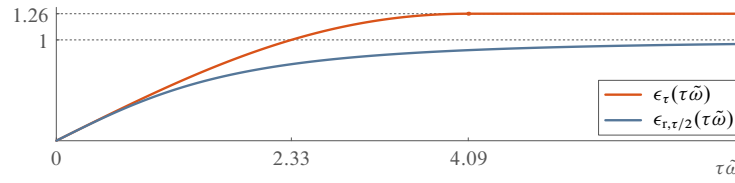
Fig. 8.4: Errors of approximating the derivative by (8.21) and (8.22)

The situation might be different for infinite-dimensional plants. We already saw that DTC elements, which contain delays, play an important role in the control of dead-time systems. As another example, consider the LTI system G_x defined via its transfer function in (1.21) on p. 9, which describes the acoustic pressure in a duct of length L, measured at the distance x from the actuation point. For $x = L$ and the static reflectance $R(s) = 1$ it becomes

$$G_L(s) = \frac{2Z_{\mathrm{m}}}{1 - \mathrm{e}^{-2\tau s}}\,\mathrm{e}^{-\tau s},$$

where $\tau = L/c$. It might not be easy to design a finite-dimensional stabilizing controller for it. However, this system is clearly stabilized by the delayed control law $u(t) = -p_L(t - \tau)/(2Z_{\mathrm{m}})$, which actually renders the closed-loop system FIR. Still, this is more a toy example, as the delayed control law above has zero tolerance to uncertainty in τ.

8.4 Delays in the regulator problem: repetitive control

The term "regulator problem" is referred to the problem of rejecting the effect of non-decaying disturbances, generated as the response of known autonomous models to nonzero initial conditions, on controlled variables. Common models for such disturbances are the integrator $1/s$, which generates constant signals, the double integrator $1/s^2$, which generates ramp signals, and the harmonic oscillator $1/(s^2 + \omega_0^2)$, which generates sine waves with the frequency ω_0. The *internal model principle* [15], by which models of exogenous signals should be incorporated into the controller, is one of fundamental principles of the control theory. For example, the need in the use of integral actions to counteract the effect of constant or slowly varying unmeasured disturbances has been known for aeons. Likewise, harmonic disturbances of a known frequency can be asymptotically canceled if the feedback loop includes a harmonic oscillator. Incorporating models of disturbances into feedback loops reduces the regulator problem to mere stabilization problems.

The use of delays can generalize this idea to a substantially wider class of exogenous signals, viz. all periodic signals of a known period. Indeed, consider the system described by the autonomous difference equation

$$w(t) = w(t - \tau), \quad \breve{w}_0 = \phi \tag{8.23}$$

for some function $\phi(t)$ defined in $[-\tau, 0]$, where $\breve{w}_t$ is defined according to (1.6) on p. 2. It is readily seen that this equation generates the τ-periodic function $w(t) = \phi(t - \tau\lceil t/\tau \rceil)$. Thus, any τ-periodic signal can be generated by (8.23) by an appropriate choice of the initial condition function ϕ.

The application of the internal model principle to (8.23) is conceptually straightforward. Namely, this system has the transfer function $1/(1 - \mathrm{e}^{-\tau s})$, so it should be incorporated into the controller. The application of this logic in the unity-feedback setting is shown in Fig. 8.5(a), where P is a SISO plant and R is a free part of the controller to be designed. This is a paraphrase of the architecture proposed in [23], dubbed *repetitive control*. As with any other controller constructed according to the internal model principle, it guarantees asymptotic rejection of all τ-periodic disturbances d and asymptotically perfect
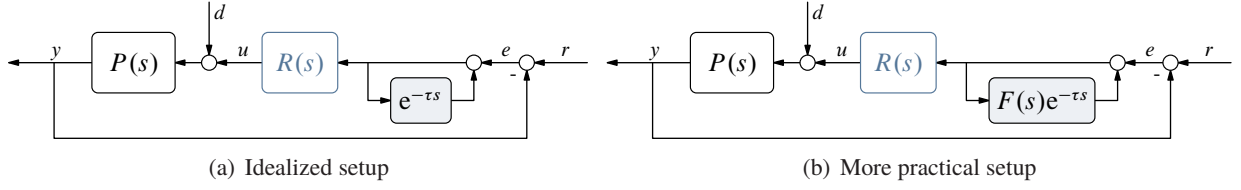
(a) Idealized setup (b) More practical setup

Fig. 8.5: Unity-feedback repetitive controller

tracking of all τ-periodic reference signals r, provided the closed-loop system is stable and $P(s)R(s)$ has no zeros at the poles of the repetitive element, i.e. at $s = \mathrm{j}2k\pi/\tau, k \in \mathbb{Z}$.

A way to see that is via the closed-loop disturbance sensitivity transfer function

$$T_{\mathrm{d}}(s) = \frac{P(s)(1 - \mathrm{e}^{-\tau s})}{1 - \mathrm{e}^{-\tau s} + P(s)R(s)},$$

which has zeros at $s = \mathrm{j}2k\pi/\tau$ for all $k \in \mathbb{Z}$ then. Every piecewise smooth periodic disturbance can be presented via its Fourier series as

$$d(t) = \sum_{k\in\mathbb{Z}} d_k \mathrm{e}^{\mathrm{j}(2k\pi/\tau)t} \tag{8.24}$$

for some Fourier coefficients $d_k \in \mathbb{C}$. By the frequency response theorem, if the closed-loop system is stable, then its steady-state response to this disturbance is

$$y_{\mathrm{ss}}(t) = \sum_{k\in\mathbb{Z}} T_{\mathrm{d}}(\mathrm{j}2k\pi/\tau)d_k \mathrm{e}^{\mathrm{j}(2k\pi/\tau)t} = 0. \tag{8.25}$$

The tracking error can be analyzed in a similar manner via the sensitivity transfer function,

$$S(s) = \frac{1 - \mathrm{e}^{-\tau s}}{1 - \mathrm{e}^{-\tau s} + P(s)R(s)},$$

which also has all pure imaginary poles of the controller as its zeros.

However, the stability of repetitive control system happens to be a challenge. To see why, assume that P and R are finite dimensional and rearrange the setup in Fig. 8.5(a) in the form presented in Fig. 2.1 on p. 19. Taking $\begin{bmatrix} r \\ d \end{bmatrix}$ as the "u" input there and y as its namesake, this corresponds to

$$\begin{bmatrix} G_{zw} & G_{zu} \\ G_{yw} & G_{yu} \end{bmatrix} = \begin{bmatrix} 0 & 0 & 0 \\ 1 & 1 & 0 \end{bmatrix} + \begin{bmatrix} 1 \\ -1 \end{bmatrix} \frac{1}{1 + PR} \begin{bmatrix} 1 & 1 & -P \end{bmatrix}.$$

If $P(s)R(s)$ is strictly proper, which is a reasonable assumption to make, then $G_{zw}(\infty) = 1$ and we have the case of $\rho(D_{zw}) = 1$ in terms of the discussion in §2.1.3. Hence, no matter what R is selected, the closed-loop system is practically unstable. In other words, the ability to reject all τ-periodic disturbances conflicts with the stability requirements in most situations.

The situation is not hopeless though. There are workarounds, endeavoring to regain the ability to stabilize the closed-loop system at the expense of relaxing the perfect regulation requirement. For example, one can use the architecture presented in Fig. 8.5(b) for a stable filter F such that $|F(\infty)| < 1$. In this case the equivalent

$$\begin{bmatrix} G_{zw} & G_{zu} \\ G_{yw} & G_{yu} \end{bmatrix} = \begin{bmatrix} 0 & 0 & 0 \\ 1 & 1 & 0 \end{bmatrix} + \begin{bmatrix} F \\ -1 \end{bmatrix} \frac{1}{1 + PR} \begin{bmatrix} 1 & 1 & -P \end{bmatrix}.$$

so that $G_{zw}(\infty) = F(\infty)$ satisfies $\rho(D_{zw}) < 1$ and the system can in principle be stabilized[2].

---

[2]Specific approaches to design stabilizing R's are discussed below.

The price we pay is in the ability to reject all periodic disturbances. Indeed, the disturbance sensitivity reads now

$$T_d(s) = \frac{P(s)(1 - F(s)e^{-\tau s})}{1 - F(s)e^{-\tau s} + P(s)R(s)}$$

and has a zero at $j2k\pi/\tau$ iff $F(j2k\pi/\tau) = 1$, which can happen only at a finite number of k's unless $F(s) = 1$. Still, we can choose F so that $|1 - F(j2k\pi/\tau)| \ll 1$ at $k \in \mathbb{Z}$ of interest. A well-justified requirement is to maintain this condition for a number of small indices k. This could effectively eliminate low-frequency Fourier terms in (8.25), while high-frequency components are normally filtered out by the plant itself. If $F(0) = 1$, then the controller still has an integral action. Thus, it might make sense to choose a low-pass F with the unit static gain. The bandwidth of F can then be a tuning parameter, with which the range of rejected signals can be selected. For example, consider the choice

$$F(s) = \frac{\omega_1 \alpha}{s + \omega_1 \alpha}, \tag{8.26}$$

where $\omega_1 := 2\pi/\tau$ is the fundamental frequency of the Fourier series in (8.24). The parameter $\alpha \in \mathbb{N}$ reflects the number of first frequencies of (8.24) located within the bandwidth of this F, which is $\omega_1 \alpha$. It can be shown that

$$\left| 1 - F\left(j\frac{2\pi}{\tau}k\right) \right| = \frac{1}{\sqrt{1 + \alpha^2/k^2}} \le \epsilon \quad \Longleftrightarrow \quad \alpha \ge k\sqrt{\frac{1}{\epsilon} - 1}$$

for an attenuation level $\epsilon \in (0, 1)$. Thus, we can attenuate well more and more harmonic components of a τ-periodic d by increasing α.

Consider now the design of a stabilizing R for the augmented plant

$$P_{\text{aug}} = \frac{P}{1 - F\bar{D}_\tau} \tag{8.27}$$

in the system in Fig. 8.5(b). This is not a conventional delay system, so methods studied in Chapter 3 are not readily applicable. A natural candidate may be the reduction approach of Fiagbedzi–Pearson from §3.3.3. In principle, if F is a low-pass filter having a strictly contractive frequency response gain for all nonzero frequencies, then unstable poles of $P_{\text{aug}}(s)$ are those of the plant and the pole at the origin of the repetitive transfer function $1/(1 - F(s)e^{-\tau s})$. If only those modes are intended to be shifted by feedback, then the solution of the left characteristic matrix equation (3.34) should be simplified. Still, this might not be an ideal solution, as the other modes of the repetitive element, at least several of them, are supposed to be very lightly damped.

Arguably, the prevalent approach to stabilize repetitive control schemes is via the use of robust stability arguments. As already discussed, the characteristic equation of the closed-loop system in Fig. 8.5(b) is that of the feedback interconnection of the "nominal" weighted sensitivity function $F/(1 + PR)$ with $\bar{D}_\tau$. By the Small Gain Theorem, see [82, §4.4.2] or [12, Sec. III.2], this interconnection is stable whenever $\|F/(1+PR)\|_\infty < 1$. Thus, we can design a stabilizing R via solving the weighted sensitivity H_∞ problem for the finite-dimensional plant P and weight F. Having to solve a finite-dimensional stabilization problem is convenient. However, this approach is an overkill, as the resulting system will be stable for every τ. This is not what we really need here, the delay element in Fig. 8.5 is a part of the controller and is generated by us.

An alternative approach, which leads to a surprisingly simple solution to the stabilization problem, is to exploit the loop-shifting technique discussed in §3.4.1. To see that, *assume* that the augmented plant in (8.27) can be expressed in the form

$$P_{\text{aug}} = \frac{\tilde{P}}{1 - \tilde{P}\Pi} \tag{8.28}$$

for some finite-dimensional $\tilde{P}$ and an infinite-dimensional $\Pi \in H_\infty$. This is the feedback interconnection of $\tilde{P}$ and Π and loop can now be shifted by the stable Π similarly to what is shown in Fig. 3.9 on p. 62. The difference is that now the plant and the controller are swapped, so the initial feedback part of the plant becomes a parallel addition to the controller (mind the the external feedback loop in Fig. 8.5 is negative). Hence, if required $\tilde{P}$ and Π exist, then a controller R stabilizes P_{aug} iff $\tilde{R} := R - \Pi$ stabilizes the finite-dimensional $\tilde{P}$. Thus, all we need is to stabilize a finite-dimensional $\tilde{P}$ by some controller, say $\tilde{R}$, and then implement $R = \tilde{R} + \Pi$.

In the procedure above stabilization effectively boils down to transforming (8.27) into form (8.28). To find required $\tilde{P}$ and Π, equate the reciprocals of the right-hand sides of (8.27) and (8.28), i.e.

$$\frac{1}{P} - \frac{F}{P}\bar{D}_\tau = \frac{1}{\tilde{P}} - \Pi. \tag{8.29}$$

If the system F/P is stable, then possible admissible choices are

$$\tilde{P} = P \quad \text{and} \quad \Pi = \frac{F}{P}\bar{D}_\tau. \tag{8.30}$$

The conditions for the stability of F/P are that every unstable zero of $P(s)$ is a zero of $F(s)$ as well and the pole excess of $F(s)$ is at least that of $P(s)$. These conditions are effectively nonrestrictive for minimum-phase plants, because the pole excess of $F(s)$ can be chosen arbitrarily large without affecting its properties in the repetitive control context (just add stable poles far beyond the required bandwidth). If $P(s)$ is nonminimum-phase, then the procedure is a bit more complex. Assume, for the sake of simplicity, that $F(s)/P(s)$ is proper. We know, from the discussion in §3.4.2, that there is a finite-dimensional system $\tilde{F}$, whose transfer function is proper, such that $\tilde{F} = F/P\,\bar{D}_\tau + \sigma_\tau\{F/P\,\bar{D}_\tau\}$, where $\sigma_\tau\{\cdot\}$ is the completion operator as in (3.41), always producing a stable system. Hence, (8.29) can be rewritten as

$$\frac{1}{P} - \tilde{F} + \sigma_\tau\left\{\frac{F}{P}\bar{D}_\tau\right\} = \frac{1}{\tilde{P}} - \Pi$$

and we may choose

$$\tilde{P} = \frac{P}{1 - P\tilde{F}} \quad \text{and} \quad \Pi = -\sigma_\tau\left\{\frac{F}{P}\bar{D}_\tau\right\}. \tag{8.31}$$

Thus, we again have a finite-dimensional $\tilde{P}$ and a stable Π.

With this choice, the closed-loop sensitivity and disturbance sensitivity transfer functions are

$$S(s) = \frac{1}{1 + \tilde{P}(s)\tilde{R}(s)}\frac{\tilde{P}(s)}{P(s)}(1 - F(s)e^{-\tau s}) \quad \text{and} \quad T_{\text{d}}(s) = \frac{\tilde{P}(s)}{1 + \tilde{P}(s)\tilde{R}(s)}(1 - F(s)e^{-\tau s}),$$
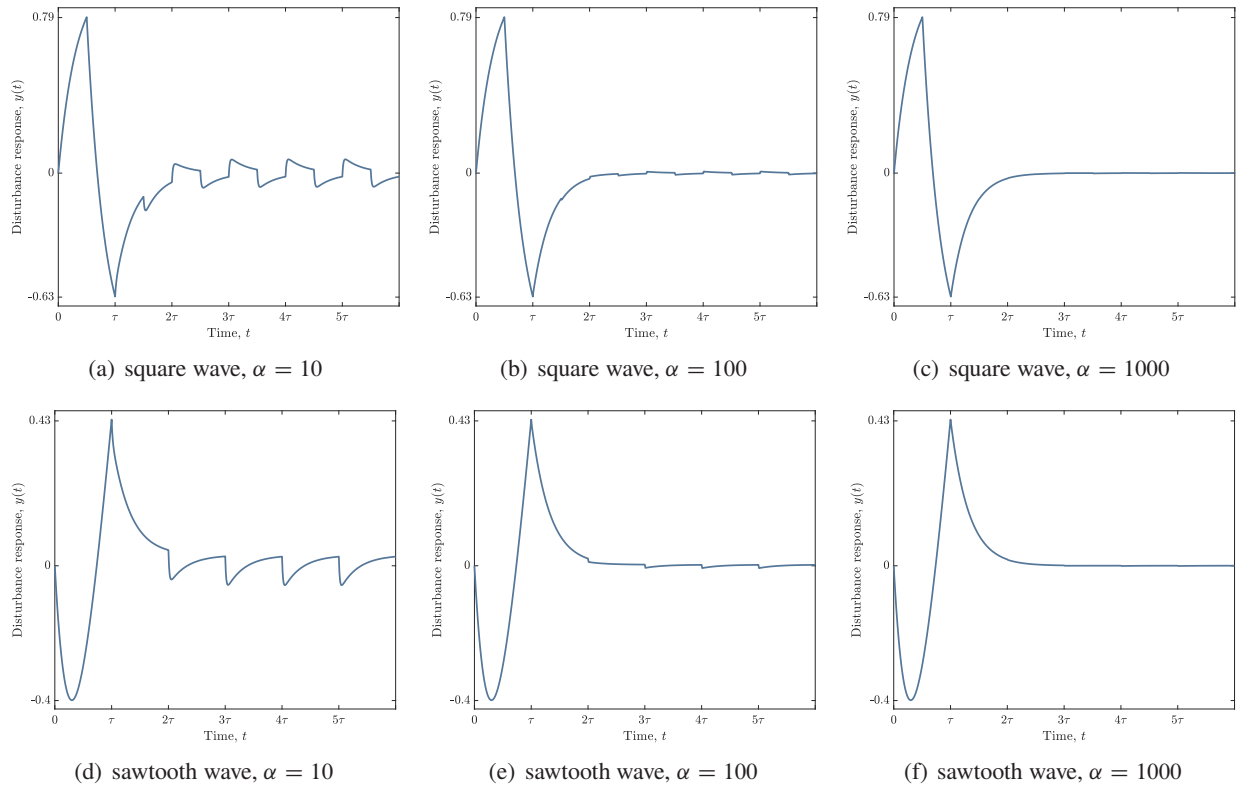
respectively. In the minimum-phase case, when $\tilde{P} = P$, the structure of these closed-loop transfer functions is reminiscent of the Smith controller in that the response is that of the system without the repetitive block, multiplied by the repetitive action. More analogies can be drawn from the fact that the closed-loop characteristic function is a plain polynomial now.

Example 8.2. Consider the problem of rejecting τ-periodic load disturbance for the plain integrator plant with the transfer function

$$P(s) = \frac{1}{s}.$$

Choosing the filter F as in (8.26), we have

$$\frac{F(s)}{P(s)} = \frac{\omega_1 \alpha s}{s + \omega_1 \alpha},$$

(a) square wave, $\alpha = 10$

(b) square wave, $\alpha = 100$

(c) square wave, $\alpha = 1000$

(d) sawtooth wave, $\alpha = 10$

(e) sawtooth wave, $\alpha = 100$

(f) sawtooth wave, $\alpha = 1000$

Fig. 8.6: Disturbance responses under $k_\mathrm{p} = 1$

which is obviously stable (it would be stable for any strictly proper $F(s)$, as a matter of fact). Thus, we can use (8.30) and design the "primary controller" $\tilde{R}$ to stabilize the plain integrator $\tilde{P} = P$. The latter problem is simple, e.g. it can be solved with any proportional controller $\tilde{R}(s) = k_\mathrm{p}$. Thus, we end up with

$$R(s) = k_\mathrm{p} + \frac{\omega_1 \alpha s}{s + \omega_1 \alpha} \mathrm{e}^{-\tau s},$$

which is easy to implement.

Simulations of the closed-loop disturbance response for this filter under $k_\mathrm{p} = 1$ and $\tau = \pi$ are presented in Fig. 8.6. The first row in Fig. 8.6 shows responses to a square wave disturbance and the second—to a sawtooth d, both of unit amplitude. The simulations agree with the analysis above that higher-bandwidth F result in a better attenuation of periodic load disturbances. Note that the disturbance response in the first interval $t \in [0, \tau]$ does not depend on α. This is because during this interval the initial conditions of the controller are zero and the repetitive part is not efficient. The controller then "learns" the actual waveform of the disturbance and compensates it. ∇

Appendix A

Mathematical Background

THIS APPENDIX collects mathematical facts required throughout the text. They can be found in many advanced books on linear MIMO control and are rather standard. Their presentation here aims at providing a convenient reference, rather then a tutorial exposition of corresponding topics. As such, the exposition is rather laconic at times.

A.1 Linear algebra

We start with a collection of results on matrices and matrix equations. These results are required throughout these notes, yet are not always a part of basic Linear Algebra courses. Some proofs are presented mostly for fun.

A.1.1 Schur complement

Let M be a square matrix partitioned as

$$M = \begin{bmatrix} M_{11} & M_{12} \\ M_{21} & M_{22} \end{bmatrix}, \tag{A.1}$$

with square M_{11} and M_{22}. If M_{11} is nonsingular, then a direct substitution yields the decomposition

$$\begin{bmatrix} M_{11} & M_{12} \\ M_{21} & M_{22} \end{bmatrix} = \begin{bmatrix} I & 0 \\ M_{21}M_{11}^{-1} & I \end{bmatrix} \begin{bmatrix} M_{11} & 0 \\ 0 & M_{22} - M_{21}M_{11}^{-1}M_{12} \end{bmatrix} \begin{bmatrix} I & M_{11}^{-1}M_{12} \\ 0 & I \end{bmatrix}. \tag{A.2a}$$

It follows from this equality that M is nonsingular iff so is the matrix

$$\Delta_{11} := M_{22} - M_{21}M_{11}^{-1}M_{12},$$

which is called the *Schur complement* of M_{11} in M. Similarly, if M_{22} is nonsingular, then

$$\begin{bmatrix} M_{11} & M_{12} \\ M_{21} & M_{22} \end{bmatrix} = \begin{bmatrix} I & M_{12}M_{22}^{-1} \\ 0 & I \end{bmatrix} \begin{bmatrix} M_{11} - M_{12}M_{22}^{-1}M_{21} & 0 \\ 0 & M_{22} \end{bmatrix} \begin{bmatrix} I & 0 \\ M_{22}^{-1}M_{21} & I \end{bmatrix} \tag{A.2b}$$

and the Schur complement of M_{22} is defined as

$$\Delta_{22} := M_{11} - M_{12}M_{22}^{-1}M_{21}.$$

Using equations (A.2) the following formulae for the inversion of block 2×2 matrices can be derived:

$$\begin{bmatrix} M_{11} & M_{12} \\ M_{21} & M_{22} \end{bmatrix}^{-1} = \begin{bmatrix} I & -M_{11}^{-1}M_{12} \\ 0 & I \end{bmatrix} \begin{bmatrix} M_{11}^{-1} & 0 \\ 0 & \Delta_{11}^{-1} \end{bmatrix} \begin{bmatrix} I & 0 \\ -M_{21}M_{11}^{-1} & I \end{bmatrix} \quad \text{(if } \det M_{11} \neq 0\text{)}$$

$$= \begin{bmatrix} M_{11}^{-1} + M_{11}^{-1}M_{12}\Delta_{11}^{-1}M_{21}M_{11}^{-1} & -M_{11}^{-1}M_{12}\Delta_{11}^{-1} \\ -\Delta_{11}^{-1}M_{21}M_{11}^{-1} & \Delta_{11}^{-1} \end{bmatrix} \tag{A.3a}$$

$$= \begin{bmatrix} I & 0 \\ -M_{22}^{-1}M_{21} & I \end{bmatrix} \begin{bmatrix} \Delta_{22}^{-1} & 0 \\ 0 & M_{22}^{-1} \end{bmatrix} \begin{bmatrix} I & -M_{12}M_{22}^{-1} \\ 0 & I \end{bmatrix} \quad \text{(if } \det M_{22} \neq 0\text{)}$$

$$= \begin{bmatrix} \Delta_{22}^{-1} & -\Delta_{22}^{-1}M_{12}M_{22}^{-1} \\ -M_{22}^{-1}M_{21}\Delta_{22}^{-1} & M_{22}^{-1} + M_{22}^{-1}M_{21}\Delta_{22}^{-1}M_{12}M_{22}^{-1} \end{bmatrix}. \tag{A.3b}$$

The formulae above are particularly simple in the case of block-triangular matrices:

$$\begin{bmatrix} M_{11} & M_{12} \\ 0 & M_{22} \end{bmatrix}^{-1} = \begin{bmatrix} M_{11}^{-1} & -M_{11}^{-1}M_{12}M_{22}^{-1} \\ 0 & M_{22}^{-1} \end{bmatrix} \tag{A.4a}$$

and

$$\begin{bmatrix} M_{11} & 0 \\ M_{21} & M_{22} \end{bmatrix}^{-1} = \begin{bmatrix} M_{11}^{-1} & 0 \\ -M_{22}^{-1}M_{21}M_{11}^{-1} & M_{22}^{-1} \end{bmatrix}. \tag{A.4b}$$

Another useful consequence of the decompositions in (A.2) is the following formulae for the determinant of block 2×2 matrices:

$$\det M_{11} \neq 0 \quad \Longrightarrow \quad \det M = \det M_{11} \det \Delta_{11} \tag{A.5a}$$

and

$$\det M_{22} \neq 0 \quad \Longrightarrow \quad \det M = \det M_{22} \det \Delta_{22} \tag{A.5b}$$

(the determinants of the triangle factors in (A.2) obviously equal one).

A.1.2   Sign-definite matrices

An $n \times n$ matrix $M = M'$ is said to be *positive definite*, denoted $M > 0$, if

$$x'Mx > 0, \quad \forall x \neq 0.$$

It is *positive semi-definite*, denoted $M \geq 0$, if

$$x'Mx \geq 0, \quad \forall x.$$

The notions of negative definite ($M < 0$) and semi-definite ($M \leq 0$) matrices can be defined in a similar way or via the relations $M < 0 \iff -M > 0$ and $M \leq 0 \iff -M \geq 0$. Compatibly dimensioned symmetric (or Hermitian) matrices can be compared. We say that $M_1 > M_2$ if $M_1 - M_2 > 0$ and that $M_1 \geq M_2$ if $M_1 - M_2 \geq 0$. A criterion of positive definiteness (positive semi-definiteness) is that all eigenvalues of $M = M'$, which are real, are positive (nonnegative). Unlike scalars, matrices need not be wither positive or negative (semi)definite. There are matrices that are not sign definite, like $M = \begin{bmatrix} 1 & 0 \\ 0 & -1 \end{bmatrix}$.

If a matrix $T \in \mathbb{R}^{n \times m}$, where $m \leq n$, has full rank, then $M > 0$ only if $T'MT > 0$. Indeed, if $T'MT \not> 0$, there is $y \neq 0$ such that $y'T'MTy \leq 0$. But then $x'Mx \leq 0$ for $x = Ty \neq 0$. If $m = n$,

then the relation goes both ways, namely, $M > 0 \iff T'MT > 0$. These properties help to simplify the analysis of block 2×2 matrices of the form (A.1). For example, it is readily seen that

$$\begin{bmatrix} M_{11} & M_{12} \\ M_{21} & M_{22} \end{bmatrix} > 0 \implies M_{11} > 0 \wedge M_{22} > 0.$$

Moreover, it follows from (A.2) that

$$\begin{bmatrix} M_{11} & M_{12} \\ M_{21} & M_{22} \end{bmatrix} > 0 \iff M_{11} > 0 \wedge \Delta_{11} > 0 \iff M_{22} > 0 \wedge \Delta_{22} > 0 \tag{A.6}$$

(these relations use the fact that the positive-definiteness of a block-diagonal matrix is equivalent to that of each its diagonal block).

A.2 Matrix equations

A.2.1 Linear matrix equations

Let $A_1 \in \mathbb{R}^{n_1 \times n_1}$, $A_2 \in \mathbb{R}^{n_2 \times n_2}$, and $Q \in \mathbb{R}^{n_1 \times n_2}$. The following linear matrix equation:

$$A_1 X - X A_2 + Q = 0 \tag{A.7}$$

is called the *Sylvester equation*. It has a unique solution $X \in \mathbb{R}^{n_1 \times n_2}$ iff

$$\mathrm{spec}(A_1) \cap \mathrm{spec}(A_2) = \emptyset,$$

i.e. iff none of the eigenvalues of A_1 is also an eigenvalue of A_2. If this condition fails to hold, then the Sylvester equation might have either no solutions or an infinite number of solutions (depending on Q). The following result establishes the connection between the solvability of (A.7) with the block-diagonalizability of certain block-triangular matrices:

Proposition A.1 (Roth's removal rule). *Equation* (A.7) *is solvable iff the matrices*

$$\begin{bmatrix} A_1 & Q \\ 0 & A_2 \end{bmatrix} \quad \text{and} \quad \begin{bmatrix} A_1 & 0 \\ 0 & A_2 \end{bmatrix}$$

are similar.

An important particular case of the Sylvester equation is the so-called (continuous-time) *Lyapunov equation*, which is defined as

$$AX + XA' + Q = 0 \tag{A.8}$$

for given $A \in \mathbb{R}^{n \times n}$ and $Q \in \mathbb{R}^{n \times n}$. If Q is symmetric (i.e. $Q = Q'$), then the solution X is symmetric too. Furthermore, if A is Hurwitz, i.e. if A has all its eigenvalues in the open left half plane $\mathbb{C} \setminus \overline{\mathbb{C}}_0$, then

$$X = \int_{\mathbb{R}_+} e^{At} Q e^{A't} \, dt \tag{A.9}$$

exists and is the solution of (A.8). Indeed, it is readily seen that

$$A e^{At} Q e^{A't} + e^{At} Q e^{A't} A' = \frac{d}{dt} \left(e^{At} Q e^{A't} \right).$$

Thus, if the integral in (A.9) exists,

$$A \int_{\mathbb{R}_+} e^{At} Q e^{A't} \, dt + \int_{\mathbb{R}_+} e^{At} Q e^{A't} \, dt \, A' + Q = \int_{\mathbb{R}_+} d(e^{At} Q e^{A't}) + Q = 0,$$

where the fact that $\lim_{t \to \infty} e^{At} Q e^{A't} = 0$ was used.

The following result reveals an important connection between the existence of positive definite solution of a Lyapunov equation and the stability of matrices:

Proposition A.2. *A matrix $A \in \mathbb{R}^{n \times n}$ is Hurwitz iff the solution $X \in \mathbb{R}^{n \times n}$ of the Lyapunov equation* (A.8) *satisfies $X = X' > 0$ whenever $Q = Q' > 0$.*

Proof. First, assume that A is Hurwitz. Clearly, (A, Q) is controllable (follows from the non-singularity of Q), so that $X > 0$ by (A.9). Now, let $X > 0$ for some $Q > 0$. Assume that A is not Hurwitz, i.e. that it has an eigenvalue λ such that $\text{Re } \lambda \geq 0$. Denote the corresponding eigenvector by $\eta \neq 0$ and pre- and post-multiply (A.8) by η' and η, respectively. We have:

$$-\eta' Q \eta = \eta'(AX + XA')\eta = \lambda \eta' X \eta + \overline{\lambda} \eta' X \eta = 2 \text{Re } \lambda \eta' X \eta.$$

This, in turn, implies that $\text{Re } \lambda \eta' X \eta < 0$, which is a contradiction. $\qquad\square$

Proposition A.2 actually says that the stability of A is equivalent to the existence of a matrix $X = X' > 0$ such that

$$AX + XA' < 0. \tag{A.10}$$

Inequality (A.10) belongs to the so-called class of *Linear Matrix Inequalities* (LMI), for the verification of which efficient numerical methods are available. For this reason (A.10) can be considered an alternative to the conventional verification of eigenvalues of A. More important is that the LMI (A.10) can be incorporated into many other analysis and design problems that also reduce to LMIs.

A.2.2   Quadratic matrix equations

A matrix equation of the form

$$A'X + XA + Q + XRX = 0 \tag{A.11}$$

for some matrices $A \in \mathbb{R}^{n \times n}$, $Q = Q' \in \mathbb{R}^{n \times n}$, and $R = R' \in \mathbb{R}^{n \times n}$ is called the (continuous-time) *algebraic Riccati equation* (ARE). Such equations can be thought of as a matrix extension of the standard quadratic equation $rx^2 + 2ax + q = 0$. Like in the quadratic equation case, a solution X of the ARE of the form (A.11) is not unique. In control applications we are mostly concerned with the so-called *stabilizing* solution, which is defined as the solution for which the matrix $A + RX$ is Hurwitz (stable). The stabilizing solution *is* unique (if exists) as proved below:

Proposition A.3. *If there is a stabilizing solution to* (A.11), *then it is unique.*

Proof. Assume, on the contrary, that there are two stabilizing solutions, say X_1 and X_2, satisfying

$$A'X_1 + X_1 A + Q + X_1 R X_1 = 0 \quad \text{and} \quad A'X_2 + X_2 A + Q + X_2 R X_2 = 0$$

with Hurwitz matrices $A_1 := A + RX_1$ and $A_2 := A + RX_2$. Subtracting the second equation from the first one and denoting $X_\delta := X_1 - X_2$ we obtain:

$$\begin{aligned}
0 &= A'X_1 + X_1 A_1 + Q - (A'X_2 + X_2 A_2 + Q) \\
&= A'X_\delta + X_1 A_1 - X_2 A_2 \pm X_2 A_1 = A'X_\delta + X_\delta A_1 + X_2(A_1 - A_2) = A'X_\delta + X_\delta A_1 + X_2 R X_\delta \\
&= A_2' X_\delta + X_\delta A_1.
\end{aligned}$$

This is a Sylvester equation and since A_1 and A_2 are Hurwitz, it has a unique solution, which is obviously $X_\delta = 0$. Thus, $X_1 = X_2$. $\qquad\square$

Crucial for studying AREs, as well as for their numerical solutions, is the fact that solutions of (A.11) can be expressed in terms of the eigenstructure of certain matrices. To see this, note that (A.11) can be equivalently written as

$$\begin{bmatrix} A & R \\ -Q & -A' \end{bmatrix} \begin{bmatrix} I \\ X \end{bmatrix} = \begin{bmatrix} I \\ X \end{bmatrix} (A + RX) \tag{A.12}$$

(here the first row is an obvious equality, whereas the second row is just a rewritten (A.11)). This equation is actually reminiscent of the eigenvalue equation. Connections indeed exist. To see them, denote

$$H := \begin{bmatrix} A & R \\ -Q & -A' \end{bmatrix} \in \mathbb{R}^{2n \times 2n}. \tag{A.13}$$

Let η be an eigenvector of $A + RX$ corresponding to an eigenvalue λ. Post-multiplying (A.12) by η and denoting $\eta_H := \begin{bmatrix} I \\ X \end{bmatrix} \eta$, we obtain that $H \eta_H = \lambda \eta_H$. This implies that any eigenvalue of the $n \times n$ matrix $A + RX$ is an eigenvalue of the $2n \times 2n$ matrix H as well.

To understand properties of H, introduce the $2n \times 2n$ skew-symmetric matrix

$$J := \begin{bmatrix} 0 & -I \\ I & 0 \end{bmatrix}. \tag{A.14}$$

It is readily verified that $J^{-1} = -J$, so J is also unitary. The direct substitution then shows that

$$J^{-1} H J = -H' \tag{A.15}$$

(such matrices are called *Hamiltonian*). This implies that H and $-H'$ are similar. Hence, λ is an eigenvalue of H iff its imaginary axis mirror, $-\bar{\lambda}$, is an eigenvalue of H.

Now, if $A + RX$ is stable, H should have n eigenvalues in $\mathbb{C} \setminus \bar{\mathbb{C}}_0$. This, in turn, means that the other n eigenvalues of H must be in $\mathbb{C}_0$ and this partition of the spectrum of H (n eigenvalues in $\mathbb{C} \setminus \bar{\mathbb{C}}_0$ and the other n—in the $\mathbb{C}_0$) is unique. Of course, this partition is possible iff H has no jω-axis eigenvalues, which is thus necessary for the ARE (A.11) to have a stabilizing solution. This is not sufficient though. Some insight why is this true can be gained through the reexamination of the eigenvector structure of H. Indeed, it follows from the formula $\eta_H = \begin{bmatrix} \eta \\ X\eta \end{bmatrix}$ and the fact that η is a (non-zero) eigenvector of $A + RX$ that at least one of the first n components of η_H must be non-zero. This is not necessarily true for all stable (i.e. those corresponding to stable eigenvalues) eigenvectors of Hamiltonian matrices as can be seen in the following simple example:

$$H = \left[\begin{array}{cc|cc} -1 & 0 & 1 & 0 \\ 0 & 1 & 0 & 0 \\ \hline -1 & -1 & 1 & 0 \\ -1 & -1 & 0 & -1 \end{array} \right], \quad \text{for which spec}(H) = \{\pm 1, \pm \sqrt{2}\} \text{ and } \lambda = -1 \text{ has } \eta_H = \left[\begin{array}{c} 0 \\ 0 \\ \hline 0 \\ 1 \end{array} \right]. \tag{A.16}$$

The corresponding ARE has no stabilizing solutions indeed, which can be easily seen from the fact that the pair $(A, R) = \left(\begin{bmatrix} -1 & 0 \\ 0 & 1 \end{bmatrix}, \begin{bmatrix} 1 & 0 \\ 0 & 0 \end{bmatrix} \right)$ is not stabilizable, so that there is no X for which $A + RX$ is stable.

For general R, there might not be an easy criterion, in terms of A, Q, and R, for the existence of a stabilizing solution X to (A.11). The situation is more transparent for sign semi-definite R's as the following result shows:

Theorem A.4. *If either $R \geq 0$ or $R \leq 0$, then there is a stabilizing solution of the ARE* (A.11) *iff H has no jω-axis eigenvalues and the pair (A, R) is stabilizable. Moreover, a stabilizing solution is always symmetric, i.e. $X = X'$.*

Proof. The necessity of $\mathrm{spec}(H) \cap j\mathbb{R} = \emptyset$ was shown before. Hence, we may assume that H has no $j\omega$-axis eigenvalues. Then there always exists a nonsingular $T \in \mathbb{R}^{2n \times 2n}$ such that

$$
T^{-1}HT = \begin{bmatrix} T_{11} & T_{12} \\ T_{21} & T_{22} \end{bmatrix}^{-1} \begin{bmatrix} A & R \\ -Q & -A' \end{bmatrix} \begin{bmatrix} T_{11} & T_{12} \\ T_{21} & T_{22} \end{bmatrix} = \begin{bmatrix} H_\mathrm{s} & H_{12} \\ 0 & H_{\bar{\mathrm{s}}} \end{bmatrix},
$$

where H_s and $-H_{\bar{\mathrm{s}}}$ are Hurwitz (one such T, which is orthogonal, can be obtained by the Schur decomposition of H). Equivalently,

$$
\begin{bmatrix} A & R \\ -Q & -A' \end{bmatrix} \begin{bmatrix} T_{11} & T_{12} \\ T_{21} & T_{22} \end{bmatrix} = \begin{bmatrix} T_{11} & T_{12} \\ T_{21} & T_{22} \end{bmatrix} \begin{bmatrix} H_\mathrm{s} & H_{12} \\ 0 & H_{\bar{\mathrm{s}}} \end{bmatrix},
$$

from which

$$
\begin{bmatrix} A & R \\ -Q & -A' \end{bmatrix} \begin{bmatrix} T_{11} \\ T_{21} \end{bmatrix} = \begin{bmatrix} T_{11} \\ T_{21} \end{bmatrix} H_\mathrm{s}. \tag{A.17}
$$

In fact, for any such T we have that $T_{21}'T_{11}$ is symmetric. To see this, pre-multiply (A.17) by $\begin{bmatrix} T_{11}' & T_{21}' \end{bmatrix} J$, where J is defined in (A.14), to get

$$
\begin{bmatrix} T_{11}' & T_{21}' \end{bmatrix} \begin{bmatrix} 0 & -I \\ I & 0 \end{bmatrix} \begin{bmatrix} A & R \\ -Q & -A' \end{bmatrix} \begin{bmatrix} T_{11} \\ T_{21} \end{bmatrix} = \begin{bmatrix} T_{11}' & T_{21}' \end{bmatrix} \begin{bmatrix} 0 & -I \\ I & 0 \end{bmatrix} \begin{bmatrix} T_{11} \\ T_{21} \end{bmatrix} H_\mathrm{s}
$$

or, equivalently (mind the fact that $JH = -H'J$ as H is Hamiltonian),

$$
-H_\mathrm{s}'(T_{11}'T_{21} - T_{21}'T_{11}) = (T_{11}'T_{21} - T_{21}'T_{11})H_\mathrm{s}.
$$

This is a Lyapunov equation of the form (A.8) with Hurwitz $A = H_\mathrm{s}$ and $Q = 0$, hence its unique solution is $T_{11}'T_{21} - T_{21}'T_{11} = 0$.

Now, show that there is a stabilizing solution iff T_{11} is nonsingular. The "if" part follows by construction, as in this case $X = T_{21}T_{11}^{-1}$ is the required solution with $A + RX = T_{11}H_\mathrm{s}T_{11}^{-1}$ (can be verified by a direct substitution). To prove the "only if" part, assume that there is a stabilizing solution X. Eqn. (A.12) can then be complemented to

$$
\begin{bmatrix} A & R \\ -Q & -A' \end{bmatrix} \begin{bmatrix} I & 0 \\ X & I \end{bmatrix} = \begin{bmatrix} I & 0 \\ X & I \end{bmatrix} \begin{bmatrix} A + RX & R \\ 0 & -(A' + XR) \end{bmatrix}
$$

(as a matter of fact, this shows that $A' + XR$ is Hurwitz because the $(2, 2)$ block in the last matrix above should contain all n RHP eigenvalues of H). This implies that

$$
\begin{bmatrix} A + RX & R \\ 0 & -(A' + XR) \end{bmatrix} = \begin{bmatrix} I & 0 \\ -X & I \end{bmatrix} \begin{bmatrix} T_{11} & T_{12} \\ T_{21} & T_{22} \end{bmatrix} \begin{bmatrix} H_\mathrm{s} & H_{12} \\ 0 & H_{\bar{\mathrm{s}}} \end{bmatrix} \left(\begin{bmatrix} I & 0 \\ -X & I \end{bmatrix} \begin{bmatrix} T_{11} & T_{12} \\ T_{21} & T_{22} \end{bmatrix} \right)^{-1},
$$

which, in turn, leads to

$$
\begin{bmatrix} A + RX & R \\ 0 & -(A' + XR) \end{bmatrix} \begin{bmatrix} T_{11} \\ T_{21} - XT_{11} \end{bmatrix} = \begin{bmatrix} T_{11} \\ T_{21} - XT_{11} \end{bmatrix} H_\mathrm{s}.
$$

The second row above reads $(A' + XR)(T_{21} - XT_{11}) + (T_{21} - XT_{11})H_\mathrm{s} = 0$, which is a Sylvester equation having the unique solution (as the matrices $A' + XR$ and H_s are Hurwitz) $T_{21} - XT_{11} = 0$. This equality implies that if there is a vector $\eta \neq 0$ such that $T_{11}\eta = 0$, then $T \begin{bmatrix} \eta \\ 0 \end{bmatrix} = 0$, which is a contradiction because T is nonsingular.

Next, show that T_{11} is nonsingular iff the pair (A, R) is stabilizable. The "only if" part here is straightforward, otherwise $A + RT_{21}T_{11}^{-1} = T_{11}H_\mathrm{s}T_{11}^{-1}$ cannot be stable. The "if" part, i.e. the proof that the

stabilizability of (A, R) implies $\det(T_{11}) \neq 0$, is more involved. To show it, assume the opposite, i.e. that $\det(T_{11}) = 0$ despite the stabilizability of (A, R). Pick any $0 \neq \eta \in \ker T_{11}$ and pre- and post-multiply the first row of (A.17) by $\eta' T_{21}'$ and η, respectively. This yields (mind the symmetry of $T_{21}' T_{11}$)

$$\eta' T_{21}'(AT_{11} + RT_{21})\eta = \eta' T_{21}' T_{11} H_s \eta = \eta' T_{11}' T_{21} H_s \eta$$

and then $\eta' T_{21}' R T_{21} \eta = 0$. This is the part where the sign definiteness of R is used as then the last equality implies that $RT_{21}\eta = 0$. This, in turn, leads to $T_{11} H_s \eta = 0$ from the first row of (A.17). Since $\eta \in \ker T_{11}$ is arbitrary, we actually just proved that $H_s \ker T_{11} \subset \ker T_{11}$, i.e. that $\ker T_{11}$ is H_s-invariant. It is a known fact that any (nonzero) invariant subspace of a matrix M contains at least one eigenvector of M. So there is a vector $0 \neq \zeta \in \ker T_{11}$ such that $H_s \zeta = \lambda \zeta$ for some $\operatorname{Re} \lambda < 0$. Post-multiplying (A.17) by this ζ we have:

$$\begin{bmatrix} R \\ -A' \end{bmatrix} T_{21}\zeta = \begin{bmatrix} 0 \\ \lambda I \end{bmatrix} T_{21}\zeta \iff \begin{bmatrix} R \\ A' + \lambda I \end{bmatrix} T_{21}\zeta = 0 \iff \zeta' T_{21}' \begin{bmatrix} A - (-\lambda)I & R \end{bmatrix} = 0.$$

The detectability of (A, R) then yields (via the PBH test) that the latter necessarily yields $T_{21}\zeta = 0$. As $T_{11}\zeta = 0$ too and T is nonsingular, we have a contradiction. Hence, $\det(T_{11}) \neq 0$.

Thus, we just proved that there is a stabilizing solution X iff (A, R) is stabilizable and this stabilizing $X = T_{21} T_{11}^{-1}$ for any T_{11} and T_{21} satisfying (A.17). Rewrite

$$X = (T_{11}^{-1})' T_{11}' T_{21} T_{11}^{-1} = (T_{11}^{-1})' T_{21}' T_{11} T_{11}^{-1} = (T_{11}^{-1})' T_{21}' = X'.$$

This completes the proof. □

A.3 Linear-fractional transformations

Linear fractional transformations (LFTs) of Δ by G can be seen as a general interconnection of two mappings (operators),

$$G = \begin{bmatrix} G_{11} & G_{12} \\ G_{21} & G_{22} \end{bmatrix} : (u_1, u_2) \mapsto (y_1, y_2)$$

and Δ, in the forms presented in Fig. A.1. The lower LFT is the mapping $\mathcal{F}_l(G, \Delta) : u_1 \mapsto y_1$, which corresponds to the choice $\Delta : y_2 \mapsto u_2$ as shown in Fig. A.1(a), equals

$$\mathcal{F}_l(G, \Delta) = G_{11} + G_{12}(I - \Delta G_{22})^{-1} \Delta G_{21} = G_{11} + G_{12}\Delta(I - G_{22}\Delta)^{-1} G_{21}, \qquad \text{(A.18a)}$$

It is well defined if $I - \Delta G_{22}$ (equivalently, $I - G_{22}\Delta$) is invertible. The upper LFT is the mapping $\mathcal{F}_u(G, \Delta) : u_2 \mapsto y_2$, which corresponds to the choice $\Delta : y_1 \mapsto u_1$ as in Fig. A.1(b), equals

$$\mathcal{F}_u(G, \Delta) = G_{22} + G_{21}(I - \Delta G_{11})^{-1} \Delta G_{12} = G_{22} + G_{21}\Delta(I - G_{11}\Delta)^{-1} G_{12}. \qquad \text{(A.18b)}$$

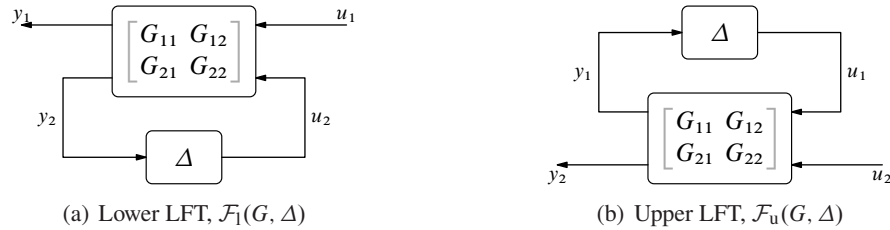(a) Lower LFT, $\mathcal{F}_l(G, \Delta)$ (b) Upper LFT, $\mathcal{F}_u(G, \Delta)$

Fig. A.1: Linear fractional transformations (LFTs)

It is well defined whenever $I - \Delta G_{11}$ (equivalently, $I - G_{11}\Delta$) is invertible. These transformations are differentiated merely for convenience, they are essentially equivalent. This follows from the equality

$$\mathcal{F}_u(G, \Delta) = \mathcal{F}_l\left(\begin{bmatrix} 0 & I \\ I & 0 \end{bmatrix} G \begin{bmatrix} 0 & I \\ I & 0 \end{bmatrix}, \Delta\right),$$

which is easy to verify.

Standard addition, multiplication, and feedback interconnection of mappings can be viewed as special cases of this LFT, e.g.

$$G_1 + G_2 = \mathcal{F}_l\left(\begin{bmatrix} G_1 & I \\ I & 0 \end{bmatrix}, G_2\right) = \mathcal{F}_u\left(\begin{bmatrix} 0 & I \\ I & G_1 \end{bmatrix}, G_2\right),$$

$$G_2 G_1 = \mathcal{F}_l\left(\begin{bmatrix} 0 & I \\ G_1 & 0 \end{bmatrix}, G_2\right) = \mathcal{F}_u\left(\begin{bmatrix} 0 & G_1 \\ I & 0 \end{bmatrix}, G_2\right),$$

and

$$G_1(I - G_2 G_1)^{-1} = \mathcal{F}_l\left(\begin{bmatrix} G_1 & G_1 \\ G_1 & G_1 \end{bmatrix}, G_2\right) = \mathcal{F}_u\left(\begin{bmatrix} G_1 & G_1 \\ G_1 & G_1 \end{bmatrix}, G_2\right)$$

(these choices are not unique).

The two propositions below present some useful algebraic properties of LFTs.

Proposition A.5. *Suppose $\mathcal{F}_l(G, \Delta)$ is square and well posed and G_{11} is nonsingular. Then $\mathcal{F}_l(G, \Delta)$ is invertible and*

$$[\mathcal{F}_l(G, \Delta)]^{-1} = \mathcal{F}_l(\hat{G}, \Delta), \quad \text{where} \quad \hat{G} = \begin{bmatrix} G_{11}^{-1} & -G_{11}^{-1} G_{12} \\ G_{21} G_{11}^{-1} & G_{22} - G_{21} G_{11}^{-1} G_{12} \end{bmatrix}.$$

Similarly, if $\mathcal{F}_u(G, \Delta)$ is square and well posed and G_{22} is nonsingular, then $\mathcal{F}_u(G, \Delta)$ is invertible and

$$[\mathcal{F}_u(G, \Delta)]^{-1} = \mathcal{F}_u(\tilde{G}, \Delta), \quad \text{where} \quad \tilde{G} = \begin{bmatrix} G_{11} - G_{12} G_{22}^{-1} G_{21} & G_{12} G_{22}^{-1} \\ -G_{22}^{-1} G_{21} & G_{22}^{-1} \end{bmatrix}.$$

Proof. We prove only the lower LFT part, the upper LFT part is proved similarly. The logic is that the sought $[\mathcal{F}_l(G, \Delta)]^{-1}$ is a mapping $y_1 \mapsto u_1$, so what we need is to swap u_1 with y_1. Because Δ is still supposed to have y_2 as its input and u_2 as its output, these signals remain untouched. The result then follows from the relation

$$\begin{bmatrix} y_1 \\ y_2 \end{bmatrix} = \begin{bmatrix} G_{11} & G_{12} \\ G_{21} & G_{22} \end{bmatrix} \begin{bmatrix} u_1 \\ u_2 \end{bmatrix} \iff \begin{bmatrix} u_1 \\ y_2 \end{bmatrix} = \begin{bmatrix} G_{11}^{-1} & -G_{11}^{-1} G_{12} \\ G_{21} G_{11}^{-1} & G_{22} - G_{21} G_{11}^{-1} G_{12} \end{bmatrix} \begin{bmatrix} y_1 \\ u_2 \end{bmatrix} = \hat{G} \begin{bmatrix} y_1 \\ u_2 \end{bmatrix},$$

which is verified by direct substitution. $\qquad \square$

Proposition A.6. *If G is invertible and such that G_{12} and G_{21} are square and invertible too, then*

$$T = \mathcal{F}_l(G, \Delta) \iff \Delta = \mathcal{F}_u(G^{-1}, T).$$

Proof. Let $T = \mathcal{F}_l(G, \Delta)$. Since G is nonsingular, $\begin{bmatrix} u_1 \\ u_2 \end{bmatrix} = G^{-1} \begin{bmatrix} y_1 \\ y_2 \end{bmatrix}$. Then, taking into account that T is the mapping $u_1 \mapsto y_1$ and Δ is the mapping $y_2 \mapsto u_2$, we have that Δ satisfies the following set of equations:

$$\begin{bmatrix} u_1 \\ u_2 \end{bmatrix} = G^{-1} \begin{bmatrix} y_1 \\ y_2 \end{bmatrix} \quad \text{and} \quad y_1 = T u_1.$$

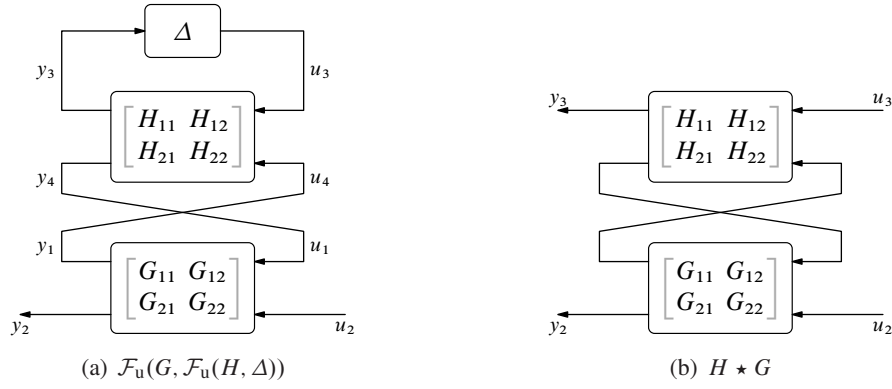(a) $\mathcal{F}_u(G, \mathcal{F}_u(H, \Delta))$ (b) $H \star G$

Fig. A.2: Nested LFTs and the Redheffer star product

This defines exactly $\mathcal{F}_u(G^{-1}, T)$. Similar arguments yield that $\Delta = \mathcal{F}_u(G^{-1}, T) \implies T = \mathcal{F}_l(G, \Delta)$. To complete the proof we only need to show that $\mathcal{F}_l(G, \Delta)$ is well posed iff so is $\mathcal{F}_u(G^{-1}, T)$. To show this, assume first that $\mathcal{F}_l(G, \Delta)$ is well posed, i.e. that $I - G_{22}\Delta$ is nonsingular. The well-posedness of $\mathcal{F}_u(G^{-1}, T)$ reads then as the non-singularity of $I - \begin{bmatrix} I & 0 \end{bmatrix} G^{-1} \begin{bmatrix} I \\ 0 \end{bmatrix} T$ or, because $I - M_1 M_2$ is nonsingular iff $I - M_2 M_1$ is nonsingular, of

$$I - G^{-1} \begin{bmatrix} I \\ 0 \end{bmatrix} T \begin{bmatrix} I & 0 \end{bmatrix} = G^{-1} \left(\begin{bmatrix} G_{11} & G_{12} \\ G_{21} & G_{22} \end{bmatrix} - \begin{bmatrix} G_{11} + G_{12}\Delta(I - G_{22}\Delta)^{-1}G_{21} & 0 \\ 0 & 0 \end{bmatrix} \right)$$

$$= G^{-1} \begin{bmatrix} -G_{12}\Delta(I - G_{22}\Delta)^{-1}G_{21} & G_{12} \\ G_{21} & G_{22} \end{bmatrix}$$

$$= G^{-1} \begin{bmatrix} G_{12} & -G_{12}\Delta(I - G_{22}\Delta)^{-1}G_{21} \\ G_{22} & G_{21} \end{bmatrix} \begin{bmatrix} 0 & I \\ I & 0 \end{bmatrix}.$$

Now, G_{12} is assumed to be invertible. Its Schur complement in the system in the middle of the right-hand side above,

$$G_{21} + G_{22}\Delta(I - G_{22}\Delta)^{-1}G_{21} = (I - G_{22}\Delta)^{-1}G_{21},$$

is invertible too, because G_{21} is also assumed to be invertible. Hence, $\mathcal{F}_u(G^{-1}, T)$ is well posed. The other direction follows by similar arguments. □

An important property of linear fractional transformations is that they can be nested one into another one. Namely, $\mathcal{F}_u(G, \mathcal{F}_u(H, R))$ is again an upper LFT. This can be seen via the block-diagram in Fig. A.2. The interconnection of G and H, which is obtained by equating $u_1 = y_4$ and $u_4 = y_1$, is known as the *Redheffer star-product*, denoted $G \star H$. The star product is a mapping $(u_3, u_2) \mapsto (y_3, y_2)$. Algebraically, the relations between input and output signals in Fig. A.2 is

$$\begin{bmatrix} y_1 \\ y_2 \\ y_3 \\ y_4 \end{bmatrix} = \begin{bmatrix} G_{11} & G_{12} & 0 & 0 \\ G_{21} & G_{22} & 0 & 0 \\ 0 & 0 & H_{11} & H_{12} \\ 0 & 0 & H_{21} & H_{22} \end{bmatrix} \begin{bmatrix} u_1 \\ u_2 \\ u_3 \\ u_4 \end{bmatrix} \quad \text{and} \quad \begin{bmatrix} y_4 \\ y_1 \end{bmatrix} = \begin{bmatrix} u_1 \\ u_4 \end{bmatrix}.$$

Thus, the internal signals u_1 and u_4 verify

$$\begin{bmatrix} u_1 \\ u_4 \end{bmatrix} = \begin{bmatrix} 0 & 0 & H_{21} & H_{22} \\ G_{11} & G_{12} & 0 & 0 \end{bmatrix} \begin{bmatrix} u_1 \\ u_2 \\ u_3 \\ u_4 \end{bmatrix} \iff \begin{bmatrix} I & -H_{22} \\ -G_{11} & I \end{bmatrix} \begin{bmatrix} u_1 \\ u_4 \end{bmatrix} = \begin{bmatrix} H_{21} & 0 \\ 0 & G_{12} \end{bmatrix} \begin{bmatrix} u_3 \\ u_2 \end{bmatrix},$$

from which, assuming the invertibility of $I - H_{22}G_{11}$ (or, equivalently, of $I - G_{11}H_{22}$),

$$
\begin{aligned}
H \star G &= \begin{bmatrix} H_{11} & 0 \\ 0 & G_{22} \end{bmatrix} + \begin{bmatrix} 0 & H_{12} \\ G_{21} & 0 \end{bmatrix} \begin{bmatrix} I & -H_{22} \\ -G_{11} & I \end{bmatrix}^{-1} \begin{bmatrix} H_{21} & 0 \\ 0 & G_{12} \end{bmatrix} \\
&= \begin{bmatrix} H_{11} & H_{12}G_{12} \\ 0 & G_{22} \end{bmatrix} + \begin{bmatrix} H_{12}G_{11} \\ G_{21} \end{bmatrix} (I - H_{22}G_{11})^{-1} \begin{bmatrix} H_{21} & H_{22}G_{12} \end{bmatrix},
\end{aligned}
$$

where the last equality is obtained by (A.3b). The nested LFT in Fig. A.2 reads then

$$
\mathcal{F}_u(G, \mathcal{F}_u(H, \Delta)) = \mathcal{F}_u(H \star G, \Delta), \tag{A.19a}
$$

Likewise,

$$
\mathcal{F}_l(G, \mathcal{F}_l(H, \Delta)) = \mathcal{F}_l(G \star H, \Delta). \tag{A.19b}
$$

which can be derived by similar arguments.

Appendix B

Background on Linear Systems

THE PURPOSE of this appendix is to collect some basic facts about (mostly finite-dimensional and time-invariant) linear systems. The material, which is required throughout the notes, is presented in a condensed matter. More details can be found in [45], whose philosophy is followed below, as well as in many other textbooks.

B.1   Signals and systems in time domain

Signals are functions of independent variables (mainly time), conveying information about changing phenomena. Systems are constraints imposed on interdependent signals, like those between forces and positions in mechanical systems or between voltages and currents in electrical systems or between pressures and volume flow rates in hydraulic systems, et cetera. As customary, throughout these notes we treat one group of signals as an action (inputs) and another one—as a reaction (outputs), which is sufficiently general in many situations, especially for processes with delays. A system G with an input u and an output y can then be viewed as a mapping $G : u \mapsto y$.

B.1.1   Continuous-time signals and systems

Continuous-time signals are viewed as functions defined on some subset of the real axis $\mathbb{R}$. For many good reasons, control applications are mostly concerned with signals defined on the positive semi-axis $\mathbb{R}_+$, in which case an n-dimensional continuous-time signal $f(t)$ is understood as

$$f : \mathbb{R}_+ \to \mathbb{R}^n.$$

The ith component of $f(t)$, denoted $f_i(t)$, is a scalar function of time t. Signal spaces are used to constrain the set of considered signals in some way, formalizing the notion of *admissible* signals. We mostly use the space

$$L_2^n(\mathbb{R}_+) := \left\{ f : \mathbb{R}_+ \to \mathbb{R}^n \mid \|f\|_2 := \left(\int_{\mathbb{R}_+} \|f(t)\|^2 \mathrm{d}t \right)^{1/2} < \infty \right\} \tag{B.1}$$

for this purpose. The squared L_2-norm, $\|f\|_2^2$, can be interpreted as the *energy* of f. Thus, L_2 can be seen as the space of finite-energy signals.

Linear continuous-time systems with m-dimensional inputs and p-dimensional outputs are understood as linear operators $G : \mathfrak{D}_G \subset L_2^m(\mathbb{R}_+) \to L_2^p(\mathbb{R}_+)$ for some domain $\mathfrak{D}_G$. A system G is said to be *stable* (or i/o stable) if $\mathfrak{D}_G = L_2^m(\mathbb{R}_+)$ and $\|G\|_{L_2 \to L_2} := \sup_{\|u\|_2 = 1} \|Gu\|_2 < \infty$. The norm of G defined by the last expression is called its L_2-*induced norm*. We say that $G : u \mapsto y$ is *causal* if $y(t) = 0$ for all $t \le t_\mathrm{c}$ whenever $u(t) = 0$ for all $t \le t_\mathrm{c}$ for every $t_\mathrm{c} \in \mathbb{R}_+$. In other words, a system is causal if its output at

every time instance t_c can only depend on the past and present inputs. A linear system G is said to be *time invariant* (abbreviated LTI) if $GS_\tau = S_\tau G$ for all $\tau > 0$, where S_τ is the τ-shift operator, defined via

$$(S_\tau u)(t) = \begin{cases} 0 & \text{if } 0 \le t < \tau \\ u(t - \tau) & \text{if } \tau \le t \end{cases} \tag{B.2}$$

This effectively says that a time-shifted input produces a time-shifted, but otherwise unchanged, output.

A fairly general class of $p \times m$ causal LTI systems $G : u \mapsto y$ can be described by the *convolution integral*

$$y(t) = \int_{\mathbb{R}_+} g(t - s)u(s)\,\mathrm{d}s = \int_{\mathbb{R}_+} \tilde{g}(t - s)u(s)\,\mathrm{d}s + \sum_{i \in \mathbb{Z}_+} g_i u(t - \varkappa_i), \tag{B.3}$$

where

$$g(t) = \tilde{g}(t) + \sum_{i \in \mathbb{Z}_+} g_i \delta(t - \varkappa_i) \tag{B.4}$$

for a bounded on any bounded subset of $\mathbb{R}$ function $\tilde{g} : \mathbb{R} \to \mathbb{R}^{p \times m}$ such that $\tilde{g}(t) = 0$ whenever $t < 0$, bounded $g_i \in \mathbb{R}^{p \times m}$, and a strictly increasing sequence $\{\varkappa_i\}_{i \in \mathbb{Z}_+}$, such that $\varkappa_0 = 0$ and $\varkappa_i - \varkappa_{i-1} \ge \epsilon$ for all $i \in \mathbb{Z}_+$ and some constant $\epsilon > 0$, independent of i. The (generalized) function g is called the *impulse response* of G, i.e. it is the response of G to the Dirac delta impulse[1] applied at the time instance $t = 0$.

An important class of LTI systems are finite-dimensional systems. These are systems for which there are $n \in \mathbb{Z}_+$ and matrices $A \in \mathbb{R}^{n \times n}$, $B \in \mathbb{R}^{n \times m}$, $C \in \mathbb{R}^{p \times n}$, and $D \in \mathbb{R}^{p \times m}$ such that

$$g(t) = D\delta(t) + C\mathrm{e}^{At}B\mathbb{1}(t) \tag{B.5}$$

(i.e. $\tilde{g}(t) = C\mathrm{e}^{At}B\mathbb{1}(t)$, $g_0 = D$, and $g_i = 0$ for all $i > 0$ in (B.4)). Given any $t_c \ge 0$, the response of such a system at all $t \ge t_c$ can be expressed as

$$y(t) = Du(t) + \int_0^t C\mathrm{e}^{A(t-s)}Bu(s)\,\mathrm{d}s = Du(t) + \int_{t_c}^t C\mathrm{e}^{A(t-s)}Bu(s)\,\mathrm{d}s + C\mathrm{e}^{A(t-t_c)}x(t_c), \tag{B.6}$$

where the n-dimensional vector

$$x(t) := \int_0^t \mathrm{e}^{A(t-s)}Bu(s)\,\mathrm{d}s \tag{B.7}$$

is called the *state vector* of G. The meaning of the second relation in (B.6) is that the knowledge of $x(t_c)$ is sufficient to account for the effect of the past, $t < t_c$, on the behavior of the system afterwards. In other words, the state vector is a *history accumulator*. By differentiating (B.7), we get the state-space description,

$$G : \begin{cases} \dot{x}(t) = Ax(t) + Bu(t), & x(0) = 0 \\ y(t) = Cx(t) + Du(t), \end{cases} \tag{B.8}$$

which is a differential, rather than integral, equation. The state-space representation (B.8) might be more convenient to handle than the convolution integral (B.3). The quadruple (A, B, C, D) is referred to as a *state-space realization* of a system G. In some situations the initial condition $x(0)$ is more convenient to be taken equal to some $x_0 \ne 0$. This aims at accounting for the behavior of the system in $t < 0$. In such a case we can treat G as an operator $\mathfrak{D}_G \subset \mathbb{R}^n \times L_2^m(\mathbb{R}_+) \to L_2^p(\mathbb{R}_+)$.

There is also an alternative notion of the stability for systems given by their state equation (B.8). A linear system is said to be *Lyapunov stable* if for every $\epsilon > 0$ there is $\delta = \delta(\epsilon)$ such that $\|x(t)\| < \epsilon$ for all $t \in \mathbb{R}_+$ whenever $\|x(0)\| < \delta$. The *asymptotic stability* requires in addition that $\lim_{t \to \infty} \|x(t)\| = 0$. It is known that G is Lyapunov stable iff A has no eigenvalues in the open right-half plane $\mathbb{C}_0$ and its pure

---

[1]More precisely, the jth column of $g(t)$ is the response of G to the input $e_j \delta(s)$, where e_j is the jth standard basis on $\mathbb{R}^m$.

imaginary eigenvalues are simple. G is asymptotically stable iff A has no eigenvalues in the closed right-half plane $\bar{\mathbb{C}}_0$. Note that these notions do not account for exogenous input signals explicitly[2], considering the system autonomous for $t > 0$. This is unlike the i/o stability notion, which assumes equilibrium at $t = 0$ and is driven by u. Nonetheless, the i/o and Lyapunov stability properties are essentially equivalent for finite-dimensional systems. Namely, under a mild minimality assumption, G is i/o stable iff its state equation is asymptotically stable. The situation is less trivial for infinite-dimensional systems though.

B.1.2 Discrete-time signals and systems

Discrete-time signals are functions defined on some subset of the real axis $\mathbb{Z}$. An n-dimensional discrete-time signal $f[t]$ on the nonnegative semi-axis $\mathbb{Z}_+$ is understood as

$$f : \mathbb{Z}_+ \to \mathbb{R}^n.$$

The discrete counterpart of the L_2 space is

$$\ell_2^n(\mathbb{Z}_+) := \left\{ f : \mathbb{Z}_+ \to \mathbb{R}^n \mid \|f\|_2 := \left(\sum_{t \in \mathbb{Z}_+} \|f[t]\|^2 \right)^{1/2} < \infty \right\} \tag{B.9}$$

and the squared ℓ_2-norm, $\|f\|_2^2$, can be also interpreted as the *energy* of f, rendering ℓ_2 the space of finite-energy signals.

Linear discrete-time systems with m-dimensional inputs and p-dimensional outputs are understood as linear operators $G : \mathfrak{D}_G \subset \ell_2^m(\mathbb{Z}_+) \to \ell_2^p(\mathbb{Z}_+)$ for some domain $\mathfrak{D}_G$. A system G is said to be *stable* if $\mathfrak{D}_G = \ell_2^m(\mathbb{Z}_+)$ and $\|G\|_{\ell_2 \to \ell_2} := \sup_{\|u\|_2 = 1} \|Gu\|_2 < \infty$. The norm of G defined by the last expression is called its *ℓ_2-induced norm*. We say that $G : u \mapsto y$ is *causal* (*strictly causal*) if $y[t] = 0$ for all $t \le t_c$ whenever $u[t] = 0$ for all $t \le t_c$ (all $t < t_c$) for every $t_c \in \mathbb{Z}_+$. In other words, a system is causal if its output at every time instance t_c can only depend on the past and present inputs and strictly causal if its output at every t_c can only depend on the past inputs. A linear system G is said to be *shift invariant* (abbreviated LSI) if $GS_1 = S_1 G$, where the unit shift S_1 is defined similarly to the continuous-time shift in (B.2) for $\tau = 1$.

A general class of $p \times m$ causal LSI systems $G : u \mapsto y$ can be described by the *convolution sum*

$$y[t] = \sum_{s \in \mathbb{Z}} g[t - s]u[s] \tag{B.10}$$

for a bounded on any bounded subset of $\mathbb{Z}$ function $g : \mathbb{Z} \to \mathbb{R}^{p \times m}$ such that $g[t] = 0$ whenever $t < 0$. The function g, which is the response of the system to the unit pulse applied at $t = 0$, is called the *impulse response* of G. Finite-dimensional LSI systems are those with

$$g[t] = D\delta[t] + CA^t B \mathbb{1}[t] \tag{B.11}$$

for some $n \in \mathbb{Z}_+$ and matrices $A \in \mathbb{R}^{n \times n}$, $B \in \mathbb{R}^{n \times m}$, $C \in \mathbb{R}^{p \times n}$, and $D \in \mathbb{R}^{p \times m}$. For such systems there is a (non-unique) n-dimensional *state vector*

$$x[t] := \sum_{s=0}^{t} A^{t-s} Bu[s]. \tag{B.12}$$

It is a *history accumulator*, exactly like in the continuous-time case. Finite-dimensional systems can be presented in their state-space description,

$$G : \begin{cases} x[t+1] = Ax[t] + Bu[t], & x[0] = 0 \\ y[t] = Cx[t] + Du[t], \end{cases} \tag{B.13}$$

which is a difference equation, similarly to the differential equation in the continuous-time case.

---

[2]If we think of variables in (B.8) as deviations from an equilibrium, then a possibly constant u is involved into the definition.

B.2   Signals and systems in transformed domains

The Fourier transform of a continuous-time signal $f : \mathbb{R}_+ \to \mathbb{F}^n$ is defined as

$$\mathcal{F}\{f\} = F(\mathrm{j}\omega) := \int_{\mathbb{R}_+} f(t)\mathrm{e}^{-\mathrm{j}\omega t}\,\mathrm{d}t, \tag{B.14}$$

where $\omega \in \mathbb{R}$ is called the (angular) frequency and measured in radians per time unit (e.g. per second). The signal $\mathcal{F}\{f\}$ is called the *frequency-domain* representation of f. The term "frequency" becomes apparent in the inverse Fourier transform formula,

$$\mathcal{F}^{-1}\{F\} = f(t) = \frac{1}{2\pi} \int_{\mathbb{R}} F(\mathrm{j}\omega)\mathrm{e}^{\mathrm{j}\omega t}\,\mathrm{d}\omega, \tag{B.15}$$

which effectively says that $f(t)$ is a superposition of *harmonic signals* $\mathrm{e}^{\mathrm{j}\omega t}$ with frequencies ω. The Fourier transform $F(\mathrm{j}\omega)$, called also the *spectrum* of f, can then be viewed as the weight of the harmonic $\mathrm{e}^{\mathrm{j}\omega t}$ in $f(t)$. The set of Fourier transformable signals is quite limited. The integral in (B.14) converges, in norm, essentially only for $L_2(\mathbb{R}_+)$-signals. The one-sided (or unilateral) Laplace transform of $f : \mathbb{R}_+ \to \mathbb{C}^n$, defined as

$$\mathcal{L}\{f\} = F(s) := \int_{\mathbb{R}_+} f(t)\mathrm{e}^{-st}\,\mathrm{d}t \tag{B.16}$$

for all $s \in \mathbb{C}$ for which the integral converges, can be viewed as a generalization of the Fourier transform, rendering a wider class of signals transformable. The set of $s \in \mathbb{C}$ for which (B.16) exists is called the *region of convergence* (or RoC) of $F(s)$.

An important property of integral transforms is that they turn convolutions into products. Namely, if $G : u \mapsto y$ is LTI, then

$$\mathcal{F}\{y\} = \mathcal{F}\{g\}\,\mathcal{F}\{u\} \quad \text{or} \quad Y(\mathrm{j}\omega) = G(\mathrm{j}\omega)U(\mathrm{j}\omega)$$

provided $\mathcal{F}\{g\}$ and $\mathcal{F}\{u\}$ exist. The Fourier transform of the impulse response g of an LTI G is called its *frequency response* and denoted $G(\mathrm{j}\omega)$. Likewise,

$$\mathcal{L}\{y\} = \mathcal{L}\{g\}\,\mathcal{L}\{u\} \quad \text{or} \quad Y(s) = G(s)U(s).$$

for all s in the RoCs of both $G(s)$ and $U(s)$. The Laplace transform of the impulse response g of an LTI G is called its *transfer function*, denoted $G(s)$.

Properties of LTI systems can be analyzed in terms of their transfer functions. An important fact is that an LTI continuous-time system is causal and stable iff its transfer function $G(s)$ belongs to the space

$$H_\infty^{p \times m} := \big\{ G : \mathbb{C}_0 \to \mathbb{C}^{p \times m} \mid G \text{ is holomorphic in } \mathbb{C}_0 \text{ and } \|G\|_\infty := \sup_{s \in \mathbb{C}_0} \|G(s)\| < \infty \big\}, \tag{B.17}$$

where $\|G(s)\|$ stands for the matrix spectral norm on $\mathbb{C}^{p \times m}$. The H_∞ system norm defined in (B.17) actually equals the L_2-induced norm of G, i.e. $\|G\|_\infty = \|G\|_{L_2 \to L_2}$. Also, every $G \in H_\infty$ has a unique *boundary function* $\tilde{G} \in L_\infty(\mathrm{j}\mathbb{R})$ such that $\tilde{G}(\mathrm{j}\omega) = \lim_{\sigma \downarrow 0} G(\sigma + \mathrm{j}\omega)$ for almost all ω and $\|\tilde{G}\|_\infty = \|G\|_\infty$, where

$$L_\infty^{p \times m}(\mathrm{j}\mathbb{R}) := \big\{ \tilde{G} : \mathrm{j}\mathbb{R} \to \mathbb{C}^{p \times m} \mid \|\tilde{G}\|_\infty := \operatorname{ess\,sup}_{\omega \in \mathbb{R}} \|\tilde{G}(\mathrm{j}\omega)\| < \infty \big\}. \tag{B.18}$$

It is customary to identify G with $\tilde{G}$ and regard H_∞ as a closed subspace of $L_\infty(\mathrm{j}\mathbb{R})$, in which case

$$\|G\|_\infty = \operatorname*{ess\,sup}_{\omega \in \mathbb{R}} \|G(\mathrm{j}\omega)\|. \tag{B.19}$$

It should be emphasized that this equality holds only for functions $G \in H_\infty$ as defined by (B.17).

The counterpart of the Laplace transform for discrete sequences is the z-transform, defined as

$$\mathfrak{Z}\{f\} = F(z) := \sum_{t \in \mathbb{Z}_+} f[t] z^{-t} \tag{B.20}$$

for all $z \in \mathbb{C}$ for which the sum converges (RoC). The z-transform of the impulse response g of a discrete-time LSI system G is also called its transfer function, denoted $G(z)$. In full analogy with the continuous-time case, the relation between the z-transforms of the input and output to G reads $Y(z) = G(z)U(z)$ in the z-domain and G is causal and stable iff its transfer function is holomorphic and bounded in the exterior of the closed unit disk, i.e. in $\mathbb{C} \setminus \overline{\mathbb{D}}$.

Transfer functions, in both the Laplace and z-domains, can be expressed in terms of corresponding spate-space realizations (A, B, C, D) as

$$G(s) = D + C(sI - A)^{-1}B =: \left[\begin{array}{c|c} A & B \\ \hline C & D \end{array} \right] := D + C(zI - A)^{-1}B = G(z).$$

Transfer functions of finite-dimensional causal systems are rational functions of s and z and are proper, in the sense that their limits for $\operatorname{Re} s \to \infty$ and $|z| \to \infty$, respectively, exist. Finite-dimensional systems are stable iff they are proper and all poles of their transfer functions are in the open left-half plane $\mathbb{C} \setminus \overline{\mathbb{C}}_0$ (or in the open unit disk $\mathbb{D}$ in the discrete-time case). All these poles are among the eigenvalues of the "A" matrix of a state-space realization of G, cf. the relation between i/o and Lyapunov's asymptotic stability notions.

B.2.1 System norms

Norms are used to measure sizes. Applying to control systems, norms are frequently used to quantify performance, which requires to construct a meaningful *error system*. There is a plenty of system norms that could be defined for continuous-time LTI systems, such as H_2, H_∞, L_1, $\star$, you name it. In some situations norms on various Sobolev spaces may be used (although this is frequently just a matter of an appropriate dynamics scaling). It is important that unlike matrix norms, i.e. norms on finite-dimensional spaces, system norms are not equivalent. It might happen that a system has a finite H_2-norm but infinite H_∞-nor, or vice versa. Thus, one should be careful with the choice of the norm, which suits a concrete application.

Below we briefly review two, arguably the most widely used in control applications, systems norms, viz. H_∞ and H_2 ones.

H_∞ system norm

We already defined the H_∞ space and the corresponding norm of an LTI continuous-time system in §B.2 in the context of the L_2-stability of G. Just add that if G is finite dimensional, then $G \in H_\infty$ iff the transfer function $G(s)$ is proper and has no poles in the closed right-hand plane $\overline{\mathbb{C}}_0$. By (B.19), the H_∞ norm can be determined from the Bode frequency response plot as the peak value of the magnitude, or of the largest singular value of $G(j\omega)$ for MIMO systems.

The H_∞-norm of G is important also in performance considerations, especially those motivated by the classical frequency-domain analysis and in robust control applications. For instance, it is readily seen, via (B.19), that

$$\|WG\|_\infty \leq 1 \quad \Longleftrightarrow \quad |G(j\omega)| \leq \frac{1}{|W(j\omega)|}, \quad \forall \omega \in \mathbb{R}$$

for all SISO systems G and W. This relation can be useful in situations when G is a closed-loop system of interest and W is a weighing function, whose reciprocal represents a required upper bound (shape) on

the frequency response magnitude of G. For example, if G represents the closed-loop sensitivity ($S = 1/(1 + PC)$ in the conventional unity-feedback setup with a plant P and a controller C), a required $1/W$ may be some low-pass filter, whose magnitude at low frequencies would represent the error tolerance in the system, the high-frequency magnitude would represent limitations on the peak of $|S(j\omega)|$, and the corner frequency would reflect our requirements on the closed-loop bandwidth. The minimization of $\|WG\|_\infty$ could then be a tool of validating the feasibility of this kind of requirements and, if the problem of rendering $\|WG\|_\infty \le 1$ is feasible, of designing a required controller.

H_2 system norm

Introduce now another space of matrix-valued complex functions on $\mathbb{C}_0$,

$$H_2^{p\times m} := \left\{ G : \mathbb{C}_0 \to \mathbb{C}^{p\times m} \mid G(s) \text{ is holomorphic}\right.$$
$$\left. \text{in } \mathbb{C}_0 \text{ and } \|G\|_2 := \left(\sup_{\sigma>0} \frac{1}{2\pi} \int_{\mathbb{R}} \|G(\sigma + j\omega)\|_F^2 \, d\omega \right)^{1/2} < \infty \right\}. \quad \text{(B.21)}$$

The norm in this definition, known as the H_2-norm of G, is not quite intuitive. To gain insight into it, note that like in the H_∞ case, every $G \in H_2$ has a unique boundary function $\tilde{G} \in L_2(j\mathbb{R})$, where

$$L_2^{p\times m}(j\mathbb{R}) := \left\{ \tilde{G} : j\mathbb{R} \to \mathbb{C}^{p\times m} \mid \|\tilde{G}\|_2 := \left(\frac{1}{2\pi} \int_{\mathbb{R}} \|\tilde{G}(j\omega)\|_F^2 \, d\omega \right)^{1/2} < \infty \right\}, \quad \text{(B.22)}$$

such that $\|G\|_2 = \|\tilde{G}\|_2$. The space H_2 is regarded then as a closed subspace of $L_2(j\mathbb{R})$. We can then identify G with $\tilde{G}$ and regard H_2 as a closed subspace of $L_2(j\mathbb{R})$, in which case

$$\|G\|_2 = \left(\frac{1}{2\pi} \int_{\mathbb{R}} \|G(j\omega)\|_F^2 \, d\omega \right)^{1/2} = \left(\int_{\mathbb{R}_+} \|g(t)\|_F^2 \, dt \right)^{1/2}. \quad \text{(B.23)}$$

where the second equality follows by the Paley–Wiener theorem. Thus, H_2 is the space of transfer functions of *causal* systems, whose impulse responses have *finite energy*. The expressions in (B.23) are both intuitive and quite convenient from the computational viewpoint, see §B.3.2. If G is finite dimensional, then $G \in H_2$ iff the transfer function $G(s)$ is strictly proper, i.e. is such that $\lim_{|s|\to\infty} \|G(s)\| = 0$, and has no poles in the closed right-hand plane $\overline{\mathbb{C}}_0$.

Another interpretation of the H_2 system norm takes the stochastic viewpoint. Namely, assume that $G : u \mapsto y$ is LTI. If the input u is a unit-intensity white Gaussian process, then the output y is asymptotically stationary process and $\|G\|_2^2$ equals its steady-state variance. This property renders the H_2 system norm a powerful tool to address performance issues in systems driven by stochastic processes. Specifically, this is the norm of choice in Kalman filtering and LQG.

Remark B.1 (H_2 vs. H_∞). It should be emphasized that the belonging of a transfer function to H_2 does not guarantee its stability, i.e. belonging to H_∞. For example, the transfer function of a system, whose impulse response $g(t) = \text{sinc}(t)\mathbb{1}(t)$, does belong to H_2 (it can be verified that $\|G\|_2 = \|g\|_2 = \sqrt{\pi/2} < \infty$), but not to H_∞ (as $G(s) = \arctan(1/s)$ is unbounded on any path in $\mathbb{C}_0$ approaching $s = \pm j$). Thus, this system is L_2-unstable. It might also happen that the transfer function of a stable system does not belong to H_2, which is the case with static systems, for instance. ∇

The H_2 space is Hilbert and as such it is equipped with an inner product, which is

$$\langle G_1, G_2 \rangle_2 := \frac{1}{2\pi} \int_{\mathbb{R}} \text{tr}\big([G_2(j\omega)]' G_1(j\omega)\big) \, d\omega = \int_{\mathbb{R}_+} \text{tr}\big(g_2'(t) g_1(t)\big) \, dt$$

in this case. The notion of the inner product facilitates defining angles between systems, which is a useful technical tool in minimizing the H_2 norm via the Projection Theorem.

B.3 State-space techniques

The state-space representation of LTI system is quite convenient for carrying our operations on them, normally reducing these operations to manipulations over plain matrices. This is a power property, several examples of which are reviewed in this section.

B.3.1 System interconnections in terms of state-space realizations

State-space realizations of parallel and cascade (series) interconnections of two compatibly dimensioned systems G_1 and G_2 are

$$
\left[\begin{array}{c|c} A_1 & B_1 \\ \hline C_1 & D_1 \end{array}\right] + \left[\begin{array}{c|c} A_2 & B_2 \\ \hline C_2 & D_2 \end{array}\right] = \left[\begin{array}{cc|c} A_1 & 0 & B_1 \\ 0 & A_2 & B_2 \\ \hline C_1 & C_2 & D_1 + D_2 \end{array}\right] \tag{B.24}
$$

and

$$
\left[\begin{array}{c|c} A_2 & B_2 \\ \hline C_2 & D_2 \end{array}\right]\left[\begin{array}{c|c} A_1 & B_1 \\ \hline C_1 & D_1 \end{array}\right] = \left[\begin{array}{cc|c} A_1 & 0 & B_1 \\ B_2 C_1 & A_2 & B_2 D_1 \\ \hline D_2 C_1 & C_2 & D_2 D_1 \end{array}\right] = \left[\begin{array}{cc|c} A_2 & B_2 C_1 & B_2 D_1 \\ 0 & A_1 & B_1 \\ \hline C_2 & D_2 C_1 & D_2 D_1 \end{array}\right], \tag{B.25}
$$

respectively. These realizations can be derived by stacking state vectors of G_1 and G_2 and equating corresponding input and output signals. Likewise, the transfer function of the star product of two systems is terms of corresponding state-space realizations is

$$
\left[\begin{array}{c|cc} A & B_1 & B_2 \\ \hline C_1 & D_{11} & D_{12} \\ C_2 & D_{21} & D_{22} \end{array}\right] \star \left[\begin{array}{c|cc} \tilde{A} & \tilde{B}_1 & \tilde{B}_2 \\ \hline \tilde{C}_1 & \tilde{D}_{11} & \tilde{D}_{12} \\ \tilde{C}_2 & \tilde{D}_{21} & \tilde{D}_{22} \end{array}\right] = \left[\begin{array}{c|c} A_\star & B_\star \\ \hline C_\star & D_\star \end{array}\right],
$$

where

$$
A_\star := \left[\begin{array}{cc} A & B_2 \tilde{C}_1 \\ 0 & \tilde{A} \end{array}\right] + \left[\begin{array}{c} B_2 \tilde{D}_{11} \\ \tilde{B}_1 \end{array}\right](I - D_{22}\tilde{D}_{11})^{-1}\left[\begin{array}{cc} C_2 & D_{22}\tilde{C}_1 \end{array}\right],
$$

$$
B_\star := \left[\begin{array}{cc} B_1 & B_2 \tilde{D}_{12} \\ 0 & \tilde{B}_2 \end{array}\right] + \left[\begin{array}{c} B_2 \tilde{D}_{11} \\ \tilde{B}_1 \end{array}\right](I - D_{22}\tilde{D}_{11})^{-1}\left[\begin{array}{cc} D_{21} & D_{22}\tilde{D}_{12} \end{array}\right],
$$

$$
C_\star := \left[\begin{array}{cc} C_1 & D_{12}\tilde{C}_1 \\ 0 & \tilde{C}_2 \end{array}\right] + \left[\begin{array}{c} D_{12}\tilde{D}_{11} \\ \tilde{D}_{21} \end{array}\right](I - D_{22}\tilde{D}_{11})^{-1}\left[\begin{array}{cc} C_2 & D_{22}\tilde{C}_1 \end{array}\right],
$$

$$
D_\star := \left[\begin{array}{cc} D_{11} & D_{12}\tilde{D}_{12} \\ 0 & \tilde{D}_{22} \end{array}\right] + \left[\begin{array}{c} D_{12}\tilde{D}_{11} \\ \tilde{D}_{21} \end{array}\right](I - D_{22}\tilde{D}_{11})^{-1}\left[\begin{array}{cc} D_{21} & D_{22}\tilde{D}_{12} \end{array}\right].
$$

Finally, the transfer function of the inverse system, which can be derived by swapping its input and output, is

$$
\left[\begin{array}{c|c} A & B \\ \hline C & D \end{array}\right]^{-1} = \left[\begin{array}{c|c} A - BD^{-1}C & BD^{-1} \\ \hline -D^{-1}C & D^{-1} \end{array}\right]. \tag{B.26}
$$

It exists, as a proper transfer function, iff $\det(D) \neq 0$.

B.3.2 System norms in terms of state-space realizations

State-space representations are also convenient in reducing the computation of system norms, both H_2 and H_∞, to algebraic manipulations of matrices. Assume that G is LTI and is given in terms of its realization (A, B, C, D) with a Hurwitz A.

We start with the H_2 case:

Proposition B.1. *If $D = 0$, then*

$$\|G\|_2^2 = \text{tr}(B'QB) = \text{tr}(CPC'),$$

where Q and P are the observability and controllability Gramians of (C, A) and (A, B), satisfying

$$AP + PA' + BB' = 0 \quad \text{and} \quad A'Q + QA + C'C = 0,$$

respectively.

Proof. Let $g(t) = Ce^{At}B$ be the impulse response of G, see (B.5). It follows from the second equality of (B.23) that

$$\|G\|_2^2 = \int_{\mathbb{R}_+} \text{tr}\big(g(t)'g(t)\big)\,dt = \int_{\mathbb{R}_+} \text{tr}\big(B'e^{A't}C'Ce^{At}B\big)\,dt = \text{tr}\bigg(B'\int_{\mathbb{R}_+} e^{A't}C'Ce^{At}\,dt\,B\bigg),$$

which yields the first equality of the proposition. Now, by the property $\text{tr}(M_1M_2) = \text{tr}(M_2M_1)$,

$$\|G\|_2^2 = \int_{\mathbb{R}_+} \text{tr}\big(g(t)g(t)'\big)\,dt = \int_{\mathbb{R}_+} \text{tr}\big(Ce^{At}BB'e^{A't}C'\big)\,dt = \text{tr}\bigg(C\int_{\mathbb{R}_+} e^{At}BB'e^{A't}\,dt\,C'\bigg),$$

which yields the second equality of the proposition. $\square$

This result offers an efficient algorithm to compute the H_2 norm. The Lyapunov equations for computing P and Q are linear and can thus be solved in a finite number of steps.

Unlike the H_2 case, there are no closed-form formulae for the H_∞ norm of a stable LTI system. Rather, an iterative search procedure can be organized on every step of which one has to check whether $\|G\|_\infty < \gamma$ for a given $\gamma > 0$. The basis for this procedure is given by the following result:

Proposition B.2. $\|G\|_\infty < \gamma$ *for a given $\gamma > 0$ iff $\|D\| < \gamma$ and the matrix*

$$H := \begin{bmatrix} A & 0 \\ C'C & -A' \end{bmatrix} - \begin{bmatrix} B \\ C'D \end{bmatrix} (\gamma^2 I - D'D)^{-1} \begin{bmatrix} -D'C & B' \end{bmatrix}$$

has no pure imaginary eigenvalues.

Using the result of Proposition B.2, the H_∞ norm can be found by a bisection algorithm. To this end, we select an upper bound γ_u and a lower bound γ_l (e.g. $\gamma_l = \bar{\sigma}(D)$) for $\|G\|_\infty$ and then check whether $\|G\|_\infty < (\gamma_l + \gamma_u)/2$ (in this case $\gamma_u \to (\gamma_l + \gamma_u)/2$) or not (in this case $\gamma_l \to (\gamma_l + \gamma_u)/2$). The iterations are repeated until the relative error $1 - \gamma_l/\gamma_u \in (0, 1)$ falls within a required tolerance level.

Bibliography

[1] I. Alterman and L. Mirkin, "On the robustness of sampled-data systems to uncertainty in continuous-time delays," *IEEE Trans. Automat. Control*, vol. 3, pp. 686–692, 2011.

[2] R. J. Anderson and M. W. Spong, "Bilateral control of teleoperators with time delay," *IEEE Trans. Automat. Control*, vol. 34, no. 5, pp. 494–501, 1989.

[3] Z. Artstein, "Linear systems with delayed control: A reduction," *IEEE Trans. Automat. Control*, vol. 27, no. 4, pp. 869–879, 1982.

[4] K. J. Åström and T. Hägglund, *Advanced PID Control*. Research Triangle Park, NC: ISA, 2006.

[5] M. Athans and P. L. Falb, *Optimal Control: An Introduction to the Theory and Its Applications*. New York, NY: McGraw-Hill, 1966.

[6] R. Bellman and K. L. Cooke, *Differential-Difference Equations*. New York, NY: Academic Press, 1963.

[7] S. Boyd and L. Vandenberghe, *Convex Optimization*. Cambridge, UK: Cambridge University Press, 2004.

[8] R. F. Curtain and K. Glover, "Robust stabilization of infinite dimensional systems by finite dimensional controllers," *Syst. Control Lett.*, vol. 7, pp. 41–47, 1986.

[9] R. F. Curtain and K. Morris, "Transfer functions of distributed parameter systems: A tutorial," *Automatica*, vol. 45, no. 5, pp. 1101–1116, 2009.

[10] R. F. Curtain and H. Zwart, *An Introduction to Infinite-Dimensional Linear Systems Theory*. New York, NY: Springer-Verlag, 1995.

[11] R. Datko, "A procedure for determination of the exponential stability of certain differential-difference equations," *Quart. Appl. Math.*, vol. 36, pp. 279–292, 1978.

[12] C. A. Desoer and M. Vidyasagar, *Feedback Systems: Input-Output Properties*. New York, NY: Academic Press, 1975.

[13] Y. A. Fiagbedzi and A. E. Pearson, "Feedback stabilization of linear autonomous time lag systems," *IEEE Trans. Automat. Control*, vol. 31, no. 9, pp. 847–855, 1986.

[14] B. A. Francis, *A Course in H_∞ Theory*, ser. Lecture Notes in Control and Inform. Sci. New York, NY: Springer-Verlag, 1987, vol. 88.

[15] B. A. Francis and W. M. Wonham, "The internal model principle for linear multivariable regulators," *Appl. Math. Opt.*, vol. 2, no. 2, pp. 170–412, 1975.

[16] E. Fridman, "New Lyapunov–Krasovskii functionals for stability of linear retarded and neutral type systems," *Syst. Control Lett.*, vol. 43, pp. 309–319, 2001.

[17] A. T. Fuller, "Optimal nonlinear control of systems with pure delay," *Int. J. Control*, vol. 8, no. 2, pp. 145–168, 1968.

[18] T. Furukawa and E. Shimemura, "Predictive control for systems with time delay," *Int. J. Control*, vol. 37, no. 2, pp. 399–412, 1983.

[19] G. C. Goodwin, S. F. Graebe, and M. E. Salgado, *Control System Design*. Englewood Cliffs, NJ: Prentice-Hall, 2000.

[20] K. Gu, V. L. Kharitonov, and J. Chen, *Stability of Time-Delay Systems*. Boston, MA: Birkhäuser, 2003.

[21] R. Gudin and L. Mirkin, "On the delay margin of dead-time compensators," *Int. J. Control*, vol. 80, no. 8, pp. 1316–1332, 2007.

[22] J. K. Hale and S. M. Verduyn Lunel, *Introduction to Functional Differential Equations*. New York, NY: Springer-Verlag, 1993.

[23] T. Inoue, M. Nakano, and S. Iwai, "High accuracy control of servomechanism for repeated contouring," in *Proc. 10th Annual Symp. Incremental Motion Control Systems and Devices*, Urbana–Champaign, IL, 1981, pp. 285–292.

[24] N. F. Jerome and W. H. Ray, "High-performance multivariable control strategies for systems having time delays," *AIChE Journal*, vol. 32, no. 6, pp. 914–931, 1986.

[25] T. Kailath, *Linear Systems*. Englewood Cliffs, NJ: Prentice-Hall, 1980.

[26] C.-Y. Kao and B. Lincoln, "Simple stability criteria for systems with time-varying delays," *Automatica*, vol. 40, no. 8, pp. 1429–1434, 2004.

[27] C.-Y. Kao and A. Rantzer, "Stability analysis of systems with uncertain time-varying delays," *Automatica*, vol. 43, no. 6, pp. 959–970, 2007.

[28] V. L. Kharitonov, *Time-Delay Systems: Lyapunov Functionals and Matrices*. New York, NY: Birkhäuser, 2013.

[29] O. Kidron and O. Yaniv, "Robust control of uncertain resonant systems," *European J. Control*, vol. 1, no. 2, pp. 104–112, 1995.

[30] D. L. Kleinman, "Optimal control of linear systems with time-delay and observation noise," *IEEE Trans. Automat. Control*, vol. 14, no. 5, pp. 524–527, 1969.

[31] N. N. Krasovskiĭ, *Stability of Motion: Applications of Lyapunov's Second Method to Differential Systems and Equations With Delay*. Stanford, CA: Stanford Univ. Press, 1963.

[32] W. H. Kwon and A. E. Pearson, "Feedback stabilization of linear systems with delayed control," *IEEE Trans. Automat. Control*, vol. 25, no. 2, pp. 266–269, 1980.

[33] D. G. Luenberger, *Optimization by Vector Space Methods*. New York, NY: John Wiley & Sons, 1969.

[34] A. Z. Manitius and A. W. Olbrot, "Finite spectrum assignment problem for systems with delay," *IEEE Trans. Automat. Control*, vol. 24, pp. 541–553, 1979.

[35] I. Masubuchi, Y. Kamitane, A. Ohara, and N. Suda, "H_∞ control for descriptor systems: A matrix inequalities approach," *Automatica*, vol. 33, no. 4, pp. 669–673, 1997.

[36] D. Q. Mayne, "Control of linear systems with time delay," *Electronics Letters*, vol. 4, no. 20, pp. 439–440, 1968.

[37] A. Megretski and A. Rantzer, "System analysis via integral quadratic constraints," *IEEE Trans. Automat. Control*, vol. 42, no. 6, pp. 819–830, 1997.

[38] G. Meinsma and L. Mirkin, "H^∞ control of systems with multiple I/O delays via decomposition to adobe problems," *IEEE Trans. Automat. Control*, vol. 50, no. 2, pp. 199–211, 2005.

[39] G. Meinsma and H. Zwart, "On $\mathcal{H}_\infty$ control for dead-time systems," *IEEE Trans. Automat. Control*, vol. 45, no. 2, pp. 272–285, 2000.

[40] R. H. Middleton and D. E. Miller, "On the achievable delay margin using LTI control for unstable plants," *IEEE Trans. Automat. Control*, vol. 52, no. 7, pp. 1194–1207, 2007.

[41] D. E. Miller and D. E. Davison, "Stabilization in the presence of an uncertain arbitrarily large delay," *IEEE Trans. Automat. Control*, vol. 50, no. 8, pp. 1074–1089, 2005.

[42] L. Mirkin, "On the extraction of dead-time controllers and estimators from delay-free parametrizations," *IEEE Trans. Automat. Control*, vol. 48, no. 4, pp. 543–553, 2003.

[43] ——, "On the approximation of distributed-delay control laws," *Syst. Control Lett.*, vol. 55, no. 5, pp. 331–342, 2004.

[44] ——, "Intermittent redesign of analog controllers via the Youla parameter," *IEEE Trans. Automat. Control*, vol. 62, no. 4, pp. 1838–1851, 2017.

[45] ——, "Linear Control Systems," course notes, Faculty of Mechanical Eng., Technion—IIT, 2024. [Online]. Available: http://leo.technion.ac.il/Courses/LCS/LCSnotes.pdf

[46] L. Mirkin, Z. J. Palmor, and D. Shneiderman, "Dead-time compensation for systems with multiple I/O delays: A loop shifting approach," *IEEE Trans. Automat. Control*, vol. 56, no. 11, pp. 2542–2554, 2011.

[47] L. Mirkin and N. Raskin, "Every stabilizing dead-time controller has an observer-predictor-based structure," *Automatica*, vol. 39, no. 10, pp. 1747–1754, 2003.

[48] L. Mirkin, H. Rotstein, and Z. J. Palmor, "H^2 and H^∞ design of sampled-data systems using lifting. Part II: Properties of systems in the lifted domain," *SIAM J. Control Optim.*, vol. 38, no. 1, pp. 197–218, 1999.

[49] L. Mirkin and G. Tadmor, "Imposing FIR structure on H^2 preview tracking and smoothing solutions," *SIAM J. Control Optim.*, vol. 48, no. 4, pp. 2433–2460, 2009.

[50] L. Mirkin and D. Zanutto, "Dead-time compensation as an observer-based design," *IEEE Control Syst Lett*, vol. 6, pp. 1604–1609, 2022.

[51] S.-I. Niculescu and W. Michiels, "Stabilizing a chain of integrators using multiple delays," *IEEE Trans. Automat. Control*, vol. 49, no. 4, pp. 802–807, 2004.

[52] M. Nordin and P.-O. Gutman, "Digital QFT design for the benchmark problem," *European J. Control*, vol. 1, no. 2, pp. 97–103, 1995.

[53] J. E. Normey-Rico and E. F. Camacho, *Control of Dead-time Processes*. London, UK: Springer-Verlag, 2007.

[54] N. Olgac and B. T. Holm-Hansen, "A novel active vibration absorption technique: delayed resonator," *J. Sound Vibration*, vol. 176, no. 1, pp. 93–104, 1994.

[55] D. H. Owens and A. Raya, "Robust stability of Smith predictor controllers for time-delay systems," *IEE Proc. – Control Theory Appl.*, vol. 129, no. 6, pp. 298–304, 1982.

[56] A. Packard and J. Doyle, "The complex structured singular value," *Automatica*, vol. 29, no. 1, pp. 71–109, 1993.

[57] P. Park, "A delay-dependent stability criterion for systems with uncertain time-invariant delays," *IEEE Trans. Automat. Control*, vol. 44, no. 4, pp. 876–877, 1999.

[58] J. R. Partington, *Linear Operators and Linear Systems: An Analytical Approach to Control Theory*. Cambridge, UK: Cambridge University Press, 2004.

[59] J. R. Partington and C. Bonnet, "H_∞ and BIBO stabilization of delay systems of neutral type," *Syst. Control Lett.*, vol. 52, no. 8, pp. 283–288, 2004.

[60] J. R. Partington and P. M. Mäkilä, "Rational approximation of distributed-delay controllers," *Int. J. Control*, vol. 78, no. 16, pp. 1295–1301, 2005.

[61] R. Rabah, G. M. Sklyar, and A. V. Rezounenko, "Stability analysis of neutral type systems in Hilbert space," *J. Differential Equations*, vol. 214, no. 2, pp. 391–428, 2005.

[62] B. S. Razumikhin, "On the stability of delay systems," *Prikl. Mat. i Meh.*, vol. 20, no. 4, pp. 500–512, 1956, (in Russian).

[63] Z. V. Rekasius, "A stability test for systems with delays," in *Proc. 1980 Joint Automatic Control Conf.*, vol. II, San Francisco, CA, 1980, p. TP9–A.

[64] R. D. Robinett, B. J. Petterson, and J. C. Fahrenholtz, "Time-domain validation for sample-data uncertainty models," *J. Intell. Robot. Syst.*, vol. 21, pp. 277–285, 1998.

[65] W. Rudin, *Real and Complex Analysis*, 3rd ed. New York, NY: McGraw-Hill, 1987.

[66] C. W. Scherer and S. Weiland, *Linear Matrix Inequalities in Control*, DISC course notes, 2015. [Online]. Available: https://www.imng.uni-stuttgart.de/mst/files/LectureNotes.pdf

[67] A. Seuret, F. Gouaisbaut, and L. Baudouin, "D1.1 - Overview of Lyapunov methods for time-delay systems," LAAS-CNRS, Research Report no. 16308, Sep. 2016. [Online]. Available: https://hal.archives-ouvertes.fr/hal-01369516

[68] J. S. Shamma, "Robust stability with time-varying structured uncertainty," *IEEE Trans. Automat. Control*, vol. 39, no. 4, pp. 714–724, 1994.

[69] W. Singhose, "Command shaping for flexible systems: A review of the first 50 years," *Int. J. Precis. Eng. Manuf.*, vol. 10, no. 4, pp. 153–168, 2009.

[70] O. J. M. Smith, "Closer control of loops with dead time," *Chem. Eng. Progress*, vol. 53, no. 5, pp. 217–219, 1957.

[71] ——, "Posicast control of damped oscillatory systems," *Proc. IRE*, vol. 45, no. 9, pp. 1249–1255, 1957.

[72] I. H. Suh and Z. Bien, "Proportional minus delay controller," *IEEE Trans. Automat. Control*, vol. 24, no. 2, pp. 370–372, 1979.

[73] P. K. S. Tam and J. B. Moore, "Stable realization of fixed-lag smoothing equations for continuous-time signals," *IEEE Trans. Automat. Control*, vol. 19, no. 1, pp. 84–87, 1974.

[74] O. Troeng and L. Mirkin, "Toward a more efficient implementation of distributed-delay elements," in *Proc. 52nd IEEE Conf. Decision and Control*, Florence, Italy, 2013, pp. 294–299.

[75] Y. Z. Tsypkin, "Stability of systems with delayed feedback," *Avtomatika i Telemekhanica*, vol. 7, no. 2–3, pp. 107–129, 1946.

[76] V. Van Assche, M. Dambrine, J.-F. Lafay, and J.-P. Richard, "Some problems arising in the implementation of distributed-delay control laws," in *Proc. 38th IEEE Conf. Decision and Control*, Phoenix, AZ, 1999, pp. 4668–4672.

[77] J. Veenman and C. W. Scherer, "IQC-synthesis with general dynamic multipliers," *Int. J. Robust and Nonlinear Control*, vol. 24, no. 17, pp. 3027–3056, 2014.

[78] K. Walton and J. E. Marshall, "Direct method for TDS stability analysis," *IEE Proc. – Control Theory Appl.*, vol. 134, pp. 101–107, 1987.

[79] Z. Q. Wang, P. Lundström, and S. Skogestad, "Representation of uncertain time delays in the H_∞ framework," *Int. J. Control*, vol. 59, no. 3, pp. 627–638, 1994.

[80] K. Watanabe and M. Ito, "A process-model control for linear systems with delay," *IEEE Trans. Automat. Control*, vol. 26, no. 6, pp. 1261–1269, 1981.

[81] B. Wie and K.-W. Byun, "New generalized structural filtering concept for active vibration control synthesis," *J. Guidance, Control, and Dynamics*, vol. 12, no. 2, pp. 147–154, 1989.

[82] J. C. Willems, *The Analysis of Feedback Systems*.   Cambridge, MA: The MIT Press, 1971.

[83] S. Xu and J. Lam, "A survey of linear matrix inequality techniques in stability analysis of delay systems," *Int. J. Systems Sciences*, vol. 39, no. 12, pp. 1095–1113, 2008.

[84] J. Zhang, C. R. Knospe, and P. Tsiotras, "Stability of time-delay systems: Equivalence between Lyapunov and scaled small-gain conditions," *IEEE Trans. Automat. Control*, vol. 46, no. 3, pp. 482–486, 2001.

[85] X.-M. Zhang, Q.-L. Han, A. Seuret, F. Gouaisbaut, and Y. He, "Overview of recent advances in stability of linear systems with time-varying delays," *IET Control Theory Appl.*, vol. 13, no. 1, pp. 1–16, 2018.

Index